Theory of Elastic Waves

Gerhard Müller

Editors

Michael Weber - GFZ & Universität Potsdam

Georg Rümpker - Universität Frankfurt

Dirk Gajewski - Universität Hamburg

Germany

tew_2007.ps + tew_2007.pdf

Preface

When Gerhard Müller chose to leave us on 9 July 2002 because of his illness, we lost a teacher and colleague. Part of his legacy is several lecture notes which he had worked on for more then 20 years. These notes have become the backbone of teaching seismics and seismology at basically all German universities. When asked some years before his death if he had considered to translate "Theorie Elastischer Wellen" into English and publish it as a book, his answer was "I plan to do it when I am retired". We hope that our effort would have found his approval.

We would like to thank R. and I. Coman (Universität Hamburg) for preparing a first, German draft in LATEX of this script, A. Siebert (GFZ Potsdam) for her help in preparing the figures and our students for pointing out errors and asking questions. We would like to thank A. Priestley for proof-reading the script and turning Deutschlish into English and K. Priestley for his many comments.

We thank the GFZ Potsdam and the Dublin Institute for Advanced Studies for their support during a sabbatical of MW in Dublin, where most of this book was prepared. We would also like to thank the GFZ for continuing support in the preparation of this book.

M. Weber G. Rümpker D. Gajewski

Potsdam, Frankfurt, Hamburg

January 2007

This file can be downloaded from **http://gfz-potsdam.de/mhw/tew/**

$tew\_2007.ps(64MB) + tew\_2007.pdf(3.5MB)$

Preface of the German Lecture Notes

This script is the revised and extended version of a manuscript which was used for several years in a 1- to 2-semester lecture on the theory of elastic waves at the universities of Karlsruhe and Frankfurt. The aim of this manuscript is to give students with some background in mathematics and theoretical physics the basic knowledge of the theory of elastic waves, which is necessary for the study of special literature in monographs and scientific journals. Since this is an introductory text, theory and methods are explained with simple models to keep the computational complexity and the formulae as simple as possible. This is why often liquid media instead of solid media are considered, and only horizontally polarised waves (SH-waves) are discussed, when shear waves in layered, solid media are considered. A third example is that the normal mode theory for point sources is derived for an ideal wave guide with free or rigid boundaries. These simplifications occasionally hide the direct connection to seismology. In my opinion, there is no other approach if one aims at presenting theory and methods in detail and introducing at least some aspect from the wide field of seismology. After working through this script students should, I hope, be better prepared to read the advanced text books of Pilant (1979), Aki and Richards (1980, 2000), Ben-Menahem and Sing (1981), Dahlen and Tromp (1998), Kennett (2002) and Chapman (2004), which treat models as realistically as possible.

This manuscript has its emphasis in the wave seismic treatment of elastic body and surface waves in layered media. The understanding of the dynamic properties of these two wave types, i.e., their amplitudes, frequencies and impulse forms, are a basic prerequisite-requisite for the study of the structure of the Earth, may it be in the crust, the mantle or the core, and for the study of processes in the earthquake source. Ray seismics in inhomogeneous media and their relation with wave seismics are discussed in more detail than in earlier versions of the script, but seismologically interesting topics like eigen-modes of the Earth and extended sources of elastic waves are still not treated, since they would exceed the scope of an introductory lecture.

At several places of the manuscript, exercises are included, the solution of these is an important part in understanding the material. One of the appendices tries to cover in compact form the basics of the Laplace and Fourier transform and of the delta function, so that these topics can be used in the main part of the script.

I would like to thank Ingrid Hörnchen for the often tedious writing and correcting of this manuscript.

Gerhard Müller

Contents

Chapter 1

Literature

The following list contains only books, that treat the propagation of elastic waves and a few text books on continuum mechanics. Articles in journals are mentioned if necessary. Their number is kept to a minimum.

Achenbach, J.D.: Wave propagation in elastic solid, North-Holland Publ. Comp., Amsterdam, 1973

Aki, K. and P.G. Richards: Quantitative seismology - theory and methods (2 volumes), Freeman and Co., San Francisco, 1980 and 2002

Ben-Menahem, A. and S.J. Singh: Seismic waves and sources, Springer, Heidelberg, 1981

Bleistein, N.: Mathematical methods for wave phenomena, Academic Press, New York, 1984

Brekhovskikh, L.M.: Waves in layered media, Academic Press, New York, 1960

Brekhovskikh, L., and Goncharov, V.: Mechanics of continua and wave dynamics, Springer-Verlag, Berlin, 1985

Budden, K.G.: The wave-guide mode theory of wave propagation, Logos Press, London, 1961

Bullen, K.E., and Bolt, B.A.: An introduction to the theory of seismology, Cambridge University Press, Cambridge, 1985

Cagniard, L.: Reflection and refraction of progressive waves, McGraw-Hill Book Comp., New York, 1962

*Č*ervený, V., I.A. Molotov and I. P*š*encík: Ray method in seismology, Univerzita Karlova, Prague, 1977

Chapman, Ch.: Fundamentals of seismic wave propagation, Cambridge University Press, 2004

Dahlen, F. A. and J. Tromp: Theoretical global seismology, Princeton University, Princeton, New Jersey, 1998

Ewing, M., W.S. Jardetzky and F. Press: Elastic waves in layered media, McGraw-Hill Book Comp., New York, 1957

Fung, Y.C.: Foundations of solid mechanics, Prentice-Hall, Englewood Cliffs, N.Y., 1965

Grant, F.S. and G.F. West: Interpretation theory in applied geophysics, McGraw-Hill Book Comp., New York, 1965

Hudson, J.A.: The excitation and propagation of elastic waves, Cambridge University Press, Cambridge, 1980

Kennett, B.L.N.: The seismic wave field (2 volumes), Cambridge University Press, Cambridge, 2002

Landau, L.D. and E.M. Lifschitz: Elastizitätstheorie, Akademie Verlag, Berlin, 1977

Love, A.E.H.: A treatise on the mathematical theory of elasticity, 4th edition, Dover Publications, New York, 1944

Pilant, W.L.: Elastic waves in the Earth, Elsevier, Amsterdam, 1979

Riley, K.F., M.P. Hobson and S.J. Bence: Mathematical methods for physics and engineering, A comprehensive guide, Cambridge University Press, Cambridge, 2nd edition, 2002

Sommerfeld, A.: Mechanik der deformierbaren Medien, Akad. Verlagsgesellschaft, Leipzig, 1964

Tolstoy, I.: Wave propagation, McGraw-Hill Book Comp., New York, 1973

Tolstoy, I. and C.S. Clay: Ocean acoustics-theory and experiment in underwater sound, McGraw-Hill Book Comp., New York, 1966

White, J.E.: Seismic waves-radiation, transmission and attenuation, McGraw-Hill Book Comp., New York, 1965

Chapter 2

Foundations of elasticity theory

Comments

In this chapter symbolic and index notation is used, i.e., a vector (symbolic notation $\overrightarrow{f}$) is also written as f_i (components $f_1, f_2, \ldots, f_n$), the location vector (symbolic $\overrightarrow{x}$) as x_i (components $x_1,\ x_2,\ x_3$), and a matrix (symbolic $\underline{a}$) as a_{ij} ($i =$ line index $= 1, 2, \ldots, m, j =$ row index$= 1, 2, \ldots, n$). The product of matrix a_{ij} with the vector f_j is the vector

$$g_i = \sum_{j=1}^{n} a_{ij} f_j \qquad (i = 1, 2, \ldots, m).$$

A short notation for this is (*summation convention* $= SC$)

$$g_i = a_{ij} f_j.$$

In the following text, if a product on the right occurs in which there is a repeated index, this index takes all values from 1, 2, ..., n (usually n = 3) and all products are summed.

If the symbolic notation is simpler, e.g., for the cross product of two vectors or for divergence or rotation, the symbolic notation is used.

2.1 Analysis of strain

2.1.1 Components of the displacement vector

Consider a body that is deformed by an external force. Before deformation, the point P has the location vector x_i and the infinitesimal close point Q has the location vector $x_i + y_i$. The components of y_i are assumed to be independent variables; this is why dx_i was not used. After deformation, P has been displaced by the displacement vector u_i to P', and Q has been displaced to Q' by the vector (expansion up to linear terms)

$$z_i = u_i + du_i = u_i + \frac{\partial u_i}{\partial x_j} y_j \quad \text{(SC)}.$$

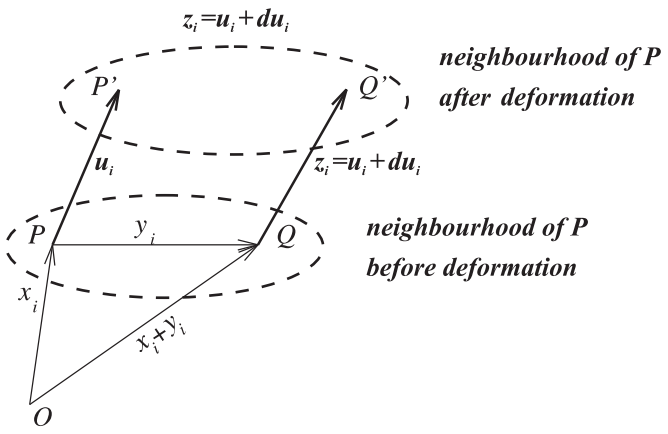

Fig. 2.1: Neighbourhood of P and Q before and after deformation.

Vector z_i describes (for variable Q in the neighbourhood of P) the changes near P due to the deformation. In general, these changes consist of: a translation, a rotation of the *whole* region around an axis through P and the actual deformation, which changes the length of lines (rotation and deformation will be discussed later in more detail)

$$z_i = u_i + du_i = \underbrace{u_i}_{\text{translation}} + \underbrace{\epsilon_{ij} y_j}_{\text{deformation}} + \underbrace{\xi_{ij} y_j}_{\text{rotation}}$$

$$\epsilon_{ij} = \frac{1}{2}\left(\frac{\partial u_i}{\partial x_j} + \frac{\partial u_j}{\partial x_i}\right), \qquad \xi_{ij} := \frac{1}{2}\left(\frac{\partial u_i}{\partial x_j} - \frac{\partial u_j}{\partial x_j}\right) \tag{2.1}$$

$$\epsilon_{ij} = \epsilon_{ji} \tag{2.2}$$

$$\xi_{ij} = -\xi_{ji} \qquad (\Rightarrow \xi_{11} = \xi_{22} = \xi_{33} = 0)\,. \tag{2.3}$$

The matrices ϵ_{ij} and ξ_{ij} are *tensors of 2nd degree*. ϵ_{ij} is symmetric due to (2.2) and ξ_{ij} is anti-symmetric due to (2.3). ϵ_{ij} is called *deformation tensor* and ξ_{ij} is called *rotation tensor*.

2.1.2 Tensors of 2nd degree

A tensor of 2nd degree, t_{ij}, transforms a vector into another vector (e.g., ϵ_{ij} transforms vector y_i into the deformation part of du_i; another example of this is the inertial tensor transforms the vector of the angular velocity into the rotation impulse vector (rotation of a rigid body)). If the coordinate system is rotated, the tensor components have to be transformed as follows to yield the original vector

$$\begin{aligned} t'_{kl} &= a_{ik}a_{jl}t_{ij} \qquad \text{(SC twice)} \\ a_{mn} &= \cos\gamma_{mn} \qquad \text{(see sketch).} \end{aligned} \tag{2.4}$$

t'_{kl} = Tensor component in the rotated coordinate system (dashed line in sketch).

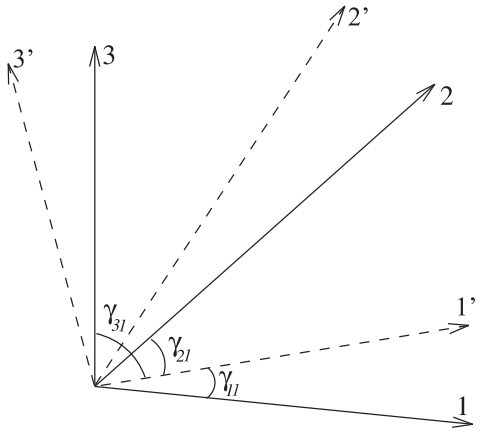

Fig. 2.2: Coordinate system of tensors of 2nd degree.

For a certain orientation of the rotated system, the non-diagonal elements $t'_{12}, t'_{13}, t'_{21}$, ... vanish. These coordinate axis are called *main axes* of the tensor, and the tensor is in diagonal form. In the diagonal form, many physical relations become simpler. Certain combinations of tensor components are independent of the coordinate system of the tensor. These are the three *invariants* (T_1, T_2, T_3 are the diagonal elements of the tensor in diagonal form). More on tensors can be found in, e.g., Riley, Hobson and Bence.

$$
\begin{aligned}
I_1 = &\begin{vmatrix} t_{11} & t_{12} & t_{13} \\ t_{21} & t_{22} & t_{23} \\ t_{31} & t_{32} & t_{33} \end{vmatrix} && = T_1T_2T_3 && \text{(determinant)}\\
I_2 = &\ t_{11}+t_{22}+t_{33} && = T_1+T_2+T_3 && \text{(trace)}\\
I_3 = &\ t_{11}t_{22}+t_{22}t_{33}+t_{33}t_{11}- && && \\
&\ t_{12}t_{21}-t_{23}t_{32}-t_{31}t_{13} && = T_1T_2+T_2T_3+T_3T_1. &&
\end{aligned}
$$

2.1.3 Rotation component of displacement

The rotation component of displacement follows from

$$
\begin{pmatrix} 0 & \xi_{12} & \xi_{13} \\ -\xi_{12} & 0 & \xi_{23} \\ -\xi_{13} & -\xi_{23} & 0 \end{pmatrix}
\begin{pmatrix} y_1 \\ y_2 \\ y_3 \end{pmatrix} =
\begin{pmatrix} \xi_{12}y_2+\xi_{13}y_3 \\ -\xi_{12}y_1+\xi_{23}y_3 \\ -\xi_{13}y_1-\xi_{23}y_2 \end{pmatrix} = \vec{\xi}\times\vec{y}
$$

$$
\text{with} \qquad \vec{\xi} = (-\xi_{23}, \xi_{13}, -\xi_{12}) = \frac{1}{2}\nabla\times\vec{u}.
$$

Vector $\vec{\xi}\times\vec{y}$ describes an *infinitesimal rotation* of the region of P around an axis through P with the direction of $\vec{\xi}$. The rotation angle has the absolute value $\left|\vec{\xi}\right|$ and is independent of $\vec{y}$ (show). A prerequisite is that $\vec{\xi}$ is infinitesimal. A sufficient condition for this is that

$$
\left|\frac{\partial u_i}{\partial x_j}\right| \ll 1 \qquad \text{for all } i \text{ and } j. \tag{2.5}
$$

2.1.4 Deformation component of displacement

After separating out the rotation term, only the deformation term is of interest since it describes the forces which act in a body. The deformation is described completely by the six components ϵ_{ij} which are, in general, different. These dimensionless components will now be interpreted physically.

The starting point is $du_i = \epsilon_{ij}y_j$, i.e., we assume no rotation.

a) During this transformation, a line remains a line, a plane remains a plane, a sphere becomes an ellipsoid and parallel lines remain parallel.

b) *Deformation components* $\epsilon_{11}, \epsilon_{22}, \epsilon_{33}$

Coordinate origin at P and special selection of $Q:\ y_1 \neq 0, y_2 = y_3 = 0$.

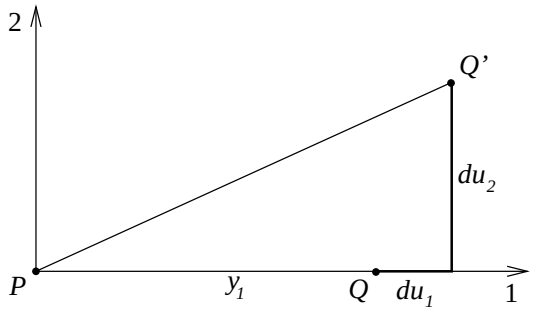

Fig. 2.3: Sketch for deformation components.

$$
\begin{aligned}
du_1 &= \epsilon_{11} y_1 \\
du_2 &= \epsilon_{21} y_1 \\
du_3 &= \epsilon_{31} y_1 = 0 \qquad \text{(assumption : } \quad \epsilon_{31} = 0\text{)}.
\end{aligned}
$$

$\epsilon_{11} = \frac{du_1}{y_1}$ is the relative change in length in direction 1 (*not* the relative change in length of PQ, see also d). Stretching occurs if $\epsilon_{11} > 0$ and shortening if $\epsilon_{11} < 0$. Similarly, ϵ_{22} and ϵ_{33} are the relative length changes in direction 2 and 3.

c) *Shear components* $\epsilon_{12}, \epsilon_{13}, \epsilon_{23}$

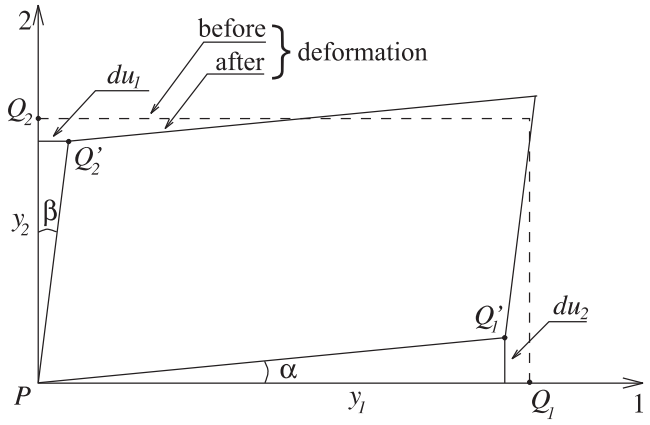

Fig. 2.4: Sketch for shear components.

$$
\begin{aligned}
Q_1 \to Q_1' \ : \ du_2 &= \epsilon_{21} y_1 = \epsilon_{12} y_1 \\
Q_2 \to Q_2' \ : \ du_1 &= \epsilon_{12} y_2
\end{aligned}
$$

$$\begin{aligned} \tan\alpha \simeq \alpha \simeq \frac{du_2}{y_1} &= \epsilon_{12} \\ \tan\beta \simeq \beta \simeq \frac{du_1}{y_2} &= \epsilon_{12}. \end{aligned}$$

This means, ϵ_{12} is the angle around which the 1- or 2-axis is rotated. The right angle at P is reduced by $2\epsilon_{12}$. If the parallelogram is not in the 1-2 plane after deformation (since $\epsilon_{13}, \epsilon_{23}$ or ϵ_{33} is non-zero), these statements hold for the vertical projection in this plane.

Similar results hold for ϵ_{13} and ϵ_{23}.

d) *Length changes of distance* $\overline{PQ}$

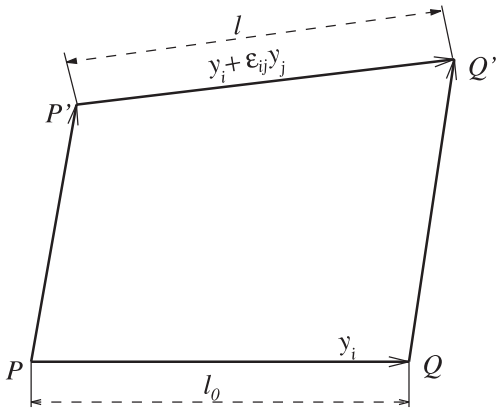

Fig. 2.5: Sketch for length changes of distance $\overline{PQ}$.

$$\begin{aligned} \overline{PQ} &= l_0 = \left\{ \sum_{i=1}^{3} y_i^2 \right\}^{1/2} \\ \overline{P'Q'} &= l = \left\{ \sum_{i=1}^{3} (y_i + \epsilon_{ij} y_j)^2 \right\}^{1/2} = \\ &= \left\{ \sum_{i=1}^{3} y_i^2 + 2\epsilon_{ij} y_i y_j + \sum_{i=1}^{3} (\epsilon_{ij} y_j)^2 \right\}^{1/2}. \end{aligned}$$

The 1st, 2nd and 3rd term require SC once, twice and three times, respectively. The 3rd term contains only squares of ϵ_{ij} and can, within the framework of *infinitesimal strain theory* treated here, be neglected relative to the 2nd term (the prerequisite for this is (2-5))

$$l = l_0 \left(1 + \frac{2}{l_0^2}\epsilon_{ij} y_i y_j\right)^{\frac{1}{2}} = l_0 + \frac{1}{l_0}\epsilon_{ij} y_i y_j.$$

Relative length changes

$$\frac{l - l_0}{l_0} = \epsilon_{ij}\frac{y_i y_j}{l_0^2} = \epsilon_{ij} n_i n_j \text{ (SC twice; quadratic form in } n_k)$$

$$n_i = \frac{y_i}{l_0} = \text{unit vector in direction of } y_i.$$

Approaches for **finite** *strain theory* exist (see, e.g., Bullen and Bolt). Such a theory has to be developed from the very start. Then, for example, the simple separation of the rotation term in the displacement vector, which is possible for infinitesimal deformations, is no longer possible. The deformation tensor ϵ_{ij} also becomes more complicated.

e) *Volume changes (cubic dilatation)*

We consider a finite (not infinitesimal) volume V containing point P surface with S. After deformation, for which we assume without loss of generality that P remains in its position, volume V is changed by ΔV.

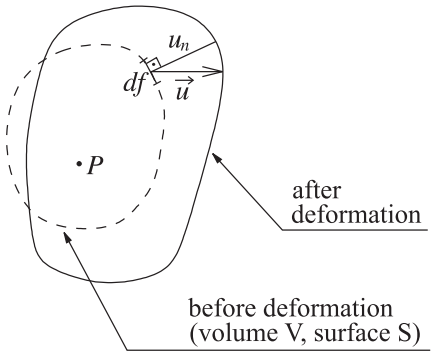

Fig. 2.6: Sketch for volume changes.

$$\Delta V = \int_S u_n df.$$

Transformation of this surface integral with Gauss' law gives

$$\Delta V = \int_V \nabla \cdot \vec{u}\, dV,$$

and the relative volume change can be written as

$$\frac{\Delta V}{V} = \frac{1}{V}\int_V \nabla \cdot \overrightarrow{u}\, dV. \tag{2.6}$$

Into the limit $V \to 0$ (shrinking to point P), this becomes

$$\lim_{V\to 0} \frac{\Delta V}{V} = \Theta.$$

This limit is called *cubic dilatation*.

From (2.6) with (2.1), it follows that

$$\Theta = \nabla\cdot\overrightarrow{u} := \frac{\partial u_1}{\partial x_1}+\frac{\partial u_2}{\partial x_2}+\frac{\partial u_3}{\partial x_3} = \epsilon_{11}+\epsilon_{22}+\epsilon_{33} \quad \text{(trace of the deformation tensor)}.$$

For $\Theta > 0$ the volume increases, for $\Theta < 0$ the volume decreases.

2.1.5 Components of the deformation tensor in cylindrical and spherical coordinates

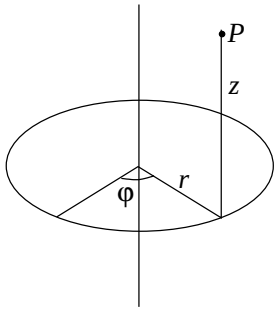

Fig. 2.7: Cylindrical coordinates r, φ, z.

$$\begin{aligned}
\overrightarrow{u} &= (u_r, u_\varphi, u_z) \\
\epsilon_{rr} &= \frac{\partial u_r}{\partial r} \\
\epsilon_{\varphi\varphi} &= \frac{1}{r}\frac{\partial u_\varphi}{\partial \varphi} + \frac{u_r}{r} \\
\epsilon_{zz} &= \frac{\partial u_z}{\partial z} \\
2\epsilon_{r\varphi} &= \frac{1}{r}\frac{\partial u_r}{\partial \varphi} + \frac{\partial u_\varphi}{\partial r} - \frac{u_\varphi}{r}
\end{aligned}$$

$$\begin{aligned} 2\epsilon_{rz} &= \frac{\partial u_r}{\partial z} + \frac{\partial u_z}{\partial r} \\ 2\epsilon_{\varphi z} &= \frac{\partial u_\varphi}{\partial z} + \frac{1}{r}\frac{\partial u_z}{\partial \varphi}. \end{aligned}$$

The components refer to the local Cartesian coordinate system in P.

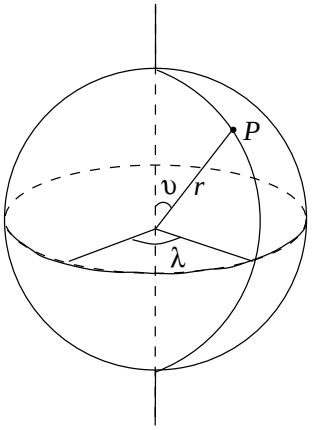

Fig. 2.8: Spherical coordinates r, ϑ, λ.

$$\begin{aligned} \overrightarrow{u} &= (u_r, u_\vartheta, u_{\lambda)} \\ \epsilon_{rr} &= \frac{\partial u_r}{\partial r} \\ \epsilon_{\vartheta\vartheta} &= \frac{1}{r}\frac{\partial u_\vartheta}{\partial \vartheta} + \frac{u_r}{r} \\ \epsilon_{\lambda\lambda} &= \frac{1}{r\sin\vartheta}\frac{\partial u_\lambda}{\partial \lambda} + \frac{u_r}{r} + \frac{\cot\vartheta}{r}u_\vartheta \\ 2\epsilon_{r\vartheta} &= \frac{1}{r}\frac{\partial u_r}{\partial \vartheta} + \frac{\partial u_\vartheta}{\partial r} - \frac{u_\vartheta}{r} \\ 2\epsilon_{r\lambda} &= \frac{1}{r\sin\vartheta}\frac{\partial u_r}{\partial \lambda} + \frac{\partial u_\lambda}{\partial r} - \frac{u_\lambda}{r} \\ 2\epsilon_{\vartheta\lambda} &= \frac{1}{r\sin\vartheta}\frac{\partial u_\vartheta}{\partial \lambda} + \frac{1}{r}\frac{\partial u_\lambda}{\partial \vartheta} - \frac{\cot\vartheta}{r}u_\lambda. \end{aligned}$$

Exercise 2.1

How does a rectangular cube with edges parallel to the main axis system of the deformation tensor deform (length of edges a, b, c)? Confirm the equation

$$\Theta = \epsilon_{11} + \epsilon_{22} + \epsilon_{33} \quad .$$

Exercise 2.2

Split the deformation tensor into one part that is pure shear (no volume change) and another part that is pure volume change (no shear).

Exercise 2.3:

Derive the components of the deformation tensor in cylindrical coordinates. Hint:

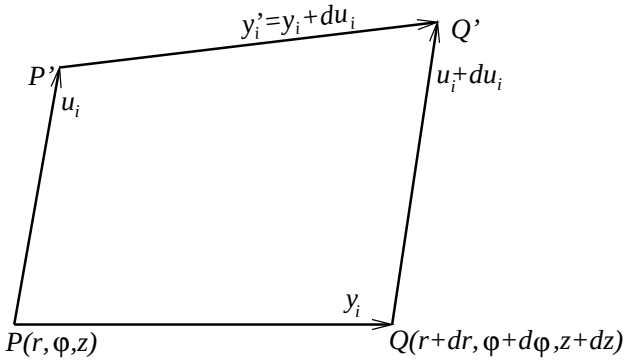

Fig. 2.9: Displacement vectors to be used.

With respect to the local Cartesian coordinate system in P, it holds that

$$\begin{array}{lcllcl} y_1 &=& dr & u_1 &=& u_r \\ y_2 &=& r d\varphi & u_2 &=& u_\varphi \\ y_3 &=& dz & u_3 &=& u_z. \end{array}$$

Determine first the cylindrical coordinates of P' and Q' under the condition of infinitesimal displacement and deformation. Then give the components of the vector $y'_i = y_i + du_i$ in the local Cartesian coordinate system of P', similar to the definition of y_i, in the system of P. This requires linearisation. This then allows the derivation of vector du_i in the form

$$du_i = v_{ij} y_j$$

and the determination of tensor v_{ij}. The deformation tensor is the symmetric part of v_{ij}

$$\epsilon_{ij} = \frac{1}{2}(v_{ij} + v_{ji}).$$

2.2 Analysis of stress

2.2.1 Stress

In a deformed body, a volume element is subject to *body forces* (proportional to volume, e.g., gravity, centrifugal force, inertial force) and to *surface forces*, which originate from neighbouring volume elements (proportional to surface). The later is the topic here. We consider a body K_1 with the surface S within a deformed body K_2 (see Fig. 2.10). If K_2 is removed, K_1 will, in general, assume a new equilibrium configuration. This indicates that K_2 has exerted forces through S on K_1. To bring K_1 back to its original form, *Ersatz* forces $\vec{P}\Delta f$ (Δf=surface element) have to be applied on S.

The same forces were exerted by K_2. $\vec{P}$ with the dimension force/surface is called *traction*. Its direction and size depend on:

1. The location of the surface element Δf
2. Its normal direction $\vec{n}$ (defined as the direction pointing *out* of K_1).

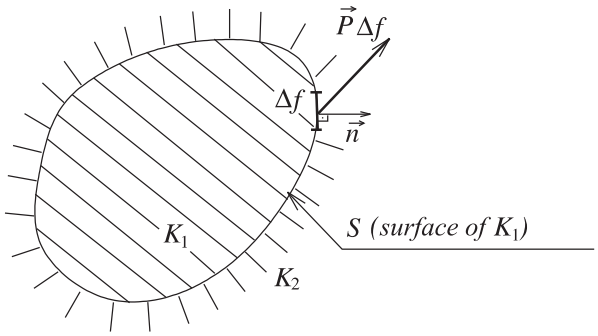

Fig. 2.10: Body K_1 within a deformed body K_2.

The component of $\vec{P}$ parallel to $\vec{n}$ is called normal traction (= pull or pressure traction).

The component of $\vec{P}$ perpendicular to $\vec{n}$ is called tangential traction, shear traction or thrust traction.

If $\vec{P}$ is known everywhere in the body and for all directions $\vec{n}$, the stress within the body is known. For this, six functions must be known.

2.2.2 Stress tensor p_{ij}

We consider a body in an infinitesimal tetrahedron *ABCD* and assume, that the traction of the three sides *ABD, ABC,* and *ACD* are known.

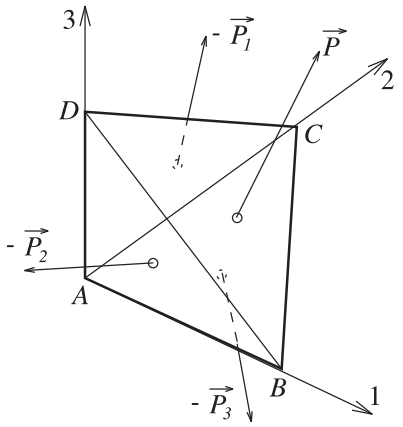

Fig. 2.11: Infinitesimal tetrahedron *ABCD*.

From this, we will compute the traction tensor $\vec{P}$ of *BCD*. Because the tetrahedron is small, all tractions are constant over their corresponding surfaces. The normal directions and surfaces are

ABD: negative 2-direction, Δf_2

ABC: negative 3-direction, Δf_3

ACD: negative 1-direction, Δf_1

BCD: $\vec{n} = (n_1, n_2, n_3),\ \Delta f$

$$\Delta f_j = \Delta f n_j. \tag{2.7}$$

We assume that the forces and traction vectors on *ABD, ABC* and *ACD* are known for the *positive* 2-, 3- and 1-direction, respectively

ABD: $\vec{P_2}\Delta f_2,\ \vec{P_2} = (p_{21}, p_{22}, p_{23})$

ABC: $\vec{P_3}\Delta f_3,\ \vec{P_3} = (p_{31}, p_{32}, p_{33})$

ACD: $\vec{P_1}\Delta f_1,\ \vec{P_1} = (p_{11}, p_{12}, p_{13})$.

This means that nine functions p_{ij} are known. After neglecting the body forces (which decrease faster then the surface forces for a shrinking tetrahedron), the force balance at the tetrahedron can be written as

$$-\vec{P_j}\Delta f_j + \vec{P}\Delta f = 0.$$

With (2.7), it follows (SC)

$$\vec{P} = \vec{P_j} n_j. \tag{2.8}$$

Therefore, it is sufficient to know the traction vectors of three perpendicular surface elements to determine the traction vector for an arbitrarily oriented surface element. In index notation, (2.8) can be written as (note: P_j is a component of $\overrightarrow{P}, \overrightarrow{P_j}$ is a vector)

$$P_1 = p_{11}n_1 + p_{21}n_2 + p_{31}n_3.$$

In general, it holds that $P_j = p_{ij}n_i$. (SC)

The nine functions p_{ij} form the *stress tensor*. It is valid for a certain right-angle coordinate system. The components p_{i1}, p_{i2}, p_{i3} give the traction vector for a surface element, the normal of which is in the direction of the positive i-axis. p_{ii} (e.i., p_{11}, p_{22}, or p_{33}) is the normal stress, the two other components are the tangential stresses, respectively. As will be shown in the next section (see also exercise 2.6), the stress tensor is symmetric, i.e.,

$$p_{ij} = p_{ji}.$$

Therefore, $P_j = p_{ji}n_i$ or in the usual notation

$$P_i = p_{ij}n_j. \tag{2.9}$$

In general, the stress tensor has six independent components.

Exercise 2.4

a) Give the stress tensor for hydrostatic pressure p.

b) Give the stress tensor for the interior of an infinite plate which is fixed at one side (bottom), whereas at the other side (top) the shear traction τ acts everywhere in the same direction.

Exercise 2.5

Show that if $\overrightarrow{P}$ is the traction for direction $\overrightarrow{n}$, and $\overrightarrow{P'}$ for the direction $\overrightarrow{n'}$, it holds that $\overrightarrow{P}\overrightarrow{n'} = \overrightarrow{P'}\overrightarrow{n}$.

2.3 Equilibrium conditions

The equilibrium conditions for a finite volume V in a deformable body require that the resulting force and the resulting angular moment vanish

$$\int_V \overrightarrow{F} dV + \int_S \overrightarrow{P} df = 0 \qquad \text{(resulting force)} \tag{2.10}$$

$$\int_V (\overrightarrow{x} \times \overrightarrow{F}) dV + \int_S (\overrightarrow{x} \times \overrightarrow{P}) df = 0 \quad \text{(resulting moment)} \tag{2.11}$$

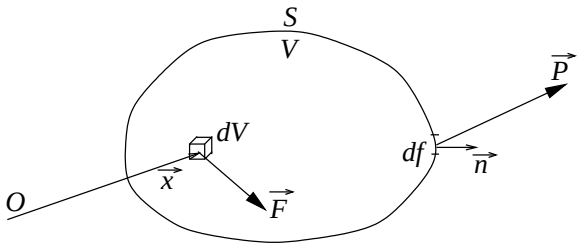

Fig. 2.12: Finite volume V in a deformable body.

where $\overrightarrow{F}$= body forces including inertial force (dimension: force/ volume = force density) and

$\overrightarrow{P}$= traction vector on S (normal $\overrightarrow{n}$ towards the outside).

Equation (2.10) gives the equation of motion of the elastic continuum. For each component (only Cartesian components can be used)

$$\int_V F_i dV + \int_S P_i df = \int_V F_i dV + \int_S p_{ij} n_j df = 0.$$

$p_{ij} n_j$ can be understood as the normal component P_{in} of the traction $\overrightarrow{P_i} = (p_{i1}, p_{i2}, p_{i3})$ relative to the ith-direction. Application of Gauss' theorem gives

$$\int_S P_{in} df = \int_V \nabla \cdot \overrightarrow{P_i} dV,$$

therefore,

$$\int_V (F_i + \nabla \cdot \overrightarrow{P_i}) dV = 0.$$

This holds for every arbitrary volume V. Therefore, the integrand has to vanish

$$F_i + \frac{\partial p_{i1}}{\partial x_1} + \frac{\partial p_{i2}}{\partial x_2} + \frac{\partial p_{i3}}{\partial x_3} = 0$$

or

$$F_i + \frac{\partial p_{ij}}{\partial x_j} = 0 \qquad \text{(SC)}$$

with the components of F : $F_i = -\rho \frac{d^2 u_i}{dt^2} + f_i \qquad (\rho = \text{density}).$

The first term is the inertial force; f_i contains all other body forces. Within the framework of the theory of infinitesimal deformation, the implicit differentiation $\frac{d}{dt}$ can be replaced by the local differentiation, i.e., partial differentiation $\frac{\partial}{\partial t}$

$$\frac{dA}{dt} = \frac{\partial A}{\partial t} + \frac{\partial A}{\partial x_i}\frac{\partial x_i}{\partial t} \approx \frac{\partial A}{\partial t} \quad (A = \text{infinitesimal parameter, e.g. } u_i).$$

Then, this gives the *equation of motion* (SC)

$$\rho \frac{\partial^2 u_i}{\partial t^2} = \frac{\partial p_{ij}}{\partial x_j} + f_i. \tag{2.12}$$

At rest, normally $p_{ij} \neq 0$ and the remaining stress is called the initial stress. It exists, when objects composed of materials with different thermal expansions coefficients are cooled, or by the self-compression of objects in their own gravity field (in this case the initial stress is the hydrostatic pressure). Assume that for a body at rest $p_{ij} = p_{ij}^{(0)}$ and $f_i = f_i^{(0)}$. Then (2.12) holds and

$$\frac{\partial p_{ij}^{(0)}}{\partial x_j} + f_i^{(0)} = 0. \tag{2.13}$$

The pre-stressed body will be deformed by time-dependent body forces (e.g., an earthquake in the Earth's crust). In the case of a sufficiently small additional stress (and only then), the following separation is valid

$$p_{ij} = p_{ij}^{(0)} + p_{ij}^{(1)} \qquad f_i = f_i^{(0)} + f_i^{(1)}.$$

With (2.13), it follows from (2.12), that

$$\rho \frac{\partial^2 u_i}{\partial t^2} = \frac{\partial p_{ij}^{(1)}}{\partial x_j} + f_i^{(1)}.$$

This means that the displacement u_i from the pre-stressed state depends only on the additional stress and the additional body forces. In the following, p_{ij} and f_i in (2.12) will always be understood in that sense, i.e., at rest $p_{ij} = 0$ and

$f_i = 0$. This assumption is sufficient for the study of elastic body and surface waves in the Earth. In the case of normal modes and tides, where large depth ranges and even the whole Earth moves, p_{ij} in (2.12) is the complete stress tensor, including the hydrostatic contribution. In this case, f_i represents all external forces, including the gravitational force of the Earth itself. The reason for this is that, in this case, because of the large size of the hydrostatic pressure during deformation, the change of this pressure cannot be neglected. A simple example is seen in the the radial modes of a sphere which have *larger* periods if hydrostatic pressure and gravitational force are included.

Exercise 2.6

Derive the equation of motion without assuming the symmetry of the stress tensor p_{ij}; then derive this symmetry from the moment equation (2.11). Hint: In the first part, use the stress vector in the form $P_i = p_{ji}n_j$ instead of (2.9). In the second part, write (2.11) by components and use the result of the first part.

2.4 Stress-strain relations

2.4.1 Generalised Hooke's Law

If a body in an unperturbed configuration shows a deformation associated with a length change, this body is under stress. This means that in each point of the body a relation between the components of the stress tensor and the deformation tensor exists

$$p_{ij} = f_{ij}(\epsilon_{11}, \epsilon_{12}, \ldots, \epsilon_{33}; a_1, a_2, \ldots, a_n). \tag{2.14}$$

As indicated, other independent parameters a_k, such as time and temperature, can occur. Generally, p_{ij} at time t can depend on the previous history at times τ with $-\infty < \tau < t$. If, for example, a beam has suffered extreme bending in the past, its behaviour will be different. The general study of (2.14) and a corresponding classification of materials as elastic, plastic and visco-elastic, *etc.* is the topic of *rheology*. For seismology, generally the most simple form of (2.14) is sufficient, namely that p_{ij} at a point depends only on the present values of ϵ_{kl} at that point. In this case, from $\epsilon_{kl} = 0$, it follows $p_{ij} = 0$, i.e., deformation ceases instantly if the stress ceases. This means

$$\begin{aligned} p_{ij} &= f_{ij}(\epsilon_{11}, \epsilon_{12}, \ldots, \epsilon_{33}) \\ & f_{ij}(0, 0, \ldots, 0) = 0. \end{aligned} \tag{2.15}$$

If these conditions hold, this state is called *ideal elasticity*. Under infinitesimal deformation, p_{ij} is a linear function of all ϵ_{kl} (expansion of (2.15) at $\epsilon_{kl} = 0$)

$$\begin{aligned} p_{ij} &= c_{ijkl}\epsilon_{kl} \qquad \text{(SC twice)} \\ c_{ijkl} &= \text{elasticity constants.} \end{aligned} \tag{2.16}$$

Linear elasticity theory studies elastic processes in bodies under the following assumptions:

1. The deformations are infinitesimal.
2. The stress-strain relations are linear.

The important assumption is 1.

The well-known *Hooke's Law*, for the stretching of a wire or the shearing of a cube, is a special case of (2.16). Equation (2.16) is, therefore, called generalised Hooke's law. Its range of applicability has to be determined by experiments or observation. The relation in the following sketch holds, for example, for the stretching of a wire. Between A and B the relation between force per square unit of the cross section p_{11} and the relative change in length ϵ_{11} is linear and corresponds to (2.16) (E = Young's modulus).

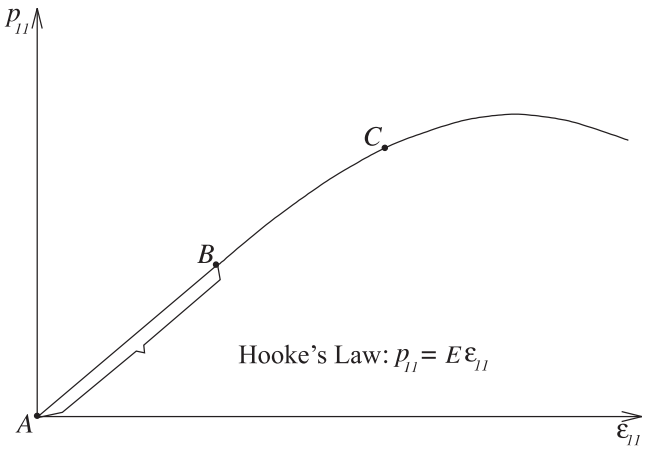

Fig. 2.13: Sketch for the stretching of a wire.

Between B and C the relation is no longer linear but still corresponds to ideal elastic behaviour, i.e., if p_{11} is reduced to zero, no deformation ϵ_{11} remains. Beyond C irreversible deformation occurs (plastic behaviour, flow of material). Finally the wire ruptures.

The tensor of 4th degree c_{ijkl} has 81 (9 x 9 =) components. Due to the symmetry of the deformation and stress tensors, only 36 (6 x 6 =) components are independent from each other. Since the elastic deformation energy (= elastic energy per unit volume) is conserved, this number reduces further to 21 components (see, e.g., pg. 268-269 in Sommerfeld). This is the maximum number of elasticity constants an *anisotropic* body can have. For special forms of anisotropy, and especially for isotropy, this number reduces further. For isotropic bodies which do not have preferred directions, only two elastic constants remain. The *stress-strain relations* (2.16) can then be written as

$$p_{ij} = \lambda\theta\delta_{ij} + 2\mu\epsilon_{ij} \tag{2.17}$$

where λ and μ are Lamés elasticity constant and elasticity parameter, respectively (both of which can be spatially dependent),

$\theta = \epsilon_{11} + \epsilon_{22} + \epsilon_{33}$ is the cubic dilatation, and

$\delta_{ij} = \left\{ \begin{array}{ll} 1 & \text{for } i = j \\ 0 & \text{otherwise} \end{array} \right\}$: is the Kronecker symbol or unit tensor

2.4.2 Derivation of (2.17)

We choose the main axis system of the stress tensor as the coordinate system, which under isotropy is identical to that of the deformation tensor. We, furthermore, have the main stress and deformation components P_1, P_2, P_3 and the main deformations E_1, E_2, E_3, respectively, which have a linear relation. In the isotropic case, this becomes

$$\begin{aligned} P_1 &= aE_1 + b(E_2 + E_3) \\ P_2 &= aE_2 + b(E_1 + E_3) \\ P_3 &= aE_3 + b(E_1 + E_2). \end{aligned}$$

The coefficient of E_2 and E_3 in the equation for P_1 have to be the same, since for an isotropic body the main axes 2 and 3 contribute equally to the main stress P_1. The same holds for the other two equations. From this, it follows that

$$\begin{aligned} P_i &= (a-b)E_i + b(E_1 + E_2 + E_3) \\ &= 2\mu E_i + \lambda(E_1 + E_2 + E_3), \end{aligned} \tag{2.18}$$

where the constants a and b have been replaced by the Lamé parameters λ and μ, respectively. This shows that (2.17) for the main axis coordinate system has no shear component of the deformation tensor and no shear stress.

Using (2.4) for the transformation of tensor components, the stress and deformations components in any coordinate system can be given as

$$\begin{aligned}
p_{11} &= a_{11}^2 P_1 + a_{21}^2 P_2 + a_{31}^2 P_3 & \epsilon_{11} &= a_{11}^2 E_1 + a_{21}^2 E_2 + a_{31}^2 E_3 \\
p_{22} &= a_{12}^2 P_1 + a_{22}^2 P_2 + a_{32}^2 P_3 & &\vdots \\
p_{12} &= a_{11}a_{12} P_1 + a_{21}a_{22} P_2 + a_{31}a_{32} P_3 & \epsilon_{12} &= a_{11}a_{12} E_1 + a_{21}a_{22} E_2 \\
& & & \quad + a_{31}a_{32} E_3 \\
p_{23} &= a_{12}a_{13} P_1 + a_{22}a_{23} P_2 + a_{32}a_{33} P_3 & &\vdots \\
&\vdots & &\vdots
\end{aligned} \tag{2.19}$$

For the directional cosines it holds that

$$a_{ik} a_{il} = \delta_{kl} \qquad \text{(SC)}.$$

Using (2.18) in the left equation of (2.19) and using the equations on the right gives

$$\begin{aligned}
p_{11} &= 2\mu\epsilon_{11} + \lambda(E_1 + E_2 + E_3) \\
p_{22} &= 2\mu\epsilon_{22} + \lambda(E_1 + E_2 + E_3) \\
p_{12} &= 2\mu\epsilon_{12} \\
p_{23} &= 2\mu\epsilon_{23} \\
&\vdots
\end{aligned}$$

The relations for shear stress already have the final form; those for the normal stress can be brought to the final form with the tensor invariants $E_1 + E_2 + E_3 = \epsilon_{11} + \epsilon_{22} + \epsilon_{33}$. This concludes the proof of (2.17).

Expressing ϵ_{kl} in terms of the derivative of the displacement vector, (2.17) can be written in Cartesian coordinates as

$$\begin{aligned}
p_{ii} &= \lambda\left(\frac{\partial u_1}{\partial x_1} + \frac{\partial u_2}{\partial x_2} + \frac{\partial u_3}{\partial x_3}\right) + 2\mu\frac{\partial u_i}{\partial x_i} \qquad \text{(no SC!)} \\
p_{ij} &= \mu\left(\frac{\partial u_i}{\partial x_j} + \frac{\partial u_j}{\partial x_i}\right) \qquad (i \neq j).
\end{aligned}$$

Equation (2.17) also holds in curved, orthogonal coordinates, like cylinder and spherical coordinates, respectively, if the deformation tensor is given in these coordinates (compare section 2.1.5). p_{ij} refers then to the coordinate surfaces

of the corresponding system. Finally, it should be noted that p_{ij} is usually understood as a stress added to a pre-stressed configuration.

The assumption that rocks and material of the deep Earth are isotropic is often valid. The crystals which make up the rock building minerals are, on the other hand, mostly anisotropic, but if they are randomly oriented, the material appears macroscopically isotropic.

2.4.3. Additions

Thermo-elastic stress-strain relations

These are examples of relations in which stress not only depends on deformation, but also on other parameters, e.g., temperature (α = volume expansion coefficient, $T - T_0$ = temperature change)

$$p_{ij} = \lambda\Theta\delta_{ij} + 2\mu\epsilon_{ij} - (\lambda + \frac{2}{3}\mu)\alpha(T - T_0)\delta_{ij}.$$

Relation between λ and μ and other elasticity parameters

E = Young's modulus
σ = Poisson's ratio
k = Bulk modulus
τ = Rigidity

$$E = \frac{\mu(3\lambda + 2\mu)}{\lambda + \mu} \qquad \sigma = \frac{\lambda}{2(\lambda+\mu)} \qquad k = \lambda + \frac{2}{3}\mu$$
$$\tau = \mu \qquad \lambda = \frac{\sigma E}{(1+\sigma)(1-2\sigma)} \qquad \mu = \frac{E}{2(1+\sigma)}.$$

In ideal fluids $\tau = \mu = 0$, there is no resistance to shearing. Then $k = \lambda$ and $\sigma = 0.5$. Within the framework of elasticity theory, fluids and gases behave identically, but the bulk modulus of fluids is significantly larger than that of gases. Their Poisson's ratio σ lies between -1 and 0.5; negative σ values are rare (compare Exercise 2.8). For rocks, σ is usually close to 0.25; $\sigma = 0.25$ means $\lambda = \mu$.

Exercise 2.7

Derive the formula for k. k is defined as the ratio $-\frac{p}{\Theta}$ in an experiment in which a body is under pressure p from all sides and has the relative volume change $\Theta < 0$. Describe the deformation and the stress tensor and then the stress-strain relation.

Exercise 2.8

Derive the formula for E and σ. E is defined as the ratio $\frac{p_{11}}{\epsilon_{11}}$ and σ is the ratio $-\frac{\epsilon_{22}}{\epsilon_{11}}$ in an experiment, in which a wire or rod is under extension force p_{11} in the 1-direction (ϵ_{11} = extension, $-\epsilon_{22}=$ perpendicular contraction, $\epsilon_{33}=$?, $p_{22}=$?, $p_{33}=$?). Proceed as in exercise 2.7. What is the meaning of $\sigma < 0$?

2.5 Equation of motion, boundary and initial conditions

2.5.1 Equation of motion

Using (2.17) in the equation of motion (2.12), which depends on p_{ij}, this equation only depends on the components of the displacement vector

$$\begin{aligned}\rho\frac{\partial^2 u_i}{\partial t^2} &= \tfrac{\partial}{\partial x_j}(\lambda\Theta\delta_{ij}+2\mu\epsilon_{ij})+f_i \\ &= \tfrac{\partial}{\partial x_i}(\lambda\Theta)+\tfrac{\partial}{\partial x_j}\left[\mu\left(\tfrac{\partial u_i}{\partial x_j}+\tfrac{\partial u_j}{\partial x_i}\right)\right]+f_i \quad .\end{aligned} \tag{2.20}$$

If λ and μ are independent of location (homogeneous medium) it follows that

$$\rho\frac{\partial^2 u_i}{\partial t^2}=\lambda\frac{\partial\Theta}{\partial x_i}+\mu\left[\frac{\partial^2 u_i}{\partial x_1^2}+\frac{\partial^2 u_i}{\partial x_2^2}+\frac{\partial^2 u_i}{\partial x_3^2}+\frac{\partial}{\partial x_i}\left(\frac{\partial u_1}{\partial x_1}+\frac{\partial u_2}{\partial x_2}+\frac{\partial u_3}{\partial x_3}\right)\right]+f_i$$

$$\rho\frac{\partial^2 u_i}{\partial t^2}=(\lambda+\mu)\frac{\partial\Theta}{\partial x_i}+\mu\nabla^2 u_i+f_i. \tag{2.21}$$

This is the *equation of motion for homogeneous media* in Cartesian coordinates.

In symbolic notation ($\Theta=\nabla\cdot\overrightarrow{u}$)

$$\rho\frac{\partial^2 u_i}{\partial t^2}=(\lambda+\mu)\nabla\,\nabla\cdot\overrightarrow{u}+\mu\nabla^2\overrightarrow{u}+\overrightarrow{f}. \tag{2.22}$$

This is only valid for Cartesian coordinates. $\nabla^2\overrightarrow{u}$ is the vector $(\nabla^2 u_1,\nabla^2 u_2,\nabla^2 u_3)$. In Cartesian coordinates

$$\nabla^2\overrightarrow{u}=\nabla\,\nabla\cdot\overrightarrow{u}-\nabla\times\,\nabla\times\overrightarrow{u}. \tag{2.23}$$

(Verify that in curved orthogonal coordinates (2.23) *defines* the vector $\nabla^2\overrightarrow{u}$, and it is not identical with the vector, which results from the application of ∇^2 on the components.) Inserting (2.23) in (2.22) gives

$$\rho \frac{\partial^2 \vec{u}}{\partial t^2} = (\lambda + 2\mu) \nabla \nabla \cdot \vec{u} - \mu \nabla \times \nabla \times \vec{u} + \vec{f}. \tag{2.24}$$

This form of the equation of motion is independent of the coordinate system. It is the starting point for the following section: according to section 2.3, $\vec{f}$ contains only the body forces which act in addition to those of the forces at rest.

2.5.2 Boundary conditions

On a surface in which at least one material parameter ρ, λ or μ is discontinuous, the stress vector, relative to the normal direction of this surface, is continuous. To show this, consider a small flat circular cylinder of thickness 2d which encloses the boundary between the two media. The sum of all forces acting on the cylinder (body forces in the interior and surface forces on its surface) has to be zero.

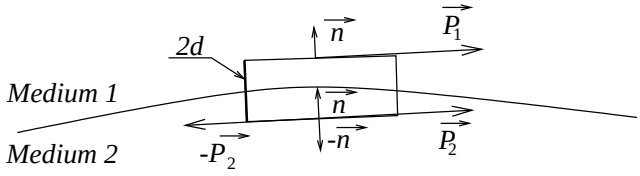

Fig. 2.14: Circular cylinder of thickness 2d enclosing the boundary between two media.

In the limit $d \to 0$, only the surface forces on the top and bottom surface Δf, have to be considered

$$\vec{P_1} \Delta f + (-\vec{P_2}) \Delta f = 0.$$

From this, it follows that $\vec{P_1} = \vec{P_2}$. This means that at boundaries *normal and tangential stress are continuous.*

For the displacement, it holds that at a solid-solid boundary, all components are continuous (no sliding possible). At a solid-liquid or liquid-liquid boundary only the normal displacement is continuous.

Example: A body consists of two half-spaces, separated by a plane at $z = 0$. The displacements are $u_x, u_y, u_z,$ and the stresses are $p_{xx}, p_{yy}, p_{zz}, p_{xy}, p_{xz}, p_{yz}$. The boundary conditions $z = 0$ for the different combinations of half-spaces are

$$
\begin{array}{lcl}
\text{solid} - \text{solid} & : & u_x, u_y, u_z, p_{xz}, p_{yz}, p_{zz} \text{ continuous} \\
\text{solid} - \text{fluid} & : & u_z, p_{zz} \text{ continuous}, p_{xz} = p_{yz} = 0 \\
\text{fluid} - \text{fluid} & : & u_z, p_{zz} \text{ continuous} \\
\text{solid} - \text{rigid} & : & u_x = u_y = u_z = 0 \\
\text{fluid} - \text{rigid} & : & u_z = 0 \\
\left.\begin{array}{lcl} \text{solid} - \text{vacuum} & : & p_{xz} = p_{yz} = p_{zz} = 0 \\ \text{fluid} - \text{vacuum} & : & p_{zz} = 0 \end{array}\right\} & & \text{free surface .}
\end{array}
$$

If at a surface with the normal vector n_i, the stress is not zero (stress vector P_i), the stress vector in the body has to acquire this boundary value

$$p_{ij}^{(r)} n_j = P_i. \tag{2.25}$$

$p_{ij}^{(r)}$ are the boundary values of the components of the stress tensor at the surface, and they can be calculated from (2.25).

Example: $P(t)$ on a plane surface. For the case of pressure

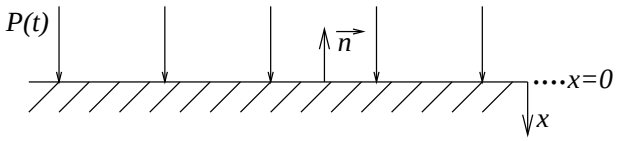

Fig. 2.15: Pressure on a plane surface.

$$
\begin{aligned}
\overrightarrow{n} &= (-1, 0, 0) = (n_1, n_2, n_3) \\
\overrightarrow{P} &= (P(t), 0, 0) = (P_1, P_2, P_3) \qquad .
\end{aligned}
$$

Equation (2.25) yields $-p_{i1}^{(r)} = P_i$ or

$$
\left.\begin{array}{l} p_{11} = p_{xx} = -P(t) \\ p_{12} = p_{xy} = 0 \\ p_{13} = p_{xz} = 0 \end{array}\right\} \quad \text{for } x = 0.
$$

Similarly, displacements can be prescribed on the surfaces of a body.

2.5.3 Initial conditions

The initial conditions prescribe the spatial distribution of certain parameters, in our case the displacement $u_i(x_1, x_2, x_3, t)$ and the particle velocity $\partial u_i/\partial t$ for $t = 0$

$$u_i(x_1, x_2, x_3, 0) = f_1(x_1, x_2, x_3), \qquad \frac{\partial u_i}{\partial t}(x_1, x_2, x_3, 0) = f_2(x_1, x_2, x_3).$$

The general wave propagation solution is an initial and a boundary problem, i.e., in addition to the equation of motion, the boundary and initial conditions have to be satisfied. Normally in seismological applications $f_1 = f_2 = 0$, and no special initial conditions have to be satisfied. The main problems are then to consider the boundary conditions.

2.6 Displacement potentials and wave types

2.6.1 Displacement potentials

A vector $\vec{u}$ can, in general, be described as

$$\vec{u} = \nabla\Phi + \nabla \times \vec{\Psi} \tag{2.26}$$

where Φ is a *scalar potential* and $\vec{\Psi}$ a *vector potential*. In our case, where $\vec{u}$ is a displacement field, both are called displacement potentials. (Do not confuse them with the *elastic* potential, i.e., the elastic deformation energy.)

Φ is called *compression potential* and $\vec{\Psi}$ *shear potential*. If the vector $\vec{u}$ is given, Φ and $\vec{\Psi}$ can be computed (compare exercise 2.9)

$$\begin{aligned} \Phi &= \frac{1}{4\pi} \int \frac{\vec{u} \cdot \vec{r}}{r^3} dV \\ \vec{\Psi} &= \frac{1}{4\pi} \int \frac{\vec{u} \times \vec{r}}{r^3} dV. \end{aligned} \tag{2.27}$$

Vector $\vec{r}$ (with absolute value r) points from the volume element dV to the point where Φ and $\vec{\Psi}$ are computed. The integration covers the whole volume. For $\vec{\Psi}$, there is the additional requirement that

$$\nabla \cdot \vec{\Psi} = 0. \tag{2.28}$$

$\vec{\Psi}$ has to be determined in Cartesian coordinates.

$\nabla\,\Phi$ in (2.26) is called *compressional part* of $\overrightarrow{u}$. It is free of rotation and curl. According to section 2.1.4, the volume elements suffer no rigid rotation, but only a deformation, which, in general, consists of a volume change and a shear component (in the sense of exercise 2.2; section 2.1). In the main axis system of the deformation tensor, only volume changes occur (compression or dilatation). The contribution $\nabla \times \overrightarrow{\Psi}$ in (2.26) is called *shear component.* It is free of divergence and source contributions; the volume elements suffer no volume change, but shear deformation and rigid rotation.

Similarly to (2.26), the body force $\overrightarrow{f}$ in (2.24) can be split into

$$\overrightarrow{f} = \nabla\,\varphi + \nabla \times \overrightarrow{\psi}. \tag{2.29}$$

Do not confuse the vector potentials $\overrightarrow{\Psi}$ and $\overrightarrow{\psi}$.

Using (2.26) and (2.29) in (2.24) gives

$$\rho\left[\nabla\frac{\partial^2\Phi}{\partial t^2} + \nabla \times \frac{\partial^2\overrightarrow{\Psi}}{\partial t^2}\right] = (\lambda+2\mu)\nabla\,\nabla^2\Phi - \mu\,\nabla\times\,\nabla\times\,\nabla\times\,\overrightarrow{\Psi} + \nabla\,\varphi + \nabla\times\,\overrightarrow{\psi}. \tag{2.30}$$

We try now to equate all the gradient terms and also, separately, the rotation terms of this equation. If the resulting differential equations can be solved, (2.30) and, therefore, (2.24) are satisfied. This leads to

$$\begin{aligned} \nabla\left[\rho\frac{\partial^2\Phi}{\partial t^2} - (\lambda+2\mu)\nabla^2\Phi - \varphi\right] &= 0 \\ \nabla\times\left[\rho\frac{\partial^2\overrightarrow{\Psi}}{\partial t^2} + \mu\,\nabla\times\,\nabla\times\,\overrightarrow{\Psi} - \overrightarrow{\psi}\right] &= 0. \end{aligned}$$

Since the content of the square brackets has to vanish

$$\begin{aligned} \nabla^2\Phi - \frac{1}{\alpha^2}\frac{\partial^2\Phi}{\partial t^2} &= -\frac{\varphi}{\lambda+2\mu} \qquad \alpha^2 = \frac{\lambda+2\mu}{\rho} \\ -\nabla\times\,\nabla\times\,\overrightarrow{\Psi} - \frac{1}{\beta^2}\frac{\partial^2\overrightarrow{\Psi}}{\partial t^2} &= -\frac{\overrightarrow{\psi}}{\mu} \qquad \beta^2 = \frac{\mu}{\rho}. \end{aligned} \tag{2.31}$$

The potentials φ and $\overrightarrow{\psi}$ have to be determined from $\overrightarrow{f}$ using (2.27). If no body forces act, $\varphi = 0$ and $\overrightarrow{\psi} = 0$. The equation for Φ is an inhomogeneous wave equation. In Cartesian coordinates the components of $\overrightarrow{\Psi}$ give also inhomogeneous wave equations due to (2.23) and (2.28). In other coordinates, the equations for the components of $\overrightarrow{\Psi}$ look different (compare exercise 2.10).

Both simplifications used are, as experience has shown, justified. The problem can, therefore, be solved either via (2.24) or (2.31). In more complicated cases, (2.31) is easier to solve. In this case, the boundary conditions for displacement and stress have to be expressed as those for Φ and $\vec{\Psi}$.

2.6.2 Wave types

The general discussion of the differential equations (2.31) shows that they have solutions which correspond to *waves* (for details, see section 3.1). Perturbations in the compressional part of the displacement vector propagate as *compressional waves* with the velocity $\alpha = ((\lambda + 2\mu)/\rho)^{1/2}$ through the medium. Perturbations in the shear part propagate as shear waves with the velocity $\beta = (\mu/\rho)^{1/2}$. Thus, we have found the two basic wave types, which can propagate in a solid medium. For rocks, it usually holds that $\lambda = \mu$. In this case, it follows that $\alpha/\beta = 3^{1/2}$. In liquid or gases, only compressional waves (*sound waves*) can propagate since $\mu = 0$.

Often compressional waves are called *longitudinal waves* and shear waves are called *transverse waves*. The displacement vector in a longitudinal wave is parallel to the propagation direction and perpendicular to it in a transverse wave. A compressional wave is, in general, primarily longitudinally polarised, and a shear wave is primarily transversely polarised. The identification is, therefore, not fully valid. There exist special cases in which a compressional wave is transversal and a shear wave is longitudinal (see section 3.5.1 and exercise 3.5 in chapter 3).

The seismological names for compressional and shear waves are *P-waves* and *S-waves*, respectively. This indicates that the P-wave is the first wave arriving at a station from an earthquake (P from primary), whereas the S-wave arrives later (S from secondary).

In a homogeneous medium, compressional waves and shear waves are *decoupled*, i.e., they propagate independently from each other. This no longer holds for inhomogeneous media in which λ, μ and/or ρ, and, therefore, α and β, vary from point to point. But in this case, usually two wave types propagate through the medium, and the travel times of their first onsets are determined by the velocity distribution of α and β, respectively. The faster of the two waves is no longer a pure compressional wave but contains a shear component. The slower wave is, correspondingly, not a pure shear wave but contains a compressional contribution. This becomes plausible if one approximates an inhomogeneous medium by piece-wise homogeneous media. Satisfying the boundary conditions at the interfaces between the homogeneous media usually requires, on *both* sides, the existence of compressional and shear waves. Details on this will be given in section 3.6.2. Compressional and shear waves which are decoupled in homogeneous sections of the medium, create reflected and refracted waves of the other type, respectively, at interfaces. This change in wave type occurs continuously in continuous media and is stronger the stronger the changes in α, β,

and/or ρ per wave length are. The theory for continuous inhomogeneous media is much more complicated then the theory for piece-wise homogeneous media. Media in which α, β and ρ depend only on *one* coordinate, e.g., depth, can, for many seismological applications, be approximated by layers of homogeneous media. For such configurations, effective methods for the use of computers exist.

Exercise 2.9

Show (2.27) by comparing (2.26) with the equation

$$\nabla^2 \vec{a} = \nabla \, \nabla \cdot \vec{a} - \nabla \times \, \nabla \times \vec{a}$$

and consider, that the Possion equation $\nabla^2 \vec{a} = \vec{u}$ has (in Cartesian coordinates) the solution

$$\vec{a} = -\frac{1}{4\pi} \int \vec{u} \frac{1}{r} dV.$$

Exercise 2.10

Write (2.26) in cylindrical coordinates (r, φ, z) under the condition that the medium is cylindrically symmetric, and the φ-component of $\vec{u}$ is zero ($\Psi_r = \Psi_z = 0$). What is the form of (2.31) for vanishing body forces?

Exercise 2.11

Show that in a liquid with constant density ρ, but variable compressional module k and pressure p, satisfies the wave equation $\nabla^2 p = \frac{1}{\alpha^2} \frac{\partial^2 p}{\partial t^2}$ with spatially varying sound velocity $\alpha = (k/\rho)^{1/2}$.

Hint: Derive from the equation of motion (2.12) without body forces, the equation $\rho \partial^2 \vec{u} / \partial t^2 = -\nabla p$ and apply then the divergence operation i.e. ($p = -k \, \nabla \cdot \vec{u}$).

Chapter 3

Body waves

3.1 Plane body waves

The most simple types of waves can be derived, if for an unbounded medium (full-space), solutions of the equation of motion are determined which depend only on *one* spatial coordinate. For example, we look for a solution of (2.21) or (2.24) in the form of $\vec{u} = (u_x(x,t), 0, 0)$, i.e., $\vec{u}$ points in x-direction and depends only on x and the time t. Alternatively, we look for a solution in the form of $\vec{u} = (0, u_y(x,t), 0)$, i.e., $\vec{u}$ points in y-direction and depends also only on x and t. In the first case, it follows from (2.21) for $f_i = 0$

$$\frac{\partial^2 u_x}{\partial x^2} = \frac{1}{\alpha^2}\frac{\partial^2 u_x}{\partial t^2}, \qquad \alpha^2 = \frac{\lambda + 2\mu}{\rho},$$

and in the second case,

$$\frac{\partial^2 u_y}{\partial x^2} = \frac{1}{\beta^2}\frac{\partial^2 u_y}{\partial t^2}, \qquad \beta^2 = \frac{\mu}{\rho}.$$

These are *one dimensional wave equations.* In the following, we consider the general form

$$\frac{\partial^2 u}{\partial x^2} = \frac{1}{c^2}\frac{\partial^2 u}{\partial t^2}. \tag{3.1}$$

The most general solution of this equation is

$$u(x,t) = F(x - ct) + G(x + ct), \tag{3.2}$$

where *F(x)* and *G(x)* are any twice differentiable functions (check that (3.2) solves (3.1)). Another form is

$$u(x,t) = F\left(t - \frac{x}{c}\right) + G\left(t + \frac{x}{c}\right). \tag{3.3}$$

The first and the second term in (3.2) and (3.3) have to be interpreted as waves propagating in the positive and negative x-direction, respectively. For example, the first term in (3.3) for $x = x_1$ can be written as

$$u(x_1,t) = F\left(t - \frac{x_1}{c}\right) = F_1(t).$$

For another distance $x_2 > x_1$

$$u(x_2,t) = F\left(t - \frac{x_2}{c}\right) = F\left(t - \frac{x_2 - x_1}{c} - \frac{x_1}{c}\right) = F_1\left(t - \frac{x_2 - x_1}{c}\right).$$

This means that for time t at distance x_2 the same effects occur as at distance x_1 at the earlier time $t - (x_2 - x_1)/c$. This corresponds to a wave which has travelled from x_1 to x_2 in the time $(x_2 - x_1)/c$. The *propagation velocity* is, therefore, c. The *wavefronts* of this wave, i.e., the surfaces between perturbed and unperturbed regions, are the planes $x = \text{const}$. Therefore, these are *plane* waves. If G(x) in (3.2) or G(t) in (3.3) are not zero, two plane waves propagate in opposite directions.

In the case of $u = u_x$, we have a longitudinal wave (polarisation *in* the direction of propagation); in case of $u = u_y$, we have a transverse wave (polarisation *perpendicular* to the direction of propagation).

Harmonic waves can be represented as

$$u(x,t) = A\,exp\left[i\omega(t - \frac{x}{c})\right] = A\,exp\left[i(\omega t - kx)\right]$$

with A= Amplitude (real or complex), ω= angular frequency $\nu = \omega/2\pi$= frequency, $T = 1/\nu$= period, $k = \omega/c$= wavenumber and $\Lambda = 2\pi/k$= wave length. Between c, Λ and ν the well-known relation $c = \Lambda\nu$ holds. The use of the complex exponential function in the description of plane harmonic waves is more convenient than the use of the real sine and cosine functions. In the following, only the exponential function will be used.

3.2 The initial value problem for plane waves

We look for the solution of the one-dimensional wave equation (3.1) which satisfies the initial conditions

$u(x,0) = f(x)$ for displacement and

$$\frac{\partial u}{\partial t}(x,0) = g(x) \text{ for particle velocity.}$$

This is an initial value problem of a linear *ordinary* differential equation, e.g., the problem to determine the movement of a pendulum, if initial displacement and initial velocity are given. We start from (3.2). For $t=0$, it also holds that

$$F(x) + G(x) = f(x) \tag{3.4}$$
$$-cF'(x) + cG'(x) = g(x). \tag{3.5}$$

Integrating (3.5) with respect to x, gives

$$F(x) - G(x) = -\frac{1}{c}\int_{-\infty}^{x} g(\xi)d\xi. \tag{3.6}$$

From the addition of (3.4) and (3.6), it follows that

$$F(x) = \frac{1}{2}\left\{f(x) - \frac{1}{c}\int_{-\infty}^{x} g(\xi)d\xi\right\},$$

and from the subtraction of these two equations that

$$G(x) = \frac{1}{2}\left\{f(x) + \frac{1}{c}\int_{-\infty}^{x} g(\xi)d\xi\right\}.$$

From this, it follows that

$$u(x,t) = \frac{1}{2}\left\{f(x-ct) + f(x+ct)\right\} + \frac{1}{2c}\int_{x-ct}^{x+ct} g(\xi)d\xi.$$

This solution satisfies the wave equation and the initial conditions (check). We will discuss *two special cases.*

3.2.1 Case 1

$g(x) = 0$, i.e., the initial velocity is zero. Then

$$u(x,t) = \frac{1}{2}\left\{f(x-ct) + f(x+ct)\right\}.$$

Two snap shots (Fig. 3.1) for t=0 and for t>0, illustrate this result.

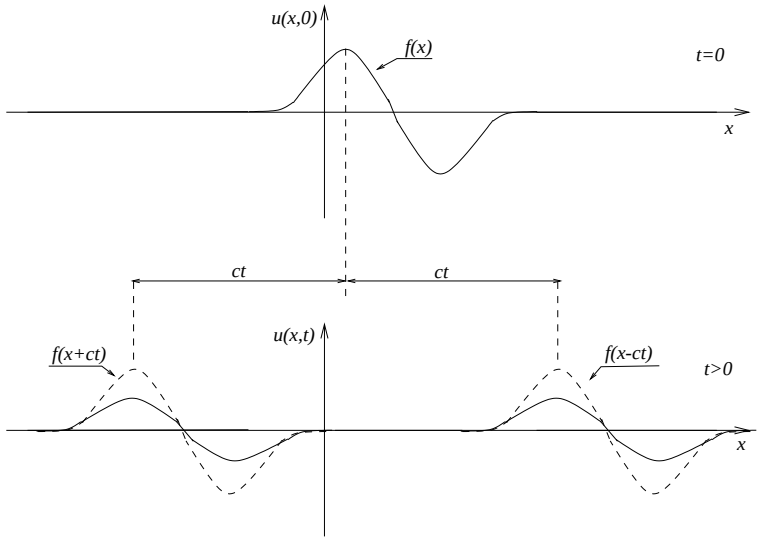

Fig. 3.1: Snap shots of two plane waves.

Two plane waves propagate from the point of excitation in both directions with the velocity c. A practical example is a stretched rope with the form $f(x)$ for $t=0$.

3.2.2 Case 2

$f(x) = 0$, i.e., the initial displacement is zero. Furthermore, we assume $g(x) = \overline{V_0}\delta(x)$. $\delta(x)$ is *Dirac's delta function* (see appendix A.3). $g(x)$ corresponds to an "impulse" at $x = 0$. $\overline{V_0}$ has the dimension of velocity times length. Then

$$u(x,t) = \frac{\overline{V_0}}{2c} \int_{x-ct}^{x+ct} \delta(\xi) d\xi.$$

The sketch (Fig. 3.2) shows the value of the integrand and the integration interval for a fixed point in time $t > 0$ and for a location $x > 0$.

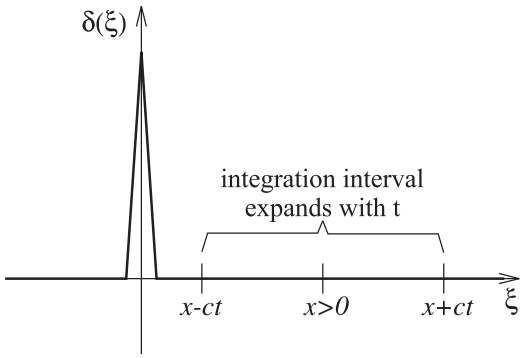

Fig. 3.2: Value of the integrand and the integration interval of u(x,t).

Only when the integration interval includes the point $\xi = 0$, does the integral become non-zero. Then it always has the value of 1

$$u(x,t) = \begin{cases} \frac{\overline{V_0}}{2c} H(t - \frac{x}{c}) & \text{for x}>0 \\ \frac{\overline{V_0}}{2c} H(t + \frac{x}{c}) & \text{for x}<0 \end{cases}$$

$H(t)$ is the *Heaviside step function*, $H(t) = 0$ for $t < 0$, $H(t) = 1$ for $t \geq 0$.

The displacement jumps at $t = |x|/c$ from zero to the value $\overline{V_0}/2c$.

3.3 Simple boundary value problems for plane waves

The simplest boundary value problem is to determine the displacement within a half-space for a time dependent pressure $P(t)$ at the surface $x = 0$ of this half-space. Since the displacement $\vec{u}$ only has an x-component, u_x and since x is the only explicit spatial coordinate, the one-dimensional wave equation (3.1) for a plane compressional wave is applicable

$$\frac{\partial^2 u_x}{\partial x^2} = \frac{1}{\alpha^2} \frac{\partial^2 u_x}{\partial t^2}.$$

The solution for the case considered here is

$$u_x(x,t) = F\left(t - \frac{x}{\alpha}\right),$$

since a wave can only propagate in $+x$-direction. Function $F(t)$ has to be determined from the boundary condition that the stress vector adapts without jump to the imposed stress vector at the free surface $x = 0$ (compare (2.25) and in section 2.5.2)

$$p_{xx} = -P(t) \text{ and } p_{xy} = p_{xz} = 0 \text{ for } x = 0.$$

The stress-strain relation (2.17) gives first, that p_{xy} and p_{xz} are zero everywhere in the medium, and second that

$$p_{xx} = (\lambda + 2\mu)\frac{\partial u_x}{\partial x} = -\frac{\lambda + 2\mu}{\alpha}F'\left(t - \frac{x}{\alpha}\right) = -\rho\alpha F'\left(t - \frac{x}{\alpha}\right).$$

For $x = 0$, it follows that

$$-\rho\alpha F'(t) = -P(t)$$

and after integration

$$F(t) = \frac{1}{\rho\alpha}\int_{-\infty}^{t} P(\tau)d\tau = \frac{1}{\rho\alpha}\int_{o}^{t} P(\tau)d\tau.$$

For this, we assumed that $P(t) = 0$ for $t < 0$. Then, the displacement can be written as

$$u(x,t) = \frac{1}{\rho\alpha}\int_{0}^{t-x/\alpha} P(\tau)d\tau.$$

The displacement is proportional to the time integral of the pressure on the surface of the half-space. If a short impulse $P(t) = \overline{P_0}\delta(t)$ acts, it follows that,

$$u_x(x,t) = \frac{\overline{P_0}}{\rho\alpha}H\left(t - \frac{x}{\alpha}\right).$$

$\overline{P_0}$ has the dimension pressure times time (see also appendix A, section A.3.1). At the time $t = x/\alpha$, all points in the half-space are displaced instantly by $\overline{P}_0/\rho\alpha$ in $+x$-direction and remain fixed in this position. For $\overline{P}_0 = 1$ bar sec $= 9.81$ Nsec/cm$^2 \approx 10^6$ dyn sec/cm^2, $\rho = 3\,$g/cm^3 and $\alpha = 6\,$km/sec the displacement is approximately $0.5\,$cm.

This boundary value problem is simple enough so that it could be solved directly with the equation of motion (2.21) or (2.24). One could have also worked with

displacement potentials Φ and $\vec{\Psi}$ and their differential equations (2.31) (show).

Exercise 3.1

The tangential stress $T(t)$ acts on the surface of a half-space. What is the displacement in the half-space? Application: The tangential stress on the rupture surface of earthquakes is $50\,\mathrm{bar} = 50 \cdot 10^6\,\mathrm{dyn/cm^2}$ (stress drop). What is the particle velocity (on the rupture surface) for ($\rho = 3\,\mathrm{g/cm^3}$, $\beta = 3.5\,\mathrm{km/sec}$)?

Exercise 3.2

An elastic layer of thickness H overlies a rigid half-space. Pressure $P(t)$ acts on the top of the elastic layer. What is the movement in the layer? Examine the case $P(t) = \overline{P}_0\delta(t)$.

Exercise 3.3

Solve the static problem of exercise 3.2 (constant pressure P_1 on the surface).

3.4 Spherical waves from explosion point sources

In the previous sections, we considered infinitely extended waves. They are an idealisation, because they cannot be produced in reality since they require infinitely extended sources. The most simple wave type from sources with finite extension are *spherical waves*, i.e., waves which originate at a point (*point source*) and propagate in the full-space. Their wavefronts are spheres.

In the most simple case, the displacement vector is *radially* oriented and also *radially symmetric* relative to the point source, i.e., the radial displacement on a sphere around the point source is the same everywhere. If a spherical explosion in a homogeneous medium far from interfaces is triggered, the resulting displacement has these two properties. Therefore, we call these *explosions point sources*. The results derived with the linear elasticity theory can only be applied to spherical waves from explosions in the distance range in which the prerequisites of the theory (infinitesimal deformation, linear stress-strain relation) are satisfied. In the *plastic zone*, the *shattered zone* and the *non-linear zone* (this is a rough classification with increasing distance from the centre of the explosion) these requirements are not met. For a nuclear explosion of 1 Megaton TNT equivalent (approximately mb = 6.5 to 7.0), the shattered zone is roughly 1 to 2 km wide.

We plan to solve the following boundary problem: given the radial displacement at distance $r = r_1$ from the point source $U(r_1, t) = U_1(t)$, we want to find $U(r, t)$ for $r > r_1$.

We start from the equation of motion (2.24) with $\vec{f} = 0$. This is how the problem is solved in appendix A (appendix A.2.2) using the Laplace transform.

Here, more simply, the displacement potential from section 2.6 will be used. In this case, the shear potential is zero, since a radially symmetric radial vector can be derived solely from the compressional potential

$$\Phi(r,t) = \int^r U(r',t)dr'.$$

In spherical coordinates (r, ϑ, λ), it holds that

$$\nabla\Phi = \left(\tfrac{\partial\Phi}{\partial r}, \tfrac{1}{r}\tfrac{\partial\Phi}{\partial\vartheta}, \tfrac{1}{r\sin\vartheta}\tfrac{\partial\Phi}{\partial\lambda}\right) = (U(r,t), 0, 0).$$

For Φ, the wave equation with $\varphi = 0$ can by written according to (2.31) as

$$\nabla^2\Phi = \frac{\partial^2\Phi}{\partial r^2} + \frac{2}{r}\frac{\partial\Phi}{\partial r} = \frac{1}{r}\frac{\partial^2(r\Phi)}{\partial r^2} = \frac{1}{\alpha^2}\frac{\partial^2\Phi}{\partial t^2}$$

$$\frac{\partial^2(r\Phi)}{\partial r^2} = \frac{1}{\alpha^2}\frac{\partial^2(r\Phi)}{\partial t^2}. \tag{3.7}$$

In the case of radial symmetry, the wave equation can be reduced to the form of a one-dimensional wave equation for Cartesian coordinates for the function $r\Phi$,

$$\frac{\partial^2 u}{\partial x^2} = \frac{1}{\alpha^2}\frac{\partial^2 u}{\partial t^2},$$

.

The most general solution for (3.7) is ,therefore,

$$\Phi(r,t) = \frac{1}{r}\left\{F(t - \frac{r}{\alpha}) + G(t + \frac{r}{\alpha})\right\}.$$

This describes the superposition of two compressional waves, one propagating outward from the point source and the other propagating inwards towards the point source. In realistic problems, the second term is always zero and

$$\Phi(r,t) = \frac{1}{r}F\left(t - \frac{r}{\alpha}\right). \tag{3.8}$$

Function $F(t)$ is often called the *excitation function* or reduced displacement potential. The wavefronts are the spheres r =const. The potential as a function of time has the same form everywhere, and the amplitudes decrease with distance as $1/r$. The radial displacement of the spherical wave consists of two contributions with different dependence on r

$$U(r,t) = \frac{\partial \Phi}{\partial r} = -\frac{1}{r^2} F\left(t - \frac{r}{\alpha}\right) - \frac{1}{r\alpha} F'\left(t - \frac{r}{\alpha}\right). \tag{3.9}$$

These two terms, therefore, change their form with increasing distance. Generally, this holds for the displacement of waves from a point source. The first term in (3.9) is called *near-field term* since it dominates for sufficiently small r. The second term is the *far-field term* and describes with sufficient accuracy the displacement for distances from the point source which are larger then several wave lengths (show this for $F(t) = e^{i\omega t}$). That means there the displacement reduces proportional to $1/r$.

From the boundary condition $r = r_1$, it follows that

$$-\frac{1}{r_1\alpha} F'\left(t - \frac{r_1}{\alpha}\right) - \frac{1}{r_1^2} F\left(t - \frac{r_1}{\alpha}\right) = U_1(t).$$

We choose the origin time so that $U_1(t)$ only begins to be non-zero for $t = r_1/\alpha$. It, therefore, appears as if the wave starts at time $t = 0$ at the point source ($r = 0$). If $\overline{U}_1\left(t - \frac{r_1}{\alpha}\right) = U_1(t)$, it holds that $\overline{U}_1(t)$ is already non-zero for $t > 0$. With $\tau = t - \frac{r_1}{\alpha}$, it follows that

$$\frac{1}{r_1\alpha} F'(\tau) + \frac{1}{r_1^2} F(\tau) = -\overline{U}_1(\tau). \tag{3.10}$$

The solution of (3.10) can be found with the Laplace transform (see section A.2.1.1 of appendix A).

Since the criterion (A.16) of appendix A is satisfied for all physically realistic displacements $\overline{U}_1(\tau)$, the initial value $F(+0)$ of $F(\tau)$ is zero. Therefore, transformation of (3.10)with $F(\tau) \longleftrightarrow f(s)$ and $\overline{U}_1(\tau) \longleftrightarrow \overline{u}_1(s)$ gives

$$\begin{aligned} \frac{1}{r_1}\left(\frac{s}{\alpha} + \frac{1}{r_1}\right) f(s) &= -\overline{u}_1(s) \\ f(s) &= -r_1\alpha \frac{1}{s + \frac{\alpha}{r_1}} \overline{u}_1(s) \qquad . \end{aligned} \tag{3.11}$$

With $\left(s + \frac{\alpha}{r_1}\right)^{-1} \longleftrightarrow e^{-\frac{\alpha}{r_1}\tau}$ (see appendix A, section A.1.4), and using convolution (see appendix A, equation A.7), the inverse transformation of (3.11) reads as

$$F(\tau) = -r_1\alpha \int_0^\tau \overline{U}_1(\vartheta) e^{-\frac{\alpha}{r_1}(\tau - \vartheta)} d\vartheta.$$

From this, it follows

$$F'(\tau) = -r_1\alpha\overline{U}_1(\tau) + \alpha^2 \int_0^\tau \overline{U}_1(\vartheta) e^{-\frac{\alpha}{r_1}(\tau-\vartheta)} d\vartheta.$$

The radial displacement for $r > r_1$ then can be written using (3.9) as

$$U(r,t) = \frac{r_1}{r}\left\{\overline{U}_1(\tau) + \alpha\left(\frac{1}{r} - \frac{1}{r_1}\right)\int_0^\tau \overline{U}_1(\vartheta) e^{-\frac{\alpha}{r_1}(\tau-\vartheta)} d\vartheta\right\} \tag{3.12}$$

with the *retarded time* $\tau = t - \frac{r}{\alpha}$. This solves the boundary problem.

Applications

1. $U_1(t) = \overline{U}_0\delta\left(t - \frac{r_1}{\alpha}\right)$, i.e., $\overline{U}_1(t) = \overline{U}_0\delta(t)$.

   The dimension of $\overline{U}_0$ is time times length. Equation (3.12) is valid also in this case (see appendix A)

   $$U(r,t) = \frac{r_1}{r}\overline{U}_0\left\{\delta(\tau) + \alpha\left(\frac{1}{r} - \frac{1}{r_1}\right)e^{-\frac{\alpha}{r_1}\tau} H(\tau)\right\}.$$

   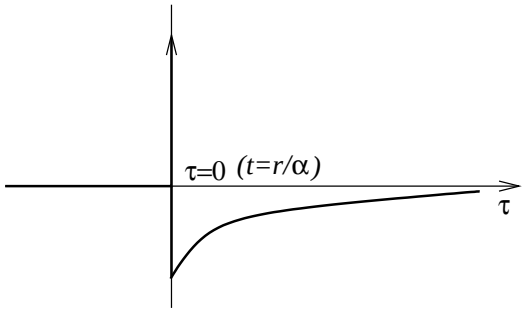

   Fig. 3.3: U(r,t) as a function of time.

2. $U_1(t) = U_0 H\left(t - \frac{r_1}{\alpha}\right)$, i.e. $\overline{U}_1(t) = U_0 H(t)$.

   The dimension of U_0 is length. From (3.12), it follows

   $$\begin{aligned} U(r,t) &= \frac{r_1}{r}U_0\left\{H(\tau) + \alpha\left(\frac{1}{r} - \frac{1}{r_1}\right)e^{-\frac{\alpha}{r_1}\tau}\left[\frac{r_1}{\alpha}e^{\frac{\alpha}{r_1}\vartheta}\right]_{\vartheta=0}^{\vartheta=\tau} H(\tau)\right\} \\ &= \frac{r_1}{r}U_0 H(\tau)\left\{1 + \left(\frac{r_1}{r} - 1\right)\left(1 - e^{-\frac{\alpha}{r_1}\tau}\right)\right\} \\ &= \frac{r_1}{r}U_0 H(\tau)\left\{\frac{r_1}{r} + \left(1 - \frac{r_1}{r}\right)e^{-\frac{\alpha}{r_1}\tau}\right\}. \end{aligned}$$

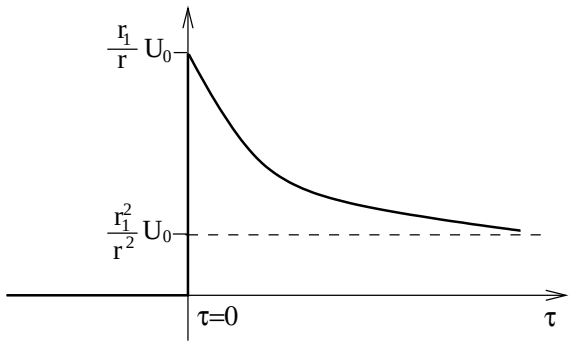

Fig. 3.4: U(r,t) as a function of time.

Exercise 3.4

Pressure $P(t)$ $\left(P(t) = 0 \,\text{for}\, t < \frac{r_1}{\alpha}\right)$ acts in a spherical cavity with radius r_1. What is the differential equation for the excitation function $F(t)$ (analogue to 3.10)? In the case of radial symmetry, the radial stress p_{rr} is connected to the radial displacement U as (show)

$$p_{rr} = (\lambda + 2\mu)\frac{\partial U}{\partial r} + 2\lambda\frac{U}{r}.$$

Which frequencies are preferably radiated (eigenvibrations of the cavity)? This can be derived / seen from the differential equation without solving it (compare to the differential equation of the mechanical oscillator, see appendix A.2.1.1). Solve the differential equation of $P(t) = \overline{P}_0\delta(t - r_1/\alpha)$.

3.5 Spherical waves from single force and dipole point sources

3.5.1 Single force point source

A single force in the centre of a Cartesian coordinate system acting in z-direction with a force-time law $K(t)$ has the force density (compare appendix A.3.3)

$$\overrightarrow{f} = (0, 0, \delta(x)\,\delta(y)\,\delta(z)\,K(t))\,.$$

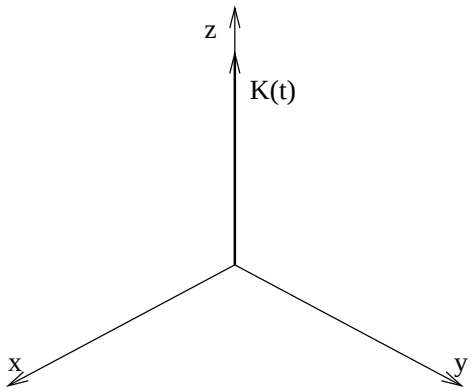

Fig. 3.5: Cartesian coordinate system with force-time law $K(t)$.

The separation $\overrightarrow{f} = \nabla\varphi + \nabla \times \overrightarrow{\psi}$ is possible with the help of (2.27)

$$\begin{aligned} \varphi(x,y,z,t) &= \frac{1}{4\pi}\iiint_{-\infty}^{+\infty} \frac{1}{r'^3}(z-\zeta)\delta(\xi)\delta(\eta)\delta(\zeta)K(t)d\xi d\eta d\zeta \\ &= \frac{K(t)z}{4\pi r^3}, \qquad r^2 = x^2+y^2+z^2 \end{aligned} \tag{3.13}$$

$$\begin{aligned} \overrightarrow{\psi}(x,y,z,t) &= \frac{1}{4\pi}\iiint_{-\infty}^{+\infty} \frac{1}{r^3}\{-(y-\eta), x-\xi, 0\}\,\delta(\xi)\delta(\eta)\delta(\zeta)K(t)d\xi d\eta d\zeta \\ &= \frac{K(t)}{4\pi r^3}(-y, x, 0). \end{aligned} \tag{3.14}$$

If (3.13) and (3.14) are used in the differential equation (2.31) of the displacement potentials, it follows that for the shear potential $\overrightarrow{\Psi} = (\Psi_x, \Psi_y, \Psi_z) \quad \Psi_z = 0$ and that for Ψ_x and Ψ_y, due to (2.23) and (2.28), the following wave equations hold; the same is true for the compression potential Φ

$$\begin{aligned} \nabla^2\Phi - \frac{1}{\alpha^2}\frac{\partial^2\varphi}{\partial t^2} &= -\frac{K(t)z}{4\pi\rho\alpha^2 r^3} \\ \nabla^2\Psi_x - \frac{1}{\beta^2}\frac{\partial^2\Psi_x}{\partial t^2} &= \frac{K(t)y}{4\pi\rho\beta^2 r^3} \\ \nabla^2\Psi_y - \frac{1}{\beta^2}\frac{\partial^2\Psi_y}{\partial t^2} &= -\frac{K(t)x}{4\pi\rho\beta^2 r^3}. \end{aligned}$$

The solution of the inhomogeneous wave equation

$$\nabla^2 a - \frac{1}{c^2}\frac{\partial^2 a}{\partial t^2} = f(x,y,z,t)$$

can for vanishing initial conditions, be written as

$$a(x,y,z,t) = -\frac{1}{4\pi}\iiint_{-\infty}^{+\infty}\frac{1}{r'}f\left(\xi,\eta,\zeta,t-\frac{r'}{c}\right)d\xi d\eta d\zeta \qquad (3.15)$$

with

$$r'^2 = (x-\xi)^2 + (y-\eta)^2 + (z-\zeta)^2.$$

Equation (3.15) is *Kirchhoff's Equation* for an infinite medium. It is the analogue to the well-known Poisson's differential equation which is also a volume integral over the perturbation function (compare exercise 2.9). Equation (3.15) can also be computed in non-Cartesian coordinates, something we now use.

Application of the wave equation for Φ

We introduce the spherical coordinates (r', ϑ, λ) relative to point P. λ is defined, see sketch, via an additional Cartesian coordinate system $(\overline{x}, \overline{y}, \overline{z})$.

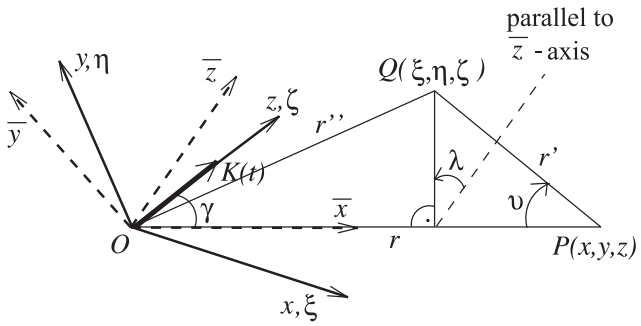

Fig. 3.6: Additional Cartesian coordinate system $(\overline{x}, \overline{y}, \overline{z})$.

The $\overline{x}$-axis of of this coordinate system is identical to the line OP. The $\overline{z}$-axis is in the plane defined by the $zand\zeta$-axis and the line OP. Then the z,ζ-axis has then in the $\overline{x}-\overline{y}-\overline{z}$-system the direction of the unit vector

$$\overrightarrow{n} = (\cos\gamma, 0, \sin\gamma) = \left\{\frac{z}{r}, 0, \left(1-\frac{z^2}{r^2}\right)^{\frac{1}{2}}\right\}.$$

Vector $\overrightarrow{r''}$ from O to Q can be written in the same system as

$$\overrightarrow{r''} = (r - r'\cos\vartheta, r'\sin\vartheta\sin\lambda, r'\sin\vartheta\cos\lambda).$$

These two vectors are needed later. Equation (3.15) can for Φ then be written as

$$\Phi(x,y,z,t) = \frac{1}{16\pi^2\rho\alpha^2}\int_0^\infty\int_0^\pi\int_0^{2\pi}\frac{\zeta}{r''^3}\cdot\frac{K\left(t-\frac{r'}{\alpha}\right)}{r'}\cdot r'^2\sin\vartheta\,d\lambda\,d\vartheta\,dr'.$$

We still must express ζ and r'' in terms of r', ϑ and λ

$$\begin{aligned}\xi &= \overrightarrow{r''}\cdot\overrightarrow{n} = \frac{z}{r}(r - r'\cos\vartheta) + \left(1-\frac{z^2}{r^2}\right)^{\frac{1}{2}} r'\sin\vartheta\cos\lambda\\ r''^2 &= r^2 + r'^2 - 2rr'\cos\vartheta \qquad \text{(rule of cosine)}.\end{aligned}$$

This gives

$$\Phi(x,y,z,t) = \frac{1}{16\pi^2\rho\alpha^2}\int_0^\infty\int_0^\pi\int_0^{2\pi}\frac{z\left(1-\frac{r'}{r}\cos\vartheta\right)+r'\left(1-\frac{z^2}{r^2}\right)^{\frac{1}{2}}\sin\vartheta\cos\lambda}{r^3\left(1+\frac{r'^2}{r^2}-2\frac{r'}{r}\cos\vartheta\right)^{\frac{3}{2}}}$$
$$\cdot K\left(t-\frac{r'}{\alpha}\right)\cdot r'\sin\vartheta\,d\lambda\,d\vartheta\,dr'.$$

The part of the integrand with $\cos\lambda$ does not contribute to the integration over λ. The other part has only to be multiplied by 2π. With $a = r/r'$ and

$$\begin{aligned}\int_0^\pi\frac{(1-a\cos\vartheta)\sin\vartheta}{(1+a^2-2a\cos\vartheta)^{\frac{3}{2}}}d\vartheta &= \int_{(1-a)^2}^{(1+a)^2}\frac{1+\frac{1}{2}(u-1-a^2)}{2au^{\frac{3}{2}}}du\\ &= \frac{1}{4a}\int_{(1-a)^2}^{(1+a)^2}\left(\frac{1}{u^{\frac{1}{2}}}+\frac{1-a^2}{u^{\frac{3}{2}}}\right)du\\ &= \frac{1}{4a}\left\{2u^{\frac{1}{2}}+2(a^2-1)u^{-\frac{1}{2}}\right\}_{(1-a)^2}^{(1+a)^2}\\ &= \frac{1}{2a}\{1+a-|1-a|\}\\ &\quad +\frac{1}{2a}\left\{(a+1)(a-1)\cdot\left(\frac{1}{1+a}-\frac{1}{1-a}\right)\right\}\\ &= \begin{cases}2 & for \quad 0<a<1\\ 0 & for \quad a>1\end{cases}\end{aligned}$$

$$\begin{aligned}u &= 1+a^2-2a\cos\vartheta\\ du &= 2a\sin\vartheta d\vartheta\end{aligned}$$

it follows that

$$\begin{aligned}\Phi(x,y,z,t) &= \frac{z}{4\pi\rho\alpha^2 r^3}\int_0^r r' K\left(t-\frac{r'}{\alpha}\right)dr' \\ &= \frac{z}{4\pi\rho r^3}\int_0^{\frac{r}{\alpha}} K(t-\tau)\tau d\tau.\end{aligned}$$

The wave equations for Ψ_x and Ψ_y are solved in a similar fashion. Therefore, it is possible to write the potentials of the single force point source as

$$\left.\begin{aligned}\Phi(x,y,z,t) &= \tfrac{z}{4\pi\rho r^3}\textstyle\int_0^{\frac{r}{\alpha}} K(t-\tau)\tau d\tau \\ \Psi_x(x,y,z,t) &= -\tfrac{y}{4\pi\rho r^3}\textstyle\int_0^{\frac{r}{\beta}} K(t-\tau)\tau d\tau \\ \Psi_y(x,y,z,t) &= \tfrac{x}{4\pi\rho r^3}\textstyle\int_0^{\frac{r}{\beta}} K(t-\tau)\tau d\tau \\ \Psi_z(x,y,z,t) &= 0 \\ with & \\ r^2 &= x^2+y^2+z^2.\end{aligned}\right\} \qquad (3.16)$$

Before we derive the displacements, we change to spherical coordinates (r,ϑ,λ) relative to the single force point source

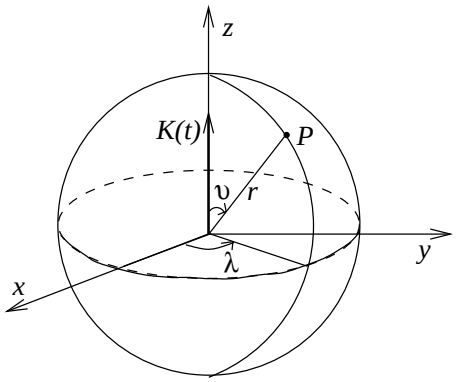

Fig. 3.7: Spherical coordinates (r,ϑ,λ).

$$\begin{aligned} x &= r\sin\vartheta\cos\lambda \\ y &= r\sin\vartheta\sin\lambda \\ z &= r\cos\vartheta. \end{aligned}$$

In spherical coordinates, the shear potential has no r- and ϑ-component (show), and for the λ-component it holds that

$$\Psi_\lambda = -\Psi_x \sin\lambda + \Psi_y \cos\lambda.$$

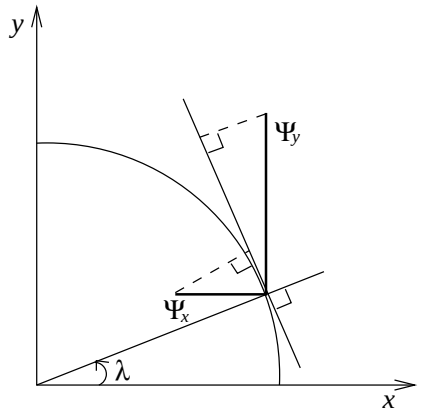

Fig. 3.8: x-y-plane of Fig. 3.7.

This gives

$$\left.\begin{aligned} \Phi(r,\vartheta,t) &= \tfrac{\cos\vartheta}{4\pi\rho r^2}\int_0^{\frac{r}{\alpha}} K(t-\tau)\tau d\tau \\ \Psi_\lambda(r,\vartheta,t) &= \tfrac{\sin\vartheta}{4\pi\rho r^2}\int_0^{\frac{r}{\beta}} K(t-\tau)\tau d\tau. \end{aligned}\right\} \tag{3.17}$$

This equation does not depend on λ. The *displacement vector* $\overrightarrow{u} = \nabla\Phi + \nabla\times\overrightarrow{\Psi}$ can be written in spherical coordinates (show) as

$$\left.\begin{aligned} u_r &= \tfrac{\partial\Phi}{\partial r} + \tfrac{1}{r\sin\vartheta}\tfrac{\partial}{\partial\vartheta}(\sin\vartheta\Psi_\lambda) \\ u_\vartheta &= \tfrac{1}{r}\tfrac{\partial\Phi}{\partial\vartheta} - \tfrac{1}{r}\tfrac{\partial}{\partial r}(r\Psi_\lambda) \\ u_\lambda &= 0. \end{aligned}\right\} \tag{3.18}$$

This shows that the P-wave following from Φ is not purely longitudinal, but it contains a transverse component (in u_ϑ). Similarly, the S-wave following from Ψ_λ is not purely transverse since u_r contains a shear component. The first term in u_ϑ and the second in u_r are *near field terms* (compare exercise 3.5). Here we compute only the *far-field terms* of u_r and u_ϑ (*only* differentiation of the integrals in(3.17))

$$\left.\begin{aligned} u_r &\simeq \frac{\cos\vartheta}{4\pi\rho\alpha^2 r} K\left(t-\frac{r}{\alpha}\right) \qquad \text{(longitudinal } P-\text{wave)} \\ u_\vartheta &\simeq \frac{-\sin\vartheta}{4\pi\rho\beta^2 r} K\left(t-\frac{r}{\beta}\right) \qquad \text{(transversal } S-\text{wave).} \end{aligned}\right\} \tag{3.19}$$

The far-field displacements have, therefore, the form of the force $K(t)$ decreasing with $1/r$. The single force point source has directionally dependent radiation, and the *far-field radiation characteristics* are shown in Fig. 3.9.

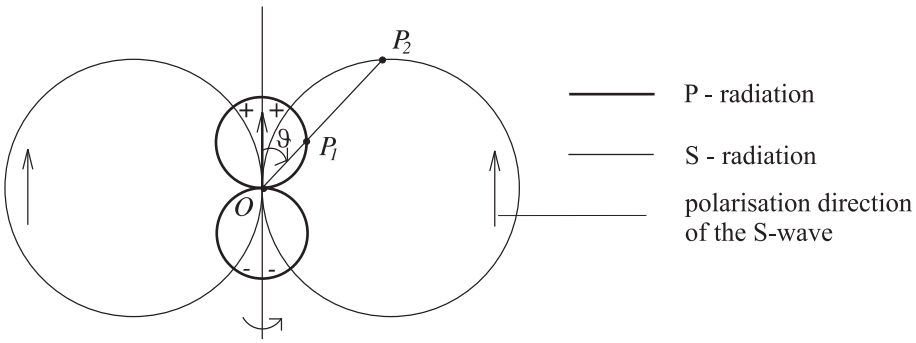

Fig. 3.9: Far field radiation characteristics of single force point source.

The radiation characteristics (P- and S-waves) are each two circles. Those for the S-waves have a radius which is α^2/β^2 larger then those of the P-waves. If the *radiation angle* ϑ is varied for fixed r, the displacements u_r are proportional to the distance $\overline{OP}_1$, and the displacements u_ϑ are proportional to the distance $\overline{OP}_2$. The sign of the displacement u_r changes in transition from the first P-radiation circle to the second. The full 3-D radiation characteristics follows from that shown in Fig. 3.9 by rotation around the direction of the force. Within the framework of the far-field equations (3.19), no S-wave is radiated in the direction of the force, and perpendicular to it, no P-wave is radiated (but compare exercise 3.5).

The practical use of the single force point source, acting perpendicular on the free surface, is that it is a good model for the effect of a *drop weight*, excitation by *vibro-seis* and often also for *explosions* detonated close to the surface. A complete solution requires the consideration of the effects of the free surface, but that is significantly more complicated. Furthermore, the differences to the

full-space models for all P-waves and for S-waves, for radiation angles smaller then 30 to 40 degrees, are small, respectively.

Exercise 3.5

Compute the complete displacement (3.18) using (3.17) and examine in particular, the directions $\vartheta = 0$ and $\vartheta = 90^0$. Which polarisation does the displacement vector have, and at which times are arrivals to be expected? Compute for $K(t) = K_0 H(t)$ the static displacement ($t > r/\beta$).

3.5.2 Dipole point sources

A force dipole can be constructed from two opposing single forces which are acting on two neighbouring points. Fig. 3.10 shows, on the left, a *dipole with moment* for which the line connecting the forces is perpendicular to the direction of the force. The connecting line for a "*dipole without moment*" points in the direction of the force.

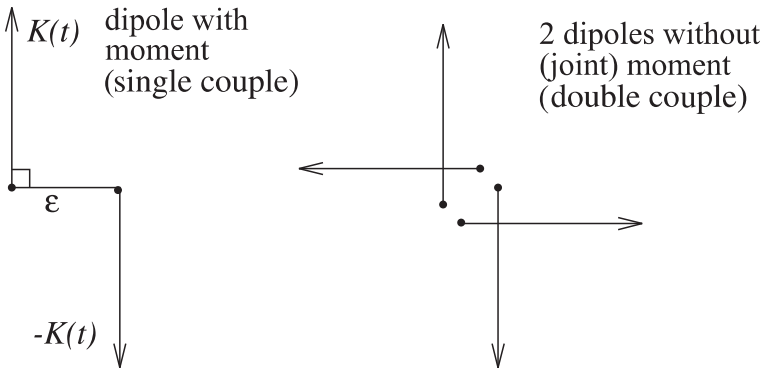

Fig. 3.10: Single couple and double couple constructed from single forces.

Two dipoles with moment for which the sum over the moments is zero (right in Fig. 3.10), are a good model for many earthquake sources, i.e., in the case where the spatial radiation of earthquake waves of sufficiently large wave length is similar to that of a double couple model. The actual processes acting in the earthquake source are naturally not four single forces. Usually, the rock breaks along a surface if the shear strength is exceeded by the accumulation of shear stress (*shear rupture*). Another possibility is that the shear stress exceeds the static friction on a pre-existing rupture surface. Source models from single forces and dipoles are only *equivalent point sources.*

In the following, we derive the far-field displacement of the single couple model and give the results for the double couple model. We start from the single couple (with $x_0 \neq 0$) in Fig. 3.11 and compute first from (3.19) the P-wave

displacement of force $K(t)$ with *Cartesian* components $\cos\vartheta = z/r, r^2 = (x - x_0)^2 + y^2 + z^2$

$$\left.\begin{matrix} u_x \\ u_y \\ u_z \end{matrix}\right\} = \frac{z}{4\pi\rho\alpha^2 r^2} K\left(t - \frac{r}{\alpha}\right) \cdot \left\{\begin{matrix} (x - x_0)/r \\ y/r \\ z/r. \end{matrix}\right.$$

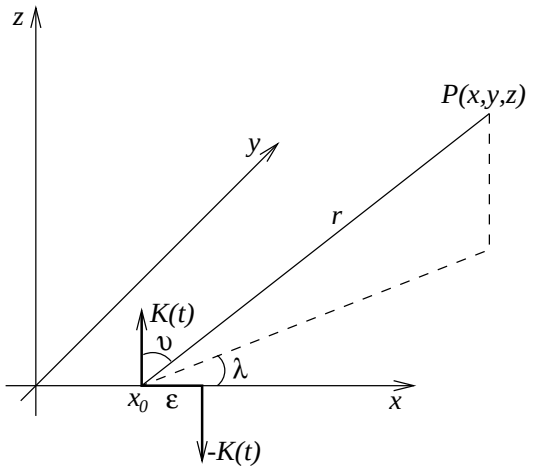

Fig. 3.11: Single couple model.

The displacements u'_x, u'_y, u'_z of force $-K(t)$ with the two neighbouring points of action shifted by ϵ, can be determined using the Taylor expansion of u_x, u_y, u_z at the source coordinate x_0 and truncating after the linear term. This leads, for example, to

$$u'_x = -\left(u_x + \frac{\partial u_x}{\partial x_0}\epsilon\right).$$

The single couple displacement then follows by superposition

$$u''_x = u_x + u'_x = -\frac{\partial u_x}{\partial x_0}\epsilon.$$

To obtain the far-field displacement requires only the differentiation of the force $K(t - r/\alpha)$ with respect to r, and additional differentiation $\partial r/\partial x_0 = -(x - x_0)/r$. The other terms with x_0 contribute only to the near field, the amplitude of which decreases faster then $1/\mathrm{r}$. This leads to

$$u''_x = -\frac{z}{4\pi\rho\alpha^2 r^2} K'\left(t - \frac{r}{\alpha}\right) \frac{-1}{\alpha} \frac{-(x - x_0)}{r} \epsilon \frac{x - x_0}{r}.$$

The y- and z-displacement are treated similarly. Therefore,

$$\left.\begin{matrix} u''_x \\ u''_y \\ u''_z \end{matrix}\right\} = -\tfrac{z(x-x_0)}{4\pi\rho\alpha^3 r^3} K'\left(t-\tfrac{r}{\alpha}\right)\epsilon\cdot \quad \left\{\begin{matrix} (x-x_0)/r \\ y/r \\ z/r. \end{matrix}\right. \tag{3.20}$$

As expected, the P-displacement of the single couple is also longitudinal.

The force dipole is defined strictly by the limit $\epsilon \to 0$, combined with a simultaneous increase of $K(t)$, so that

$$\lim_{\epsilon\to 0} K(t)\,\epsilon = M(t)$$

remains finite (but non-zero). $M(t)$ is called *moment function* of the dipole with the dimensions of a rotational moment.

From (3.20) with $z/r = \cos\vartheta$ and $(x-x_0)/r = \sin\vartheta\cos\lambda$, it follows that the P-wave displacement of the single couple in r-direction is

$$u_r = -\frac{\cos\vartheta\sin\vartheta\cos\lambda}{4\pi\rho\alpha^3 r} M'\left(t-\frac{r}{\alpha}\right).$$

In concluding, we now assume that $x_0 = 0$. For the S-wave, it follows similarly

$$u_\vartheta = \frac{\sin\vartheta\sin\vartheta\cos\lambda}{4\pi\rho\beta^3 r} M'\left(t-\frac{r}{\beta}\right).$$

As for the single force, the azimuthal component is zero. The following shows the results for the single couple and the radiation in the $x-z$-plane ($y=0$)

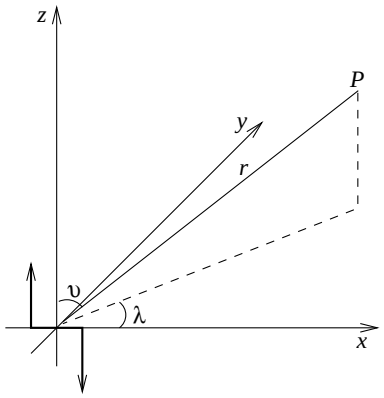

Fig. 3.12: Single couple in the x-z-plane.

$$\left.\begin{aligned} u_r &= -\tfrac{\sin 2\vartheta \cos\lambda}{8\pi\rho\alpha^3 r} M'\left(t-\tfrac{r}{\alpha}\right) \\ u_\vartheta &= \tfrac{\sin^2\vartheta\cos\lambda}{4\pi\rho\beta^3 r} M'\left(t-\tfrac{r}{\beta}\right) \\ u_\lambda &= 0. \end{aligned}\right\} \qquad (3.21)$$

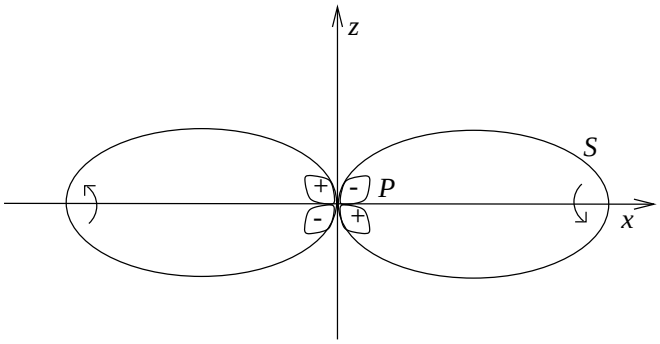

Fig. 3.13: Far field displacement of a single couple.

The ratio of the maximum S-radiation (for $\vartheta = 90^0$) to the maximum P-radiation (for $\vartheta = 45^0$) is about 10, if $\alpha \approx \beta\sqrt{3}$. The radiation characteristics in planes other then $y = 0$ follow from the one shown by multiplication with $\cos\lambda$. Plane $x = 0$ is a *nodal plane* for P- as well as for S-radiation; the plane $z = 0$ is one only for P.

The far-field displacements for a double couple in the $x-z$-plane are (see exercise 3.6)

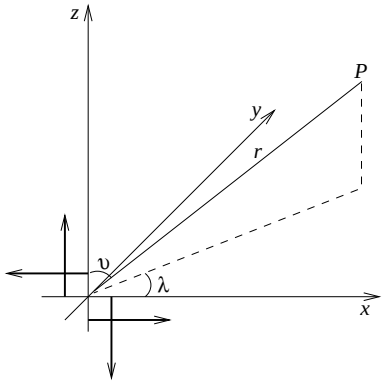

Fig. 3.14: Double couple in the x-z-plane.

$$\left.\begin{aligned} u_r &= -\tfrac{\sin 2\vartheta \cos\lambda}{4\pi\rho\alpha^3 r} M'\left(t-\tfrac{r}{\alpha}\right) \\ u_\vartheta &= -\tfrac{\cos 2\vartheta \cos\lambda}{4\pi\rho\beta^3 r} M'\left(t-\tfrac{r}{\beta}\right) \\ u_\lambda &= \tfrac{\cos\vartheta \sin\lambda}{4\pi\rho\beta^3 r} M'\left(t-\tfrac{r}{\beta}\right). \end{aligned}\right\} \tag{3.22}$$

The moment function in (3.22) is that of *one* of the two dipoles of the double couple. The radiation characteristics in the $x-z$-plane are shown in Fig. 3.15.

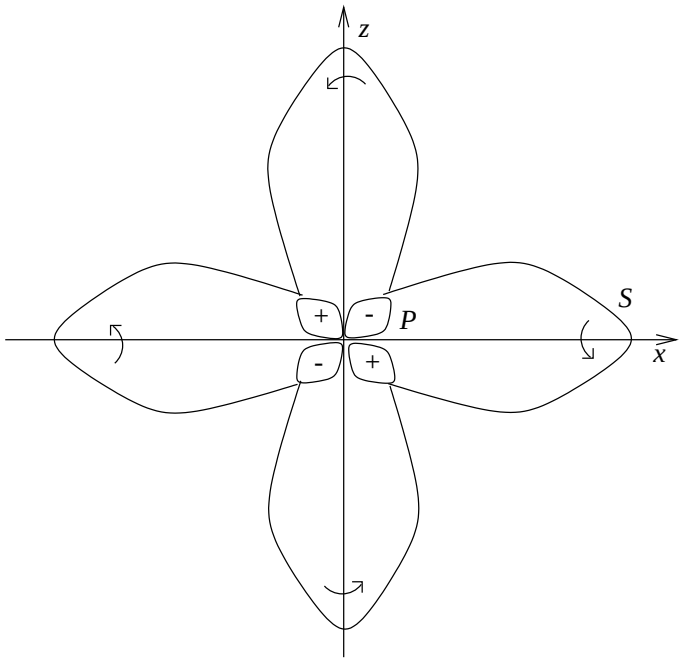

Fig. 3.15: Far field displacement of a double couple.

The P-radiation of the double couple has the same form as that of a single couple but is twice as large; the ratio of the maximum radiation of S to P is now about 5 (for $\lambda \approx \beta\sqrt{3}$). P-nodal planes are the planes with $x = 0$ and $z = 0$. The S-wave has no nodal planes, but only nodal directions (which?).

An (infinitesimal) *shear rupture*, either in the plane $z = 0$ with relative displacement in x-direction or in the plane $x = 0$ with relative displacement in z-direction, radiates waves as a double couple, i.e., (3.22) holds. A shear rupture or earthquake, therefore, radiates no P-waves in the direction of its rupture and perpendicular to it. If, by using the *distributions of the signs of first motion* of the P wave, the two nodal planes have been determined, the two possible rupture surfaces are found. The determination of the P-nodal plane of earthquakes

(*fault plane solution*), is an important aid in the study of source processes as well as the study of large-scale tectonics of a source region. Often the decision between the two options for the rupture surface can be made based on geological arguments.

The moment function of an earthquake with a smooth rupture, is, to a good approximation, a step function with non-vanishing rise time T and final value M_0, the *moment* of the earthquake (see Fig. 3.16). The far-field displacements are then, according to (3.22), one-sided impulses.

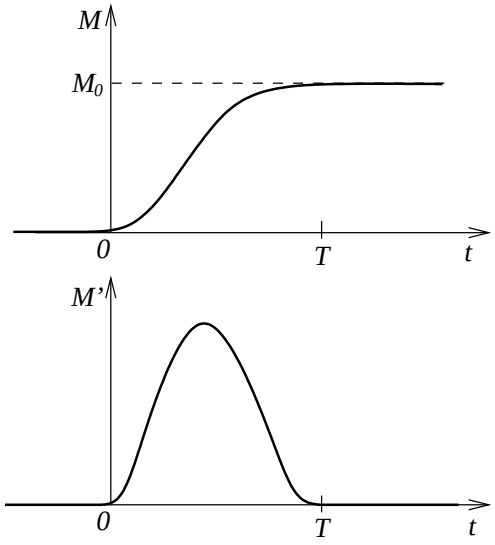

Fig. 3.16: Moment function and far-field displacement of a smooth rupture.

Propagation effects in layered media, e.g., the Earth's crust, can change the impulse form. In reality, the displacements look very often different, relative to the one shown here, due to complicated rupture processes.

Exercise 3.6

Derive the double couple displacement u_r in (3.22) from the corresponding single couple displacement in (3.21). Use equation (3.20) in Cartesian coordinates.

3.6 Reflection and refraction of plane waves at plane interfaces

3.6.1 Plane waves with arbitrary propagation direction

In sections 3.1 to 3.3 plane waves travelling in the direction of a coordinate axis were used. In the following, we need plane waves with an arbitrary direction of propagation. They can be described by the following potentials

$$\Phi = A \exp\left[i\omega\left(t - \frac{\overrightarrow{x}\,\overrightarrow{k}}{\alpha}\right)\right] \tag{3.23}$$

$$\overrightarrow{\Psi} = B \exp\left[i\omega\left(t - \frac{\overrightarrow{x}\,\overrightarrow{k}}{\beta}\right)\right] \overrightarrow{n}. \tag{3.24}$$

Their variation with time is also harmonic. This assumption is sufficient for most conclusions. A and B are constant, $\overrightarrow{k}$ and $\overrightarrow{n}$ are constant unit vectors, $\overrightarrow{x}$ is the location vector, ω is the angular frequency and i the imaginary unit. Φ and the components of $\overrightarrow{\Psi}$ satisfy the wave equation (please confirm)

$$\nabla^2\Phi = \frac{1}{\alpha^2}\frac{\partial^2\Phi}{\partial t^2}, \qquad \nabla^2\Psi_j = \frac{1}{\beta^2}\frac{\partial^2\Psi_j}{\partial t^2} \qquad \text{(Cartesian coordinates)}.$$

Since, according to (3.23) and (3.24), the movement at all times and locations is non-zero, the wavefronts can no longer be defined as surfaces separating undisturbed-disturbed from disturbed regions. We, therefore, consider wave fronts as *surfaces of constant phase* $\omega(t - \overrightarrow{x}\,\overrightarrow{k}/c)$ with $c = \alpha$ or $c = \beta$. These surfaces are defined by

$$\frac{d}{dt}\left(t - \frac{\overrightarrow{x}\,\overrightarrow{k}}{c}\right) = 0.$$

They are perpendicular to vector $\overrightarrow{k}$, which also gives the *direction of propagation*. The wavefronts move parallel with respect to themselves with the *phase velocity* c. Vector $\overrightarrow{k}$ multiplied by the wavenumber ω/α or ω/β, is called the *wavenumber vector*.

The *polarisation direction* of the compressional part

$$\nabla\,\Phi = -\frac{i\omega}{\alpha} A \exp\left[i\omega\left(t - \frac{\overrightarrow{x}\,\overrightarrow{k}}{\alpha}\right)\right] \overrightarrow{k} \tag{3.25}$$

is longitudinal (parallel to $\overrightarrow{k}$) and that of the shear component

$$\nabla \times \overrightarrow{\Psi} = -\frac{i\omega}{\beta} B \exp\left[i\omega\left(t - \frac{\overrightarrow{x}\,\overrightarrow{k}}{\beta}\right)\right] \overrightarrow{k} \times \overrightarrow{n} \tag{3.26}$$

$(rot(f \cdot \overrightarrow{n}) = f \cdot \nabla \times \overrightarrow{n} - \overrightarrow{n} \times \nabla f)$ is transversal (perpendicular to $\overrightarrow{k}$). From (3.26), it follows, that for $\overrightarrow{\Psi}$, without loss of generality, the additional condition of orthogonality of $\overrightarrow{k}$ and $\overrightarrow{n}$ can be introduced. (Separation of $\overrightarrow{n}$ in components parallel and perpendicular to $\overrightarrow{k}$).

3.6.2 Basic equations

We consider a combination of two half-spaces which are separated by a plane at z = 0. The combination is arbitrary (solid-solid, solid-vacuum, liquid-liquid, ...). We use Cartesian coordinates as shown in Fig. 3.17.

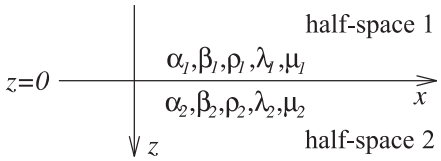

Fig. 3.17: Two half-spaces in Cartesian coordinates.

The y-axis points out of the plane. The displacement vector is

$$\overrightarrow{u} = (u, v, w),$$

and its components are *independent of* y, i.e., we treat a *plane problem* in which on all planes parallel to the $x - z$-plane, the same conditions hold. The most simple way to study elastic waves, under these conditions, is to derive u and w but not v, from potentials. Writing

$$\overrightarrow{u} = \nabla\,\Phi + \nabla \times \overrightarrow{\Psi}$$

by components,

$$\begin{aligned} u &= \frac{\partial \Phi}{\partial x} - \frac{\partial \Psi_2}{\partial z} \\ v &= \frac{\partial \Psi_1}{\partial z} - \frac{\partial \Psi_3}{\partial x} \\ w &= \frac{\partial \Phi}{\partial z} + \frac{\partial \Psi_2}{\partial x}, \end{aligned}$$

it is obvious that for v *two* potentials Ψ_1 and Ψ_3 are required, and these do not occur in u and w. For v, it is better to use directly the equation of motion (2.21) without body forces, which under these conditions becomes a wave equation

$$\nabla^2 v = \frac{1}{\beta^2}\frac{\partial^2 v}{\partial t^2}.$$

The *basic equations*, therefore, are, if Ψ instead of Ψ_2 is used

$$\left.\begin{aligned} \nabla^2\Phi &= \frac{1}{\alpha^2}\frac{\partial^2\Phi}{\partial t^2} \\ \nabla^2\Psi &= \frac{1}{\beta^2}\frac{\partial^2\Psi}{\partial t^2} \\ \nabla^2 v &= \frac{1}{\beta^2}\frac{\partial^2 v}{\partial t^2} \\ \nabla^2 &= \frac{\partial^2}{\partial x^2}+\frac{\partial^2}{\partial z^2} \end{aligned}\right\} \tag{3.27}$$

$$\left.\begin{aligned} u &= \tfrac{\partial\Phi}{\partial x}-\tfrac{\partial\Psi}{\partial z} \\ w &= \tfrac{\partial\Phi}{\partial z}+\tfrac{\partial\Psi}{\partial x}. \end{aligned}\right\} \tag{3.28}$$

The *boundary conditions* on the surface $z = 0$ between the half-spaces requires continuity of the stress components

$$\begin{aligned} p_{zz} &= \lambda\nabla\cdot\vec{u}+2\mu\frac{\partial w}{\partial z} = \lambda\nabla^2\Phi+2\mu\frac{\partial w}{\partial z} \\ p_{zx} &= \mu\left(\frac{\partial w}{\partial x}+\frac{\partial u}{\partial z}\right) \\ p_{zy} &= \mu\frac{\partial v}{\partial z}, \end{aligned}$$

or

$$\left.\begin{aligned} p_{zz} &= \tfrac{\lambda}{\alpha^2}\tfrac{\partial^2\Phi}{\partial t^2}+2\mu\left(\tfrac{\partial^2\Phi}{\partial z^2}+\tfrac{\partial^2\Psi}{\partial x\partial z}\right) \\ p_{zx} &= \mu\left(2\tfrac{\partial^2\Phi}{\partial x\partial z}+\tfrac{\partial^2\Psi}{\partial x^2}-\tfrac{\partial^2\Psi}{\partial z^2}\right) \\ p_{zy} &= \mu\tfrac{\partial v}{\partial z}. \end{aligned}\right\} \tag{3.29}$$

Which of the displacement components is continuous depends on the special combination of the half-spaces.

Since no connection of v with Φ and Ψ exists via the boundary conditions and, therefore, with u and w, it follows, that the S-waves, the displacement of which is *only* horizontal (in y-direction: *SH-waves*), propagate independently from the P-waves, following from Φ, and the S-waves, following from Ψ, that also have a vertical component (in z-direction: *SV-waves*). If a *SH-wave* impinges on an interface, only reflected and refracted *SH-waves* occur, but no *P- or SV-waves*. If, on the other hand, a $P-(SV-)$wave interacts with an interface, reflected and refracted $SV-(P-)$waves occur, but no *SH*-waves occur. These statements hold, in general, only for the case of an interface between two solid half-spaces. In liquids, neither *SH*- nor *SV*-waves propagate; in a vacuum a rigid half-space, or no waves propagate at all. Correspondingly, the situation is even more simple if such half-spaces are involved.

The *decoupling* of *P-SV*- and *SH*-waves holds for plane problems not only in the simple case of an interface z=const between two homogeneous half-spaces, but also in the more complicated case of an inhomogeneous medium, as long as density, wave velocity, and module are only functions of x and z. One consequence of this decoupling is that in the following, reflection and refraction of *P*- and *SV*-waves can be treated independently from that of the *SH*-waves. Furthermore, it is possible to dissect an S-wave of arbitrary polarisation in its *SV*- and *SH*-component and to study their respective reflection and refraction independently from each other.

In each case, we assume for the incident plane wave a potential Φ or $\vec{\Psi}$ in the form of (3.23) or (3.24), respectively, (in the second case $\vec{\Psi}$ has only the y-component Ψ). In case of a *SH*-wave, we assume that v can be described by an equation in the form of (3.23) with β instead of α. The angle of incidence φ is part of the direction vector $\vec{k}$

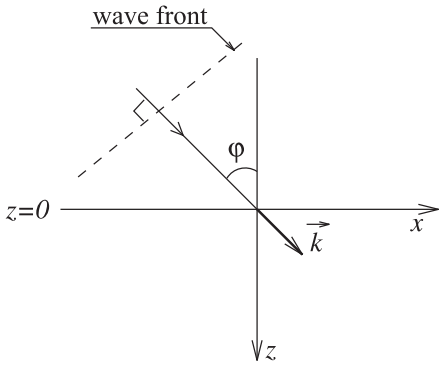

Fig. 3.18: Incident plane wave and angle of incidence φ.

$$\vec{k} = (\sin\varphi, 0, \cos\varphi). \tag{3.30}$$

For the reflected and refracted wave an ansatz is made with *different* amplitudes A and B, respectively, and *different* direction vectors $\overrightarrow{k}$. The relation between the new direction vectors and (3.30) is via Snell's law. The relation between the displacement amplitudes of the reflected and the refracted wave with the incident wave, is called *reflection coefficient* and *refraction coefficient*, respectively, and it depends on the angle of incidence and the material properties in the half-spaces. R_{pp}, R_{ps}, B_{pp}, B_{ps}, R_{ss}, R_{sp}, B_{ss}, B_{sp} will be the coefficients for *P-SV*-waves, r_{ss} and b_{ss} those for the *SH*-waves. The first index indicates the type of incident wave, the second the reflected and refracted wave type, respectively.

We discuss, in the following, only relatively simple cases, for which illustrate the main effects to be studied.

3.6.3 Reflection and refraction of SH-waves

Reflection and refraction coefficients

The displacement v_0 of the incident *SH*-wave in y-direction is

$$v_0 = C_0 \exp\left[i\omega\left(t - \frac{\sin\varphi}{\beta_1}x - \frac{\cos\varphi}{\beta_1}z\right)\right]. \tag{3.31}$$

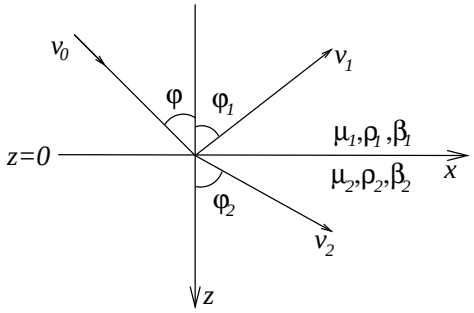

Fig. 3.19: Incident, reflected and diffracted SH-waves at a plane interface.

The *ansatz* for the reflected and refracted *SH*-wave as plane waves with reflection angle φ_1 and the refraction angle φ_2, respectively, and the *same frequency* as the incident wave is

$$\text{reflection}: \quad v_1 = C_1 \exp\left[i\omega\left(t - \frac{\sin\varphi_1}{\beta_1}x + \frac{\cos\varphi_1}{\beta_1}z\right)\right] \tag{3.32}$$

$$\text{refraction}: \quad v_2 = C_2 \exp\left[i\omega\left(t - \frac{\sin\varphi_2}{\beta_2}x - \frac{\cos\varphi_2}{\beta_2}z\right)\right]. \tag{3.33}$$

The unknowns are the angles φ_1 and φ_2, the reflection coefficient $r_{ss} = C_1/C_0$ and the refraction coefficient $b_{ss} = C_2/C_0$.

The *boundary conditions* require at $z = 0$ the continuity of displacement (that is a reasonable requirement) and continuity for the normal and tangential stresses. This leads to

$$\left.\begin{array}{rcl} v_0 + v_1 & = & v_2 \\ \mu_1 \frac{\partial}{\partial z}(v_0 + v_1) & = & \mu_2 \frac{\partial v_2}{\partial z} \end{array}\right\} \quad \text{for } z = 0. \tag{3.34}$$

The stress components p_{zz} and p_{zx} are zero everywhere, since no P- and/or SV-wave occur. Insert (3.31), (3.32) and (3.33) into (3.34). From the first boundary condition this leads to

$$C_0 \exp\left[i\omega\left(t - \frac{\sin\varphi}{\beta_1}x\right)\right] + C_1 \exp\left[i\omega\left(t - \frac{\sin\varphi_1}{\beta_1}x\right)\right] = C_2 \exp\left[i\omega\left(t - \frac{\sin\varphi_2}{\beta_2}x\right)\right]. \tag{3.35}$$

We plan to find solutions v_1 and v_2 of the problem, for which the amplitudes C_1 and C_2 are independent of location, since only then can we be sure that v_1 and v_2 are solutions of the corresponding wave equation. C_1 and C_2 become only independent of location if in (3.35)

$$\frac{\sin\varphi}{\beta_1} = \frac{\sin\varphi_1}{\beta_1} = \frac{\sin\varphi_2}{\beta_2}, \tag{3.36}$$

since only then the exponential term can be cancelled. Equation (3.36) is the well-known *Snell's Law* which states that the reflection angle φ_1 is equal to the angle of incidence φ and that for the refraction angle φ_2 is

$$\frac{\sin\varphi_2}{\sin\varphi} = \frac{\beta_2}{\beta_1}.$$

With (3.35), this leads to

$$C_2 - C_1 = C_0. \tag{3.37}$$

The second boundary condition in (3.34) gives

$$\mu_1 i\omega\left(-\frac{\cos\varphi}{\beta_1}C_0 + \frac{\cos\varphi_1}{\beta_1}C_1\right) = -\mu_2 i\omega\frac{\cos\varphi_2}{\beta_2}C_2.$$

With $\varphi_1 = \varphi$ and $\mu_{1,2}/\beta_{1,2} = \rho_{1,2}\beta_{1,2}$, it follows that

$$\rho_1\beta_1\cos\varphi(C_1 - C_0) = -\rho_2\beta_2\cos\varphi_2 C_2$$

or

$$\frac{\rho_2\beta_2\cos\varphi_2}{\rho_1\beta_1\cos\varphi}C_2 + C_1 = C_0. \tag{3.38}$$

From (3.37) and (3.38) follow the reflection and refraction coefficients

$$r_{ss} = \frac{C_1}{C_0} = \frac{\rho_1\beta_1\cos\varphi - \rho_2\beta_2\cos\varphi_2}{\rho_1\beta_1\cos\varphi + \rho_2\beta_2\cos\varphi_2} \tag{3.39}$$

$$b_{ss} = \frac{C_2}{C_0} = \frac{2\rho_1\beta_1\cos\varphi}{\rho_1\beta_1\cos\varphi + \rho_2\beta_2\cos\varphi_2}. \tag{3.40}$$

With (3.36), this leads to

$$\cos\varphi_2 = (1 - \sin^2\varphi_2)^{\frac{1}{2}} = \left(1 - \frac{\beta_2^2}{\beta_1^2}\sin^2\varphi\right)^{\frac{1}{2}}. \tag{3.41}$$

For *perpendicular* incidence ($\varphi = 0$)

$$r_{ss} = \frac{\rho_1\beta_1 - \rho_2\beta_2}{\rho_1\beta_1 + \rho_2\beta_2} \text{ and } b_{ss} = \frac{2\rho_1\beta_1}{\rho_1\beta_1 + \rho_2\beta_2}.$$

In this case, r_{ss} and b_{ss} depend only on the *impedances* $\rho_1\beta_1$ and $\rho_2\beta_2$ of the two half-spaces. For *grazing* incidence ($\varphi = \pi/2$), $r_{ss} = -1$ and $b_{ss} = 0$. The absolute value of the amplitude of the reflected wave is never larger then that of the incident wave; that of the refracted wave can be larger if $\rho_2\beta_2 < \rho_1\beta_1$ (e.g., for $\varphi = 0$).

If r_{ss} is negative, this means that in one point of the interface the displacement vector of the reflected wave points in $-y$-direction, *if* the displacement vector of the incident wave points in $+y$-direction. For impulsive excitation (see also later), this means that the direction of first motion of the incident and the reflected wave are opposite.

The following figure shows $|r_{ss}|$ as a function of φ for different velocity ratios $\beta_1/\beta_2 > 1$ and $\rho_1 = \rho_2$.

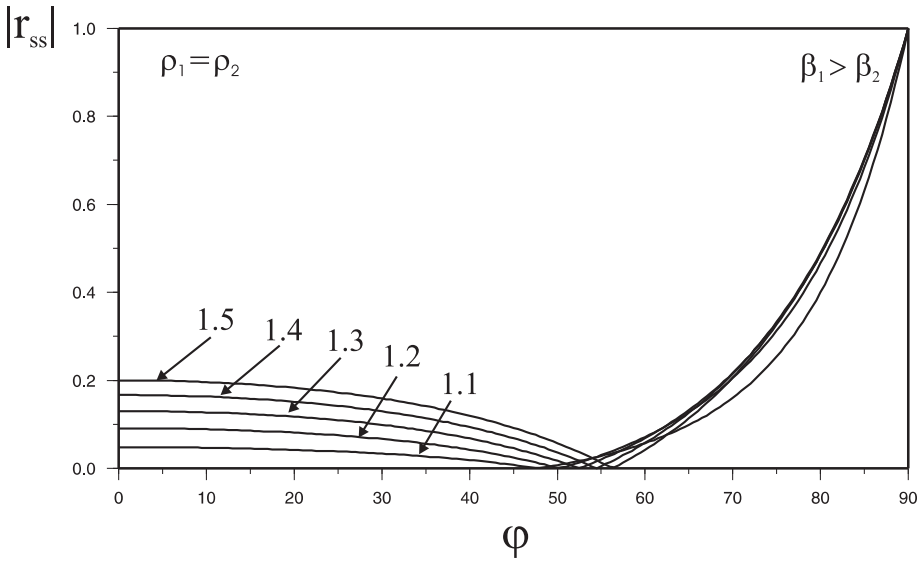

Fig. 3.20: $|r_{ss}|$ as a function of φ for different velocity ratios.

Total reflection

If $\beta_2 < \beta_1$, as in Fig. 3.20, $\cos\varphi_2$ is real for all angles of incident φ, the same is true for r_{ss} and b_{ss}. *Total reflection,*, i.e., $|r_{ss}| = 1$, is then only possible for grazing incidence.

If $\beta_2 > \beta_1$, $\cos\varphi_2$ is only real as long as

$$\varphi =< \varphi^* = \arcsin\frac{\beta_1}{\beta_2}.$$

φ^* is the *critical angle* (or *limiting angle of total reflection*). According to (3.41), $\varphi = \varphi^*$ is connected to the case with grazing propagation of the wave in the second half-space ($\varphi_2 = \pi/2$).

If $\varphi > \varphi^*$, $\cos\varphi_2$ becomes imaginary, or, to be more exact, negative imaginary for positive ω and positive imaginary for negative ω, since only then v_2 for $z \to +\infty$ remains limited. r_{ss} and b_{ss} become complex. v_1 and v_2 still solve the wave equations and satisfy the boundary conditions, even when posing the ansatz (3.32) and (3.33) have not explicitly been chosen in complex form. The reflection coefficient can then be written as

$$\left.\begin{aligned} r_{ss} &= \tfrac{a-ib}{a+ib} = \exp\left(-2i\arctan\tfrac{b}{a}\right) \\ a &= \rho_1\beta_1\cos\varphi \\ b &= -\rho_2\beta_2\left(\tfrac{\beta_2^2}{\beta_1^2}\sin^2\varphi - 1\right)^{\frac{1}{2}}\tfrac{\omega}{|\omega|} \end{aligned}\right\}. \qquad (3.42)$$

It has the absolute value 1 and a phase that depends on the angle of incidence. *Its sign changes with the sign of the frequency.* Values of $|r_{ss}|$ are shown in Fig. 3.21 for a few combinations.

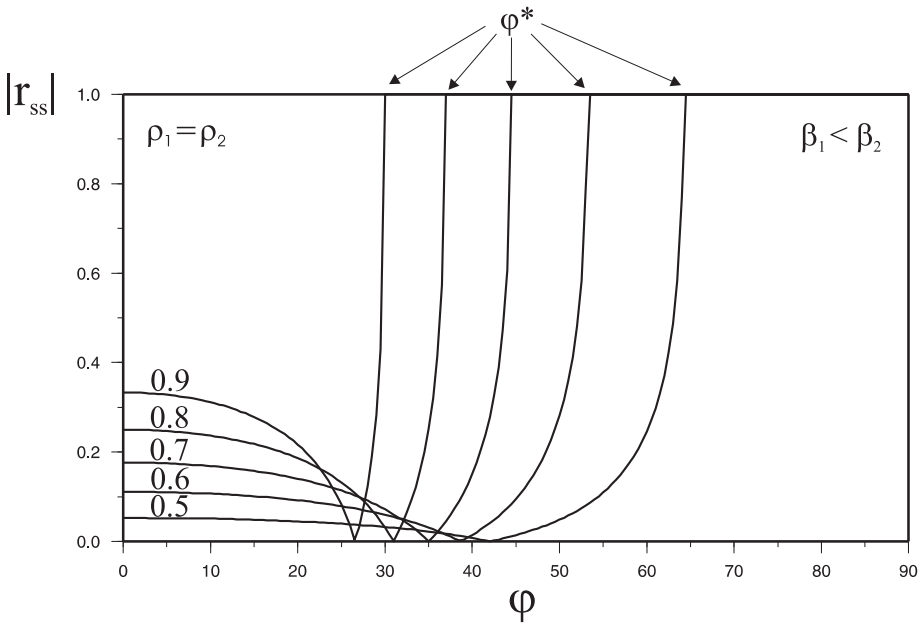

Fig. 3.21: $|r_{ss}|$ as a function of φ for different velocity ratios.

The refracted wave propagates for $\varphi > \varphi^*$ parallel to the interface with the velocity $\beta_1/\sin\varphi$. Its amplitude is not only controlled by b_{ss}, but is also controlled by the exponential term which depends on z. The amplitude of the refracted wave decays, therefore, exponentially with increasing distance from the interface (*inhomogeneous* or *boundary layer wave*). It follows that (please check)

$$v_2 = b_{ss} C_0 \exp\left[-\frac{|\omega|}{\beta_2}\left(\frac{\beta_2^2}{\beta_1^2}\sin^2\varphi - 1\right)^{\frac{1}{2}} z\right] \exp\left[i\omega\left(t - \frac{\sin\varphi}{\beta_1}x\right)\right].$$

Other cases

The treatment of the reflection of plane P-waves at an interface between two *liquids* gives similar results to the one discussed above (see also exercise 3.9). If the interface between two *solid half-spaces* is considered, the computational effort is significantly larger, since now reflected and refracted SV-waves have to be included. We, therefore, skip the details. The absolute value of the reflection coefficient R_{pp} is shown in Fig. 3.22.

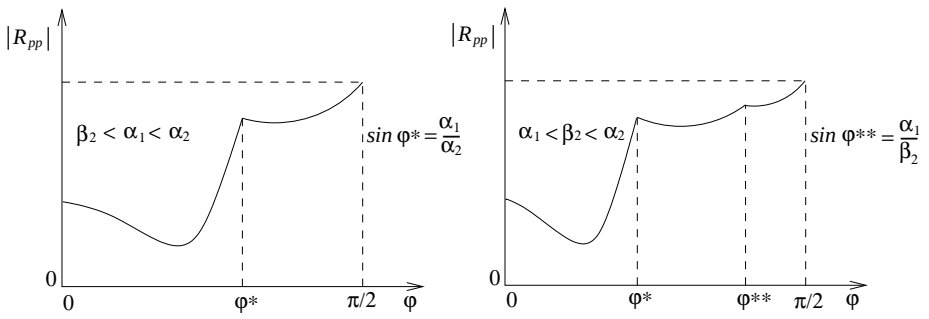

Fig. 3.22: Absolute value of the reflection coefficient R_{pp}.

For $\varphi = 0$, $R_{pp} = \frac{\rho_2\alpha_2 - \rho_1\alpha_1}{\rho_2\alpha_2 + \rho_1\alpha_1}$ (compare also exercise 3.9).

$|R_{pp}|$ for $\varphi^* < \varphi < \pi/2$ is smaller then 1 for two reasons. First, the reflected SV-wave also carries energy; second, for the case on the left of Fig. 3.22, a SV-wave propagates in the lower half-space for *all* φ, and, similarly, for the case on the right of Fig. 3.22, for $\varphi < \varphi^{**}$. $\varphi < \varphi^{**}$ is the *second critical angle* which exists only for $\alpha_1 < \beta_2 < \alpha_2$

$$\varphi^{**} = \arcsin\frac{\alpha_1}{\beta_2} > \varphi^* = \arcsin\frac{\alpha_1}{\alpha_2}.$$

For angles φ larger then φ^{**}, the second energy loss is no longer possible, and total reflection occurs. The reflected energy is then, to a smaller part, also transported in the SV-wave.

Some numerical results for reflection and refraction coefficients for a P-SV-case are given in Fig. 3.23 (model of the crust-mantle boundary (Moho) with $\alpha_1 = 6.5km/sec, \beta_1 = 3.6km/sec, \rho_1 = 2.8g/cm^3, \alpha_2 = 8.2km/sec, \beta_2 = 4.5km/sec, \rho_2 = 3.3g/cm^3$).

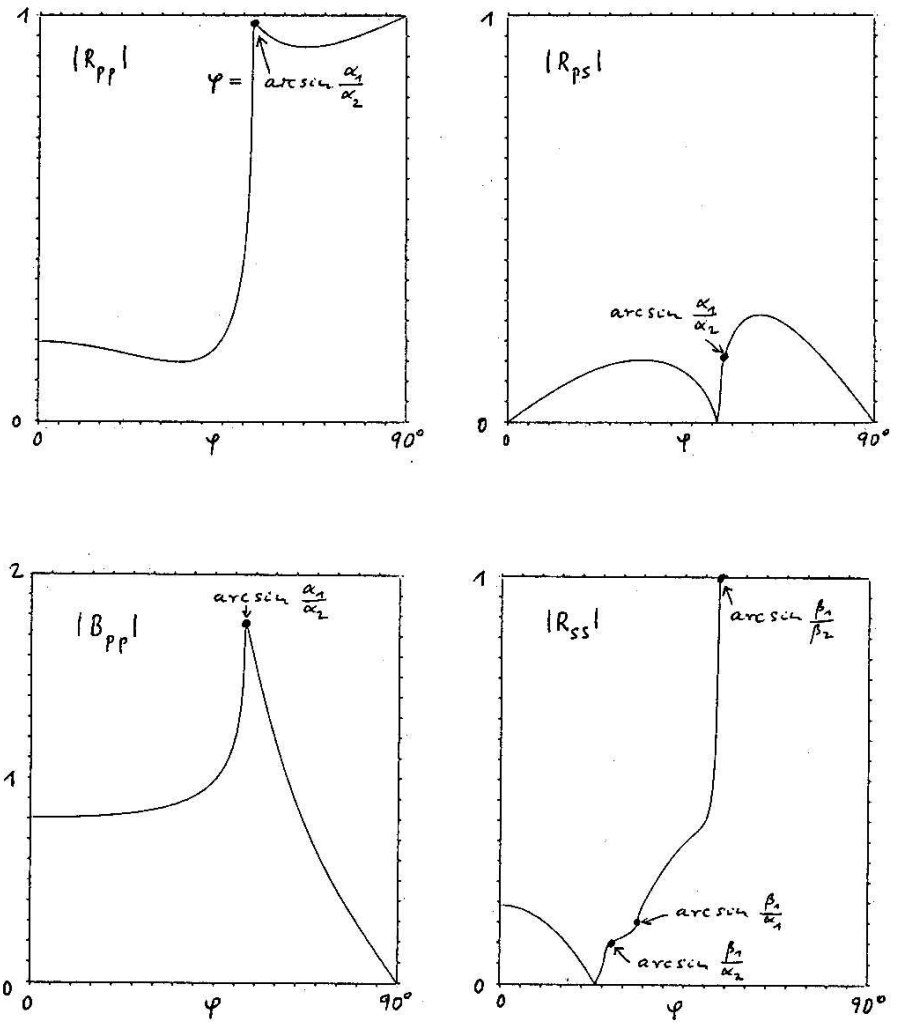

Fig. 3.23: Absolute value of reflection and refraction coefficients R_{pp}, R_{ps}, B_{pp} and R_{ss}.

Transition to impulsive excitation

The transition from the harmonic case, treated up to now, to the impulse case, can be done with the *Fourier transform* (compare appendix A.1.7). Instead of (3.31), the *SH*-wave

$$v_0 = F\left(t - \frac{\sin\varphi}{\beta_1}x - \frac{\cos\varphi}{\beta_1}z\right)$$

may impinge on the interface, and we dissect $F(t)$ with the aid of the Fourier integral in *partial vibration*

$$\begin{aligned} F(t) &= \frac{1}{2\pi}\int_{-\infty}^{+\infty}\overline{F}(\omega)e^{i\omega t}d\omega \\ \overline{F}(\omega) &= \int_{-\infty}^{+\infty}F(t)e^{-i\omega t}dt \qquad \text{Fourier transform of } F(t). \end{aligned}$$

We then study, as before, reflection and refraction of the *partial waves*

$$dv_0 = \frac{1}{2\pi}\overline{F}(\omega)\exp\left[i\omega\left(t-\frac{\sin\varphi}{\beta_1}x-\frac{\cos\varphi}{\beta_1}z\right)\right]d\omega$$

and then sum the reflected partial waves to derive the reflected *SH*-wave

$$v_1 = \frac{1}{2\pi}\int_{-\infty}^{+\infty}r_{ss}\overline{F}(\omega)\exp\left[i\omega\left(t-\frac{\sin\varphi}{\beta_1}x+\frac{\cos\varphi}{\beta_1}z\right)\right]d\omega. \tag{3.43}$$

As long as the reflection coefficient r_{ss} is frequency independent (which is the case for $\beta_2 < \beta_1$ or for $\varphi < \varphi^*$ with $\beta_2 > \beta_1$), it can be moved before the integral, thus, yielding

$$v_1 = r_{ss}F\left(t-\frac{\sin\varphi}{\beta_1}x+\frac{\cos\varphi}{\beta_1}z\right).$$

The reflected impulse has, in this case, the same form as the incident impulse. The amplitude ratio of the two impulses is equal to the reflection coefficient.

Then r_{ss}, according to (3.42), becomes dependent from ω for $\varphi > \varphi^*$ with $\beta_2 > \beta_1$. One then has to proceed differently. We dissect r_{ss} into real and imaginary parts

$$\begin{aligned} r_{ss} &= R(\varphi) + iI(\varphi)\frac{\omega}{|\omega|} \\ R(\varphi) &= \frac{a^2-b^2}{a^2+b^2} \\ I(\varphi) &= -\frac{2ab}{a^2+b^2} \qquad (b \text{ for } \omega > 0). \end{aligned}$$

According to (3.43), it holds that

$$v_1 = R(\varphi)F(\tau) + I(\varphi)\frac{1}{2\pi}\int_{-\infty}^{+\infty}\frac{i\omega}{|\omega|}\overline{F}(\omega)e^{i\omega\tau}d\omega \tag{3.44}$$

with

$$\tau = t - \frac{\sin\varphi}{\beta_1}x + \frac{\cos\varphi}{\beta_1}z.$$

The function, with which $I(\varphi)$ in (3.44) is multiplied, can be written, here via its Fourier transform, as $(i\omega/|\omega|)\cdot\overline{F}(\omega)$. This is a simple *filter* of function $F(\tau)$ (compare general comments on filters in appendix A.3.4). Each frequency ω in $F(\tau)$ keeps its amplitude, but its phase is changed. The phase change is $+90^0$ for $\omega > 0$ and -90^0 for $\omega < 0$. This corresponds to a *Hilbert transform* and is shown in appendix B. The function with which $I(\varphi)$ in (3.44) is multiplied is, therefore, the *Hilbert transform* $F_H(\tau)$ of $F(\tau)$

$$F_H(\tau) = \frac{1}{\pi}P\int_{-\infty}^{+\infty}\frac{F(t)}{t-\tau}dt = \frac{1}{\pi}\int_{-\infty}^{+\infty}\ln|t|\,F'(\tau-t)dt. \qquad (3.45)$$

P indicates the main value (without the singularity at $t = \tau$), and the second form of $F_H(\tau)$ follows from the first by partial integration. Thus,

$$v_1 = R(\varphi)F(\tau) + I(\varphi)F_H(\tau). \qquad (3.46)$$

Due to the second term in (3.46), the form of the reflected wave is *different* from that of the incident wave. Fig. 3.24 shows the *results* of the reflection of *SH*-waves and angle of incidence φ from 0 to 90^0.

For pre-critical angles of incidence $\varphi < \varphi^* = 48^0$, the reflection has the form of the incident wave with positive and negative signs. Beyond the critical angle, in the range of total reflection, impulse deformations occur until at $\varphi = 90^0$ the incident wave form appears again, but with opposite sign (corresponding to a reflection coefficient $r_{ss} = -1$). The phase shift of r_{ss} at $\varphi = 55^0$ is about $\pm 90^0$, with the consequence that $R(\varphi) \approx 0$. The reflection impulse for this angle of incidence is, therefore, close to the Hilbert transform $F_H(\tau)$ of $F(\tau)$ (the exact Hilbert transform is an impulse that is symmetric with respect to its minimum).

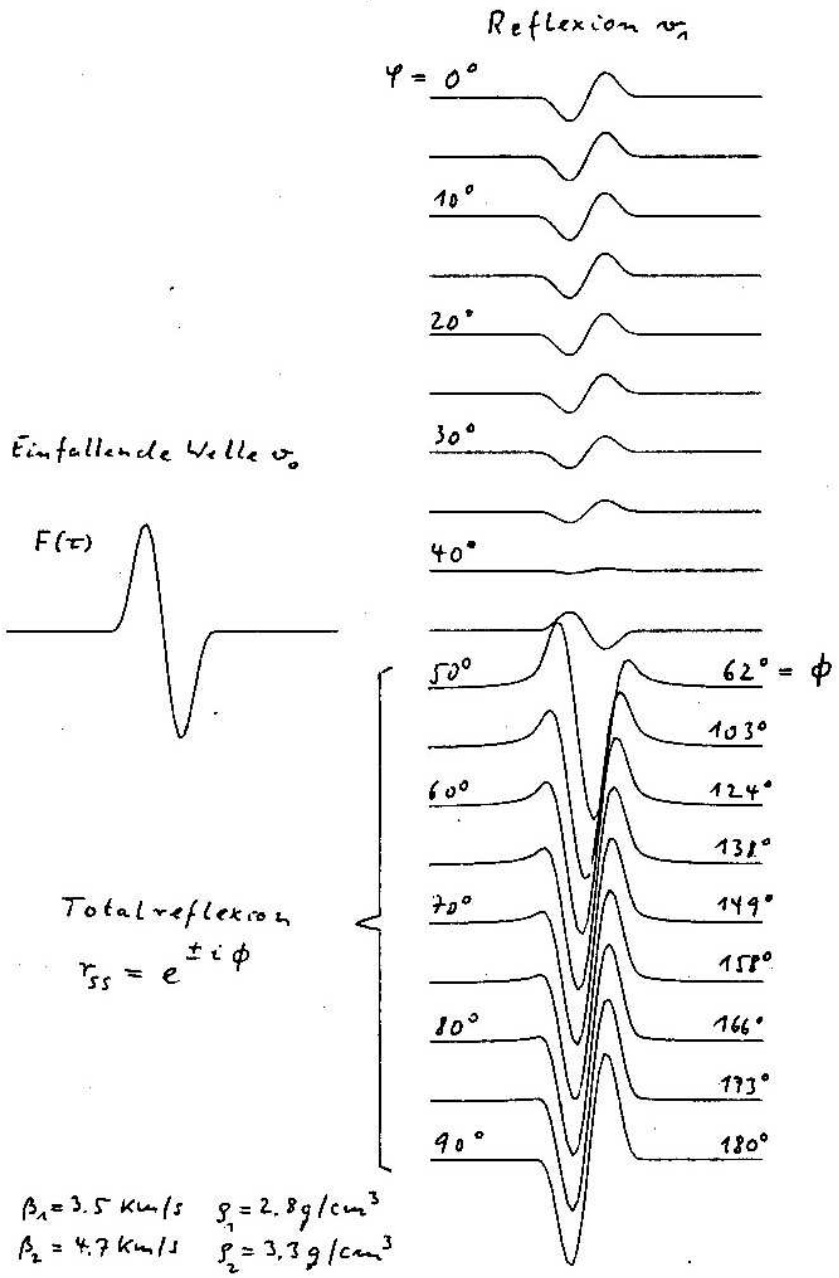

Fig. 3.24: Reflection of *SH*-waves for different angle of incidence φ.

Exercise 3.7:

Which sign does the reflection coefficient r_{ss} have in Fig. 3.20 and Fig. 3.21, in the regions where it is real?

Exercise 3.8:

Determine the angle of incidence for which r_{ss} is zero (*Brewster angle)*, and give the conditions under which this actually happens (compare $\varphi \approx 40^0$ in Fig. 3.24).

Exercise 3.9

Compute the reflection and refraction coefficients for a plane surface between two liquids and for a plane harmonic longitudinal wave under angle of incidence φ impinges. Give, qualitatively, the trend of the coefficients for $\rho_1 = \rho_2$ with $\alpha_1 > \alpha_2$ and $\alpha_1 < \alpha_2$. Hint: Use an ansatz for the displacement potential in the form of (3.31) to (3.33) and express the boundary conditions via potentials as discussed in section 3.6.2.

3.6.4 Reflection of P-waves at a free surface

Reflection coefficients

The study of the reflection of P-waves from a free surface is of practical importance for seismology. P-waves from earthquakes and explosions propagate through the Earth and impinge at the seismic station from below. Horizontal and vertical displacement are modified by the free surface. Furthermore, reflected P- and S-waves are reflected downwards and recorded at larger distances, sometimes with large amplitudes. It is, therefore, useful and necessary to know the reflection coefficient of the Earth's surface. For the moment, we neglect the layered nature of the crust in our model, thus, only giving a first approximation to reality.

Based on the comments given at the end of section 3.6.2, we select the following ansatz for the potentials

$$\text{incident } P-\text{wave}$$
$$\Phi_0 = A_0 \exp\left[i\omega\left(t - \frac{\sin\varphi}{\alpha}x - \frac{\cos\varphi}{\alpha}z\right)\right] \quad (3.47)$$
$$\text{reflected } P-\text{wave}$$
$$\Phi_1 = A_1 \exp\left[i\omega\left(t - \frac{\sin\varphi_1}{\alpha}x + \frac{\cos\varphi_1}{\alpha}z\right)\right] \quad (3.48)$$
$$\text{reflected } SV-\text{wave}$$
$$\Psi_1 = B_1 \exp\left[i\omega\left(t - \frac{\sin\varphi_1'}{\beta}x + \frac{\cos\varphi_1'}{\beta}z\right)\right]. \quad (3.49)$$

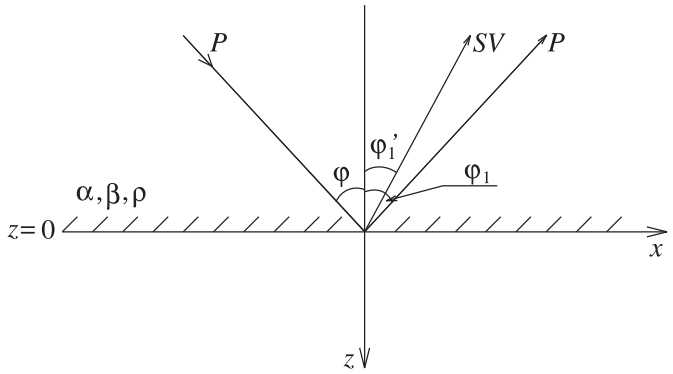

Fig. 3.25: Incident P-wave and reflected P- and S-wave .

The boundary conditions at $z = 0$ require vanishing normal and tangential stress $p_{zz} = p_{zx} = 0$. No boundary conditions for the displacement exist. With (3.29) and $\Phi = \Phi_0 + \Phi_1 \quad (\Psi = \Psi_1 = y - \text{component of } \vec{\Psi})$, it follows that

$$\frac{1}{\alpha^2}\frac{\partial^2}{\partial t^2}(\Phi_0 + \Phi_1) + \frac{2\mu}{\lambda}\left[\frac{\partial^2}{\partial z^2}(\Phi_0 + \Phi_1) + \frac{\partial^2 \Psi_1}{\partial x \partial z}\right] = 0 \qquad z = 0 \quad (3.50)$$

$$2\frac{\partial^2}{\partial x \partial z}(\Phi_0 + \Phi_1) + \frac{\partial^2 \Psi_1}{\partial x^2} - \frac{\partial^2 \Psi_1}{\partial z^2} = 0 \qquad z = 0. \quad (3.51)$$

As in the last section, Snell's law follows from the boundary conditions

$$\frac{\sin\varphi}{\alpha} = \frac{\sin\varphi_1}{\alpha} = \frac{\sin\varphi_1'}{\beta}. \qquad (3.52)$$

From this, it follows that $\varphi_1 = \varphi$ and $\varphi_1' = \arcsin\left(\frac{\beta}{\alpha} \cdot \sin\varphi\right) < \varphi$.

With (3.47), (3.48), (3.49) and

$$\frac{\mu}{\lambda} = \frac{\mu}{\lambda + 2\mu - 2\mu} = \frac{\rho\beta^2}{\rho\alpha^2 - 2\rho\beta^2} = \frac{\beta^2}{\alpha^2 - 2\beta^2}$$

(3.50) leads to

$$\frac{1}{\alpha^2}(A_0 + A_1)(i\omega)^2$$

$$+\frac{2\beta^2}{\alpha^2 - 2\beta^2}\left[(A_0 + A_1)\left(\frac{i\omega}{\alpha}\cos\varphi\right)^2 + B_1\left(-\frac{i\omega}{\beta}\sin\varphi_1'\right)\left(\frac{i\omega}{\beta}\cos\varphi_1'\right)\right] = 0.$$

Then

$$A_0 + A_1 + \frac{2\alpha^2\beta^2}{\alpha^2 - 2\beta^2}\left[(A_0 + A_1)\frac{\cos^2\varphi}{\alpha^2} - B_1\frac{\sin\varphi_1'\cos\varphi_1'}{\beta^2}\right] = 0.$$

with

$$\begin{aligned} 1 + \frac{2\beta^2}{\alpha^2 - 2\beta^2}\cos^2\varphi &= \frac{2\beta^2}{\alpha^2 - 2\beta^2}\left(\frac{\alpha^2}{2\beta^2} - 1 + \cos^2\varphi\right) \\ &= \frac{2\beta^2}{\alpha^2 - 2\beta^2}\left(\frac{\alpha^2}{2\beta^2} - \sin^2\varphi\right) \\ &= \frac{\beta^2}{\alpha^2 - 2\beta^2}\left(\frac{\alpha^2}{\beta^2} - 2\sin^2\varphi\right) \\ &= \frac{\gamma - 2\sin^2\gamma}{\gamma - 2} \end{aligned}$$

and $\left(\gamma = \frac{\alpha^2}{\beta^2} > 2\right)$, it follows that

$$\frac{\gamma - 2\sin^2\varphi}{\gamma - 2}(A_0 + A_1) - \frac{2\gamma\sin\varphi_1'\cos\varphi_1'}{\gamma - 2}B_1 = 0.$$

From this

$$(\gamma - 2\sin^2\varphi)\frac{A_1}{A_0} - 2\sin\varphi(\gamma - \sin^2\varphi)^{\frac{1}{2}}\frac{B_1}{A_0} = 2\sin^2\varphi - \gamma. \tag{3.53}$$

Equation (3.51) then gives

$$\begin{aligned} &2A_0\left(-\frac{i\omega}{\alpha}\sin\varphi\right)\left(-\frac{i\omega}{\alpha}\cos\varphi\right) + 2A_1\left(-\frac{i\omega}{\alpha}\sin\varphi\right)\left(\frac{i\omega}{\alpha}\cos\varphi\right) \\ &\quad + B_1\left(-\frac{i\omega}{\beta}\sin\varphi_1'\right)^2 - B_1\left(\frac{i\omega}{\beta}\cos\varphi_1'\right)^2 = 0 \end{aligned}$$

or

$$\frac{2\sin\varphi\cos\varphi}{\alpha^2}(A_0 - A_1) + \frac{\sin^2\varphi_1' - \cos^2\varphi_1'}{\beta^2}B_1 = 0.$$

Equation (3.52) then gives

$$2\sin\varphi\cos\varphi\frac{A_1}{A_0} + \left(\gamma - 2\sin^2\varphi\right)\frac{B_1}{A_0} = 2\sin\varphi\cos\varphi. \tag{3.54}$$

From (3.53) and (3.54), it follows that the amplitude ratios are

$$\frac{A_1}{A_0} = \frac{4\sin^2\varphi\cos\varphi\left(\gamma-\sin^2\varphi\right)^{\frac{1}{2}} - \left(\gamma-2\sin^2\varphi\right)^2}{4\sin^2\varphi\cos\varphi\left(\gamma-\sin^2\varphi\right)^{\frac{1}{2}} + \left(\gamma-2\sin^2\varphi\right)^2} \tag{3.55}$$

$$\frac{B_1}{A_0} = \frac{4\sin\varphi\cos\varphi\left(\gamma-2\sin^2\varphi\right)}{4\sin^2\varphi\cos\varphi\left(\gamma-\sin^2\varphi\right)^{\frac{1}{2}} + \left(\gamma-2\sin^2\varphi\right)^2}. \tag{3.56}$$

To derive displacement amplitudes (that is how the coefficients R_{pp} and R_{ps} in section 3.6.2 were defined) from the ratios of potential amplitudes given here, we use (3.25) and (3.26). The displacement amplitude of the incident P-wave is $-\frac{i\omega}{\alpha}A_0$; that of the reflected P-wave is $-\frac{i\omega}{\alpha}A_1$. This then gives the PP-reflection coefficient (see also (3.55))

$$R_{pp} = \frac{A_1}{A_0}. \tag{3.57}$$

Equation (3.26) gives the displacement amplitude of the reflected SV-wave as $-\frac{i\omega}{\beta}B_1$. Thus, the PS-reflection coefficient is (see also (3.56))

$$R_{ps} = \frac{\alpha}{\beta}\frac{B_1}{A_0}. \tag{3.58}$$

R_{pp} and Rps are *real* and *frequency independent* for all angles of incident φ. R_{ps} is always positive. For $\varphi = 0$ and $\varphi = \frac{\pi}{2}$, $R_{pp} = -1$ and $R_{ps} = 0$, respectively, and only a P-wave is reflected.

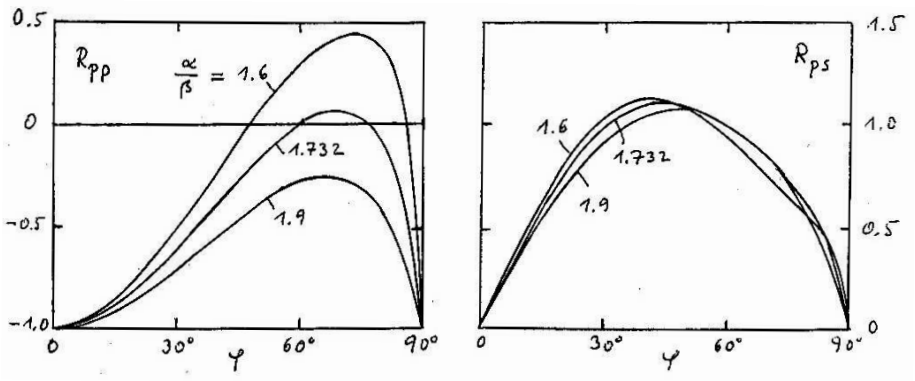

Fig. 3.26: Reflection and refraction coefficients of P-waves for different angles of incidence φ.

The meaning of the *negative signs* in the reflection coefficients becomes clear, if the displacement vector of the incident and reflected waves are represented via (3.25) and (3.26)

$$\begin{aligned}
\vec{u}_0 &= \nabla\,\Phi_0 = -\frac{i\omega}{\alpha}A_0 \exp\left[i\omega\left(t - \frac{\sin\varphi}{\alpha}x - \frac{\cos\varphi}{\alpha}z\right)\right]\vec{k}_0 \\
\vec{u}_1 &= \nabla\,\Phi_1 = -\frac{i\omega}{\alpha}A_0 R_{pp} \exp\left[i\omega\left(t - \frac{\sin\varphi}{\alpha}x + \frac{\cos\varphi}{\alpha}z\right)\right]\vec{k}_1 \\
\vec{u}_1' &= \nabla\times\vec{\Psi} = -\frac{i\omega}{\alpha}A_0 R_{ps} \exp\left[i\omega\left(t - \frac{\sin\varphi_1'}{\beta}x + \frac{\cos\varphi_1'}{\beta}z\right)\right]\vec{k}_1' \times \vec{n}.
\end{aligned}$$

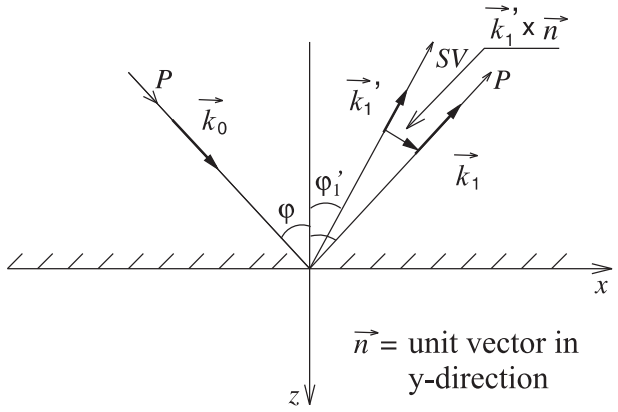

Fig. 3.27: Polarity of reflected P- and SV-waves.

$R_{pp} < 0$, therefore, means that if the displacement of the reflected P-wave in a point on the interface ($z = 0$) points in the direction of $-\vec{k}_1$, the incident wave points in the direction of $\vec{k}_0$. For $R_{ps} < 0$, the displacement of the reflected SV-wave would, for such an incident wave, be pointing in the direction of $-\vec{k}_1' \times \vec{n}$.

These connections become more obvious if we go from the harmonic case to the *impulsive case* (compare section 3.6.3, transition to impulse excitation). For the problem studied, the reflection coefficients are frequency independent. Therefore, the reflected waves have always the same form as the incident wave

$$\vec{u}_0 = F\left(t - \frac{\sin\varphi}{\alpha}x - \frac{\cos\varphi}{\alpha}z\right)\vec{k}_0 \tag{3.59}$$

$$\vec{u}_1 = R_{pp}F\left(t - \frac{\sin\varphi}{\alpha}x + \frac{\cos\varphi}{\alpha}z\right)\vec{k}_1 \tag{3.60}$$

$$\begin{aligned} \overrightarrow{u}'_1 &= R_{ps} F\left(t - \frac{\sin\varphi'_1}{\beta}x + \frac{\cos\varphi'_1}{\beta}z\right) \overrightarrow{k}'_1 \times \overrightarrow{n} \\ \varphi'_1 &= \arcsin\left(\frac{\beta}{\alpha}\sin\varphi\right). \end{aligned} \tag{3.61}$$

In the case $R_{pp} < 0$, if the *first motion* of the incident P-wave is directed towards the interface $z = 0$, this also holds for the reflected SV-wave and the reflected P-wave; otherwise, the first motion of the reflected P-wave points away from the interface. Fig. 3.28 shows the case for $R_{pp} < 0$.

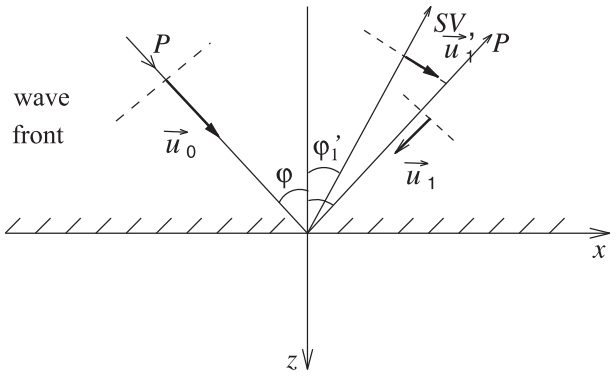

Fig. 3.28: Definition of the first motion of reflected P- and SV-waves.

Displacements at the surface

Finally, we compute the resulting displacement at the free surface (z=0) in which the three waves (3.59), (3.60) and (3.61) superimpose.

Horizontal displacement (positive in x-direction):

$$\begin{aligned} u &= \left[(1 + R_{pp})\sin\varphi + R_{ps}\cos\varphi'_1\right] F\left(t - \frac{\sin\varphi}{\alpha}x\right) \\ u &= f_u(\varphi) F\left(t - \frac{\sin\varphi}{\alpha}x\right) \\ f_u(\varphi) &= \frac{4\gamma\sin\varphi\cos\varphi\left(\gamma - \sin^2\varphi\right)^{\frac{1}{2}}}{4\sin^2\varphi\cos\varphi\left(\gamma - \sin^2\varphi\right)^{\frac{1}{2}} + \left(\gamma - 2\sin^2\varphi\right)^2} \end{aligned} \tag{3.62}$$

and *Vertical displacement* (positive in z-direction):

$$w = \left[(1 - R_{pp})\cos\varphi + R_{ps}\sin\varphi'_1\right] F\left(t - \frac{\sin\varphi}{\alpha}x\right)$$

$$
\begin{aligned}
w &= f_w(\varphi) F\left(t - \frac{\sin\varphi}{\alpha} x\right) \\
f_w(\varphi) &= \frac{2\gamma \cos\varphi \left(\gamma - 2\sin^2\varphi\right)}{4\sin^2\varphi\cos\varphi\left(\gamma - \sin^2\varphi\right)^{\frac{1}{2}} + \left(\gamma - 2\sin^2\varphi\right)^2}.
\end{aligned} \tag{3.63}
$$

The amplification factors (or transfer functions of the surface) $f_u(\varphi)$ and $f_w(\varphi)$, respectively, are given in Fig. 3.29 for the case $\gamma = 3$.

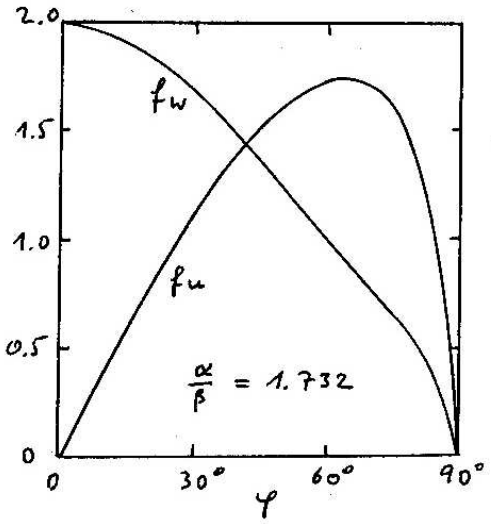

Fig. 3.29: Transfer functions of the free surface.

Therefore, a *linearly polarised* wave with the apparent velocity $\alpha/\sin\varphi$ propagates at the surface. The *polarisation angle* ϵ, (see Fig. 3.30), is not identical to the angle of incidence φ. ϵ is also called the *apparent angle of incidence*.

$$
\epsilon = \arctan\left(\frac{u}{w}\right) = \arctan\left(\frac{2\sin\varphi\left(\gamma - \sin^2\varphi\right)^{\frac{1}{2}}}{\gamma - 2\sin^2\varphi}\right).
$$

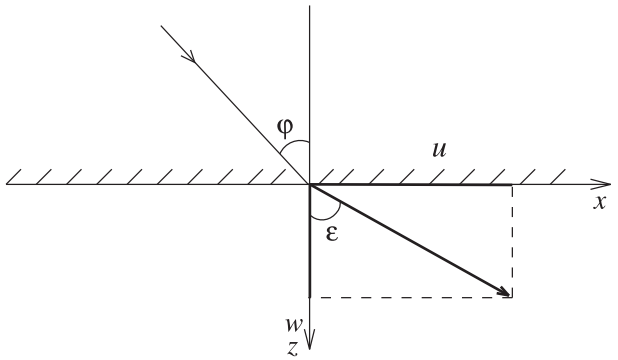

Fig. 3.30: Polarisation angle ϵ and angle of incidence φ.

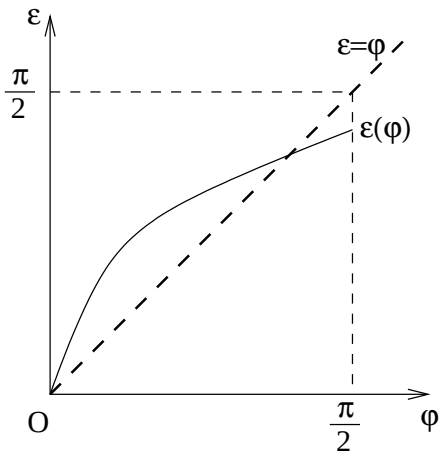

Fig. 3.31: Qualitative relationship between ϵ and φ .

$$\begin{aligned} \epsilon\left(\frac{\pi}{2}\right) &= \arctan\left(\frac{2\,(\gamma-1)^{\frac{1}{2}}}{\gamma-2}\right) \\ \epsilon'(0) &= \frac{2}{\gamma^{\frac{1}{2}}}. \end{aligned}$$

Incident SV-wave

If a SV-wave, instead of the P-wave considered up until now, impinges on the free surface, no P-wave is reflected for angles of incidence $\varphi > \varphi^* = \arcsin\frac{\beta}{\alpha}$, but only an SV-wave ($|R_{ss}| = 1$) is reflected. This follows from considerations similar to that for an incident P-wave. For $\varphi < \varphi^*$, the displacement at the free surface is linearly polarised, but for $\varphi > \varphi^*$, it is polarised *elliptically*.

This property is observed: SV-waves from earthquakes for distances smaller then about 40^0 are elliptically polarised, but are linearly polarised for larger distances.

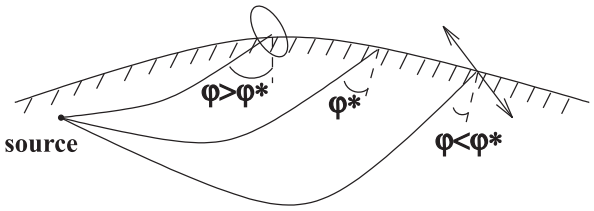

Fig. 3.32: Polarisation of SV-waves from earthquakes .

3.6.5 Reflection and refraction coefficients for layered media

Matrix formalism

In the last two sections, we studied the reflection and refraction of plane waves at *one* interface. The reflection and refraction coefficients depend, then, mainly on the properties of the half-spaces and the angle of incidence. Only if the critical angle is exceeded, a weak frequency dependence occurs: the sign of the phase (the coefficients become complex) is controlled by the sign of the frequency of the incident wave (compare section 3.6.3). The frequency dependence becomes much more pronounced when the reflection and refraction of plane waves in a (sub-parallel) *layered* media is considered (two or more interfaces). Then, generally, *interference phenomena* occur and for special frequencies (or wave lengths) *constructive* or *destructive* interferences occur.

Here, we will study the reflection and refraction of P-waves from a packet of *liquid* layers between two *liquid* half-spaces. The corresponding problem for SH-waves in solid media can be solved similarly. There is a close similarity between P-waves in layered liquid media and SH-waves in layered solid media. The treatment of P-SV-waves in solid media (possibly with interspersed liquid layers) is, in principle, the same, but the derivation is significantly more complicated. In all these approaches, a *matrix formalism* is used, which is especially effective for implementing on computers.

We choose the annotation of the liquid-layered medium as given in Fig. 3.33.

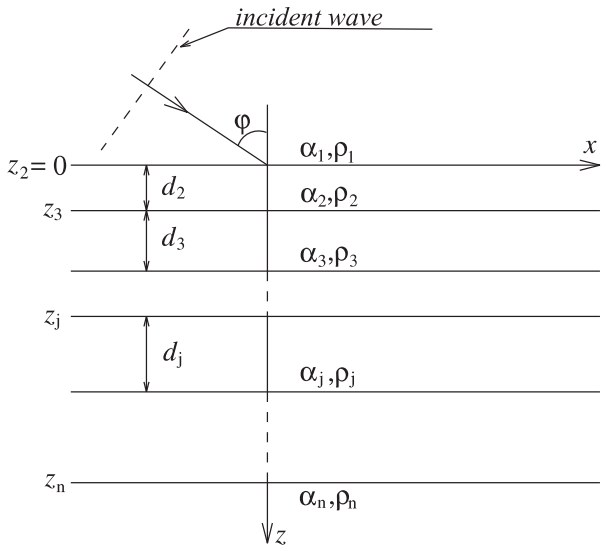

Fig. 3.33: Liquid-layered medium with n layers.

The displacement potential Φ_j in the j-th layer ($j = 1, 2, \ldots, n$) satisfies the wave equation

$$\frac{\partial^2 \Phi_j}{\partial x^2} + \frac{\partial^2 \Phi_j}{\partial z^2} = \frac{1}{\alpha_j^2} \frac{\partial^2 \Phi_j}{\partial t^2}.$$

Solutions of this equation, which can be interpreted as harmonic plane waves, have the form

$$\exp\left[i\left(\omega t \pm k_j x \pm l_j z\right)\right]$$

with $k_j^2 + l_j^2 = \omega/\alpha_j^2$, where k_j is the *horizontal*, l_j the *vertical wavenumber*, respectively. We assume positive frequencies ω and non-negative horizontal wavenumbers k_j. Then, we can disregard the sign "+" of $k_j x$, since it corresponds to waves which propagate in -x-direction. This is not possible for our selection of the incident wave, (see Fig. 3.33). The two signs of $l_j z$ have to be kept, since in all layers (except the n-th) waves propagate in $+z$- and in $-z$-direction. We then come to the *potential ansatz*

$$\begin{aligned} \Phi_j &= A_j \exp\left[i\left(\omega t - k_j x - l_j(z - z_j)\right)\right] \\ &\quad + B_j \exp\left[i\left(\omega t - k_j' x + l_j'(z - z_j)\right)\right] \end{aligned} \tag{3.64}$$

$$z_1 = z_2 = 0, \qquad k_j^2 + l_j^2 = k_j'^2 + l_j'^2 = \frac{\omega^2}{\alpha_j^2} \tag{3.65}$$

$$B_n = 0. \tag{3.66}$$

In (3.64), we have assumed, for the moment, that the wavenumbers of the waves propagating in +z- and -z-direction are different. Furthermore, we have replaced z by $z - z_j$. This does not change the meaning of the terms but simplifies the computations.

The part $A_1 \exp\left[i\left(\omega t - k_1 x - l_1 z\right)\right]$ of Φ_1 will be interpreted as incident P-wave (compare, e.g., (3.47)). This means that k_1 and l_1 are connected with the angle of incidence φ as

$$\left.\begin{array}{rcl} k_1 & = & \frac{\omega}{\alpha_1}\sin\varphi \\ l_1 & = & \frac{\omega}{\alpha_1}\cos\varphi. \end{array}\right\} \tag{3.67}$$

The part $B_1 \exp\left[i\left(\omega t - k_1' x + l_1' z\right)\right]$ of Φ_1 is the wave reflected from the layered half-space $z > 0$. We want to compute the reflection coefficient R_{pp} and the refraction coefficient B_{pp} (again defined as the ratio of the *displacement amplitudes*)

$$\left.\begin{array}{rcl} R_{pp} & = & \frac{B_1}{A_1} \\ B_{pp} & = & \frac{\alpha_1}{\alpha_n}\cdot\frac{A_n}{A_1}. \end{array}\right\} \tag{3.68}$$

The boundary conditions for the interfaces $z = z_2, z_3, \ldots, z_n$ require continuity of the vertical displacement $\partial\Phi/\partial z$ and of the normal stress $p_{zz} = \lambda\nabla^2\Phi = \rho\partial^2\Phi/\partial t^2$. For $z = z_j$, this gives

$$\frac{\partial\Phi_j}{\partial z} = \frac{\partial\Phi_{j-1}}{\partial z} \quad \text{and} \quad \rho_j\frac{\partial^2\Phi_j}{\partial t^2} = \rho_{j-1}\frac{\partial^2\Phi_{j-1}}{\partial t^2}.$$

From the first relation, it follows that (the phase term $e^{i\omega t}$ is neglected in the following since it cancels out),

$$\begin{array}{rcl} -l_j A_j \exp\left[-ik_j x\right] + l_j' B_j \exp\left[-ik_j' x\right] & = & -l_{j-1}A_{j-1}\exp\left[i\left(-k_{j-1}x - l_{j-1}d_{j-1}\right)\right] \\ & + & l_{j-1}' B_{j-1}\exp\left[i\left(-k_{j-1}' x + l_{j-1}' d_{j-1}\right)\right]. \end{array}$$

The second relation gives

$$\begin{array}{rcl} \rho_j A_j \exp\left[-ik_j x\right] + \rho_j B_j \exp\left[-ik_j' x\right] & = & \rho_{j-1}A_{j-1}\exp\left[i\left(-k_{j-1}x - l_{j-1}d_{j-1}\right)\right] \\ & + & \rho_{j-1} B_{j-1}\exp\left[i\left(-k_{j-1}' x + l_{j-1}' d_{j-1}\right)\right]. \end{array}$$

Both equations hold for $j = 2, 3, \ldots, n$, and $d_{j-1} = z_j - z_{j-1}$ ($d_1 = 0$). As before, we require that the exponential terms depending on x must cancel, leading to $k_j = k_j' = k_{j-1} = k_{j-1}'$. This, then, gives (with (3.67))

$$k'_n = k_n = k'_{n-1} = k_{n-1} = \ldots = k'_1 = k_1 = \frac{\omega}{\alpha_1} \sin\varphi.$$

This is an alternative form of *Snell's law*. With (3.65), this leads to

$$l'_j = l_j = \left(\frac{\omega^2}{\alpha_j^2} - k_1^2\right)^{\frac{1}{2}} = \frac{\omega}{\alpha_j}\left(1 - \frac{\alpha_j^2}{\alpha_1^2}\sin^2\varphi\right)^{\frac{1}{2}}. \tag{3.69}$$

If $\sin\varphi > \alpha_1/\alpha_j$, l_j is imaginary (and even *negative imaginary*), only then for $j = n$ is the amplitude of the potentials limited for $z \to \infty$. This leads to the following system of equations, which connects A_j and B_j with A_{j-1} and B_{j-1}, respectively

$$\begin{aligned} A_j - B_j &= \frac{l_{j-1}}{l_j}\left[A_{j-1}e^{-il_{j-1}d_{j-1}} - B_{j-1}e^{il_{j-1}d_{j-1}}\right] \\ A_j + B_j &= \frac{\rho_{j-1}}{\rho_j}\left[A_{j-1}e^{-il_{j-1}d_{j-1}} + B_{j-1}e^{il_{j-1}d_{j-1}}\right]. \end{aligned}$$

In matrix form, this can be written as (please check)

$$\begin{aligned} \begin{pmatrix} A_j \\ B_j \end{pmatrix} &= \frac{e^{-il_{j-1}d_{j-1}}}{2l_j\rho_j} \begin{pmatrix} l_{j-1}\rho_j + l_j\rho_{j-1} & (-l_{j-1}\rho_j + l_j\rho_{j-1})e^{2il_{j-1}d_{j-1}} \\ -l_{j-1}\rho_j + l_j\rho_{j-1} & (l_{j-1}\rho_j + l_j\rho_{j-1})e^{2il_{j-1}d_{j-1}} \end{pmatrix} \\ &\quad \cdot \begin{pmatrix} A_{j-1} \\ B_{j-1} \end{pmatrix} \\ &= m_j \cdot \begin{pmatrix} A_{j-1} \\ B_{j-1} \end{pmatrix} \end{aligned} \tag{3.70}$$

where m_j is the *layer matrix*.

Repeated application of (3.70) gives

$$\begin{aligned} \begin{pmatrix} A_n \\ B_n \end{pmatrix} &= \underline{m}_n \cdot \underline{m}_{n-1} \cdot \ldots \cdot \underline{m}_3 \cdot \underline{m}_2 \begin{pmatrix} A_1 \\ B_1 \end{pmatrix} \\ &= \underline{M} \begin{pmatrix} A_1 \\ B_1 \end{pmatrix} \\ &= \begin{pmatrix} M_{11}M_{12} \\ M_{21}M_{22} \end{pmatrix} \begin{pmatrix} A_1 \\ B_1 \end{pmatrix}. \end{aligned}$$

On computers, the product $\underline{M}$ of the layer matrices $\underline{m}_n$ to $\underline{m}_2$ can be determined quickly and efficiently. First, the angular frequency ω and the angle of incidence

φ are given; then, the l_j's are determined with (3.69), and the matrices are multiplied. This gives the elements of $\underline{M}$. From

$$A_n = M_{11}A_1 + M_{12}B_1 \text{ and } B_n = M_{21}A_1 + M_{22}B_1$$

with (3.66), it follows that

$$\frac{B_1}{A_1} = -\frac{M_{21}}{M_{22}} \text{ and } \frac{A_n}{A_1} = M_{11} - \frac{M_{12}M_{21}}{M_{22}}.$$

The reflection coefficient R_{pp} and the refraction coefficient Bpp of the layered medium, therefore, can be written according to (3.68) as

$$R_{pp} = -\frac{M_{21}}{M_{22}} \text{ and } B_{pp} = \frac{\alpha_1}{\alpha_n}\left(M_{11} - \frac{M_{12}M_{21}}{M_{22}}\right). \tag{3.71}$$

Two homogeneous half-spaces

In this very simple case, it follows (with $d_1 = 0$) that

$$\underline{M} = \underline{m}_2 = \frac{1}{2l_2\rho_2}\begin{pmatrix} l_1\rho_2 + l_2\rho_1 & -l_1\rho_2 + l_2\rho_1 \\ -l_1\rho_2 + l_2\rho_1 & l_1\rho_2 + l_2\rho_1 \end{pmatrix}$$

and, therefore, according to (3.71)

$$\begin{aligned} R_{pp} &= \frac{-l_2\rho_1 + l_1\rho_2}{l_2\rho_1 + l_1\rho_2} \\ B_{pp} &= \frac{\alpha_1}{\alpha_2}\frac{(l_1\rho_2 + l_2\rho_1)^2 - (l_2\rho_1 - l_1\rho_2)^2}{2l_2\rho_2(l_2\rho_1 + l_1\rho_2)} = \frac{\alpha_1}{\alpha_2}\frac{2l_1\rho_1}{l_2\rho_1 + l_1\rho_2}. \end{aligned}$$

With $l_1 = \frac{\omega}{\alpha_1}\cos\varphi$ and $l_2 = \frac{\omega}{\alpha_2}\left(1 - \frac{\alpha_2^2}{\alpha_1^2}\sin^2\varphi\right)^{\frac{1}{2}} = \frac{\omega}{\alpha_2}\cos\varphi_2$ (φ_2=angle of refraction), it follows that

$$\begin{aligned} R_{pp} &= \frac{\rho_2\alpha_2\cos\varphi - \rho_1\alpha_1\cos\varphi_2}{\rho_2\alpha_2\cos\varphi + \rho_1\alpha_1\cos\varphi_2} \\ B_{pp} &= \frac{2\rho_1\alpha_1\cos\varphi}{\rho_2\alpha_2\cos\varphi + \rho_1\alpha_1\cos\varphi_2} \end{aligned}$$

(compare with exercise 3.9). For $\varphi = 0\,(\rightarrow \varphi_2 = 0)$, it follows that

$$R_{pp} = \frac{\rho_2\alpha_2 - \rho_1\alpha_1}{\rho_2\alpha_2 + \rho_1\alpha_1} \text{ and } B_{pp} = \frac{2\rho_1\alpha_1}{\rho_2\alpha_2 + \rho_1\alpha_1}. \tag{3.72}$$

These are equations that also hold for an interface between two *solid* half-spaces.

Lamella in full-space

We limit our study here to *vertical reflections* from a lamella.

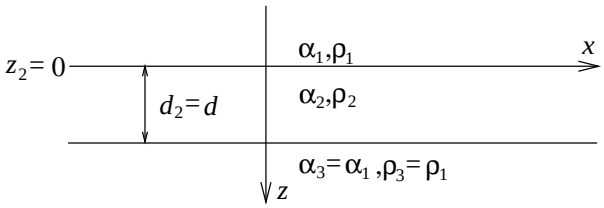

Fig. 3.34: Lamella of thickness d.

In this case, $n = 3, l_1 = l_3 = \omega/\alpha_1$ and $l_2 = \omega/\alpha_2$. Then with (3.70) and $d_1 = 0$, $d_2 = d$

$$\begin{aligned} \underline{m}_2 &= \frac{\alpha_2}{2\rho_2}\begin{pmatrix} \frac{\rho_2}{\alpha_1} + \frac{\rho_1}{\alpha_2} & -\frac{\rho_2}{\alpha_1} + \frac{\rho_1}{\alpha_2} \\ -\frac{\rho_2}{\alpha_1} + \frac{\rho_1}{\alpha_2} & \frac{\rho_2}{\alpha_1} + \frac{\rho_1}{\alpha_2} \end{pmatrix} \\ &= \frac{\alpha_2}{2\alpha_1}\begin{pmatrix} 1+\gamma & -1+\gamma \\ -1+\gamma & 1+\gamma \end{pmatrix} \end{aligned}$$

$$\underline{m}_3 = \frac{\alpha_1 e^{-i\omega\frac{d}{\alpha_2}}}{2\alpha_2}\begin{pmatrix} 1+\gamma' & (-1+\gamma')e^{2i\omega\frac{d}{\alpha_2}} \\ -1+\gamma' & (1+\gamma')e^{2i\omega\frac{d}{\alpha_2}} \end{pmatrix}$$

with $\gamma = \frac{\rho_1\alpha_1}{\rho_2\alpha_2}$ and $\gamma' = \frac{\rho_2\alpha_2}{\rho_1\alpha_1} = \frac{1}{\gamma}$. This leads to

$$\underline{M} = \underline{m}_3\underline{m}_2 = \frac{e^{-i\omega\frac{d}{\alpha_2}}}{4\gamma}\begin{pmatrix} (1+\gamma)^2 - (1-\gamma)^2 e^{2i\omega\frac{d}{\alpha_2}} & \gamma^2 - 1 + (1-\gamma^2)e^{2i\omega\frac{d}{\alpha_2}} \\ 1-\gamma^2 + (\gamma^2-1)e^{2i\omega\frac{d}{\alpha_2}} & -(1-\gamma)^2 + (1+\gamma)^2 e^{2i\omega\frac{d}{\alpha_2}} \end{pmatrix}.$$

We now compute the *reflection coefficient* R_{pp} (according to (3.71))

$$R_{pp} = -\frac{M_{21}}{M_{22}} = \frac{(1-\gamma^2)(1-e^{2i\omega\frac{d}{\alpha_2}})}{(1-\gamma)^2 - (1+\gamma)^2 e^{2i\omega\frac{d}{\alpha_2}}} = R_0\frac{1-e^{-2i\omega\frac{d}{\alpha_2}}}{1-R_0^2 e^{-2i\omega\frac{d}{\alpha_2}}} \tag{3.73}$$

with

$$R_0 = \frac{1-\gamma}{1+\gamma} = \frac{\rho_2\alpha_2 - \rho_1\alpha_1}{\rho_2\alpha_2 + \rho_1\alpha_1}.$$

R_0, according to (3.72), is the reflection coefficient of the interface $z = 0$. For relatively small reflection coefficients R_0, which are typical for discontinuities in the Earth ($|R_0| < 0.2$), one can write as a good approximation

$$R_{pp} = R_0 \left(1 - e^{-2i\omega \frac{d}{\alpha_2}}\right). \tag{3.74}$$

Discussion of R_{pp}

R_{pp}, in the form of (3.73) or (3.74), is zero for angular frequencies ω, for which $2\omega\frac{d}{\alpha_2}$ is an even multiple of π. With the frequency ν and the wave length Λ *in the lamella* ($\alpha_2 = \nu\Lambda$), the condition for destructive interference is

$$\frac{d}{\Lambda} = \frac{1}{2}, 1, \frac{3}{2}, 2, \ldots \tag{3.75}$$

The lamella has to have a thickness of a multiple of the half wave-length so that in *reflection destructive interference* occurs with $R_{pp} = 0$. In this case *refractions show constructive interference.*

According to (3.74), R_{pp} is maximum ($|R_{pp}| = 2\,|R_0|$) if $2\omega\frac{d}{\alpha_2}$ is an uneven multiple of π. Then

$$\frac{d}{\Lambda} = \frac{1}{4}, \frac{3}{4}, \frac{5}{4}, \frac{7}{4}, \ldots \tag{3.76}$$

In this case, the waves interfere *constructively for reflection* and *destructively for refraction.*

The periodicity of R_{pp}, visible in (3.75) and (3.76), holds generally so

$$R_{pp}\left(\omega + n\frac{\alpha_2\pi}{d}\right) = R_{pp}(\omega), \qquad n = 1, 2, 3, \ldots$$

To conclude, we discuss how the reflection from a lamella looks for an *impulsive excitation.* We assume that the vertically incident P-wave has the vertical displacement $w_0 = F\left(t - \frac{z}{\alpha_1}\right)$ and that $\overline{F}(\omega)$ is the spectrum of $F(t)$. The vertical displacement w_1 of the reflected wave is then (compare section 3.6.3)

$$w_1 = \frac{1}{2\pi}\int_{-\infty}^{+\infty} R_{pp}(\omega)\overline{F}(\omega)e^{i\omega\left(t+\frac{z}{\alpha_1}\right)}\,d\omega \tag{3.77}$$

with $R_{pp}(\omega)$ from (3.73). In practise, integral (3.77) is computed numerically, since fast numerical methods for *Fourier analysis* exist and computation of the spectrum from the time function ($\overline{F}(\omega)$ from $F(t)$) and *Fourier synthesis*, i.e., computation of the time function from its spectrum (w_1 from its spectrum

$R_{pp}(\omega)\overline{F}(\omega)e^{i\omega z/\alpha_1}$). Such numerical methods are known as *Fast Fourier transform (FFT)*.

Insight into the processes occurring during reflection, the topic of this chapter, can be achieved as follows: we expand (3.73) (which due to $R_0^2 < 1$ always converges)and get

$$\begin{aligned} R_{pp}(\omega) &= R_0\left(1-e^{-i\omega\frac{2d}{\alpha_2}}\right)\sum_{n=0}^{\infty}\left(R_0^2 e^{-i\omega\frac{2d}{\alpha_2}}\right)^n \\ &= R_0 - R_0\left(1-R_0^2\right)e^{-i\omega\frac{2d}{\alpha_2}} - R_0^3\left(1-R_0^2\right)e^{-i\omega\frac{4d}{\alpha_2}} \\ &\quad -R_0^5\left(1-R_0^2\right)e^{-i\omega\frac{6d}{\alpha_2}} - \ldots \end{aligned} \tag{3.78}$$

Substitution of this into (3.77) and taking the inverse transform of each element gives

$$\begin{aligned} w_1 &= R_0 F\left(t+\frac{z}{\alpha_1}\right) - R_0\left(1-R_0^2\right)F\left(t+\frac{z}{\alpha_1}-\frac{2d}{\alpha_2}\right) \\ &- R_0^3\left(1-R_0^2\right)F\left(t+\frac{z}{\alpha_1}-\frac{4d}{\alpha_2}\right) - R_0^5\left(1-R_0^2\right)F\left(t+\frac{z}{\alpha_1}-\frac{6d}{\alpha_2}\right) - \ldots \end{aligned} \tag{3.79}$$

The first term is the *reflection from the interface* $z = 0$. Its amplitude, as expected, is the reflection coefficient R_0 of this interface. The second term describes a wave which is delayed by twice the travel time through the lamella, thus, corresponding to the *reflection from the interface* $z = d$. Its amplitude has the expected size; the reflection coefficient of this interface is $-R_0$. The product of the reflection coefficients of the interface $z = 0$ for waves travelling in $+z-$ and $-z-$direction, $2\rho_1\alpha_1/(\rho_2\alpha_2+\rho_1\alpha_1)$ and $2\rho_2\alpha_2/(\rho_1\alpha_1+\rho_2\alpha_2)$, is $1-R_0^2$. In the same way, the third and fourth term of (3.79) can be interpreted as *multiple reflections* within the lamella (with three and five reflections, respectively). The terms in (3.79) correspond to the *rays* shown in Fig. 3.35.

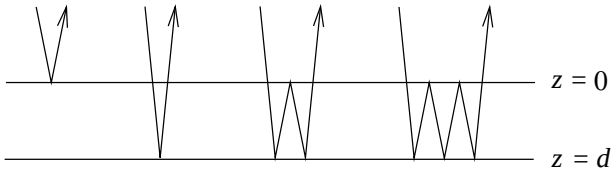

Fig. 3.35: Reflected and multiple reflected rays in a lamella.

Equation (3.79) is a decomposition of the reflected wave field in (infinite many) ray contributions. It is fully equivalent to (3.77).

The approximation (3.74) for $R_{pp}(\omega)$ corresponds to the truncation of the expansion in (3.78) after the term for $n = 0$ and, therefore, the limitation on the two *primary reflections* from the interfaces $z = 0$ and $z = d$, respectively (and neglecting R_0^2 relative to 1).

Exercise 3.10

Show that for the refraction coefficient in (3.71), it holds that

$$B_{pp} = \frac{\alpha_1}{\alpha_n} \frac{det\underline{M}}{M_{22}} \text{ with } det\underline{M} = \frac{l_1 \rho_1}{l_n \rho_n}.$$

Apply this formula in the lamella, in cases in which (3.75) and (3.76) hold.

Exercise 3.11

The P-velocity of the lamella is larger then that of the surrounding medium: $\alpha_2 > \alpha_1$. Does then total reflection occur? Discuss this qualitatively.

3.7 Reflectivity method: Reflection of spherical waves from layered media

3.7.1 Theory

The results of section 3.6.5 can, with relative ease, be extended to the excitation by spherical waves. For simplification of representation, we again assume that we deal, at the moment, only with P-waves in liquids.

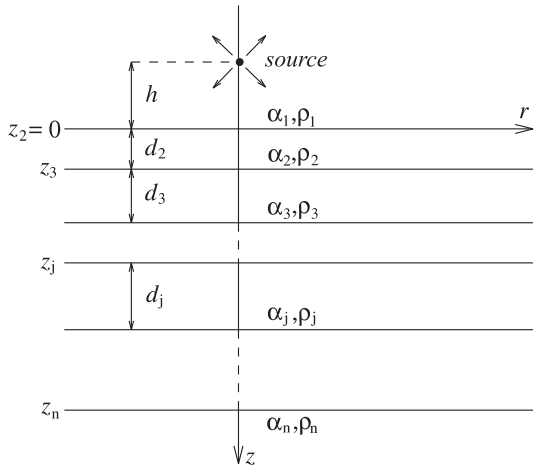

Fig. 3.36: Explosive point source over liquid, layered medium.

The spherical waves are excited by an explosion point source located at hight h above the layered medium. The displacement potential of this source for harmonic excitation is (compare section 3.4)

$$\Phi_{1e} = \frac{1}{R} e^{i\omega\left(t-\frac{R}{\alpha_1}\right)} \tag{3.80}$$

with $R^2 = r^2 + (z+h)^2$. Because of the symmetry under rotation around the z-axis, cylindrical coordinates r and z are used. The wave equation for the potential Φ_j in the j-th layer is

$$\frac{\partial^2 \Phi_j}{\partial r^2} + \frac{1}{r}\frac{\partial \Phi_j}{\partial r} + \frac{\partial^2 \Phi_j}{\partial z^2} = \frac{1}{\alpha_j^2}\frac{\partial^2 \Phi_j}{\partial t^2}. \tag{3.81}$$

Elementary solutions of this equation are (please check)

$$J_0(kr)\exp\left[i\left(\omega t \pm l_j\left(z - z_j\right)\right)\right] \text{ with } k^2 + l_j^2 = \frac{\omega^2}{\alpha_j^2}, l_j = \left(\frac{\omega^2}{\alpha_j^2} - k^2\right)^{\frac{1}{2}} \tag{3.82}$$

(compare section 3.6.5 for notation). $J_0(kr)$is the *Bessel function* of first kind and zeroth order (compare appendix C).

Equation (3.82) is an analogue to the solutions $e^{-ik_j x} \cdot e^{i(\omega t \pm l_j(z-z_j))}$ of the wave equation $\partial^2\Phi_j/\partial x^2 + \partial^2\Phi_j/\partial z^2 = (1/\alpha_j^2)\partial^2\Phi_j/\partial t^2$ discussed in the last chapter. In (3.82), the index j of the horizontal wavenumber k has been dropped, since k is a parameter over which one can integrate (furthermore, it was shown in section 3.6.5 that all k_j's are identical).

With (3.82), the functions

$$\int_0^\infty f(k) J_0(kr) e^{i(\omega t \pm l_j(z-z_j))} dk \tag{3.83}$$

are also solutions of (3.81) if the integral converges. Thus, we come to the potential ansatz

$$\Phi_j = \int_0^\infty J_0(kr)\left\{A_j(k)e^{i(\omega t - l_j(z-z_j))} + B_j(k)e^{i(\omega t + l_j(z-z_j))}\right\} dk. \tag{3.84}$$

Note the close relation of (3.84) to (3.64). Whether this ansatz actually has a solution, depends *firstly*, if Φ_{1e} from (3.80) can be represented in the integral form (3.83) and *secondly*, if Φ_j in (3.84) satisfies the boundary conditions for $z = z_2, z_3, \ldots z_n$.

The first requirement is satisfied since the following integral representation is valid (*Sommerfeld integral*, compare appendix D)

$$\frac{1}{R}e^{i\omega\left(t-\frac{R}{\alpha_1}\right)} = \int_0^\infty J_0(kr)\frac{k}{il_1}e^{i(\omega t - l_1|z+h|}dk. \tag{3.85}$$

We, therefore, can interpret the first part

$$\int_0^\infty J_0(kr)A_1e^{i(\omega t - l_1 z)}dk \tag{3.86}$$

of Φ_1 (with $z_1 = 0$) as the incident wave (see also section 3.6.5) Φ_{1e} (the second part is the reflected wave Φ_{1r}). We have to compare (3.85) and (3.86) for locations in which the spherical wave passes on incidence at the interface $z = 0$, i.e., for $-h < z \leq 0$. In this case, $|z + h| = z + h$ and the comparison gives $A_1(k) = (k/il_1)e^{-il_1h}$.

The *boundary conditions* for the interfaces can be taken from section 3.6.5. The potentials (3.84) are differentiated under the integral. The identity following from the boundary conditions is only satisfied *for all* r, if the integrands are identical. This leads to the same system of equations for $A_j(k)$ and $B_j(k)$ as in section 3.6.5, i.e., (3.70). In contrast to the previous section, the vertical wavenumbers l_j have to be considered now as functions of k (and not of the angle of incidence φ). k and φ are connected via

$$k = \frac{\omega}{\alpha_1}\sin\varphi. \tag{3.87}$$

Following section 3.6.5, the reflection coefficient $R_{pp} = B_1/A_1 = -M_{21}/M_{22}$ has been computed as a function of the angular frequency ω and angle of incidence φ;; then the dependence on k can be introduced via (3.87): $R_{pp} = R_{pp}(\omega, k)$.

The second part of Φ_1, the reflected wave, can then be written as

$$\begin{aligned}\Phi_{1r} &= \int_0^\infty J_0(kr)A_1(k)R_{pp}(\omega,k)e^{i(\omega t + l_1 z)}dk \\ &= \int_0^\infty \frac{k}{il_1}J_0(kr)R_{pp}(\omega,k)e^{i(\omega t + l_1(z-h))}dk.\end{aligned}$$

The corresponding vertical displacement is

$$w_{1r}(r,z,\omega,t) = \frac{\partial\Phi_{1r}}{\partial z} = e^{i\omega t}\int_0^\infty kJ_0(kr)R_{pp}(\omega,k)e^{il_1(z-h)}dk \tag{3.88}$$

and the horizontal displacement (with $J_0'(x) = -J_1(x)$)

$$u_{1r}(r,z,\omega,t) = \frac{\partial \Phi_{1r}}{\partial r} = e^{i\omega t} \int_0^\infty \frac{-k^2}{il_1} J_1(kr) R_{pp}(\omega,k) e^{il_1(z-h)} dk. \qquad (3.89)$$

The integrals in (3.88) and (3.89) are best computed numerically, especially, in the case of many layers. For *solid* media, (3.88) and (3.89) also hold, but the reflection coefficient $R_{pp}(\omega,k)$ is more complicated than for liquid media and w_{1r} and u_{1r} describe only the *compressional part* of the reflection from the layered half-space $z \geq 0$. For the *shear part*, similar results hold, which only now contain the reflection coefficients $R_{ps}(\omega,k)$.

The transition to *impulse excitation*

$$\Phi_{1e} = \frac{1}{R} F\left(t - \frac{R}{\alpha_1}\right)$$

instead of (3.80) is relatively simple (see section 3.6.3). If $\overline{F}(\omega)$ is the spectrum of $F(t)$, it holds that

$$\Phi_{1e} = \frac{1}{2\pi R} \int_{-\infty}^{+\infty} \overline{F}(\omega) e^{i\omega\left(t - \frac{R}{\alpha_1}\right)} d\omega.$$

The corresponding displacements of the reflected wave are

$$\left.\begin{matrix} W_{1r}(r,z,t) \\ U_{1r}(r,z,t) \end{matrix}\right\} = \frac{1}{2\pi} \int_{-\infty}^{+\infty} \overline{F}(\omega) \left\{\begin{matrix} w_{1r}(r,z,\omega,t) \\ u_{1r}(r,z,\omega,t) \end{matrix}\right\} d\omega \qquad (3.90)$$

with w_{1r} from (3.88) and u_{1r} from (3.89). The integrals in (3.88) and (3.89), multiplied by $\overline{F}(\omega)$, are, therefore, the *Fourier transforms of the displacement.*

The numerical computation of (3.88), (3.89) and (3.90) is called the *Reflectivity method*; it is a practical approach for the computation of *theoretical seismograms of body waves.* With it, the amplitudes of body waves from explosions and earthquakes can be studied, thus, progressing beyond the more classical *travel time interpretation.*

3.7.2 Reflection and head waves

An example for theoretical seismograms is given in Fig. 3.37 (from K. Fuchs: The reflection of spherical waves from transition zones with arbitrary depth-depended elastic moduli and density. Journ. of Physics of the Earth, vol. 16, Special Issue, S. 27-41, 1968). It is the result for a simple model of the crust, assumed to be homogeneous. The point source and the receivers are at the Earth's surface; the influence of which has been neglected here. The transition

of the crust to the upper mantle (*Mohorovičić-zone,* short *Moho*) is a first order *discontinuity*, i.e., the wave velocities and the density change abruptly (for a discontinuity of 2nd order these parameters would still be continuous, but their derivative with depth would have a jump).

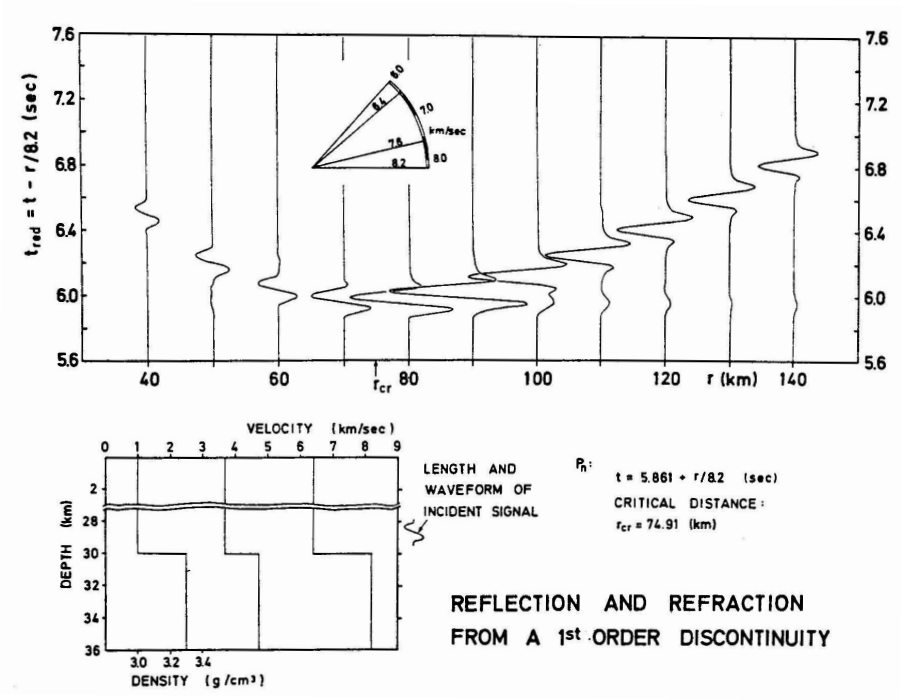

Fig. 3.37: Synthetic seismogram for reflection and refraction from a 1st order discontinuity (from K. Fuchs, 1968, Journ. of Physics of the Earth).

The dominant wave is the *reflection from the Moho.* For distances from the source beyond the *critical point* $r^* = 74.91$ km, corresponding to the *critical angle of incidence* φ^*, the first onset is the *head wave* with the apparent velocity of 8.2 km/sec. Its amplitude decays rapidly with increasing distance, and its form is the time integral of the reflection for $r < r^*$. For pre-critical distance r, the form of the reflection is practically identical to that of the incident wave. At the critical point, it begins to change its form. This was already discussed in section 3.6.3 in terms of the properties of the reflection coefficient for plane waves (this holds for *P*- and *SH*-waves, respectively). For large distances, the impulse form is roughly opposite to that for $r < r^*$. This is also expected, since the reflection coefficient R_{pp} for the angle of incidence $\varphi = \pi/2$ is equal to -1 (for liquids, this follows from the formulae given in section 3.5.6). The amplitude behaviour of the reflection is relatively similar to the trend of the absolute value $|R_{pp}|$ of the reflection coefficient, if $|R_{pp}|$ is divided by the path

length and if one considers the vertical component (see, e.g., Fig. 3.22 and corresponding equations). The main discrepancies are near the critical point. According to $|R_{pp}|$, the reflected wave should have its maximum directly at the critical point, whereas in reality, it is shifted to larger distances. This shift is larger, the lower the frequency of the incident wave.

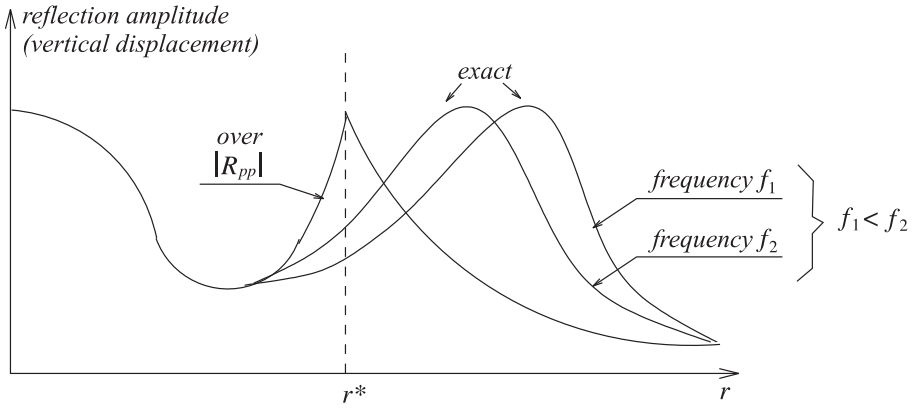

Fig. 3.38: Reflection amplitude versus offset as a function of frequency.

The consideration of this shift is important when determining the critical point from observed reflections, e.g., in reflection seismics.

3.7.3 Complete seismograms

Fig. 3.39 shows the *potential of the reflectivity method*. This shows complete *SH*-seismograms for a profile at the surface of a realistic Earth model. The source is a horizontal single force at the Earth's surface, acting perpendicular to the profile. The dominant period is 20 sec. The most pronounced phases are the dispersive Love waves (for surface waves, see chapter 4), whose amplitudes are mostly clipped. The propagation paths of the largest body wave phases (mantle wave S and SS, core reflection ScS and diffraction at the core S_{diff} are also sketched.) A detailed description of the reflectivity method is given in G. Müller: The reflectivity method: A tutorial, Journ. eophys,., vol. 58, 153-174, 1985.

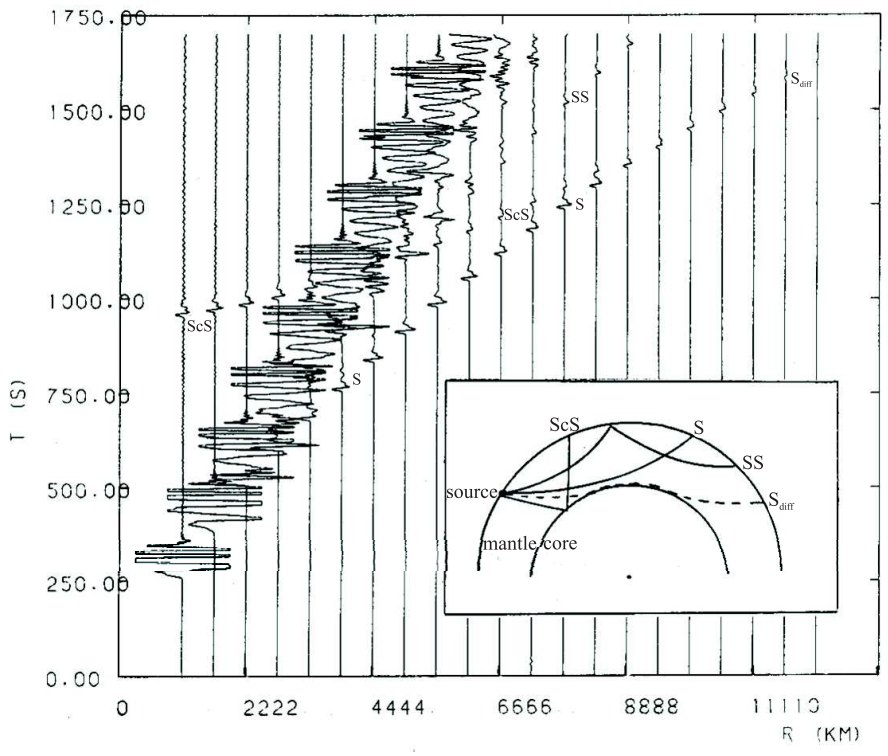

Fig. 3.39: Complete *SH*-seismograms for a profile at the surface of a realistic Earth model.

3.8 Exact or generalised ray theory - GRT

We continue the chapter on elastic body waves with the treatment of reflection and refraction of *cylindrical waves* radiated from a *line source* and reflected and refracted at a plane interface which is parallel to the line source. This problem is more simple and less practical than the case considered in section 3.7 of a point source over a layered medium. On the other hand, we will learn a totally different way of treating wave propagation which leads to relatively simple *analytical* (and not only numerically solvable) results. This is the main aim of this section. This method, originally developed by Cagniard, de Hoop and Garvin (see, e.g., W.W. Garvin: Exact transient solution of the buried line source problem, Proc. Roy. Soc. London, Ser. A, vol 234, pg. 528-541, 1956), can also be applied for layered media and be modified for point sources. In that form it is, similar to the reflectivity method, usable for the computation of theoretical body-wave seismograms in the interpretation of observations.

Again, we limit ourselves to treat the problem of a *liquid* model (see Fig. 3.40), since we can then study the main ideas with a minimum of computation.

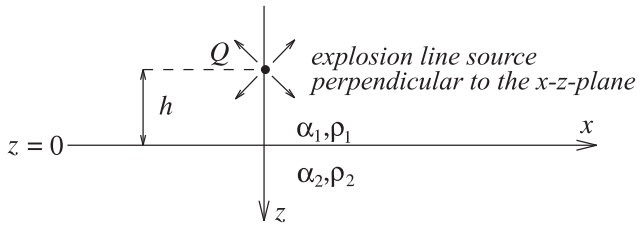

Fig. 3.40: Explosive line source in a liquid medium.

We work with the displacement potentials $\Phi_1 = \Phi_{1e} + \Phi_{1r}$ in half-space 1 ($\Phi_{1e} =$ incident, $\Phi_{1r} =$ reflected $P-$wave) and Φ_2 in half-space 2. The three potentials satisfy the wave equations

$$\nabla^2\Phi_{1e,r} = \frac{1}{\alpha_1^2}\frac{\partial^2\Phi_{1e,r}}{\partial t^2}, \qquad \nabla^2\Phi_2 = \frac{1}{\alpha_2^2}\frac{\partial^2\Phi_2}{\partial t^2}. \tag{3.91}$$

The Laplace transform of these equations gives

$$\nabla^2\varphi_{1e,r} = \frac{s^2}{\alpha_1^2}\varphi_{1e,r} \text{ and } \nabla^2\varphi_2 = \frac{s^2}{\alpha_2^2}\varphi_2, \tag{3.92}$$

where $\varphi_{1e}, \varphi_{1r}$ and φ_2 are the transforms of Φ_{1e}, Φ_{1r} and Φ_2, respectively, and s is the transform variable (see appendix A). We assume that the P-wave starts at time t=0 at the line source. Therefore, the initial values of Φ_{1e}, Φ_{1r} and Φ_2, and their time derivatives for t=+0, are zero outside the line source. The time derivatives have to be considered in the second derivative with respect to t in (3.91).

3.8.1 Incident cylindrical wave

First, we have to study the incident wave. Since the line source is explosive and has, therefore, cylindrical symmetry around its axis, it holds that

$$\nabla^2\varphi_{1e} = \frac{\partial^2\varphi_{1e}}{\partial R^2} + \frac{1}{R}\frac{\partial\varphi_{1e}}{\partial R} = \frac{s^2}{\alpha_1^2}\varphi_{1e} \tag{3.93}$$

with $R^2 = x^2 + (z+h)^2$. The solution of (3.93), which can be interpreted as a cylindrical wave in +R direction, is

$$\varphi_{1e} = f(s)\frac{1}{s}K_0(\frac{R}{\alpha_1}s), \tag{3.94}$$

where $f(s)$ is the Laplace transform of an arbitrary time function *F(t)* and $K_0(\frac{R}{\alpha_1}s)$ is one of the *modified Bessel functions* of zeroth order.

Proof: Using the substitution $x = \frac{R_s}{\alpha_1}$, (3.93) can be expressed as the differential equations of the modified Bessel function

$$x^2\frac{d^2y}{dx^2} + x\frac{dy}{dx} - (x^2 + n^2)y = 0.$$

In the case considered here, n=0. The differential equation has two independent linear solutions, $K_0(x)$ and $I_0(x)$, respectively. For real x, Fig. 3.41 shows their qualitative behaviour.

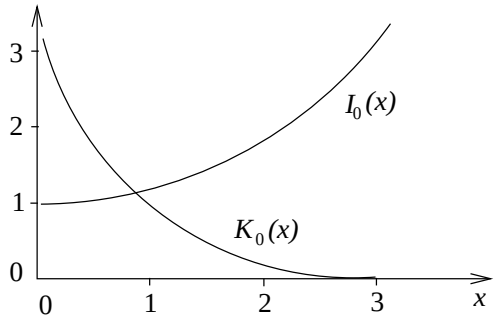

Fig. 3.41: Behaviour of linear solutions $K_0(x)$ and $I_0(x)$.

This shows that only $K_0(x)$ is a possible solution, since $I_0(x)$ grows infinitely for $x \to \infty$. (*Reference*: M. Abramovitz and I.A. Stegun: Handbook of Mathematical Functions, H. Deutsch, Frankfurt, 1985).

Taking the inverse Laplace transform of (3.94) in the time domain, and using the correspondence

$$\begin{array}{rcl} f(s) & \bullet\!\!-\!\!\circ & F(t) \qquad (F(t) \equiv 0 \text{ for } t < 0) \\ \frac{1}{s}K_0\left(\frac{R}{\alpha_1}s\right) & \bullet\!\!-\!\!\circ & \left\{ \begin{array}{lll} 0 & \text{for} & t < R/\alpha_1 \\ \cos h^{-1}(\frac{\alpha_1 t}{R}) & \text{for} & t > R/\alpha_1 \end{array} \right. \end{array}$$

with a typical behaviour of the solution given in Fig. 3.42;

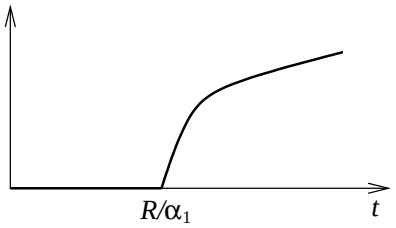

Fig. 3.42: Behaviour of the solution.

the potential can be written as

$$\Phi_{1e} = \int_{R/\alpha_1}^{t} F(t-\tau)\cos h^{-1}(\frac{\alpha_1 \tau}{R})d\tau \qquad (t \geq R/\alpha_1). \tag{3.95}$$

By varying *F(t)*, the cylindrical wave can be given different time dependencies. Equation (3.95) is the analogue to the potential $\Phi_{1e} = \frac{1}{R}F\left(t - \frac{R}{\alpha_1}\right)$ of a spherical wave from an explosive point source.

In the following, we treat the *special case* $F(t) = \delta(t)$, for which all important effects can be studied. If realistic excitations have to be treated, the results for the potentials and displacements of the reflected and diffracted waves, respectively, derived with time dependent $F(t) = \delta(t)$, have to be convolved with realistic *F(t)*. For $F(t) = \delta(t)$

$$\Phi_{1e} = \cosh^{-1}(\frac{\alpha_1 t}{R}),$$

and the corresponding radial displacement in R-direction is

$$U_R = \frac{\partial \Phi_{1e}}{\partial R} = -\frac{t}{R\left(t^2 - \frac{R^2}{\alpha_1^2}\right)^{1/2}} \qquad (t > \frac{R}{\alpha_1}). \tag{3.96}$$

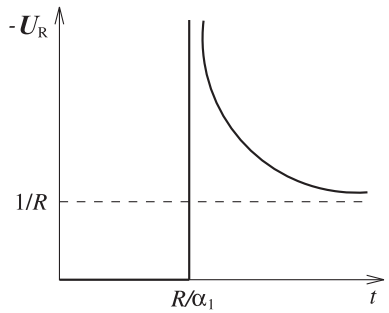

Fig. 3.43: Displacement in R direction.

The corresponding point source results are

$$\begin{aligned} \Phi_{1e} &= \frac{1}{R} H\left(t - \frac{R}{\alpha_1}\right) \\ U_R &= \frac{\partial \Phi_{1e}}{\partial R} = -\frac{1}{R^2} H\left(t - \frac{R}{\alpha_1}\right) - \frac{1}{R\alpha_1} \delta\left(t - \frac{R}{\alpha_1}\right). \end{aligned}$$

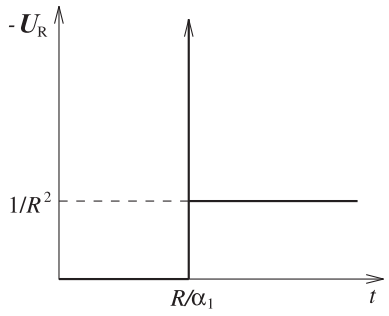

Fig. 3.44: Displacement in R direction.

3.8.2 Wavefront approximation for U_R

If we write (3.96) as

$$U_R = \frac{-t}{R\left(t + \frac{R}{\alpha_1}\right)^{1/2}\left(t - \frac{R}{\alpha_1}\right)^{1/2}},$$

and consider values of t near $\frac{R}{\alpha_1}$, we find the approximation

$$U_R \approx \frac{-1}{(2R\alpha_1)^{1/2}} \cdot \frac{1}{\left(t - \frac{R}{\alpha_1}\right)^{1/2}}. \tag{3.97}$$

This approximation is more accurate the closer t is to R/α_1, and, therefore, this is called *wavefront approximation*. It is more accurate for large R, and it is, therefore, also the *far-field approximation* of the cylindrical wave.

Within the framework of the wavefront approximation (3.97), the *impulse form* of the cylindrical wave is independent from R, and its amplitude is proportional to $R^{-1/2}$. Both statements become especially obvious if (3.97) is convolved with realistic excitation functions $F(t)$. The singularity in (3.96) and (3.97) is integrable.

3.8.3 Reflection and refraction of the cylindrical wave

The coordinates most appropriate for the study of reflection and refraction are the Cartesian coordinates x and z. Equation (3.92), then, takes the form

$$\frac{\partial^2\varphi}{\partial x^2}+\frac{\partial^2\varphi}{\partial z^2}=\frac{s^2}{\alpha^2}\varphi.$$

Appropriate elementary solutions have the form $\cos(kx)\exp(\pm imz)$ with $k^2+m^2=-s^2/\alpha^2$. From these elementary solutions, more complicated solutions in integral form (similar to section 3.7.1) can be constructed

$$\varphi=\int_0^\infty f(k)\cos(kx)e^{\pm imz}dk,$$

with which we can try to satisfy *firstly*, the potential (3.94) of the incident wave, and *secondly*, the boundary conditions for z = 0. Specifically, we use the following ansatz

$$\left.\begin{array}{lcll}\varphi_{1e} & = & \int_0^\infty A_1(k)\cos(kx)e^{-im_1z}dk & (z>-h)\\ \varphi_{1r} & = & \int_0^\infty B_1(k)\cos(kx)e^{im_1z}dk & \\ \varphi_2 & = & \int_0^\infty A_2(k)\cos(kx)e^{-im_2z}dk & \end{array}\right\} \qquad (3.98)$$

$$m_{1,2}=-i\left(k^2+\frac{s^2}{\alpha_{1,2}^2}\right)^{1/2} \quad \text{(negative imaginary for positive radicands).}$$

For $K_0\left(\frac{R}{\alpha_1}s\right)$ in (3.94) an integral representation, similar to (3.85) for the spherical wave, can be found. With this φ_{1e} (with *f(s)*=1, since $F(t)=\delta(t)$) it follows that

$$\varphi_{1e}=\frac{1}{s}\int_0^\infty\frac{1}{\left(k^2+\frac{s^2}{\alpha_1^2}\right)^{1/2}}\cos(kx)\exp\left[-|z+h|\left(k^2+\frac{s^2}{\alpha_1^2}\right)^{1/2}\right]dk. \qquad (3.99)$$

A comparison with φ_{1e} from (3.98) for z>-h gives

$$A_1(k)=\frac{e^{-im_1h}}{ism_1}.$$

The boundary conditions for z=0 are (compare section 3.6.5)

$$\frac{\partial}{\partial z}\left(\Phi_{1e}+\Phi_{1r}\right)=\frac{\partial \Phi_2}{\partial z}, \qquad \rho_1\frac{\partial^2}{\partial t^2}\left(\Phi_{1e}+\Phi_{1r}\right)=\rho_2\frac{\partial^2 \Phi_2}{\partial t^2}.$$

The Laplace transform gives

$$\frac{\partial}{\partial z}\left(\varphi_{1e}+\varphi_{1r}\right)=\frac{\partial \varphi_2}{\partial z}, \qquad \rho_1\left(\varphi_{1e}+\varphi_{1r}\right)=\rho_2\varphi_2.$$

From (3.98), it follows that

$$\begin{aligned} m_1\left(A_1(k)-B_1(k)\right) &= m_2A_2(k) \\ \rho_1\left(A_1(k)+B_1(k)\right) &= \rho_2A_2(k), \end{aligned}$$

and from this

$$B_1(k)=R_{pp}(k)A_1(k) \text{ and } A_2(k)=B_{pp}(k)A_1(k)$$

.

Thus,

$$R_{pp}(k) = \frac{\rho_2m_1-\rho_1m_2}{\rho_2m_1+\rho_1m_2} \text{ and } B_{pp}(k)=\frac{2\rho_1m_1}{\rho_2m_1+\rho_1m_2}. \tag{3.100}$$

The potentials φ_{1r} and φ_2 are, therefore,

$$\begin{aligned} \varphi_{1r} &= \int_0^\infty A_1(k)R_{pp}(k)\cos(kx)e^{im_1z}dk \\ \varphi_2 &= \int_0^\infty A_1(k)B_{pp}(k)\cos(kx)e^{-im_2z}dk. \end{aligned}$$

The Laplace transforms w and u of the vertical and horizontal displacement W and U, respectively, can, in general, be written as $w=\frac{\partial\varphi}{\partial z}$ and $u=\frac{\partial\varphi}{\partial x}$

and specifically

$$\left.\begin{array}{l} w_{1r} \\ u_{1r} \\ w_2 \\ u_2 \end{array}\right\} = \left.\begin{array}{l} \int_0^\infty \frac{R_{pp}(k)}{sim_1}\left\{\begin{array}{l} im_1\cos(kx) \\ -k\sin(kx) \end{array}\right\}e^{-im_1(h-z)}dk \\ \int_0^\infty \frac{B_{pp}(k)}{sim_1}\left\{\begin{array}{l} -im_2\cos(kx) \\ -k\sin(kx) \end{array}\right\}e^{-i(m_2z+m_1h)}dk. \end{array}\right\} \tag{3.101}$$

These Laplace transforms must now be *transformed back*. This is impossible with (A.9) in appendix A. One, rather, uses an approach that is based in transforming (3.101) several times with function theory methods until the integrals are of the form

$$\left.\begin{matrix} w \\ u \end{matrix}\right\} = \int_0^\infty Z(t) e^{-st} dt. \tag{3.102}$$

The inverse $\left\{ \begin{matrix} W(t) \\ U(t) \end{matrix} \right\} = Z(t)$ can then be identified *directly*.

An important limitation has to be mentioned first: we only consider *positive real s*, i.e., we do not consider the whole convergence half-plane of the Laplace transform, but only the positive real axis. This simplifies the computations significantly, without limitation of its generality, since the Laplace transform is an analytical function. It is, therefore, determined in the whole convergence half-plane by its values on the real axis, where the integral (3.101) is real.

With $\cos(kx) = Re(e^{-ikx})$ and $\sin(kx) = Re(ie^{-ikx})$, (3.101) can be written as

$$\left.\begin{matrix} w_{1r} \\ u_{1r} \\ w_2 \\ u_2 \end{matrix}\right\} = Re \left\{ \begin{matrix} \int_0^\infty \frac{R_{pp}(k)}{sm_1} \left\{ \begin{matrix} m_1 \\ -k \end{matrix} \right\} e^{-i(kx+m_1(h-z))} dk \\ \int_0^\infty \frac{B_{pp}(k)}{sm_1} \left\{ \begin{matrix} -m_2 \\ -k \end{matrix} \right\} e^{-i(kx+m_1 h+m_2 z)} dk \end{matrix} \right\}. \tag{3.103}$$

The next step is a change of the integration variables

$$u = \frac{ik}{s}$$

so that the integration path is now along the positive imaginary u-axis. The transformation of the square root $m_{1,2}$ gives

$$\begin{aligned} m_{1,2} &= -i \left(-s^2 u^2 + \frac{s^2}{\alpha_{1,2}^2} \right)^{1/2} = -is \left(-u^2 + \alpha_{1,2}^{-2} \right)^{1/2} \\ &= -s \left(u^2 - \alpha_{1,2}^{-2} \right)^{1/2} = -s a_{1,2} \end{aligned}$$

with

$$a_{1,2} = \left(u^2 - \alpha_{1,2}^{-2} \right)^{1/2}. \tag{3.104}$$

The transformed integration path is, therefore, in the sheet of the *Riemann plane* of the square root $a_{1,2}$, in which $a_{1,2} \simeq u$ for $|u| \to \infty$ holds (and not in the sheet with $a_{1,2} \simeq -u$). Introducing (3.104) in (3.100), gives

$$R_{pp}(u) = \frac{\rho_2 a_1 - \rho_1 a_2}{\rho_2 a_1 + \rho_1 a_2} \text{ and } B_{pp}(u) = \frac{2\rho_1 a_1}{\rho_2 a_1 + \rho_1 a_2}. \tag{3.105}$$

With $k = -isu$ and $dk = -isdu$, it follows from (3.103)

$$\left.\begin{matrix} w_{1r} \\ u_{1r} \end{matrix}\right\} = Re \int_0^{+i\infty} R_{pp}(u) \left\{ \begin{matrix} -i \\ -\frac{u}{a_1} \end{matrix} \right\} e^{-s(ux - ia_1(h-z))} du \tag{3.106}$$

$$\left.\begin{matrix} w_2 \\ u_2 \end{matrix}\right\} = Re \int_0^{+i\infty} B_{pp}(u) \left\{ \begin{matrix} i\frac{a_2}{a_1} \\ -\frac{u}{a_1} \end{matrix} \right\} e^{-s(ux - ia_1 h - ia_2 z)} du. \tag{3.107}$$

These expressions already have a certain similarity with (3.102) since s only occurs in the exponential term. The next step is, therefore, a new change in the integration variable

in (3.106)

$$t = ux - ia_1(h - z) \tag{3.108}$$

in (3.107)

$$t = ux - ia_1 h - ia_2 z. \tag{3.109}$$

From both equations, u has to be determined as a function of t and has to be inserted in (3.106) and (3.107), respectively. This will be discussed later in more detail. At the same time, the integration path has to be transformed accordingly. For $u = 0$, it follows from (3.108) and (3.109), respectively, that

$$\left.\begin{matrix} t(0) = t_0 = \frac{h-z}{\alpha_1} \\ t(0) = t_0 = \frac{h}{\alpha_1} + \frac{z}{\alpha_2}. \end{matrix}\right\} \tag{3.110}$$

The transformed integration paths C_1 (for (3.106)) and C_2 (for (3.107)), respectively, start on the positive real t-axis. For $u \to +i\infty$, they approach an asymptote in the first quadrant which passes through the centre of the coordinate system and has the slope $\tan\gamma = x/(h - z)$ (for the case (3.108)) and $\tan\gamma = x/(h + z)$ (for the case (3.109)). In (3.108), z is always negative in (3.109) always positive. The transformed integration paths are shown in Fig. 3.45.

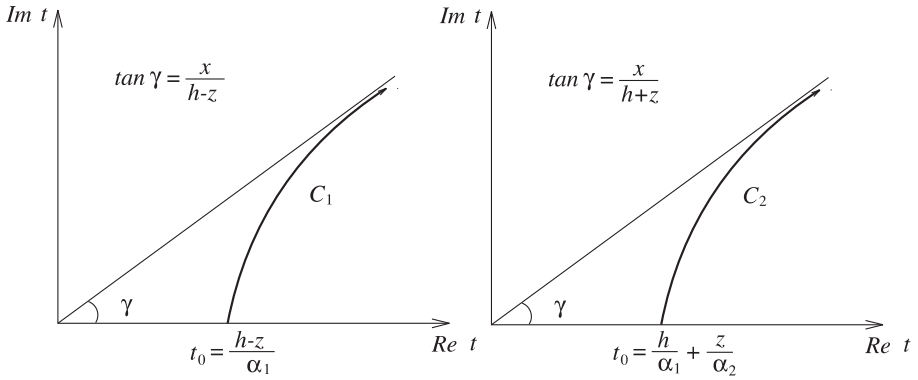

Fig. 3.45: Transformed integration paths.

In the case of the reflected wave (left in Fig. 3.45), C_1 is part of a hyperbola; in the case of the refracted wave, C_1 is part of a curve of higher order which is similar to a hyperbola. We then get

$$\left.\begin{matrix} w_{1r} \\ u_{1r} \end{matrix}\right\} = Re \int_{C_1} R_{pp}(u(t)) \left\{ \begin{matrix} -i \\ -\frac{u(t)}{a_1(u(t))} \end{matrix} \right\} \frac{du}{dt} e^{-st} dt \qquad (3.111)$$

$$\left.\begin{matrix} w_2 \\ u_2 \end{matrix}\right\} = Re \int_{C_2} B_{pp}(u(t)) \left\{ \begin{matrix} \frac{ia_2(u(t))}{a_1(u(t))} \\ -\frac{u(t)}{a_1(u(t))} \end{matrix} \right\} \frac{du}{dt} e^{-st} dt. \qquad (3.112)$$

The last step is now to deform the paths C_1 and C_2 towards the real axis according to *Cauchy's integral*. The path $C_{1,2}$ can now be replaced by the path $\overline{C}_{1,2} + C'_{1,2}$ in Fig. 3.46 if no poles of the integrands in (3.111) and (3.112) are located inside the two paths.

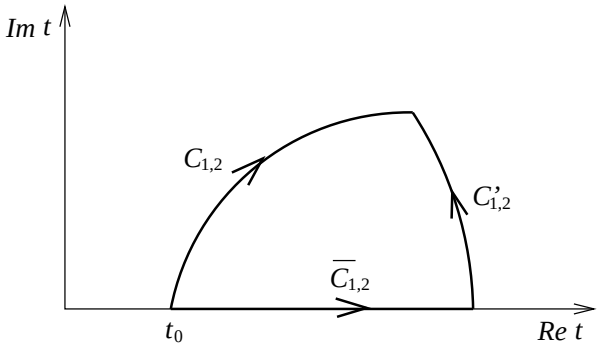

Fig. 3.46: Integration paths in the complex plane.

This is satisfied because the only singularities of a_1 and a_2 are the *branch points* $u = \pm\alpha_1^{-1}$ and $u = \pm\alpha_2^{-1}$, respectively, and these branch points are integrable singularities and not poles. Finally, the contribution of the curve $C'_{1,2}$ goes to zero if its radius becomes infinite. Thus,

$$\left.\begin{matrix} w_{1r} \\ u_{1r} \end{matrix}\right\} = \int_{\frac{h-z}{\alpha_1}}^{\infty} Re\left[R_{pp}(u(t))\left\{\begin{matrix} -i \\ -\frac{u(t)}{a_1(u(t))} \end{matrix}\right\}\frac{du}{dt}\right] e^{-st}dt + \int_0^{\frac{h-z}{\alpha_1}} [0]\, e^{-st}dt \tag{3.113}$$

$$\left.\begin{matrix} w_2 \\ u_2 \end{matrix}\right\} = \int_{\frac{h}{\alpha_1}+\frac{z}{\alpha_2}}^{\infty} Re\left[B_{pp}(u(t))\left\{\begin{matrix} \frac{ia_2(u(t))}{a_1(u(t))} \\ -\frac{u(t)}{a_1(u(t))} \end{matrix}\right\}\frac{du}{dt}\right] e^{-st}dt + \int_0^{\frac{h}{\alpha_1}+\frac{z}{\alpha_2}} [0]\, e^{-st}dt. \tag{3.114}$$

In these expressions, only the real part of the square brackets has to be considered since e^{-st} is real and the integration is only over real t. The addition of the second integral with vanishing contribution was only done for formal reasons, to allow integration over t from 0 to ∞ according to (3.102). Equation (3.113) and (3.114) have, therefore, the standard form of a Laplace transform, from which the original function can be read *directly*. The displacements W_{1r} and U_{1r} of the reflected wave are, therefore, zero between the time 0 and $(h-z)/\alpha_1$. This is not surprising since $(h-z)/\alpha_1$ is the travel time from the source perpendicular down to the reflecting interface and back to level z of the source. This time is, therefore, smaller, or at most equal, to the travel time of the first reflected onsets at this point. For $t > (h-z)/\alpha_1$ it holds that

$$\left.\begin{matrix} W_{1r} \\ U_{1r} \end{matrix}\right\} = Re\left[R_{pp}(u(t))\left\{\begin{matrix} -i \\ -\frac{u(t)}{a_1(u(t))} \end{matrix}\right\}\frac{du}{dt}\right] \tag{3.115}$$

with $u(t)$ from (3.108).

Similarly, the displacements W_2 and U_2 of the diffracted wave for $0 \le t < h/\alpha_1 + z/\alpha_2$ are zero, and for $t > h/\alpha_1 + z/\alpha_2$, it holds that

$$\left.\begin{matrix} W_2 \\ U_2 \end{matrix}\right\} = Re\left[B_{pp}(u(t))\left\{\begin{matrix} \frac{ia_2(u(t))}{a_1(u(t))} \\ -\frac{u(t)}{a_1(u(t))} \end{matrix}\right\}\frac{du}{dt}\right] \tag{3.116}$$

with $u(t)$ from (3.109).

All that is needed to calculate these relatively simple *algebraic functions*, is the solutions of (3.108) and (3.109), with respect of u as a function of real times

$t > t_0$ (from (3.110)) and the knowledge of the derivative $\frac{du}{dt}$. In the case of (3.108), this is very easy since here u can be given explicitly

$$u(t) = \begin{cases} \frac{x}{\overline{R}^2} t - \frac{h-z}{\overline{R}^2} \left(t_1^2 - t^2\right)^{\frac{1}{2}} & \text{for } \frac{h-z}{\alpha_1} \le t \le t_1 = \frac{\overline{R}}{\alpha_1} \\ \frac{x}{\overline{R}^2} t + i \frac{h-z}{\overline{R}^2} \left(t^2 - t_1^2\right)^{\frac{1}{2}} & \text{for } t > t_1. \end{cases} \tag{3.117}$$

$\overline{R} = \left(x^2 + (h-z)^2\right)^{1/2}$ is the distance of the source point from its mirror image, i.e., from the point with the coordinates $x = 0$ and $z = +h$; $t_1 = \overline{R}/\alpha_1$ is, according to *Fermat's principle*, the travel time of the actual reflection from the interface. The curve of $u(t)$ is given in Fig. 3.47. The derivative du/dt can be computed directly from (3.117). It has a singularity at $t = t_1$.

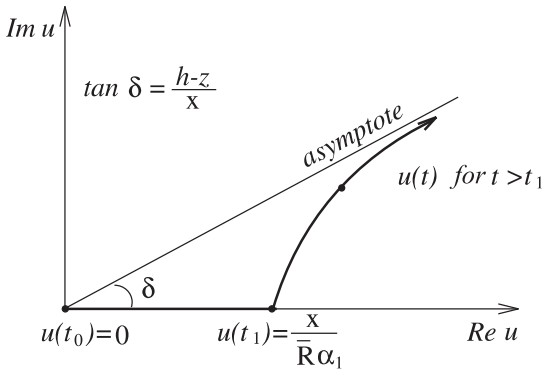

Fig. 3.47: The path of $u(t)$ in the complex plane.

In the case of the refracted wave, $u(t)$ has to be computed numerically with a similar curve as for the reflected wave (Fig. 3.47).

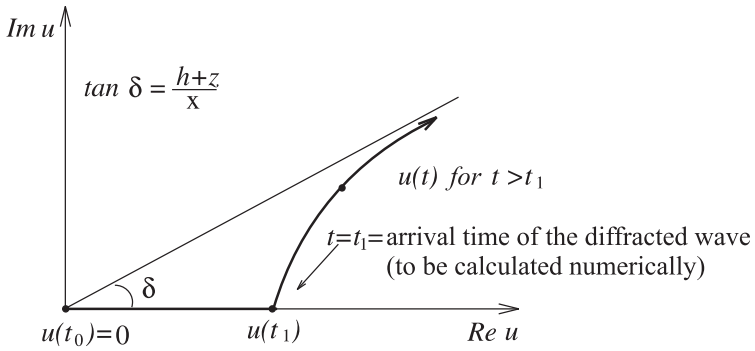

Fig. 3.47: The path of $u(t)$ for the refracted wave in the complex plane.

The numerical computations of *u(t)*, and its derivative, are possible without a large effort. In the following section, we focus on the reflected wave using (3.115) and (3.117).

3.8.4 Discussion of reflected wave types

We assume that the P-velocity in the lower half-space is larger than that of the upper half-space containing the line source; $\alpha_2 > \alpha_1$. First, we consider receivers $P(x,z)$ for which $u(t_1) = x/(\overline{R}\alpha_1) < \alpha_2^{-1}$. Since $x/\overline{R} = \sin\varphi$ (φ= angle of incidence), this means that $\sin\varphi < \alpha_1/\alpha_2 = \sin\varphi^*$ (φ^*= critical angle of incidence), and this implies *pre-critical incidence of the cylindrical wave.*

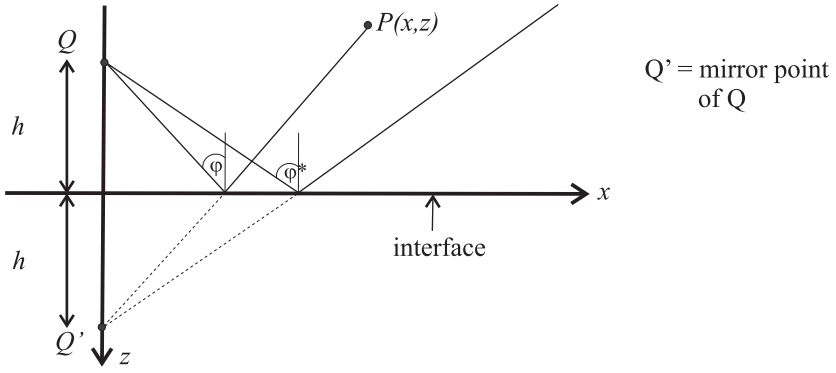

Fig. 3.49: Sketch for line source and its mirror point.

In this case, *u(t)* for $t < t_1$ is smaller than α_2^{-1} and, thus, even smaller than α_1^{-1}. Therefore, $a_1(u(t))$ and $a_2(u(t))$, according to (3.104), are positive imaginary, and $R_{pp}(u(t))$, according to (3.105), is real. Since du/dt is real for the times considered, it follows with (3.115) that the real part of the square brackets for all $t < t_1$ is zero. For $t > t_1$, $u(t)$ becomes complex, and the real part is non-zero. Not surprisingly, the displacement, therefore, starts at $t = t_1$.

If $\alpha_1 < \alpha_2$, this argument holds for arbitrary receiver locations in the upper half-space.

If $u(t_1) = x/(\overline{R}\alpha_1) > \alpha_2^{-1}$, the *angle of incidence φ is larger than the angle φ^**, and we expect a *head wave* as the first onset. In this case, $a_2(u(t))$ becomes real at the time t_2 which is defined via $u(t_2) = \alpha_2^{-1}$. The same does not hold for $a_1(u(t))$. Thus, $R_{pp}(u(t))$ has non-zero real and imaginary parts for $t > t_2$, and, therefore, (3.115) is already non-zero for $t > t_2$. Putting $u = \alpha_2^{-1}$ in (3.108), it follows that

$$t_2 = \frac{x}{\alpha_2} + (h - z)(\alpha_1^{-2} - \alpha_2^{-2})^{\frac{1}{2}} < t_1.$$

This is the arrival time of the head wave as expected according to Fermat's principle for the ray path from Q to P(x,z) in Fig. 3.50.

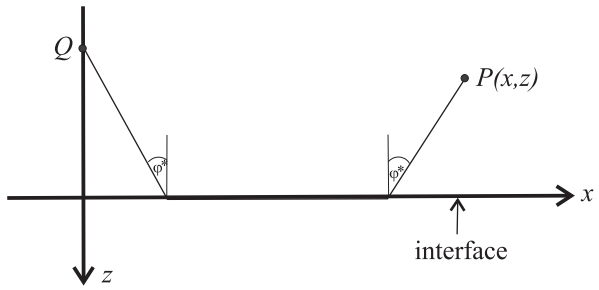

Fig. 3.50: Path of head wave from source Q to receiver P.

Considering this case at time $t = t_1$, we expect, due to the sudden change in the curve on which *u(t)* propagates, significant changes in the displacement (3.115), i.e., that the *reflection proper* gives a significant signal, and this is something which indeed can be observed.

Our derivation has shown that the head wave, and also the reflection, can be derived from the potential Φ_{1r}, i.e., no separate description was necessary for the head wave. If we had studied solid media, we, possibly, could have identified a second arrival which is an additional interface or boundary wave (P to S conversion) (compare, e.g., the work by Garvin quoted earlier). In section 3.7 (see head wave in Fig. 3.37), we encountered a similar situation in that the head wave was included in the solution. Both methods (reflectivity method in section 3.7 and GRT this section) give a complete solution unless simplifications for numerical reasons are introduced.

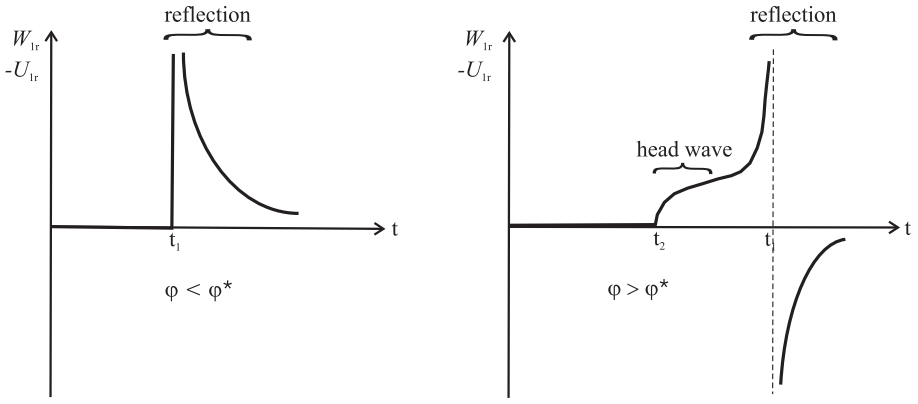

Fig. 3.51: Sketch of the displacement (in horizontal and vertical direction) for pre-critical (left) and post-critical (right) incidence, respectively.

For $t \to \infty$, the limit of the displacement is non-zero, as for the case of the incident wave (compare (3.96)). The singularities at $t = t_1$ are always integrable. Therefore, convolution with a realistic excitation function *F(t)* is always possible. On the right side of Fig. 3.51, the displacement starts before the reflection proper arriving at t_1. Fermat's principle, therefore, does not give exactly the arrival time of the first onset in the case where the reflection is not *the first arrival.*

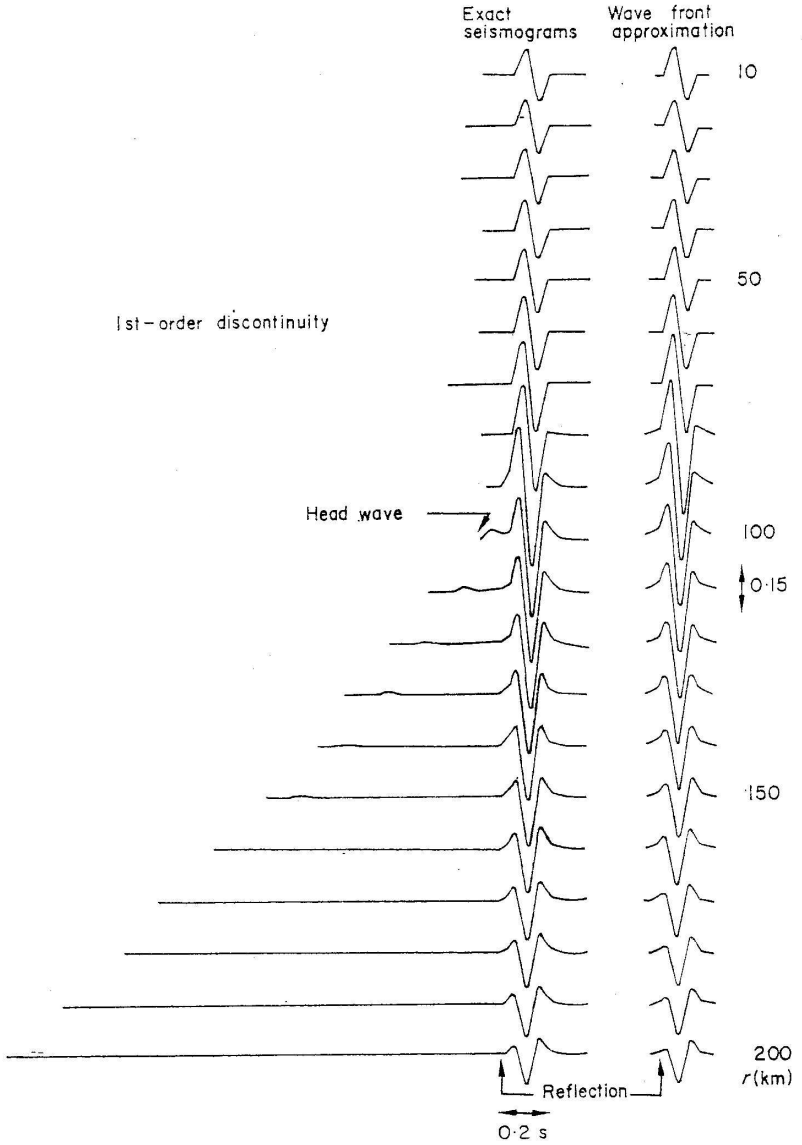

Fig. 3.52: Theoretical seismograms (vertical displacement) for a crustal model. Parameters: $\alpha_1 = 6,4$km/s, $\alpha_2 = 8,2$ km/s, $\rho_1 = 3,0$ g/cm^3, $\rho_2 = 3.3$ g/cm^3, h = 30 km, z = -30 km. On the left, the exact seismograms (GRT) and on the right a wavefront approximation is shown. From G. Müller: Exact ray theory and its application to the reflection of elastic waves from vertically inhomogeneous media, Geophys. Journ. R.A.S. 21, S. 261-283, 1970.

For realistic *F(t)*, this discrepancy is usually small. A full example using the theory of this section, is given in Fig. 3.50b. For a description of the different wave types *etc.*, see also section 3.7.2.

In the case of a layered medium with *more than one interface*, the wave field can be broken into separate ray contributions, as was done for the lamella in section 3.6.5. For each ray contribution, a formula of the type of (3.115) or (3.116) can be given, which can contain head or boundary wave contributions. This is the reason for the name "exact or generalised ray theory". Another common name is the "Cagniard-de Hoop-method".

Exercise 3.12:

Give wavefront approximations for the reflected wave and head wave, i.e., expand (3.115) around the arrival times t_1 (of the reflection) and t_2 (of the head wave), respectively. Distinguish between *slowly* varying contributions, which can be replaced by their values for $t = t_1$ and $t = t_2$, respectively, and *rapidly* varying terms, which depend on $t - t_1$, $t_1 - t$ and $t - t_2$, respectively.

3.9 Ray seismics in continuous inhomogeneous media

With the reflectivity method and the GRT, we have discussed wave-seismic methods, which if applied in *continuous inhomogeneous* media (in our case vertically inhomogeneous media), require a segmentation in homogeneous regions (in our case homogeneous layers). Wave-seismic methods for continuous inhomogeneous media, without this simplified representation of real media, are often more complicated (compare example in section 3.10). In this section, we will now sketch the *ray-seismic (or ray-optical) approximation* of the wave theory in inhomogeneous media. We will also show that it is the *high frequency approximation* of the equation of motion (2.20) for the inhomogeneous elastic continuum. We restrict our discussion again to a simplified case, namely the propagation of *SH*-waves in a two-dimensional inhomogeneous medium. The source is assumed to be a line-source in the y-direction where density ρ, *S*-velocity β and shear modulus μ depend only on x and z. The only non-zero displacement component is in the y-direction $v = v(x, z, t)$.

3.9.1 Fermat's principle and the ray equation

Fermat's principle states that the travel time of the (*SH*-)wave from the source Q to an arbitrary receiver P *along the seismic ray is an extremum and, therefore, stationary*, i.e., along each *infinitesimally adjacent path* between P and Q (dashed in Fig. 3.53) the travel time is either larger or smaller.

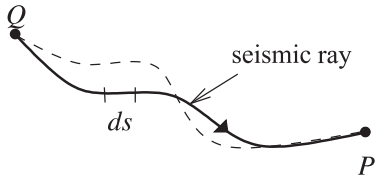

Fig. 3.53: Ray with extremum path and infinitesimally adjacent ray.

In most cases, the travel time along a seismic ray is a minimum, but there are also cases, where it is a maximum (e.g., the body waves PP, SS, PKKP). If we describe an arbitrary path from P to Q via a *parameter representation* $\{x = x(p), z = z(p)\}$, the element of the arc length s can be written as

$$ds = \left[\left(\frac{dx}{dp}\right)^2 + \left(\frac{dz}{dp}\right)^2\right]^{\frac{1}{2}} dp. \tag{3.118}$$

We consider now *many* such paths from Q to P. They all have the same value $p = p_1$ at Q and $p = p_2$ at P, respectively. Therefore, p cannot be identical to s; p could, for example, be the angle between the line connecting the coordinate centre to the point along the way and the x- or z-axis. The seismic ray is the path for which

$$T = \int_{p_1}^{p_2} \beta^{-1}\left(x(p), z(p)\right) \left[\left(\frac{dx}{dp}\right)^2 + \left(\frac{dz}{dp}\right)^2\right]^{\frac{1}{2}} dp = \int_{p_1}^{p_2} F\left(x, z, \frac{dx}{dp}, \frac{dz}{dp}\right) dp$$

$$\frac{dx}{dp} = x', \frac{dz}{dp} = z'$$

is an extremum. The determination of the seismic ray has, therefore, been reduced to a problem of *calculus of variations*. This leads to the *Euler-Lagrange equations*

$$\frac{\partial F}{\partial x} - \frac{d}{dp}\frac{\partial F}{\partial x'} = 0 \text{ and } \frac{\partial F}{\partial z} - \frac{d}{dp}\frac{\partial F}{\partial z'} = 0.$$

This gives then, for example,

$$\left(x'^2+z'^2\right)^{\frac{1}{2}}\frac{\partial}{\partial x}\left(\frac{1}{\beta(x,z)}\right)-\frac{d}{dp}\left[\frac{1}{\beta(x,z)}\frac{x'}{\left(x'^2+z'^2\right)^{\frac{1}{2}}}\right]=0.$$

Division by $(x'^2+z'^2)^{1/2}$, multiplication of nominator and denominator of the square bracket with dp, and use of (3.118) gives

$$\frac{d}{ds}\left(\frac{1}{\beta}\frac{dx}{ds}\right)=\frac{\partial}{\partial x}\left(\frac{1}{\beta}\right). \tag{3.119}$$

Similarly,

$$\frac{d}{ds}\left(\frac{1}{\beta}\frac{dz}{ds}\right)=\frac{\partial}{\partial z}\left(\frac{1}{\beta}\right). \tag{3.120}$$

Equations (3.119) and (3.120) are the *differential equations of the seismic ray* in the parameter representation $\{x=x(s), z=z(s)\}$ where s is now the arc length of the ray. With

$$\frac{dx}{ds}=\sin\varphi, \frac{dz}{ds}=\cos\varphi$$

(φ= angle of the ray versus the z-direction), it follows that

$$\left.\begin{array}{rcl}\frac{d}{ds}\left(\frac{\sin\varphi}{\beta}\right) & = & \frac{\partial}{\partial x}\left(\frac{1}{\beta}\right)\\ \frac{d}{ds}\left(\frac{\cos\varphi}{\beta}\right) & = & \frac{\partial}{\partial z}\left(\frac{1}{\beta}\right)\end{array}\right\}. \tag{3.121}$$

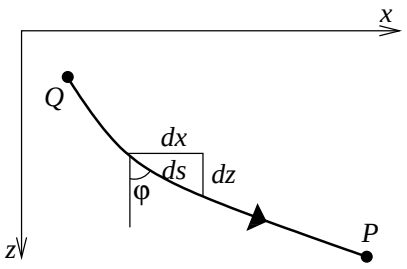

Fig. 3.54: Ray in x-z coordinate system.

These two equations can now be converted into another form of the ray equation (show)

$$\frac{\partial \varphi}{ds} = \frac{1}{\beta}\left(\sin\varphi \frac{\partial \beta}{\partial z} - \cos\varphi \frac{\partial \beta}{\partial x}\right). \tag{3.122}$$

This differential equation for $\varphi(s)$ is well suited for numerical computations of the ray path. The inverse of $d\varphi/ds$

$$r = \frac{ds}{d\varphi} = \beta\left(\sin\varphi \frac{\partial \beta}{\partial z} - \cos\varphi \frac{\partial \beta}{\partial x}\right)^{-1} \tag{3.123}$$

is the *radius of the curvature* of the ray. The ray is curved strongly (r is smaller) where the velocities change strongly ($\nabla\beta$ large).

Special cases

a) β= const.

From (3.122), it follows that $d\varphi/ds = 0$. The ray is straight.

b) $\beta = \beta(z)$ (no dependence on x)

The first equation in (3.121) gives, after integration,

$$\frac{\sin\varphi}{\beta} = q = const \tag{3.124}$$

along the whole ray (*Snell's law)* where q is the *ray parameter* of the ray. For sources and receivers at the level $z = 0$ the ray is symmetric with respect to its apex S. The ray parameter q is connected to the take-off angle φ_0, the seismic velocities $\beta(0)$ at the source and the turning point $\beta(z_s)$, respectively, via

$$q = \frac{\sin\varphi_0}{\beta(0)} = \frac{1}{\beta(z_s)}.$$

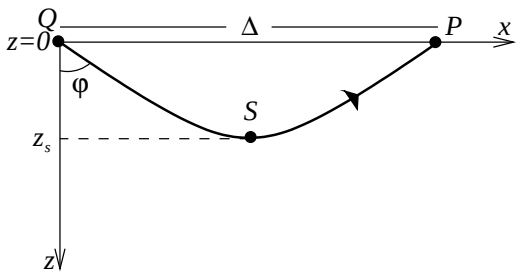

Fig. 3.55: Ray in 1-D medium.

A turning point depth z_s is only possible if $\beta(z) < \beta(z_s)$ for all $z < z_s$. For distance Δ in which the ray reappears at level $z = 0$, it holds (using (3.124)) that

$$\Delta(q) = 2\int_Q^S dx = 2\int_0^{z_s} \tan\varphi dz = 2q\int_0^{z_s} \left[\beta^{-2}(z) - q^2\right]^{\frac{1}{2}} dz. \qquad (3.125)$$

The ray's travel time is

$$T(q) = 2\int_Q^S \frac{ds}{\beta} = 2\int_0^{z_s} \frac{dz}{\beta\cos\varphi} = 2\int_0^{z_s} \beta^{-2}(z)\left[\beta^{-2}(z) - q^2\right]^{-\frac{1}{2}} dz. \quad (3.126)$$

Equations (3.126) and (3.127) are parameter representations of the *travel time curve* of the model. An example for ray paths and travel time curves in a model with a transition zone is given in Fig. 3.56.

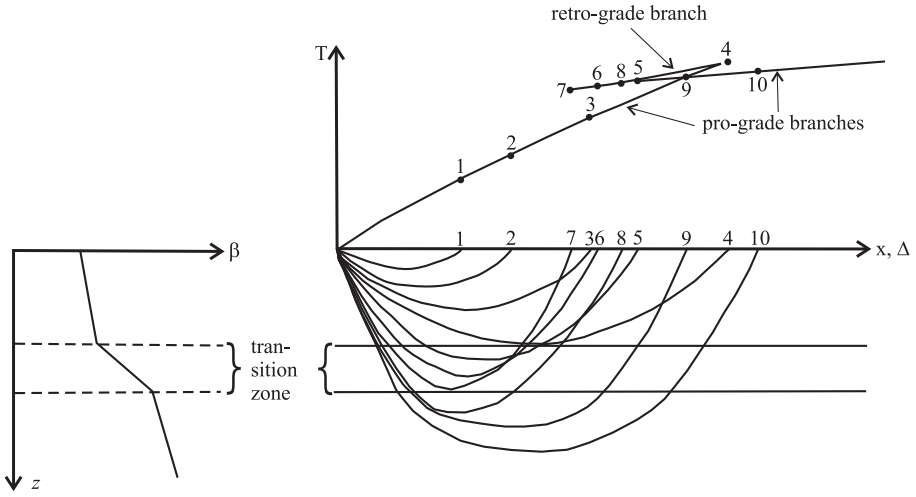

Fig. 3.56: Ray paths and travel time curves in a model with a transition zone.

The *slope* of the travel time curve is (show)

$$\frac{dT}{d\Delta} = q. \qquad (3.127)$$

c) $\beta = a + bx + cz$ (linear dependence from x and z)

In this case, it follows from

$$\frac{d\varphi}{ds} = \frac{c\sin\varphi - b\cos\varphi}{\beta}$$

and by differentiation with respect to s (φ and β are functions of s via x and z)

$$\frac{d^2\varphi}{ds^2} = \frac{c\cos\varphi + b\sin\varphi}{\beta}\frac{d\varphi}{ds} - \frac{c\sin\varphi - b\cos\varphi}{\beta^2}(b\sin\varphi + c\cos\varphi) = 0.$$

This implies $d\varphi/ds$ is a constant and, therefore, the curvature radius along the whole ray. *The ray is, therefore, a circle, or a section of it.* Its radius r follows from (3.123) if β is chosen identical to the value at the source Q and φ equal to the take-off angle φ_0. M, the centre of the circle, can be found from Q as shown in Fig. 3.57.

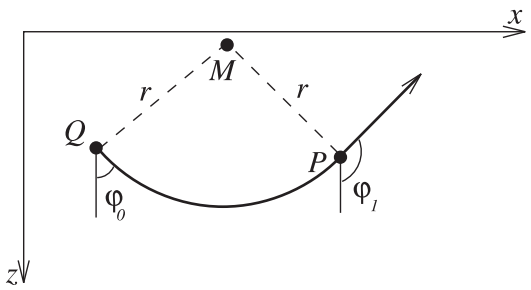

Fig. 3.57: Ray paths in a model with a linear velocity law in x and z.

The travel time from Q to P is

$$T = \int_Q^P \frac{ds}{\beta} = \int_{\varphi_0}^{\varphi_1} \frac{d\varphi}{c\sin\varphi - b\cos\varphi} = \left(c^2+b^2\right)^{-\frac{1}{2}} \ln\left\{\frac{\tan\left[\frac{(\varphi_1-\delta)}{2}\right]}{\tan\left[\frac{(\varphi_0-\delta)}{2}\right]}\right\}$$

with $\delta = \arctan(b/c)$.

An *arbitrary* velocity law $\beta(x,z)$, given at discrete points (x_n, z_n) in a model, can linearly be interpolated piece-wise between three neighbouring points. Then the laws derived here can be applied. The ray then consists of several sections of circles, and at the transition between two regions with different linear velocity laws, the tangent to the ray is continuous. A corresponding travel time and plotting program is, for many practical applications, already sufficient.

Exercise 3.13

a) Show that point M is on the line $\beta = 0$.

b) Derive the formula for T given above.

3.9.2 High frequency approximation of the equation of motion

The equation of motion for inhomogeneous, isotropic media (2.20) can for *SH*-wave propagation in two-dimensional media without volume forces, be simplified to

$$\rho \frac{\partial^2 v}{\partial t^2} = \frac{\partial}{\partial x}\left(\mu \frac{\partial v}{\partial x}\right) + \frac{\partial}{\partial z}\left(\mu \frac{\partial v}{\partial z}\right). \tag{3.128}$$

For the time harmonic case we use the ansatz

$$v(x,z,t) = A(x,z)\exp\left[i\omega\left(t - T(x,z)\right)\right]. \tag{3.129}$$

This is an ansatz for *high frequencies* since only for such frequencies can we expect that amplitude *A(x,z)* and travel time function *T(x,z)* to be frequency independent in inhomogeneous media. In homogeneous media far from interfaces, this is true for all frequencies as long as one is a few wavelengths away from the source. Using (3.129) in (3.128), and sorting with respect to powers of ω, it follows that

$$\begin{aligned}
&\omega^2 A\left\{\mu\left[\left(\frac{\partial T}{\partial x}\right)^2 + \left(\frac{\partial T}{\partial z}\right)^2\right] - \rho\right\} \\
&+i\omega A\left\{\frac{\partial \mu}{\partial x}\frac{\partial T}{\partial x} + \frac{\partial \mu}{\partial z}\frac{\partial T}{\partial z} + \mu\left(\frac{\partial^2 T}{\partial x^2} + \frac{\partial^2 T}{\partial z^2}\right) + 2\mu\left(\frac{\partial \ln A}{\partial x}\frac{\partial T}{\partial x} + \frac{\partial \ln A}{\partial z}\frac{\partial T}{\partial z}\right)\right\} \\
&- \left\{\frac{\partial \mu}{\partial x}\frac{\partial A}{\partial x} + \frac{\partial \mu}{\partial z}\frac{\partial A}{\partial z} + \mu\left(\frac{\partial^2 A}{\partial x^2} + \frac{\partial^2 A}{\partial z^2}\right)\right\} = 0.
\end{aligned} \tag{3.130}$$

For sufficiently high frequencies, the three terms of this equation are of *different* magnitudes. To satisfy (3.130), each term has then to be zero independently, *especially the first two terms*

$$\left(\frac{\partial T}{\partial x}\right)^2 + \left(\frac{\partial T}{\partial z}\right)^2 = \frac{1}{\beta^2} \tag{3.131}$$

$$2\mu\left(\frac{\partial \ln A}{\partial x}\frac{\partial T}{\partial x} + \frac{\partial \ln A}{\partial z}\frac{\partial T}{\partial z}\right) = -\frac{\partial \mu}{\partial x}\frac{\partial T}{\partial x} - \frac{\partial \mu}{\partial z}\frac{\partial T}{\partial z} - \mu\nabla^2 T. \tag{3.132}$$

Equation (3.131) is the *Eikonal equation*, and it contains on the right side the location-dependent *S*-velocity $\beta = (\mu/\rho)^{1/2}$. After solving the Eikonal, T is inserted in in the *transport equation* (3.132), and $\ln A$ and A are determined. This, in principle, solves the problem. The frequency-independent third term

in (3.130) will usually not be zero with A from (3.132). Solution (3.129) is, therefore, not exact, but becomes more accurate, the higher the frequency.

We still have to derive the conditions under which the first two terms of (3.130) are indeed of different order and, therefore, the separation into (3.131) and (3.132) is valid. The condition follows from the requirement that *each single* summand in the second term has to be small with respect to *each single* summand in the first term, for example,

$$\left|\omega \frac{\partial \mu}{\partial x}\frac{\partial T}{\partial x}\right| \ll \omega^2 \mu \left(\frac{\partial T}{\partial x}\right)^2 .$$

From (3.131), it follows roughly $|\partial T/\partial x| = 1/\beta$. Thus,

$$\left|\frac{\beta}{\mu}\frac{\partial \mu}{\partial x}\right| \ll \omega .$$

With $\mu = \rho\beta^2$, it follows

$$\left|\frac{\beta}{\rho}\frac{\partial \rho}{\partial x} + 2\frac{\partial \beta}{\partial x}\right| \ll \omega . \tag{3.133}$$

Similar relations follow from the other summands in (3.130). Usually, the required conditions are formulated as follows: the high frequency approximations (3.131) and (3.132) are valid for frequencies which are large with respect to the *velocity gradients*

$$\omega \gg |\nabla \beta| = \left[\left(\frac{\partial \beta}{\partial x}\right)^2 + \left(\frac{\partial \beta}{\partial z}\right)^2\right]^{\frac{1}{2}} . \tag{3.134}$$

Equation (3.133) shows also, that density gradients have also an influence. Equation (3.134) can be expressed even more physically: the relative change of the velocity over the distance of a wavelength has to be smaller then 2π (show).

Example

We solve (3.131) and (3.132) in the simplest case of a plane *SH*-wave propagating in z-direction with the assumption that ρ, β and μ depend only on z. Ansatz (3.129) then simplifies to

$$v(z,t) = A(z)\exp\left[i\omega\left(t - T(z)\right)\right] . \tag{3.135}$$

The solution of (3.131) is

$$\frac{dT}{dz} = \frac{1}{\beta(z)}, \; T(z) = \int_0^z \frac{d\zeta}{\beta(\zeta)}$$

where $T(z)$ is the *S-wave travel time*, with respect to the reference level $z = 0$. Equation (3.132) can be written as

$$\frac{2\mu}{\beta}\frac{d\ln A}{dz} = -\frac{1}{\beta}\frac{d\mu}{dz} + \frac{\mu}{\beta^2}\frac{d\beta}{dz}.$$

Thus,

$$\begin{aligned} \frac{d\ln A}{dz} &= \frac{1}{2}\left(\frac{d\ln\beta}{dz} - \frac{d\ln\mu}{dz}\right) = \frac{d\ln(\rho\beta)^{-\frac{1}{2}}}{dz} \\ A(z) &= A(0)\left[\frac{\rho(0)\beta(0)}{\rho(z)\beta(z)}\right]^{\frac{1}{2}}. \end{aligned}$$

The amplitudes of the *SH*-wave vary, therefore, inversely proportional to the impedance $\rho\beta$. The final solution of (3.135) is

$$v(z,t) = A(0)\left[\frac{\rho(0)\beta(0)}{\rho(z)\beta(z)}\right]^{\frac{1}{2}} \exp\left[i\omega\left(t - \int_0^z \frac{d\zeta}{\beta(\zeta)}\right)\right]. \tag{3.136}$$

From these results we conclude that, in the case considered, an *impulsive*, high frequent *SH*-wave propagates without changing its form.

Exercise 3.14

Vary the velocity β and the density ρ not *continuously* from depth 0 to depth z, but via a *step* somewhere in between. Then the amplitudes can be derived exactly via the *SH*-refraction coefficient (3.40). Show that (3.136) gives the same results if the relative change in impedance is small with respect to 1. Hint: Expansion in *both* cases.

3.9.3 Eikonal equation and seismic rays

From (3.129), it follows that surfaces of constant phase are given by

$$t - T(x,z) = const.$$

In the impulse case, these surfaces are the wavefronts separating perturbed and unperturbed regions. This is why the term wavefront is used also here. Complete differentiation with respect to t gives

$$\frac{\partial T}{\partial x}\frac{dx}{dt} + \frac{\partial T}{\partial z}\frac{dz}{dt} = \nabla T \cdot \frac{\overrightarrow{dx}}{dt} = 1, \tag{3.137}$$

where $\overrightarrow{dx}/dt = (dx/dt, 0, dz/dt)$ is the propagation velocity of the wavefront. The obvious interpretation of (3.137) for isotropic media is that $\overrightarrow{dx}/dt$ and the vector ∇T, which is perpendicular to the wavefront, are parallel, since according to the Eikonal equation (3.131) $|\nabla T| = 1/\beta$, it holds that $\left|\overrightarrow{dx}/dt\right| = \beta$. This means that the wavefronts propagate perpendicular to themselves with the local velocity β.

The *orthogonal trajectories of the wave* are defined as seismic rays. We still have to show that they are the rays defined via the Fermat's principle. We demonstrate this by showing that the differential equations of the seismic ray, (3.119) and (3.120), also follow from the Eikonal equation. As before, we describe the ray via its parameter representation $\{x = x(s),\ z = z(s)\}$ with the arc length s. Vector $\overrightarrow{dx}/ds = (dx/ds, 0, dz/ds)$ is a unit vector in ray direction for which, using the statements above, we can write

$$\frac{\overrightarrow{dx}}{ds} = \beta \nabla T = \beta(\partial T/\partial x, 0, \partial T/\partial z). \tag{3.138}$$

Instead of (3.119), we, therefore, have

$$\frac{d}{ds}\left(\frac{1}{\beta}\frac{dx}{ds}\right) = \frac{d}{ds}\left(\frac{\partial T}{\partial x}\right).$$

Using (3.138) and the Eikonal equation on the right side, we derive

$$\begin{aligned}
\frac{d}{ds}\left(\frac{1}{\beta}\frac{dx}{ds}\right) &= \frac{\partial^2 T}{\partial x^2}\frac{dx}{ds} + \frac{\partial^2 T}{\partial x \partial z}\frac{dz}{ds} = \beta\left(\frac{\partial^2 T}{\partial x^2}\frac{\partial T}{\partial x} + \frac{\partial^2 T}{\partial x \partial z}\frac{\partial T}{\partial z}\right) \\
&= \frac{\beta}{2}\frac{\partial}{\partial x}\left[\left(\frac{\partial T}{\partial x}\right)^2 + \left(\frac{\partial T}{\partial z}\right)^2\right] = \frac{\beta}{2}\frac{\partial}{\partial x}\left(\frac{1}{\beta^2}\right) \\
&= \frac{\beta}{2}\frac{(-2)}{\beta^3}\frac{\partial \beta}{\partial x} = -\frac{1}{\beta^2}\frac{\partial \beta}{\partial x} = \frac{\partial}{\partial x}\left(\frac{1}{\beta}\right).
\end{aligned}$$

That is identical to (3.119) and a similar derivation holds for (3.120). The following is the *ray equation in vector form*, which is also valid in the three-dimensional case

$$\frac{d}{ds}\left(\frac{1}{\beta}\frac{\overrightarrow{dx}}{ds}\right) = \nabla \frac{1}{\beta}. \tag{3.139}$$

This shows that *ray seismics is a high frequency approximation of wave seismics*. We have, until now, limited the discussion on *kinematic* aspects of wave propagation, i.e., on the discussion of wave paths, travel times and phases. *Dynamic* parameters, especially amplitudes, were not discussed except in the simple example in section 3.9.2. The following section gives more details on this aspect.

Before doing this, we give the form of (3.139) which is often used in numerical calculations, especially in three dimensions. The *single* ordinary differential equation of 2nd order for $\overrightarrow{x}$ (3.139) is replaced by a system of *two* equations of 1st order for $\overrightarrow{x}$ and the slowness vector $\overrightarrow{p} = \frac{1}{\beta}\frac{\overrightarrow{dx}}{ds}$ (vector in ray direction with the absolute value $\frac{1}{\beta}$)

$$\frac{\overrightarrow{dx}}{ds} = \beta\overrightarrow{p},\ \frac{\overrightarrow{dp}}{ds} = \nabla\frac{1}{\beta}.$$

Effective numerical methods for the solution of systems of ordinary differential equations of 1st order exist, e.g., the Runge-Kutta-method.

3.9.4 Amplitudes in ray seismic approximation

Within the framework of ray seismics developed from Fermat's principle, amplitudes are usually computed using the assumption that the energy radiated into a small ray bundle, remains in that bundle. This assumption implies that no energy exits the bundle sideways via diffraction or scattering and no energy is reflected or scattered backwards. This is only valid for high frequencies. In the following, we derive a formula which describes the change of the displacement amplitude along a ray radiated from a line source in a two dimensional inhomogeneous medium. The medium shall have no discontinuities.

We consider (see Fig. 3.58) a ray bundle emanating from a line source Q with a width of $dl(M)$ at the reference point M close to Q and a width of $dl(P)$ near the point P.

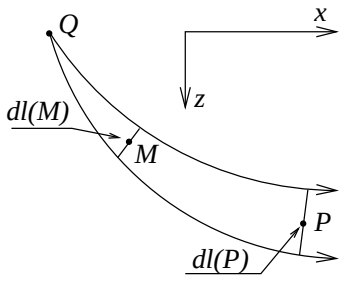

Fig. 3.58: Ray bundle emanating from the source Q.

Equation (3.129) holds for the displacement in M and P, or in real form

$$v = A \sin\left[\omega(t - T\right].$$

Our aim is the determination of the amplitude ration $A(P)/A(M)$. We first determine the energy density of the wave, i.e., the sum of kinetic and potential energy per unit volume. The kinetic energy density is $\frac{1}{2}\rho\dot{v}^2 = \frac{1}{2}\rho\omega^2 A^2 \cos^2\left[\omega(t-T)\right]$. Averaged over the period $2\pi/\omega$, the potential and kinematic energy density have the same value $\frac{1}{4}\rho\omega^2 A^2$ since the average of $\cos^2 x$ is identical to $\frac{1}{2}$. Then the energy density averaged over a period can be written as

$$\frac{\Delta E}{\Delta V} = \frac{1}{2}\rho\omega^2 A^2.$$

Consider a cube with the volume $\Delta V = dl\, dy\, ds$; its cross section $dl\, dy$ is perpendicular to the ray bundle and its length ds is exactly 1 wavelength $\beta 2\pi/\omega$. The energy

$$\Delta E = \frac{1}{2}\rho\omega^2 A^2 \Delta V = \pi\omega\rho\beta A^2 dl\, dy$$

contained within this cube flows per period through the cross section $dl\, dy$ of the ray bundle. Since no energy leaves the bundle, ΔE at P is the same as at M. From this the *amplitude ratio* follows as

$$\frac{A(P)}{A(M)} = \left[\frac{\rho(M)\beta(M)dl(M)}{\rho(P)\beta(P)dl(P)}\right]^{\frac{1}{2}}. \tag{3.140}$$

As in (3.136), impedance changes occur along the ray. The square root of the change in the cross section is the important parameter for the amplitude variation. In the most general three-dimensional case, dl has to be replaced by the cross section *surface* of the *three-dimensional* ray bundle.

Equation (3.140) can be approximated by tracing sufficiently many rays through the medium using the methods discussed previously, and then determining their perpendicular distances (or cross-section surfaces in three dimensions). These methods are based mainly on the solution of the ray equation (3.139), which is also called the equation of the *kinematic ray tracing*. A more stringent approach to calculate (3.140) is based on differential equations which are directly valid for the cross section of a ray bundle; they are called equations of the *dynamic ray tracing*. Their derivation cannot be treated here; for details, see the book of Červený, Molotov and Pšencík (1977).

For point P on a horizontal profile, e.g., at $z = 0$, a closer look at (3.140) and Fig. 3.59 helps in understanding the physical meaning.

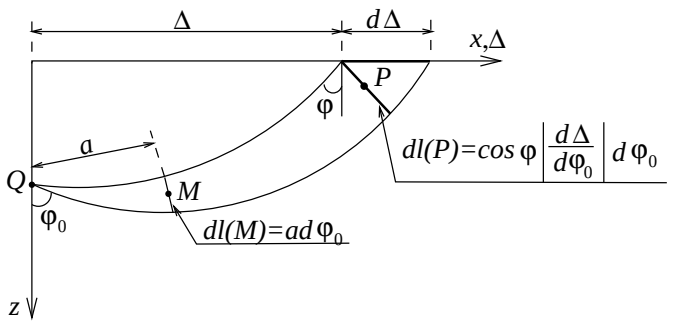

Fig. 3.59: Ray paths in an inhomogeneous medium.

The horizontal distance of P is $\Delta(\varphi_0)$ with the take-off angle φ_0 of the ray from Q to P. The distance of the reference point M from Q is a. With $dl(M)$ and $dl(P)$ from Fig. 3.59, it follows from (3.140) that

$$\frac{A(P)}{A(M)} = \left[\frac{\rho(M)\beta(M)}{\rho(P)\beta(P)}\right]^{\frac{1}{2}} \cdot \left[\frac{a}{\cos\varphi \left|\frac{d\Delta}{d\varphi_0}\right|}\right]^{\frac{1}{2}} . \tag{3.141}$$

This expression shows that problems occur if P is on, or close to, the neighbourhood of *turning points of the travel time curve* on the horizontal profile (compare, e.g., the travel time curve in Fig. 3.56). At these points, $d\Delta/d\varphi_0$ changes its sign, and that can happen either with a continuous or non-continuous pass through a zero. In the first case, infinite amplitudes occur in P; in the second case, the amplitudes become non-continuous. Both cases are unrealistic and nonphysical. Equations (3.141) and (3.140), respectively, can, therefore, only be used at some distance from the turning points (caustics) of the travel time curves. Unfortunately, this means that the points with some of the largest amplitudes cannot be treated properly under these assumptions; more sophisticated methods (like the WKBJ method, to be discussed later, or the Gaussian Beam method) must be employed.

Despite this disadvantage, the formulae given above (and their corresponding equations in three dimensions) are very useful in seismological applications. They can be easily extended to include refractions and reflections at discontinuities. This requires the determination of changes in the cross section of the ray bundle at discontinuities, and the inclusion of reflection and refraction coefficients.

A further problem of the energy ansatz used in this section is that it only gives the amplitudes of a seismic ray but no information on its phase changes that occur in *addition* to the phase changes in the travel time term. It is not always sufficient to add $\exp[i\omega(t-T)]$ to (3.140) and (3.141), respectively, e.g., on retrograde travel time branches in the case that the velocities are only a

function of z. The WKBJ method and the Gaussian Beam method solve this problem by tracking an additional parameter, the KMAH index named after Keller, Maslov, Arnold and Hormander, which counts the caustics encountered along the ray.

In the following section, the WKBJ theory for vertical inhomogeneous media, which avoids some of the ray theory problems discussed, is presented; it contains more wave seismic elements.

Exercise 3.15

Use the ray parameter q instead of the take-off angle φ_0 in the amplitude formula (3.141) in the case of a vertically inhomogeneous medium and then use (3.127). What is the relation between the amplitudes and the travel time curve $T(\Delta)$?

3.10 WKBJ method

Now we will consider total reflection at a vertically inhomogeneous medium using the WKBJ method.

3.10.1 Harmonic excitation and reflection coefficient

We consider a medium whose velocity $\beta(z)$ for $z \leq 0$ is $\beta(0)$, i.e., constant and for $z > 0$ can be any *continuous* function of z, i.e., no discontinuities exist in the medium. A plane *SH*-wave may propagate obliquely in the lower half-space $z < 0$ with the horizontal wavenumber $k = \omega \sin\varphi/\beta(0)$ (ray parameter $q = \sin\varphi/\beta(0)$ (φ = angle of incidence). Note the difference to the example in chapter 3.9.2 with vertical propagation.

Then the ray seismics of the vertically inhomogeneous medium, section 3.9.1, suggests inserting $\partial T/\partial x = q = constant$ in the Eikonal equation (3.131) (compare with (3.127)). This then, gives

$$T(x,z) = qx + \int_0^z \left[\beta^{-2}(\zeta) - q^2\right]^{\frac{1}{2}} d\zeta,$$

and, thus, the *travel time of the S-wavefront* from the intersection of the origin to the point (*x,z*). The rest of the discussion is as in section 3.9.2., and leads to

$$v_0(x,z,t) = A(0)\left[\frac{\mu(0)s(0)}{\mu(z)s(z)}\right]^{\frac{1}{2}} \exp\left[i\omega\left(t - qx - \int_0^z s(\zeta)d\zeta\right)\right] \quad (3.142)$$

$$s(\zeta) = \left[\beta^{-2}(\zeta) - q^2\right]^{\frac{1}{2}}. \quad (3.143)$$

q is the horizontal and s is the vertical *slowness* of the wave. For q=0, (3.142) is identical to (3.136). Equation (3.142) is the *WKBJ*-approximation of the S-wave. It is a useful high frequency approximation, as long as $\beta^{-1}(z) > q$, i.e., as long as the seismic ray which can be associated with the wave *is not propagating horizontally.* If the velocity, e.g., with increasing depth decreases or if it increases, but does not reach the value q^{-1}, (3.142) is applicable *for all z.*

For cases of interest and a medium with increasing velocities for increasing depth, a depth z_s is reached where $\beta(z_s) = q^{-1}$. At this depth, where the ray propagates horizontally, (3.142) diverges. Equations (3.129), (3.131) and (3.132) are *insufficient* for the description of the wavefield near the turning point of rays. If (3.142) is considered for $z > z_s$ with $\beta(z) > \beta(z_s)$, i.e., the velocity continues to increase, a stable result can, again, be obtained. The integral in the exponential term from z_s to z is imaginary, thus, giving an exponential decay of the amplitudes with increasing z, i.e., below the ray's turning point the amplitude of the *SH*-wave decreases as expected. For $z < z_s$, the wavefield is insufficiently described by (3.142) since (3.142) represents only the downward propagating *incident SH*-wave. A similar equation can be given for the *reflected SH*-wave upward propagating from the turning point

$$v_1(x,z,t) = RA(0)\left[\frac{\mu(0)s(0)}{\mu(z)s(z)}\right]^{\frac{1}{2}} \exp\left[i\omega\left(t - qx + \int_0^z s(\zeta)d\zeta\right)\right]. \qquad (3.144)$$

That this wave propagates upwards can be seen from the positive sign before the integral in the exponent. R is, as can be seen by the selection z=*0* in (3.142) and (3.144), the amplitude ratio $v_1(x,0,t)/v_0(x,0,t)$ of the reflected to the incident wave; in other words, the *reflection coefficient of the inhomogeneous half-space is* z>0. Its determination requires a quantitative connection of the whole field $v_0 + v_1$ for $z < z_s$ with the already mentioned exponentially decaying field for $z > z_s$. To tie these two solutions together is, as mentioned before, not possible with the high frequency approximation of the equation of motion used until now.

The required connection becomes possible with another high frequency approximation of (3.128), namely a wave equation with depth dependent velocity

$$\left.\begin{array}{lcl} \nabla^2 V & = & \frac{\partial^2 V}{\partial x^2} + \frac{\partial^2 V}{\partial z^2} = \frac{1}{\beta^2(z)}\frac{\partial^2 V}{\partial t^2} \\ v & = & \frac{1}{\mu^{\frac{1}{2}}(z)} V \end{array}\right\}. \qquad (3.145)$$

This high frequency approximation is valid under condition (3.134), as can be shown by inserting in (3.128). For plane waves, it follows from the ansatz

$$V(x,z,t) = B(z)\exp\left[i\omega(t - qx)\right]$$

via (3.145) an ordinary differential equation for *B(z)*

$$B''(z) + \omega^2 \left[\beta^{-2}(z) - q^2\right] B(z) = 0. \tag{3.146}$$

This equation has now to be solved for large ω. The solutions of $B''(z) + \omega^2 f(z)B(z) = 0$ in the neighbourhood of a zero of *f(z)* and for large ω is generally called *WKBJ*-solution after the authors - Wentzel, Kramers, Brillouin, Jeffreys. For $z < z_s$, the previously discussed superposition of (3.142) and (3.144) of the incident and reflected wave of v results. For $z > z_s$ the exponentially decaying solution follows. The case that z is in the immediate neighbourhood of z_s has to be examined in more detail. We approximate the coefficient $\omega^2 s^2(z)$ of $B(z)$ (with *s(z)* from (3.143)) *linearly* and get, with $s^2(z_s) = 0, \beta(z_s) = q^{-1}$ and $\beta'(z_s) > 0$,

$$B''(z) - 2\omega^2 q^3 \beta'(z_s)(z - z_s)B(z) = 0. \tag{3.147}$$

This equation can, with the substitution,

$$y(z) = \left[2\omega^2 q^2 \beta'(z_s)\right]^{\frac{1}{3}} (z - z_s) \tag{3.148}$$

be transformed into the differential equation of the *Airy functions*

$$C''(y) - yC(y) = 0.$$

The solution of interest to us, $C(y) = Ai(y)$, is discussed in appendix E (more on Airy functions can be found in M. Abramovitz and I.A. Stegun: Handbook of Mathematical Functions, H. Deutsch, Frankfurt, 1985). The depths $z < z_s$ ($z > z_s$) correspond to arguments $y < 0$ ($y > 0$) of *Ai(y)*. From Fig. E.2, it follows that the transition from the oscillatory solution *B(z)* of (3.147) with $z < z_s$ to the exponentially damped solution for $z > z_s$ is *without singularity*. This then, also holds for the displacement v, in contrast to what one would expect from (3.142) and (3.144).

The oscillatory behaviour of *B(z)* for $z < z_s$ indicates that the incident wave v_0 and the reflection v_1, build a standing wave with nodes of the displacement at depths which correspond to the zeros of the Airy function. The *reflection coefficient* R in (3.144) is now determined in such a way, that the superposition of (3.142) and (3.144), *in the term that depends on z*, is identical to the Airy function. Due to the high frequency assumption, the asymptotic form of *Ai(y)* for large negative y can be used

$$Ai(y) \simeq \pi^{-\frac{1}{2}} |y|^{-\frac{1}{4}} \sin\left(\frac{2}{3}|y|^{\frac{3}{2}} + \frac{\pi}{4}\right). \tag{3.149}$$

Furthermore, for $z < z_s$

$$\begin{aligned} v_0 + v_1 &= A(0)\left[\tfrac{\mu(0)s(0)}{\mu(z)s(z)}\right]^{\frac{1}{2}} \exp\left[i\omega\left(t - qx - \int_0^{z_s} s\,d\zeta\right)\right] \\ &\cdot \quad \left\{\exp\left[i\omega\int_z^{z_s} s\,d\zeta\right] + R\exp\left[2i\omega\int_0^{z_s} s\,d\zeta\right]\cdot\exp\left[-i\omega\int_z^{z_s} s\,d\zeta\right]\right\}. \end{aligned} \tag{3.150}$$

The z-dependence of $v_0 + v_1$ is given by the curved bracket. It will now be determined in approximation. With the approximation (3.147) $\omega^2 s^2(\zeta) = 2\omega^2 q^3 \beta'(z_s)(z_s - \zeta)$, it follows

$$\begin{aligned} \omega\int_z^{z_s} s\,d\zeta &= \pm\left[2\omega^2 q^3\beta'(z_s)\right]^{\frac{1}{2}}\int_z^{z_s}(z_s-\zeta)^{\frac{1}{2}}d\zeta \\ &= \pm\left[2\omega^2 q^3\beta'(z_s)\right]^{\frac{1}{2}}\frac{2}{3}(z-z_s)^{\frac{3}{2}} \\ &= \pm\frac{2}{3}|y|^{\frac{3}{2}} \\ &= \pm Y \end{aligned}$$

with $y = y(z)$ from (3.148). The positive (negative) sign holds for positive (negative) frequencies. Thus, for the curved brackets in (3.150)

$$\{\cdots\} = e^{\pm iY} + Ze^{\mp iY}$$

with the abbreviation

$$Z = R\exp\left[2i\omega\int_0^{z_s} s\,d\zeta\right]. \tag{3.151}$$

With $Z = \pm i$ for $\omega < 0$ (> 0), it follows that

$$\begin{aligned} \{\cdots\} &= (1\pm i)(\cos Y + \sin Y) = 2^{\frac{1}{2}}(1\pm i)\sin\left(Y + \frac{\pi}{4}\right) \\ &= 2^{\frac{1}{2}}(1\pm i)\sin\left(\frac{2}{3}|y|^{\frac{3}{2}} + \frac{\pi}{4}\right), \end{aligned}$$

and, therefore, the required agreement with the main term in (3.149). $Z = \pm i$ in (3.151) gives then the *reflection coefficient in the WKBJ-approximation*

$$\left.\begin{aligned} R &= i\tfrac{\omega}{|\omega|}\exp\left[-2i\omega\int_0^{z_s} s(\zeta)d\zeta\right] \\ s(\zeta) &= \left[\beta^{-2}(\zeta) - q^2\right]^{\frac{1}{2}} \\ \beta(z_s) &= q^{-1} = \tfrac{\beta(0)}{\sin\varphi}. \end{aligned}\right\} \tag{3.152}$$

Its absolute value is 1 (*total reflection*). It describes only the *phase shifts*, i.e., a constant phase shift of $\pm\pi/2$ for $\omega < 0$ ($\omega > 0$) is added to the phase shifts due to the travel time in the exponential term of R. Compared to the reflection coefficients of layered media, derived earlier without approximation; the form of (3.152) is *simple*. It is only valid for sufficiently high frequencies (condition (3.134)) and for angle of incidence φ with total reflection. Reflection coefficients of the type of (3.152) are useful in seismology but even more so for the propagation of sound waves in oceans or the propagation of radio waves in the ionosphere (compare, e.g., Budden (1961) and of Tolstoy and Clay (1966)).

The *reflected SH-wave* observed at the coordinate centre follows, then, by inserting (3.152) in (3.144)

$$v_1(0,0,t) = A(0)i\frac{\omega}{|\omega|}\exp\left[i\omega\left(t - 2\int_0^{z_s} s(\zeta)d\zeta\right)\right]. \qquad (3.153)$$

Then

$$\tau(q) = 2\int_0^{z_s} s(\zeta)d\zeta$$

is the *delay time*, , i.e., the time between the intersection of the incident and the reflected wave with the coordinate centre. This time delay corresponds to the ray segments *AC, BD*, or *OP*.

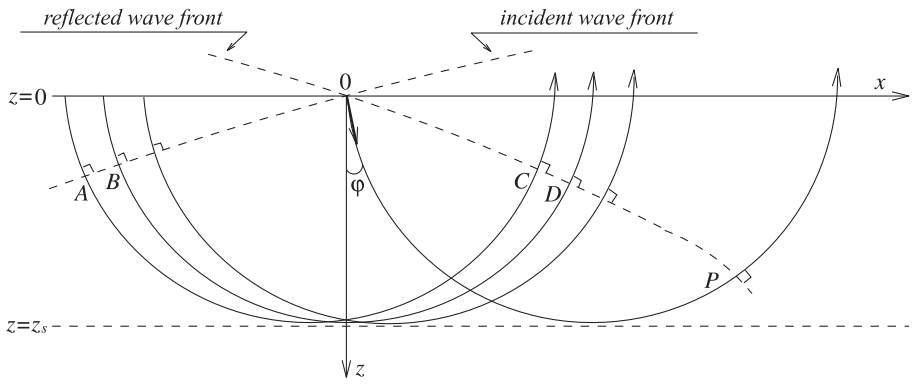

Fig. 3.60: Construction of a caustic from the envelopes of rays.

Note that the wavefronts are *curved* for $z>0$; only in the homogeneous region $z<0$ are the wavefronts plane.

Fig. 3.60 shows also that the line $z = z_s$ is the envelope of all rays. Such envelopes are called caustics, and they are characterised by large energy concentrations. Within the amplitude approximation formula (3.140), and due to

dl(P)=0 for a point P on the caustic $z = z_s$, infinite amplitudes would result there. The additional phase shift of $\pm\frac{\pi}{2}$, as discussed before, can be interpreted *physically* as the effect of the strong interaction of each ray with its neighbouring rays in the vicinity of the caustic. More complicated caustics occur in vertically inhomogeneous media, if the incident wave is from a point or line source, respectively. In such cases, the phase shift per caustic encountered, is $\pm\frac{\pi}{2}$. More complicated caustics are encountered in two and three dimensional media.

3.10.2 Impulsive excitation and WKBJ-seismograms

If an *impulsive wave*, producing a displacement $v_0(0,0,t) = F(t)$ at the coordinate centre, instead of a harmonic wave is incident, it follows from (3.153) that the corresponding reflection is the time delayed Hilbert transform of *F(t)* (compare section 3.6.3)

$$v_1(0,0,t) = F_H(t - \tau(q)). \tag{3.154}$$

This means that the reflection for *all* angles of incidence φ (or ray parameters or horizontal slowness q) have the same form except for the time delay $\tau(q)$. This is, therefore, different from the results for a discontinuity of first order in chapter 3.6.3 (there the impulse form changed in the case of total reflection also with the angle of incidence φ).

When *cylindrical waves* are considered, the principle of superposition is used. The cylindrical wave, assumed to originate from an isotropically radiating *line source in the coordinate centre*, is represented by many plane waves with radiation angles φ from 0 to $\pi/2$. This corresponds to positive values of q. The reflections are superimposed similarly. First, (3.154) is generalised for arbitrary $x > 0$

$$v_1(x,0,t) = F_H\left(t - \tau(q) - qx\right) = F_H(t) * \delta\left(t - \tau(q) - qx\right).$$

Then these plane waves are integrated over φ from 0 to $\pi/2$ and, thus, the *WKBJ-seismogram* at distance x from the line source is derived

$$v(x,0,t) = F_H(t) * \int_0^{\frac{\pi}{2}} \delta\left(t - \tau(q) - qx\right) d\varphi = F_H(t) * I(x,t). \tag{3.155}$$

The *impulse seismogram* $I(x,t)$ can now be derived numerically via

$$\left.\begin{array}{lcll} I(x,t) & = & \sum_i \delta(t - t_i)\Delta\varphi_i & \\ t_i & = & \tau(q_i) + q_i x\,, & q_i = \frac{\sin\varphi_i}{\beta(0)}. \end{array}\right\} \tag{3.156}$$

Usually, the φ_i are chosen equidistant ($\Delta\varphi_i = \Delta\varphi = const$). The delta functions are shifted from the times t_i to their immediate neighbouring time points $I(x,t)$

and possibly amass there, i.e., in the discretised version of $I(x,t)$, multiples of $\Delta\varphi$ occur there. $I(x,t)$ is then convolved with $F_H(t)$. The most time-consuming part is the computation of the delay time $\tau(q_i)$; on the other hand, efficient ray-seismic methods exist for that. In comparison to the reflectivity method and the GRT, the WKBJ-method is significantly faster. There are also other numerical realisations of this method than (3.155) and (3.156).

WKBJ-seismograms have *other phase relations and impulse forms* than expected from (3.152) and (3.154), respectively. This is due to the summation of many plane waves. Pro-grade travel time branches (see Fig. 3.56) show no phase shift, i.e., the impulse form of the incident cylindrical wave is observed there. Phase shifts and impulse form changes only occur on retro-grade travel time branches. Furthermore, the seismogram amplitudes are finite in the vicinity of the turning points of travel time curves, i.e., the WKBJ-method is valid at caustics.

WKBJ-seismograms for a simple crust-mantle model and a line source at the Earth's surface are shown in Fig. 3.61. The computations were performed with a program for *SH*-waves; even so, the velocity model (Fig. 3.62) is valid for P-waves. An acoustic P-wave computation would give, in principle, the same result for *pressure*. The travel time curve of the reflection P_MP from the crust-mantle boundary (Moho) is retrograde and the travel time branch of the refracted wave P_n from the upper mantle is prograde. Times are reduced with 8 km/s.

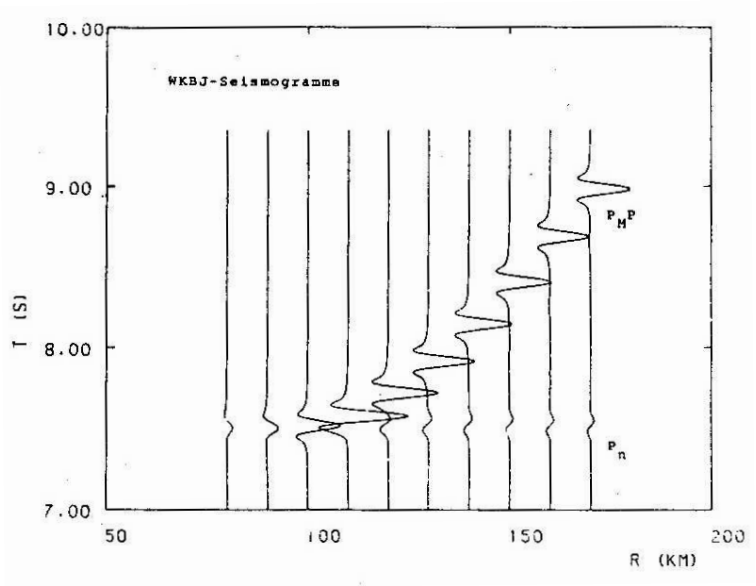

Fig. 3.61: WKBJ-seismograms for a simple crust-mantle model and a line source at the Earth's surface.

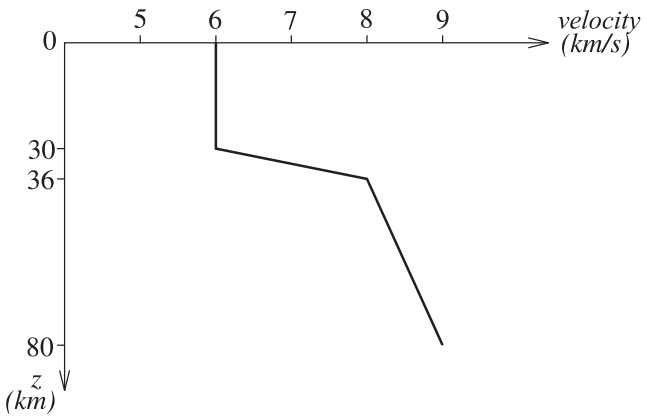

Fig. 3.62: Velocity model used in Fig. 3.61.

The impulse forms of these waves are as expected: P_n has the form of the radiated wave, whereas $P_M P$ is roughly the Hilbert transform of it. At distances smaller than the critical distance (ca. 100 km), the amplitudes increase strongly. At the critical point, which is located on a caustic within the crust, the wave field remains finite.

In seismological applications of WKBJ-seismograms, their approximate nature, due to the high frequency approximation (3.152) for the reflection coefficient, should be kept in mind. This approximation is insufficient in regions of the Earth where wave velocity and density change rapidly with depth, e.g., at the core-mantle boundary or at the boundary of the inner core of the Earth.

Chapter 4

Surface waves

4.1 Free surface waves in layered media

4.1.1 Basic equations

In addition to the body waves that penetrate to all depths in the Earth, another type of wave exists which is mostly limited to the neighbourhood of the surface of the Earth called *surface waves*. These waves propagate along the surface of the Earth, and their amplitudes are only significant down to the depth of a few wave lengths. Below that depth, the *displacement* is negligible. Because surface waves are constrained to propagate close to the Earth's surface, their amplitude decay as a function of source distance is smaller than for body waves, which propagate in three dimensions. This is why surface waves are usually the dominating signals in the earthquake record. Another significant property is their *dispersion*, i.e., their propagation velocity is frequency dependent. Therefore, the frequency within a wave group varies as a function of time (compare example in 4.1.4).

These are some of the main observations and explanations for surface waves. The first scientists to study surface waves (Rayleigh, Lamb, Love, Stoneley et al.) found the theoretical descriptions explaining the main observations. The fundamental tenet of this approach is the description of surface waves as an *eigenvalue problem but omitting the source of the elastic waves*. We consider a layered half-space with parameters as given in Fig. 4.1 with a free surface.

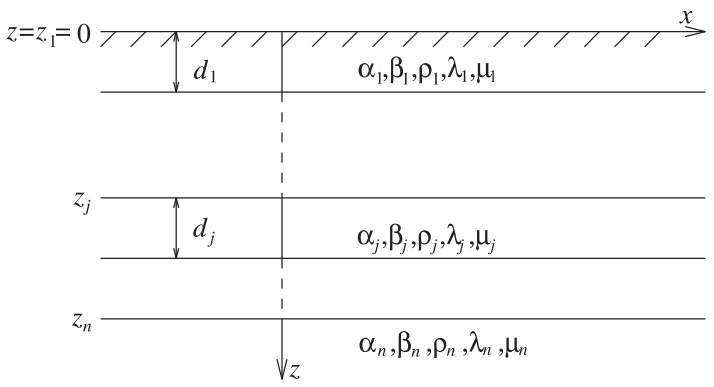

Fig. 4.1: Layered half-space with free surface.

We work with Cartesian coordinates x,y,z and assume *independence from y*. Then, the equations from section 3.6.2 can be used which have been derived to describe reflection and refraction. The separation of the displacement into *P-*, *SV-* and *SH*-contributions holds as before, as does the fact, that the *P-SV*-contributions propagate independently from the *SH*-waves. Surface waves of the *P-SV*-type are called *Rayleigh waves*. They are polarised in the x-z-plane

$$\begin{array}{lrcl} \text{horizontal displacement} & u & = & \frac{\partial \Phi}{\partial x} - \frac{\partial \Psi}{\partial z} \\ \text{vertical displacement} & w & = & \frac{\partial \Phi}{\partial z} + \frac{\partial \Psi}{\partial x}. \end{array} \tag{4.1}$$

The potentials Φ and Ψ, in each layer, satisfy the wave equation

$$\nabla^2 \Phi = \frac{1}{\alpha^2} \frac{\partial^2 \Phi}{\partial t^2}, \qquad \nabla^2 \Psi = \frac{1}{\beta^2} \frac{\partial^2 \Psi}{\partial t^2}. \tag{4.2}$$

Surface waves of the *SH*-type are called *Love waves*. They are polarised in y-direction, and for the displacement v in each layer the following wave equation holds

$$\nabla^2 v = \frac{1}{\beta^2} \frac{\partial^2 v}{\partial t^2}. \tag{4.3}$$

The boundary conditions are given in section 3.6.2. The *ansatz* for Φ_j, Ψ_j and v_j in the j-th layer of the model for harmonic excitation ($\omega > 0$) is

$$\left.\begin{array}{c} \Phi_j \\ \Psi_j \end{array}\right\} = \left\{\begin{array}{c} A_j(z) \\ B_j(z) \end{array}\right\} \exp\left[i\omega\left(t - \frac{x}{c}\right)\right] = \left\{\begin{array}{c} A_j(z) \\ B_j(z) \end{array}\right\} \exp\left[i\left(\omega t - kx\right)\right] \tag{4.4}$$

and

$$v_j = C_j(z) \exp\left[i\omega\left(t - \frac{x}{c}\right)\right] = C_j(z) \exp\left[i\left(\omega t - kx\right)\right]. \tag{4.5}$$

Consider the conditions for which a plane wave exists, which propagates in x-direction with the *phase velocity* c, where c is identical in all layers. How large is c? Then the functions $A_j(z), B_j(z)$ and $C_j(z)$ exist, so that

$$\lim_{z\to\infty} \left\{ \begin{array}{c} A_n(z) \\ B_n(z) \\ C_n(z) \end{array} \right\} = 0. \tag{4.6}$$

This problem is an *eigenvalue problem*, and c and the wavenumber $k = \omega/c$, respectively, are the corresponding *eigenvalues*. In many cases (for fixed ω), a finite number (≤ 1) of eigenvalues exist. The problem is comparable to that of determining the frequencies of *natural oscillations* (or free oscillations) of finite bodies (beams, plates, bodies *etc.*) (compare exercise 4.1).

Here we are only interested in the case where the eigenvalues are real (>0). This has the largest practical application. The corresponding surface waves are called *normal modes*. There exist also waves which can be described with complex k: $k = k_1 - ik_2$ ($k_{1,2} > 0$). These surface waves are called *leaking modes* since their amplitude decreases exponentially with $\exp(-k_2 x)$. Their phase velocity is ω/k_1.

The ansatz with plane waves neglects the influence of excitation. This, then, leads to a major simplification of the problem. Such surface waves are called *free* in contrast to *forced* surface waves which are excited by specific sources. The analogy to the free and forced resonances of limited bodies is also helpful here in the context of excitation. The treatment of free surface waves is an important requirement for the study of forced surface waves (compare section 4.2). We will soon show that the dispersive properties of both wave types are identical. Since this property depends on the medium, they can be used to determine medium parameters. This is why the study of the dispersion of free surface waves is of great practical importance.

Exercise 4.1

The radial oscillations of a liquid sphere with P-velocity α are described by the potential $\Phi_n(r,t) \sim (e^{i\omega_n t/r}) \sin(\omega_n r/\alpha)$ (n=1,2,3...). Determine the eigen frequencies ω_n from the condition that the surface of the sphere at r=R is stress free (p_{rr} from exercise 3.4); give the radial displacement. Where are the nodal planes?

4.1.2 Rayleigh waves at the surface of an homogeneous half-space

The half-space (z>0) has the velocities α and β for P- and S-waves, respectively. Inserting the ansatz

$$\Phi = A(z)\exp\left[i\left(\omega t - kx\right)\right] \text{ and } \Psi = B(z)\exp\left[i\left(\omega t - kx\right)\right] \tag{4.7}$$

into the wave equation (4.2) with $\nabla^2 = \partial^2/\partial x^2 + \partial^2/\partial z^2$, gives the differential equations for *A(z)* and *B(z)*, e.g.,

$$A''(z) + k^2\left(\frac{c^2}{\alpha^2} - 1\right)A(z) = 0.$$

The general solution of this equation is

$$A(z) = A_1 e^{-ik\delta z} + A_2 e^{ik\delta z} \text{ with } \delta = \left(\frac{c^2}{\alpha^2} - 1\right)^{\frac{1}{2}}.$$

Due to (4.6), δ has to be purely imaginary. Then, $A_2 = 0$ has to hold. From the properties of δ, a first statement on the phase velocity of the Rayleigh wave becomes possible: $c < \alpha$. It also holds that

$$A(z) = A_1 e^{-ik\delta z},$$

and, similarly, it follows that

$$B(z) = B_1 e^{-ik\gamma z}$$

with $\gamma = \left(c^2/\beta^2 - 1\right)^{1/2}$ (negative imaginary). This further limits c: $c < \beta$.

The potential ansatz (4.7) can now be written as

$$\Phi = A_1\exp\left[i\left(\omega t - kx - k\delta z\right)\right], \qquad \Psi = B_1\exp\left[i\left(\omega t - kx - k\gamma z\right)\right]. \tag{4.8}$$

Inserting the *boundary conditions* $p_{zz} = p_{zx} = 0$ for z=0 with p_{zz} and p_{zx} from (3.29), it follows that

$$\begin{aligned} -\frac{\omega^2}{\alpha^2}\frac{\lambda}{\mu}A_1 + 2\left(-k^2\delta^2 A_1 - k^2\gamma B_1\right) &= 0 \\ -2k^2\delta A_1 + \left(-k^2 + k^2\gamma^2\right)B_1 &= 0. \end{aligned}$$

Division by $-k^2$ and use of $\lambda/\mu = (\alpha^2 - 2\beta^2)/\beta^2$ gives

$$\begin{aligned} \left[\frac{c^2}{\alpha^2}\frac{\alpha^2-2\beta^2}{\beta^2} + 2\left(\frac{c^2}{\alpha^2}-1\right)\right] A_1 + 2\gamma B_1 &= 0 \\ 2\delta A_1 + \left(2 - \frac{c^2}{\beta^2}\right) B_1 &= 0. \end{aligned}$$

This leads to

$$\left.\begin{aligned} \left(\tfrac{c^2}{\beta^2}-2\right) A_1 + 2\gamma B_1 &= 0 \\ -2\delta A_1 + \left(\tfrac{c^2}{\beta^2}-2\right) B_1 &= 0. \end{aligned}\right\} \tag{4.9}$$

This system of equations only has non-trivial solutions A_1 and B_1, if its determinant is zero. *This leads to an equation for* c:

$$\left(\frac{c^2}{\beta^2}-2\right)^2 + 4\delta\gamma = 0.$$

In the range of interest $0 < c < \beta$, we have

$$\left(\frac{c^2}{\beta^2}-2\right)^2 = 4\left(1-\frac{c^2}{\beta^2}\right)^{\frac{1}{2}}\left(1-\frac{c^2}{\alpha^2}\right)^{\frac{1}{2}}.$$

Squaring this gives

$$\frac{c^2}{\beta^2}\left[\frac{c^6}{\beta^6} - 8\frac{c^4}{\beta^4} + \left(24 - 16\frac{\beta^2}{\alpha^2}\right)\frac{c^2}{\beta^2} - 16\left(1-\frac{\beta^2}{\alpha^2}\right)\right] = 0. \tag{4.10}$$

Solution $c = 0$ is not of interest, therefore, only the terms in the bracket have to be examined. For $c = 0$, it is negative, and for $c = \beta$, positive. Therefore, at least one real solution of (4.10) exists between 0 and β. The eigenvalue problem has, thus, a solution, i.e., along the surface of a homogeneous half-space a wave can propagate, the amplitudes of which decay with depth. In this simple case *no dispersion* occurs and c is independent of ω.

In the special case $\lambda = \mu$ (i.e., $\alpha = \beta\sqrt{3}$), $c = 0,92\beta$. In general, the Rayleigh wave is only slightly slower than the S-wave.

We now examine the *displacement* of the Rayleigh wave

$$u = \left(-ikA_1 e^{-ik\delta z} + ik\gamma B_1 e^{-ik\gamma z}\right)\exp\left[i\left(\omega t - kx\right)\right].$$

With $\gamma B_1 = -\left(c^2/2\beta^2 - 1\right) A_1$ (from (4.9)), it follows

$$u = -ikA_1 \left[e^{-ik\delta z} + \left(\frac{c^2}{2\beta^2} - 1 \right) e^{-ik\gamma z} \right] \exp\left[i\left(\omega t - kx\right) \right] \tag{4.11}$$

$$e^{-ik\delta z} + \left(\frac{c^2}{2\beta^2} - 1 \right) e^{-ik\gamma z} =: a(z).$$

Similarly,

$$w = \left(-ik\delta A_1 e^{-ik\delta z} - ikB_1 e^{-ik\gamma z} \right) \exp\left[i\left(\omega t - kx\right) \right].$$

With $B_1 = \delta A_1 \left(c^2/2\beta^2 - 1\right)^{-1}$ (from (4.9)), it follows

$$w = -ik\delta A_1 \left[e^{-ik\delta z} + \left(\frac{c^2}{2\beta^2} - 1 \right)^{-1} e^{-ik\gamma z} \right] \exp\left[i\left(\omega t - kx\right) \right] \tag{4.12}$$

$$e^{-ik\delta z} + \left(\frac{c^2}{2\beta^2} - 1 \right)^{-1} e^{-ik\gamma z} =: b(z).$$

We assume that A_1 is positive real and consider the real parts of (4.11) and (4.12)

$$\begin{aligned} u &= kA_1 a(z) \sin(\omega t - kx) \\ w &= -|\delta| k A_1 b(z) \cos(\omega t - kx). \end{aligned}$$

For z=0, it holds that a(0)>0 and b(0)<0. In the case of u and w, show the behaviour given in Fig. 4.2 (e.g., for x = 0). The displacement vector describes an *ellipse* with *retro-grade* motion.

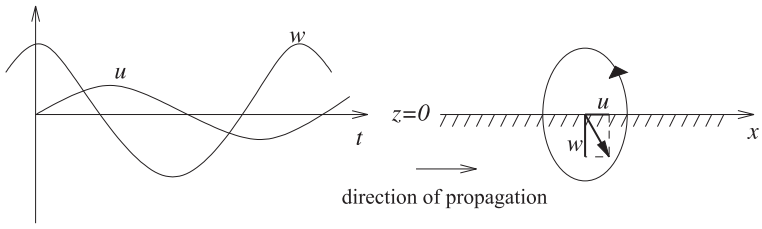

Fig. 4.2: Behaviour of u and w.

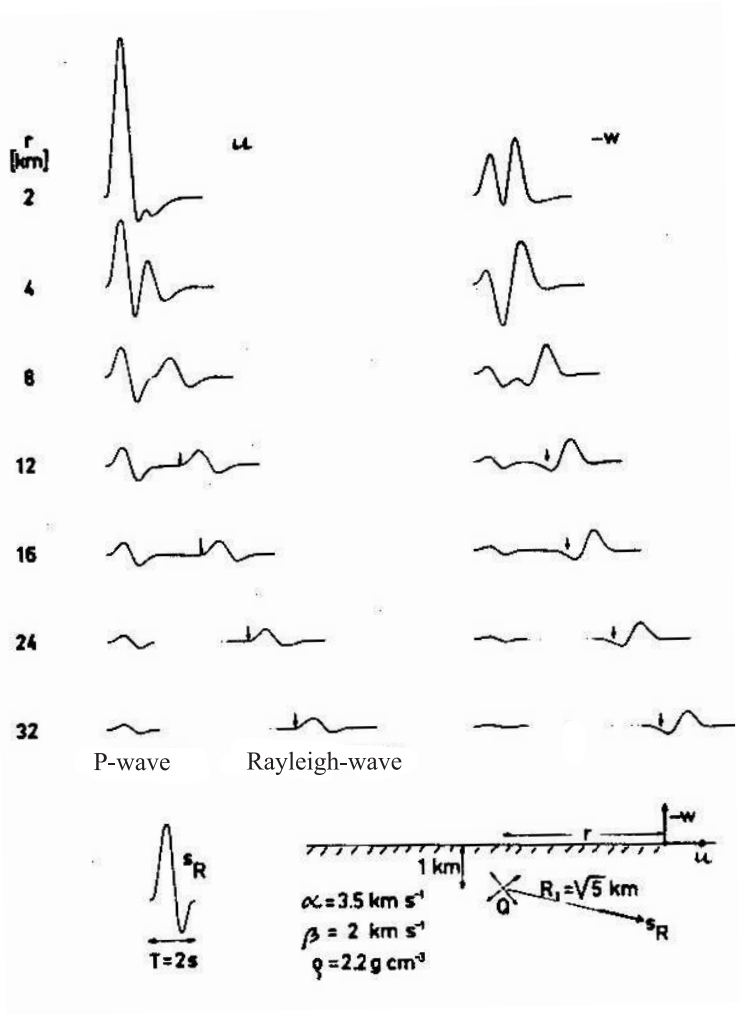

s_R = radial displacement of source

Fig. 4.3: Theoretical seismograms for an explosive point source in a homogeneous half-space and recorders at its surface (computed with the GRT for point sources, compare section 3.8).

For sufficiently large z, the second term in *a(z)* and *b(z)* dominates due to $|\gamma| < |\delta|$ so that both functions are negative there. The displacement vector, again, describes an ellipse but now with *prograde* direction. The transition from retro-grade to pro-grade motion occurs at the depth where *a(z)*=0. For $\lambda = \mu$, this is the case at about $z = 0, 2\Lambda$ where $\Lambda = 2\pi c/\omega = 2\pi/k$ is the wavelength. This depth is, therefore, a *nodal plane of the horizontal displacement.*

Elliptical polarisation of the displacement vector and the existence of nodal planes of the displacement components, are also characteristics of free Rayleigh waves in *layered* media, with the additional feature of dispersion.

The Rayleigh wave is, therefore, forced. The arrows above the seismograms indicate the theoretical arrival times r/c where c is the phase velocity of the free Rayleigh wave. Fig. 4.4 shows a hodograph of a point at the surface, i.e., its trace during the passage of a Rayleigh wave which has roughly elliptical form.

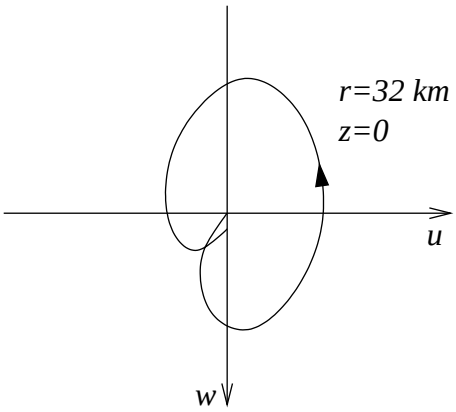

Fig. 4.4: Hodograph at a point at the surface (see Fig. 4.3).

The results of the theory of the free Rayleigh wave are, therefore, relatively well confirmed.

Exercise 4.2

Does the homogeneous half-space have free Love waves?

4.1.3 Love waves at the surface of a layered half-space

Matrix formalism and mode concept

We now study *Love waves, i.e., waves of the SH-type*, for example, surface waves in layered media. First, we discuss the general case of arbitrarily many layers and give the *numerical* method, with which the *dispersion relation* $c = c(\omega)$ or $k = k(\omega)$ can be determined; then the case of a single layer over a half-space is discussed in more detail.

We start from the basic equations in section 4.1.1 and use the ansatz (4.5) for Love waves in the wave equation (4.3) for the displacement in y-direction. By this, we derive, in analogy with (4.8), in the j-th layer

$$v_j = D_j \exp\left[i\left(\omega t - kx + k\gamma_j(z - z_j)\right)\right] + E_j \exp\left[i\left(\omega t - kx - k\gamma_j(z - z_j)\right)\right], \tag{4.13}$$

where D_j and E_j are now constants and

$$\gamma_j = \left(\frac{c^2}{\beta_j^2} - 1\right)^{\frac{1}{2}}.$$

We postulate, that γ_j is positive real or negative imaginary, depending on its radicand being positive or negative, respectively. In the half-space ($j = n$), γ_n has to be negative imaginary due to (4.6), i.e., $c < \beta_n$, and

$$D_n = 0. \tag{4.14}$$

The boundary conditions require for $z = z_1, z_2, \ldots, z_n$ continuity of the tangential stress $\mu\partial v/\partial z$ and for $z = z_2, z_3, \ldots, z_n$ continuity of the displacement v. From $\partial v_1/\partial z = 0$ for $z = z_1 = 0$, it follows that

$$E_1 = D_1. \tag{4.15}$$

For $z = z_j$ ($j \geq 2$) with $v_j = v_{j-1}$ and $\mu_j \partial v_j/\partial z = \mu_{j-1}\partial v_{j-1}/\partial z$, the following equations for D_j and E_j with dependence on D_{j-1} and E_{j-1}, can be derived

$$\begin{aligned} D_j + E_j &= D_{j-1}e^{ik\gamma_{j-1}d_{j-1}} + E_{j-1}e^{-ik\gamma_{j-1}d_{j-1}} \\ D_j - E_j &= \frac{\mu_{j-1}\gamma_{j-1}}{\mu_j\gamma_j}\left[D_{j-1}e^{ik\gamma_{j-1}d_{j-1}} - E_{j-1}e^{-ik\gamma_{j-1}d_{j-1}}\right]. \end{aligned}$$

As in section 3.6.5, this can be expressed in matrix form

$$\begin{pmatrix} D_j \\ E_j \end{pmatrix} = \frac{1}{2}e^{ik\gamma_{j-1}d_{j-1}} \begin{pmatrix} 1+\eta_j & (1-\eta_j)e^{-2ik\gamma_{j-1}d_{j-1}} \\ 1-\eta_j & (1+\eta_j)e^{-2ik\gamma_{j-1}d_{j-1}} \end{pmatrix} \begin{pmatrix} D_{j-1} \\ E_{j-1} \end{pmatrix}$$

or (4.16)

$$\begin{pmatrix} D_j \\ E_j \end{pmatrix} = \text{layer matrix } \underline{m}_j \begin{pmatrix} D_{j-1} \\ E_{j-1} \end{pmatrix}$$

$$\eta_j = \frac{\mu_{j-1}\gamma_{j-1}}{\mu_j\gamma_j}.$$

Successive application of (4.16) leads to

$$\begin{pmatrix} D_n \\ E_n \end{pmatrix} = \underline{m}_n \cdot \underline{m}_{n-1} \cdots \underline{m}_3 \cdot \underline{m}_2 \begin{pmatrix} D_1 \\ E_1 \end{pmatrix} = \underline{M} \begin{pmatrix} D_1 \\ E_1 \end{pmatrix} = \begin{pmatrix} M_{11} M_{12} \\ M_{21} M_{22} \end{pmatrix} \begin{pmatrix} D_1 \\ E_1 \end{pmatrix}.$$

$\underline{M}$ is the product of the layer matrices. With (4.14) and (4.15), the equation for c or k as a function of ω and the layer parameters can be given as a *dispersion equation*

$$M_{11} + M_{12} = 0. \tag{4.17}$$

This equation is ordinarily solved numerically. For this, a value of c within the interval from 0 to β_n is chosen, and then $M_{11} + M_{12}$ is computed via the multiplication of the layer matrices as function of ω in the relevant frequency range. Finally, their zeros are determined. Then, c is varied and the corresponding shifted zeros are determined, *etc.* If zeros exist, their location depends on the S-velocity and the density as a function of depth. Each zero gives *one branch of the dispersion curve of the phase velocity* $c_i(\omega)$ (see Fig. 4.5).

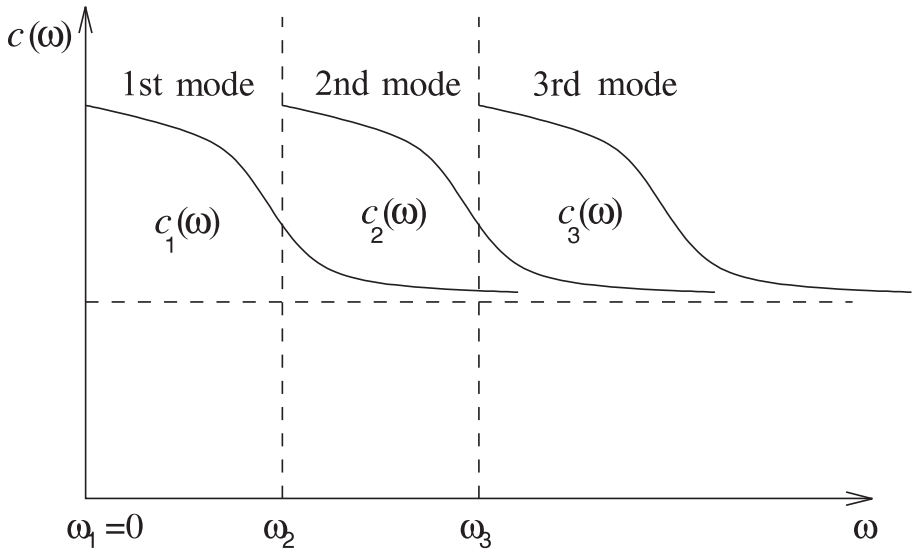

Fig. 4.5: Dispersion curves of the phase velocity.

Each branch has a *(lower) cutoff frequency* $\nu_i = \omega_i / 2\pi$. Theoretical dispersion curves are computed as a function of frequency, period or wavenumber, respectively (in the last case the frequency is fixed). Experimentally determined curves are mostly given as a function of period.

The wave behaviour in the half-space, corresponding to a certain branch of the dispersion curve, is called *mode*. For Love waves, these are *normal modes* of

the *SH*-type that propagate undamped. The concept of modes also holds for Rayleigh waves and damped surface waves. Modes are classified by their order: 1st mode, 2nd mode, *etc.* Often the first mode is also called *fundamental mode* and the numbering starts after it. Besides their dispersive properties, modes differ by their number of *node surfaces*. This number is (up to ± 1) identical with their order. Which modes occur in reality, depends on the frequency range in which the source radiates, as well as its depth (compare section 4.2). For earthquakes usually, only a few modes contribute, and often only the fundamental mode contributes to the surface waves. In Fig. 3.39, the Love waves consist mainly of the fundamental modes.

Special case n=2

In the case of a single layer over a half-space, the dispersion equation (4.17) can be written as

$$e^{-2ik\gamma_1 d_1} = \frac{\eta_2 + 1}{\eta_2 - 1} = \frac{\mu_1\gamma_1 + \mu_2\gamma_2}{\mu_1\gamma_1 - \mu_2\gamma_2} \tag{4.18}$$

with $\gamma_{1,2} = (c^2/\beta_{1,2}^2 - 1)^{1/2}$. γ_2 is negative imaginary and $c < \beta_2$.

If $\beta_1 > \beta_2$, γ_1 is also negative imaginary. Then, the right side of (4.18) is real and larger than 1. The left side is also real, but smaller than 1. Therefore, no real solution c of (4.18) exists in this case.

The S-velocity in the half-space, therefore, has to be larger than that of the layer, i.e., $\beta_2 > \beta_1$. In this case, we can exclude values of c between 0 and β_1 with the same arguments as for $\beta_1 > \beta_2$. This leaves values for c between β_1 and β_2. In this case γ_1 is positive real, and both sides in (4.18) are complex. The absolute value of both sides is 1. Thus, the matching of the phases gives the *dispersion equation of the Love waves*

$$-2k\gamma_1 d_1 = -2\arctan\frac{\mu_2|\gamma_2|}{\mu_1\gamma_1}.$$

From this, it follows with $\omega = kc$

$$\frac{\mu_2\left(c^{-2} - \beta_2^{-2}\right)^{\frac{1}{2}}}{\mu_1\left(\beta_1^{-2} - c^{-2}\right)^{\frac{1}{2}}} = \tan\left[\omega d_1\left(\beta_1^{-2} - c^{-2}\right)^{\frac{1}{2}}\right]. \tag{4.19}$$

This transcendent equation is solved by selecting c with $\beta_1 < c < \beta_2$ and inversion of the radicand, thus, giving the corresponding ω (or the the corresponding $\omega's$). For a *general* discussion, we introduce a new variable x

$$\left.\begin{aligned} x(c) &= \omega d_1 \left(\beta_1^{-2} - c^{-2}\right)^{\frac{1}{2}} \\ c(x) &= \frac{\omega d_1}{\left(\frac{\omega^2 d_1^2}{\beta_1^2} - x^2\right)^{\frac{1}{2}}}. \end{aligned}\right\} \tag{4.20}$$

The left side of (4.19) can then be written as

$$\frac{\mu_2 \left(c^{-2} - \beta_2^{-2}\right)^{\frac{1}{2}}}{\mu_1 \left(\beta_1^{-2} - c^{-2}\right)^{\frac{1}{2}}} = \frac{\mu_2}{\mu_1 x} \left[\omega^2 d_1^2 \left(\beta_1^{-2} - \beta_2^{-2}\right) - x^2\right]^{\frac{1}{2}} = f(x, \omega).$$

Equation (4.19) can then be expressed (see also Fig. 4.6) as

$$f(x, \omega) = \tan x.$$

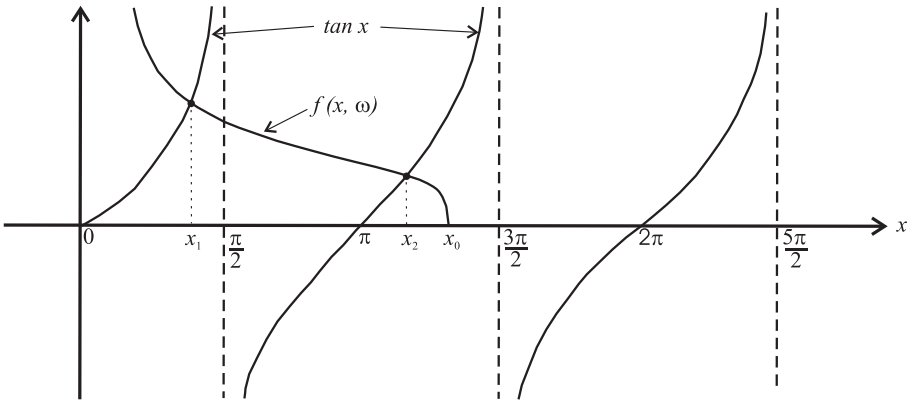

Fig. 4.6: $f(x, \omega)$ and tan x.

$f(x, \omega)$ is real between x=0 and its zero

$$x_0 = \omega d_1 \left(\beta_1^{-2} - \beta_2^{-2}\right)^{\frac{1}{2}}. \tag{4.21}$$

This zero moves to the right as a function of ω and creates, thus, more intersections of $f(x, \omega)$ with $\tan x$. The intersection $x_i = x_i(\omega)$ gives, substituting in *c(x)* from (4.20), the *dispersion relation of the i-th mode* $(i = 1, 2, \ldots)$

$$c_i(\omega) = \frac{\omega d_1}{\left(\frac{\omega^2 d_1^2}{\beta_1^2} - x_i^2(\omega)\right)^{\frac{1}{2}}}. \tag{4.22}$$

The i-th mode occurs only if $x_0 > (i-1)\pi$. With (4.21), its *cutoff frequency* becomes

$$\nu_i = \frac{\omega_i}{2\pi} = \frac{i-1}{2d_1\left(\beta_1^{-2} - \beta_2^{-2}\right)^{\frac{1}{2}}}. \tag{4.23}$$

The i-th mode exists only for frequencies $\nu > \nu_i$. The first mode (fundamental mode, i=1) exists, due to $\nu_1 = 0$, at all frequencies.

The phase velocity of each mode at its cutoff frequency is most simply derived from the fact that at this point the tangent is zero in (4.19)

$$c_i(\omega_i) = \beta_2. \tag{4.24}$$

For $\omega \to \infty$, $x_i \to (i-1/2)\pi$ and the tangent in (4.19) approaches ∞. Therefore,

$$\lim_{\omega\to\infty} c_i(\omega) = \beta_1. \tag{4.25}$$

An upper-limiting frequency does not exist, and the velocities of the layer and the half-space are the limiting values of the phase velocity.

A calculated example for the dispersion curves of the first three Love modes of a crust-mantle model, consisting of a half-space with a layer above, is given in Fig. 4.7.

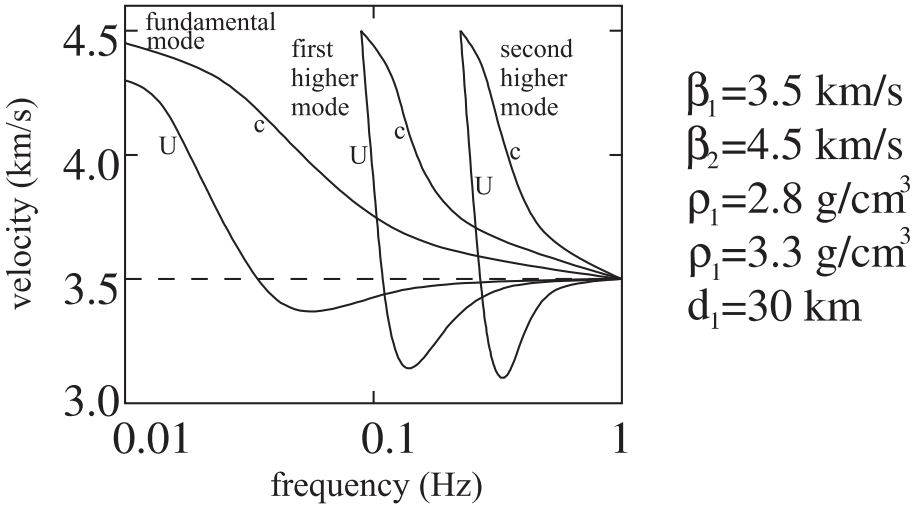

Fig. 4.7: Dispersion curves of the first three Love modes of a crust-mantle model.

In addition to the curves of the phase velocities c, the *group velocities* U are shown

$$U = \frac{d\omega}{dk} = c + k\frac{dc}{dk} = c - \Lambda\frac{dc}{d\Lambda} = \frac{c}{1 - \frac{\omega}{c}\frac{dc}{d\omega}} = \frac{c}{1 + \frac{T}{c}\frac{dc}{dT}}. \tag{4.26}$$

(Λ= wavelength, T= period). The group velocity controls, as we will see, the propagation of an impulse from the source to a receiver, i.e., each frequency travels with its group velocity from the source to the receiver, *not* with its phase velocity. Phase and group velocities can be determined from observations (see section 4.1.4 and 4.1.5). Thus, both can be used for interpretation.

Nodal planes and eigen functions

Finally, we examine the *nodal planes* of the Love modes for the case just discussed, i.e., the surfaces on which the displacement is zero. From (4.13) with (4.14) and (4.15), it follows that

$$\begin{aligned} v_1 &= 2E_1 \cos(k\gamma_1 z) \exp\left[i\left(\omega t - kx\right)\right] \\ v_2 &= E_2 \exp\left(-ik\gamma_2(z - d_1)\right) \exp\left[i\left(\omega t - kx\right)\right] \end{aligned}$$

where v_1 and v_2 are for the layer and the half-space, respectively. These expressions also hold for each individual mode, and the dispersion relation (4.22) has to be used. The relation between E_1 and E_2 is $E_2 = 2E_1 \cos(k\gamma_1 d_1)$; E_1 can be chosen arbitrarily.

This means that at the surface $z = 0$, the *maximum displacement* is always observed, and that nodal planes can only occur in the layer, but not in the half-space. Their position is determined by the zeros of the cosine. For the i-th mode they can be derived via the equation

$$k\gamma_1 z = \omega\left(\beta_1^{-2} - c_i^{-2}\right)^{\frac{1}{2}} z = (2n-1)\frac{\pi}{2} \qquad (n = 1, 2, \ldots, N_i), \tag{4.27}$$

where N_i is their number determined by $z \leq d_1$.

For the lower frequency limit $\omega = \omega_i$, from (4.23), it follows due to (4.24)

$$(i-1)\pi\frac{z}{d_1} = (2n-1)\frac{\pi}{2}.$$

This is satisfied for

$$z = \frac{2n-1}{2i-2} d_1 \text{ with } n = 1, 2, \ldots, N_i = i - 1.$$

For $\omega = \omega_i$, therefore, $i-1$ nodal planes exist. Their spacing is

$$\Delta z = \frac{d_1}{i-1} \ (i = 3, 4, \ldots).$$

The first mode (i=1) has no nodal plane, neither for $\omega = \omega_1 = 0$ nor for finite $\omega > 0$.

The other extreme on the frequency scale of each mode is $\omega = \infty$. From the discussion of the behaviour of $c_i(\omega)$ for $\omega \to \infty$ (see (4.25)), it follows that

$$\lim_{\omega\to\infty} \omega \left(\beta_1^{-2} - c_i^{-2}\right)^{\frac{1}{2}} = \lim_{\omega\to\infty} \frac{x_i(\omega)}{d_1} = \left(i - \frac{1}{2}\right) \frac{\pi}{d_1}.$$

Equation (4.27) leads to the fact that all $z \leq d_1$ have to be determined which satisfy the relation

$$\left(i - \frac{1}{2}\right) \pi \frac{z}{d_1} = (2n-1)\,\frac{\pi}{2}.$$

These are the values

$$z = \frac{2n-1}{2i-1} d_1 \text{ with } n = 1, 2, \ldots, N_i = i.$$

For $\omega = \infty$, therefore, i nodal planes exist with the spacing

$$\Delta z = \frac{d_1}{i - \frac{1}{2}} \quad (i = 2, 3, \ldots).$$

The change relative to the situation where $\omega = \omega_i$ holds, is first, the decrease in the spacing of the nodal planes, second a general move to shallower depth and finally, the addition of the i-th nodal plane $z = d_1$. This means that for $\omega = \infty$ the half-space remains at rest.

Fig. 4.8 shows quantitatively the amplitude behaviour of the first three modes as a function of depth for the crust-mantle model used for Fig. 4.7. The period is also indicated. Such amplitude distributions are called *eigen functions* of the modes. They follow from the z-dependent part of the displacement v_1 and v_2 discussed above.

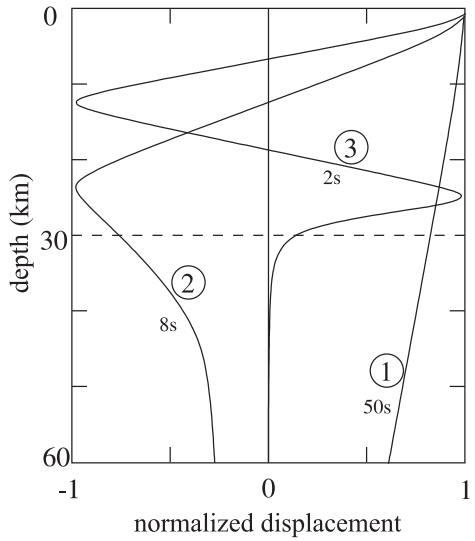

Fig. 4.8: Quantitative amplitude behaviour of the first three modes as a function of depth for the crust-mantle model used for Fig. 4.7.

Exercise 4.3

Derive the dispersion equation for free Rayleigh waves in a liquid medium consisting of a layer over a half-space and compare this to (4.19). Sketch a figure similar to Fig. 4.6. What is the difference, especially for the first mode?

4.1.4 Determination of the phase velocity of surface waves from observations

In the last section, we saw how the phase velocity of a Love mode in a layered half-space can be determined if the half-space is known. In the same way (but with more complications), the same can be done for Rayleigh waves. We now discuss the derivation of the phase velocity from *observations*. We assume that only *one* mode is present. If that is not the case, *filters* have to be used to separate the different modes. Since these are sometimes complicated methods, they are not discussed here. An overview, and applications for surface waves, can be found, e.g., in Aki and Richards, Dahlen and Tromp, and Kennett.

We work here with plane surface waves, i.e., we neglect the source term. The method for the determination of the phase velocity thus derived, is sufficiently accurate for practical purposes. The *modal seismogram* of any displacement component at the Earth's surface can be written for propagation of the mode in x-direction as

$$u(x,t) = \frac{1}{2\pi}\int_{-\infty}^{+\infty} A(\omega)\exp\left[i\omega\left(t - \frac{x}{c(\omega)}\right)\right]d\omega. \tag{4.28}$$

This is a superposition of the previously discussed harmonic surface waves with the aid of the Fourier integral. $c(\omega)$ is the phase velocity of the mode to be derived from the recordings of $u(x,t)$. Since c is frequency dependent, the seismograms for different x are different. $A(\omega)$ is the spectrum of the displacement at (arbitrary) x=0. The amplitude spectrum is $|A(\omega)|$ and the phase spectrum $\Phi(\omega) = \arg A(\omega)$, i.e.,

$$A(\omega) = |A(\omega)|e^{i\Phi(\omega)}.$$

We assume that $u(x,t)$ is known for $x = x_1$ and $x = x_2 > x_1$ and apply a Fourier analysis to the seismograms

$$u(x_{1,2},t) = \frac{1}{2\pi}\int_{-\infty}^{+\infty} G_{1,2}(\omega)e^{i\omega t}d\omega, \tag{4.29}$$

where $G_{1,2}(\omega)$ is the spectrum of the seismogram for $x = x_{1,2}$. The comparison of (4.29) with (4.28) gives

$$G_{1,2}(\omega) = |G_{1,2}(\omega)|e^{i\varphi_{1,2}(\omega)} =$$

$$A(\omega)\exp\left[-i\omega\frac{x_{1,2}}{c(\omega)}\right] = |A(\omega)|\exp\left[i\left(\Phi(\omega) - \omega\frac{x_{1,2}}{c(\omega)}\right)\right].$$

If the time t=0 is identical for both seismograms, and, if possible, jumps of $\pm 2\pi$ have been removed from the numerically determined phases $\varphi_{1,2}(\omega)$ (usually between $-\pi$ and $+\pi$), the phases of the top (observation $G_{1,2}(\omega)$...) and the bottom ($|A(\omega)|$...) can be matched and give

$$\varphi_{1,2}(\omega) = \Phi(\omega) - \omega\frac{x_{1,2}}{c(\omega)}.$$

Subtracting $\varphi_1(\omega)$ from $\varphi_2(\omega)$, the unknown phase spectrum $\Phi(\omega)$ of $u(0,t)$ cancels and the following result for the phase velocity is left

$$c(\omega) = \frac{(x_2 - x_1)\omega}{\varphi_1(\omega) - \varphi_2(\omega)}. \tag{4.30}$$

For practical applications of this method, the surface waves have to be recorded at two stations which are on a great circle path with the source. In case *three* stations are available, this requirement can be circumvented by constructing a triangle between the stations. In both approaches, the phase velocities derived are representative for the region *between* the stations.

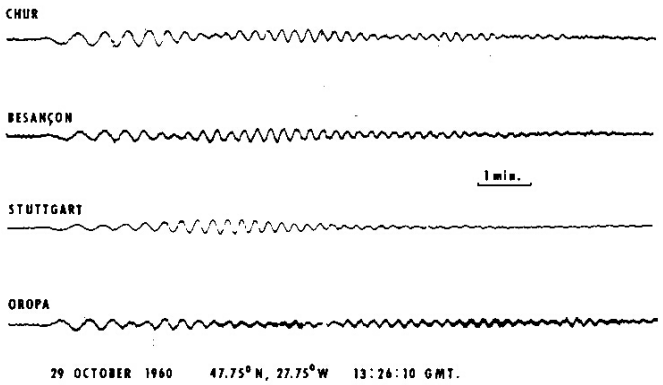

Fig. 4.9: Example for seismograms of Rayleigh waves from L. Knopoff, et al., 1966. The traces have been shifted.

The interpretation based on the phase velocity from Fig. 4.9 is given in Fig. 4.10. It shows short period group velocity observations from near earthquakes as well as phase-velocity measurements for the region of transition (Central Alps to northern Foreland, Fig. 4.9) (from L. Knopoff, St. Müller and W.L. Pilant: Structure of the crust and upper mantle in the Alps from the phase velocity of Rayleigh waves, Bull. Seism. Soc. Am. *56,* 1009-1044, 1966).

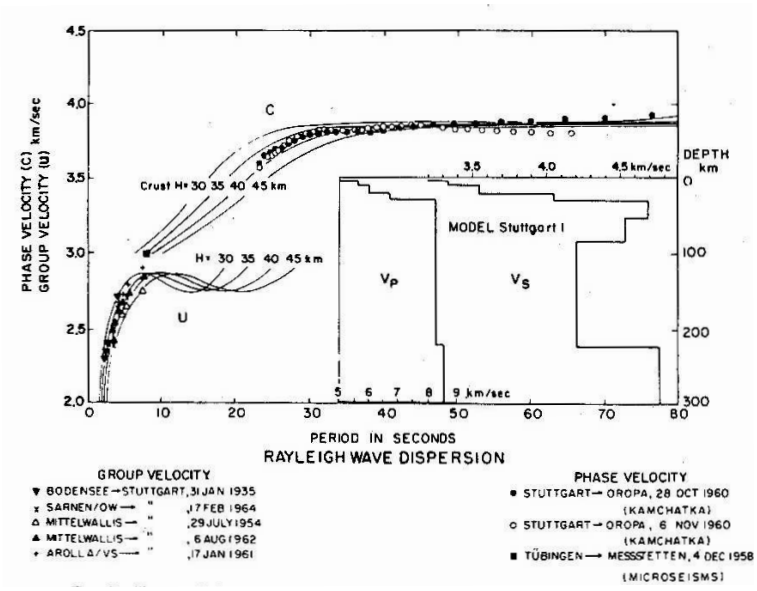

Fig. 4.10: Short period group velocity observations from L. Knopoff, et al., 1966.

4.1.5 The group velocity

Seismograms with dispersion, as shown in Fig. 4.9, often have a very slow variation of frequency with time, so that *one* frequency can be associated with a certain time. If this is done for two different distances x_1 and x_2 (on a great circle through the source), and if the times, for which frequency ω is observed are $t_1(\omega)$ and $t_2(\omega)$, it follows that

$$U(\omega) = \frac{x_2 - x_1}{t_2(\omega) - t_1(\omega)}. \tag{4.31}$$

$U(\omega)$ is the velocity with which this frequency, or a *wave group with a small frequency band* $\Delta\omega$ *around the frequency* ω, propagates. U is, therefore, called the group velocity. The theory of surface waves from point sources in section 4.2 gives the even simpler formula $U(\omega) = r/t(\omega)$, which only requires *one* seismogram; r is the distance from the source, and $t(\omega)$ is relative to the time when the wave started (source time). In practice, this seismogram is filtered in a narrow band with the central frequency ω. The arrival time $t(\omega)$ is at the maximum of the envelope of the filtered seismogram. The group velocity can, therefore, in principal be determined without difficulty from observations. Another question is, how the group velocity is connected with the phase velocity and, thus, with the parameters of the Earth, i.e., the velocity of P- and S-waves and density, as a function of depth.

To study this relation, we start from the description of the modal seismogram (4.28) and express it using the wavenumber $k = \omega/c$ as

$$u(x,t) = \frac{1}{2\pi} \int_{-\infty}^{+\infty} A(\omega) \exp\left[i\left(\omega t - kx\right)\right] d\omega. \tag{4.32}$$

For sufficiently large x and, therefore, also large t, the phase

$$\varphi(\omega) = \omega t - kx$$

is *rapidly varying* compared to $A(\omega)$. This means, for example, that for changing ω $\varphi(\omega)$ has changed by 2π, whereas $A(\omega)$ is practically unchanged, and the ω-interval, therefore, does usually not contribute to the integral (4.32). This is especially true if $\varphi(\omega)$ can be approximated linearly. This no longer holds for $\omega = \omega_0$, for which $\varphi(\omega)$ has an extremum (see Fig. 4.11), i.e., when it becomes *stationary*.

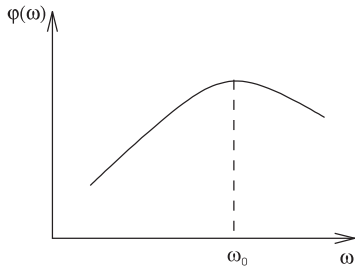

Fig. 4.11: Extremum of $\varphi(\omega)$.

This frequency ω_0 depends on t and follows from

$$\varphi'(\omega_0) = t - x\frac{dk}{d\omega}\,|_{\omega=\omega_0} = 0. \tag{4.33}$$

The frequency ω_0, which satisfies (4.33), dominates at time t in the modal seismogram. Since for *plane* surface waves location and time origin are arbitrary, (4.33) can be written for two distances x_1 and x_2 and corresponding times $t_1(\omega_0)$ and $t_2(\omega_0)$, respectively. Subtraction gives the *basic formula for the group velocity*

$$\frac{x_2 - x_1}{t_2(\omega_0) - t_1(\omega_0)} = U(\omega_0) = \frac{d\omega}{dk}\,|_{\omega=\omega_0}. \tag{4.34}$$

ω and k are connected via the phase velocity $c = \omega/k$. Using this, the explicit group velocity (4.26) can be derived directly from (4.34) (see exercise 4.4).

The arguments sketched here are the central ideas of the *method of stationary phase*. We will use it later to calculate integrals of the form (4.32) approximately; here, it was only used to demonstrate that it is the group velocity which determines the sequence and possible interference in the modal seismogram.

To make this statement more obvious, we consider an arbitrary mode of the *Rayleigh waves of a liquid half-space with a layer at the top*. Its dispersion curves for phase and group velocity look like those in Fig. 4.12 (compare exercise 4.3).

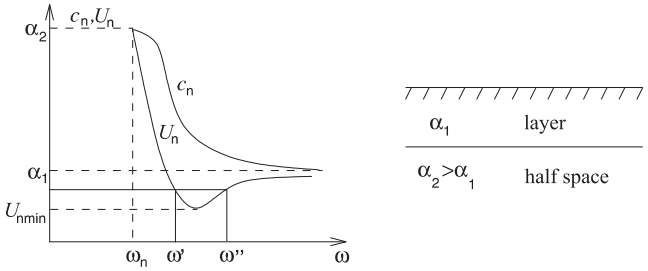

Fig. 4.12: Dispersion curves for a liquid half-space with a top layer.

Instead of (4.31), or the left of (4.34), we use $U(\omega) = r/t(\omega)$, which refers to the source, to interpret the curve of the group velocity.

From the trend in U_n, we conclude that for the mode considered, the frequencies in the neighbourhood of the lower limiting frequency ω_n arrive at an arbitrary distance r from the source. This assumes that such frequencies are actually excited at the source. Their group velocity is α_2, and their group travel time is r/α_2. For later times, which are still smaller than r/α_1, the frequency of the arriving oscillations slowly increases, corresponding to the steep trend in the curve of U_n. This wave train is called the *fundamental wave*. At later times greater then r/α_1 there are *two* frequencies, ω' and ω'', which contribute to the seismogram. This has the effect that the higher frequency waves (water waves) ride on the fundamental waves. The frequencies of the two waves approach each other for increasing time and become identical at time r/U_{nmin}. Here, U_{nmin} is the minimal group velocity. The corresponding wave group is the *Airy phase*, and it constitutes the end of the modal seismogram. Exact computations of modal seismograms, discussed later, confirm these qualitative statements. The example in Fig. 4.13 shows the behaviour of pressure of the fundamental mode (from C.L. Pekeris: Theory of propagation of explosive sound in shallow water, Geol. Soc. Am. Memoir No. 27, 1948).

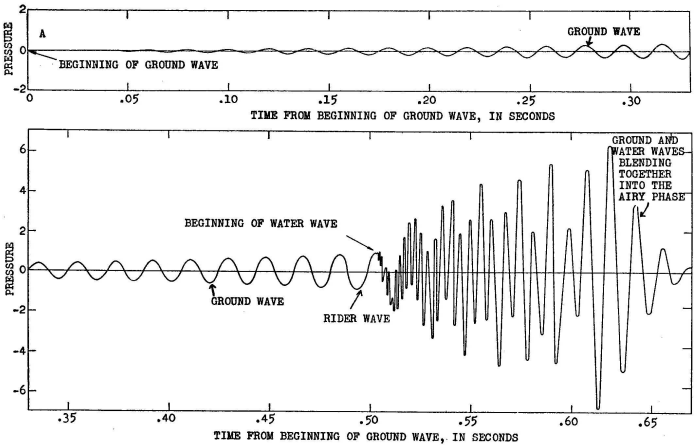

Fig. 4.13: Pressure of the fundamental mode from C.L. Pekeris, 1948. $\alpha_1 = 1500$ m/s , $\alpha_2 = 1650$ m/s, $\rho_1 = 1$ g/ cm^3, $\rho_2 = 2$ g/ cm^3, $d_1 = 20$ m.

The dispersion of the fundamental wave of the example in Fig. 4.13, shown for a source distance of 9200 m , i.e., decreasing group velocity with increasing frequency (increase of frequency with time), is called *regular dispersion*. For the water wave, the group velocity grows with the frequency (frequency increases with increasing time); this is called *inverse* dispersion. The notation regular and inverse dispersion should not be confused with the expressions *normal* and

anomal dispersion, which express, that the group velocity is larger or smaller than the phase velocity, respectively.

Fig. 4.14 is a sketch to demonstrate the basic propagation properties of a dispersive wave train. It assumes that the source radiates an impulse with constant spectrum in the frequency band $\omega_1 \leq \omega \leq \omega_2$ and that the medium produces only regular dispersion. The larger the propagation distance, the longer the wave train becomes. At the same time, the amplitudes decrease (not shown in Fig. 4.14).

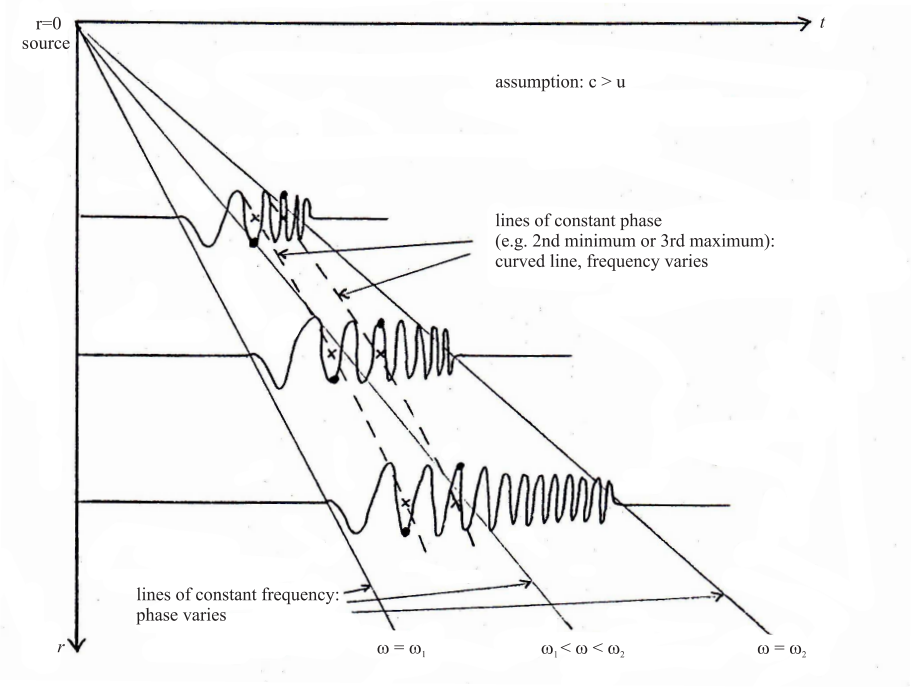

Fig. 4.14: Basic propagation properties of dispersive wave trains.

Constant frequencies occur on *straight lines* through the origin ($r = 0, t = 0$) with a slope of dr/dt that is identical to the group velocity. *Constant phases*, e.g., a certain maximum or an intersection with zero, are situated on *curved lines*, and the frequency varies along these curves. The local slope dr/dt of these curves is the phase velocity for the dominating frequency at this time.

Exercise 4.4

Derive (4.26) for the group velocity. How does $dc/d\omega$ behave for normal and abnormal dispersion, respectively?

Exercise 4.5

a) What is the form of the most general phase velocity $c(\omega)$ for which the group velocity $U(\omega)$ is constant? Interpret the corresponding seismogram (4.28).

b) What is the most general connection between phase velocities $c_1(\omega)$ and $c_2(\omega)$ with identical group velocities $U_1(\omega)$ and $U_2(\omega)$? Use $1/U = dk/d\omega = d(\omega/c)/d\omega$.

4.1.6 Description of surface waves by constructive interference of body waves

Up to this point, surface waves have been treated for the most part theoretically, namely based on an ansatz for the solution of differential equations. Input in these equations have been the concentration of the wave amplitude near the surface, propagation along the surface and dispersion. We have not reached a physical understanding how these waves can be constructed. In this section, we will show for the simple example of Love waves in a half-space with one layer at the top, that surface waves can basically be understood as arising from *constructive interference of body waves* which are reflected between the interfaces.

We consider *SH*-body waves which propagate up and down in the layer with an angle of incidence and reflection φ. The reflection at the surface is loss free; the reflection coefficient according to (3.39) equals +1. During reflection at the lower boundary of the layer ($z = d_1$), energy loss through reflection occur, as long as $\varphi < \varphi^* = \arcsin(\beta_1/\beta_2)$. In this case, the amplitude of the reflected waves decrease with the number of reflections at the lower boundary. If on the other hand, $\varphi > \varphi^*$, the reflection coefficient at the lower interface has the absolute value of +1 (see (3.42)). Thus, no wave in the lower half-space exists transporting energy away from the interface and the amplitude of each *single* multiple reflection is preserved. The wave field in this layer is then basically controlled by the interference of *all* multiple reflections. For certain values of φ there will be constructive interference and for other values there will be destructive interference, respectively. We try to determine those φ which show constructive interference. To achieve this, we approximate the momentary wavefield picture of Fig. 4.15, locally, by plane parallel wavefronts with a corresponding angle of incidence φ (see Fig. 4.16).

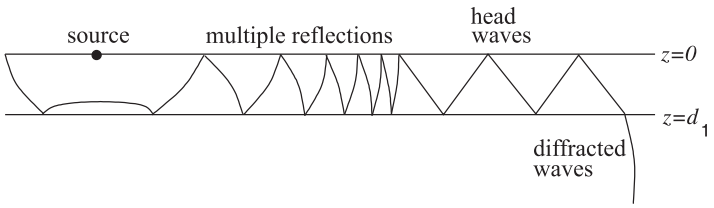

Fig. 4.15: Picture of momentary wave field.

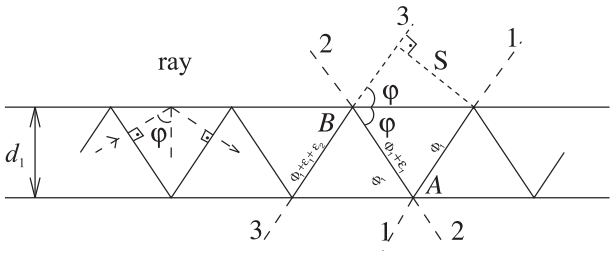

Fig. 4.16: Approximation of Fig. 4.15 by plane, parallel wavefronts.

This approximation is better at larger distances from the source. The limitation on *plane* waves means that we consider *free* normal modes.

The phases of neighbouring wavefronts 1, 2, 3 are Φ_1 (arbitrary), $\Phi_2 = \Phi_1 + \epsilon_1$ and $\Phi_3 = \Phi_1 + \epsilon_1 + \epsilon_2$, respectively, where ϵ_1 and ϵ_2 are the phase shifts of the reflections in A and B, respectively. To ensure that wave 1 and 3 are *in phase*, the phase difference $\Phi_3 - \Phi_1$ has to be equal to the phase difference due to the travel time $\omega s/\beta_1$ plus a multiple of 2π. With

$$s = 2\frac{d_1}{\tan\varphi}\sin\varphi = 2d_1\cos\varphi,$$

we derive the following condition for *constructive interference*

$$\epsilon_1 + \epsilon_2 = \frac{2\omega d_1}{\beta_1}\cos\varphi + 2n\pi, \qquad n = 0, 1, 2, \ldots. \tag{4.35}$$

The phase shifts; ϵ_1 and ϵ_2 are the phases of the reflection coefficients for plane SH-waves. Since we only consider post-critical $\varphi > \varphi^* = \arcsin(\beta_1/\beta_2)$, it follows for ϵ_1 from (3.42) and with $\omega > 0$

$$\epsilon_1 = -2\arctan\frac{b}{a} = -2\arctan\left[\frac{-\rho_2\beta_2\left(\frac{\beta_2^2}{\beta_1^2}\sin^2\varphi - 1\right)^{\frac{1}{2}}}{\rho_1\beta_1\cos\varphi}\right].$$

For the reflection at B, it holds that $\epsilon_2 = 0$, since according to (3.39), the reflection coefficient at the free surface is always $+1$.

Substituting all of the above into (4.35), we get an equation for *those* angles of incidence φ, which produce a for given ω, constructive interference

$$\arctan\left[\frac{\rho_2\beta_2\left(\frac{\beta_2^2}{\beta_1^2}\sin^2\varphi - 1\right)^{\frac{1}{2}}}{\rho_1\beta_1\cos\varphi}\right] = \frac{\omega d_1}{\beta_1}\cos\varphi + n\pi, \qquad n = 0, 1, 2, \ldots \tag{4.36}$$

In this equation, we introduce the apparent velocity

$$c = \frac{\beta_1}{\sin\varphi} \tag{4.37}$$

with which the wavefronts propagate in a *horizontal* direction. With $\cos\varphi = \beta_1(\beta_1^{-2} - c^{-2})^{1/2}$ and $\rho_{1,2}\beta_{1,2}^2 = \mu_{1,2}$, we derive by reversing (4.36), an equation for c

$$\frac{\mu_2\left(c^{-2} - \beta_2^{-2}\right)^{\frac{1}{2}}}{\mu_1\left(\beta_1^{-2} - c^{-2}\right)^{\frac{1}{2}}} = \tan\left[\omega d_1\left(\beta_1^{-2} - c^{-2}\right)^{\frac{1}{2}}\right].$$

This equation is identical with the dispersion equation (4.19) of Love waves. We would have found the same equation, if we had considered waves which propagate upwards (and not downwards) in Fig. 4.16. The superposition of both groups of waves gives, for reason of symmetry, a wave with *vertical* wavefronts. Therefore, c is not only an apparent velocity, but also the phase velocity of this resulting wave.

We also see that the Love waves in the half-space with a top layer are produced by *constructive interference of body waves* which have a *post-critical* angle of incidence. For these angles of incidence, no energy is lost from the layer into the half-space. The energy remains in the layer which acts as a perfect *wave guide*. This is generally true for normal modes of Love and Rayleigh waves in horizontally layered media, in which case that normal modes exist. From this, we can also conclude that the phase velocity of normal modes can, *at most*, be equal to the S-velocity of the half-space under the layers

$$c \leq \beta_n.$$

If it were larger, energy would be radiated into the half-space in the form of an S-wave. *Leaking modes* also occur by constructive interference of body waves. In this case, the angles of incidence are *pre-critical*, and the phase velocity is larger than β_n. Thus, radiation into the lower half-space occurs and the wave guide is not perfect.

Finally, it should be noted that the explanation of surface waves via constructive interference of body waves cannot be applied to the *fundamental mode of Rayleigh waves*. The Rayleigh wave of the homogeneous half-space, for example, exists without additional discontinuities at the surface. No simple explanation exists for the fundamental mode of Rayleigh waves.

Exercise 4.6

Determine the dispersion curves for a liquid layer whose boundaries are (1) both free, (2) both rigid, (3) one rigid and one free, respectively. Use the arguments of section 4.1.6 and compare with the solution of the corresponding eigenvalue problem. Give the group velocity and sketch the pressure-depth distributions.

4.2 Surface waves from point sources

4.2.1 Ideal wave guide for harmonic excitation

Expansion representation of the displacement potentials

We study the propagation of monochromatic sound waves from an explosive point source in a liquid layer with a free surface situated above a *rigid* half-space.

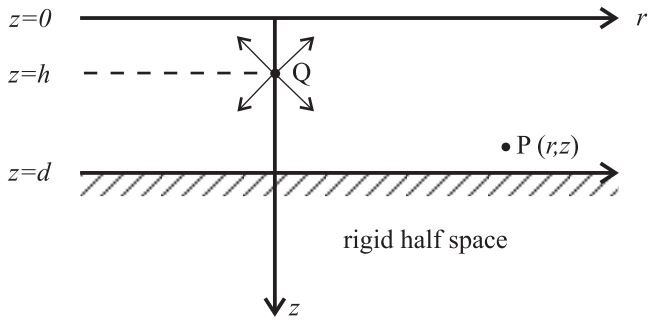

Fig. 4.17: Explosive point source in a liquid layer with a free surface atop a rigid half-space.

This is an ideal wave guide since no waves can penetrate the half-space. For such a scenario, the key features of surface waves from point sources can be studied without too much mathematical effort.

For the displacement potential Φ in the layer, we assume the following integral ansatz, using the analogy to (3.84) and applying (3.85) for the potential of the spherical wave from the source. In the following, the time-dependent term $e^{i\omega t}$ is omitted

$$\begin{aligned} \Phi &= \int_0^\infty J_0(kr)\left[\frac{k}{il}e^{-il|z-h|} + A(k)e^{-ilz} + B(k)e^{ilz}\right]dk \qquad (4.38) \\ l &= \left(\frac{\omega^2}{\alpha^2} - k^2\right)^{\frac{1}{2}}. \end{aligned}$$

$J_0(kr)$ is the Bessel function of first kind and zeroth order, k and l are the horizontal and vertical wavenumber, respectively. The square root l is, as in sections 3.6.5 and 3.7, either positive real or negative imaginary. It can be shown that Φ is a solution of the wave equations in cylindrical coordinates. The first term in (4.38) is the wave from the source, the second and third correspond to the waves

propagating in positive and negative z-direction, respectively. $A(k)$ and $B(k)$ follow from the boundary conditions for the interfaces

$$\begin{aligned} z = 0: &\qquad \text{stress} &\qquad p_{zz} = \rho\frac{\partial^2\Phi}{\partial t^2} = -\rho\omega^2\Phi = 0 \text{ or } \Phi = 0 \\ z = d: &\quad \text{normal displacement} &\quad \frac{\partial\Phi}{\partial z} = 0. \end{aligned}$$

This gives

$$\begin{aligned} A(k) + B(k) &= -\frac{k}{il}e^{-ilh} \\ A(k) - e^{2ild}B(k) &= -\frac{k}{il}e^{ilh}. \end{aligned}$$

The solution of this system of equation is (please check)

$$\begin{aligned} A(k) &= -\frac{k\cos\left[l(d-h)\right]}{il\cos(ld)} \\ B(k) &= \frac{k\sin(lh)}{l\cos(ld)}e^{-ild}. \end{aligned}$$

Inserting them into (4.38) gives

$$0 \le z \le h: \quad \Phi = 2\int_0^\infty kJ_0(kr)\frac{\sin(lz)\cos\left[l(d-h)\right]}{l\cos(ld)}dk \tag{4.39}$$

$$h \le z \le d: \quad \Phi = 2\int_0^\infty kJ_0(kr)\frac{\sin(lh)\cos\left[l(d-z)\right]}{l\cos(ld)}dk. \tag{4.40}$$

Before these expressions are solved with methods from complex analysis, it should be noted that an exchange of source and receiver does not change the value of Φ. Displacement and pressure are also the same for this case. This is an example for *reciprocity relations*, which is important in the theory of elastic waves.

The poles k_n of the integrand in (4.39) and (4.40) are determined via

$$dl_n = d\left(\frac{\omega^2}{\alpha^2} - k_n^2\right)^{\frac{1}{2}} = (2n-1)\frac{\pi}{2}, \quad n = 1, 2, 3\ldots$$

This gives

$$k_n = \left(\frac{\omega^2}{\alpha^2} - \frac{(2n-1)^2 \pi^2}{4d^2} \right)^{\frac{1}{2}}. \tag{4.41}$$

The infinite number of poles are situated on the real axis between $-\omega/\alpha$ and $+\omega/\alpha$ and on the imaginary axis, respectively. The number of poles on the real axis depends on ω. Due to these poles, the integration path in (4.39) and (4.40) have to be specified in more detail. We choose path C_1 in Fig. 4.18 which circumvents the poles in the first quadrant.

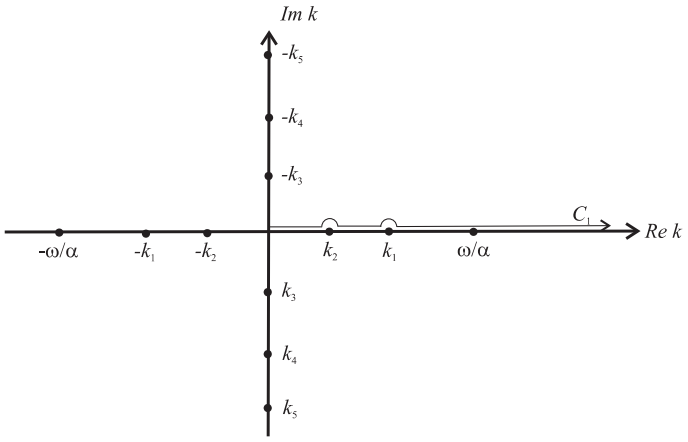

Fig. 4.18: Integration path C_1 which circumvents the poles in the first quadrant.

In the following, we discuss only (4.39) in detail. Equation (4.40) can be solved similarly. We use the identity

$$J_0(kr) = \frac{1}{2} \left[H_0^{(1)}(kr) + H_0^{(2)}(kr) \right],$$

where $H_0^{(1)}(kr)$ and $H_0^{(2)}(kr)$ are Bessel functions of the third kind (=*Hankel functions*) and zeroth order (Appendix C, equations (C.2) and (C.3), respectively). Then,

$$\Phi = \int_{C_1} k \left[H_0^{(1)}(kr) + H_0^{(2)}(kr) \right] \frac{\sin(lz)\cos\left[l(d-h)\right]}{l\cos(ld)} dk. \tag{4.42}$$

Using relation (C.6) from appendix C,

$$H_0^{(1)}(x) = -H_0^{(2)}(-x)$$

the first part of the integral in (4.42) can be written as

$$-\int_{C_1} kH_0^{(2)}(-kr)\frac{\sin(lz)\cos[l(d-h)]}{l\cos(ld)}dk = \int_{C_2} uH_0^{(2)}(ur)\frac{\sin(lz)\cos[l(d-h)]}{l\cos(ld)}du$$

where u=-k is used. The integration path C_2 is point-symmetrical to the path C_1 with respect to the coordinate centre, but it goes from $-\infty$ to 0. Inserting this in (4.42) and with consistent use of k as integration variable, gives

$$\Phi = \int_C kH_0^{(2)}(kr)\frac{\sin(lz)\cos[l(d-h)]}{l\cos(ld)}dk = \int_C I(k)dk. \qquad (4.43)$$

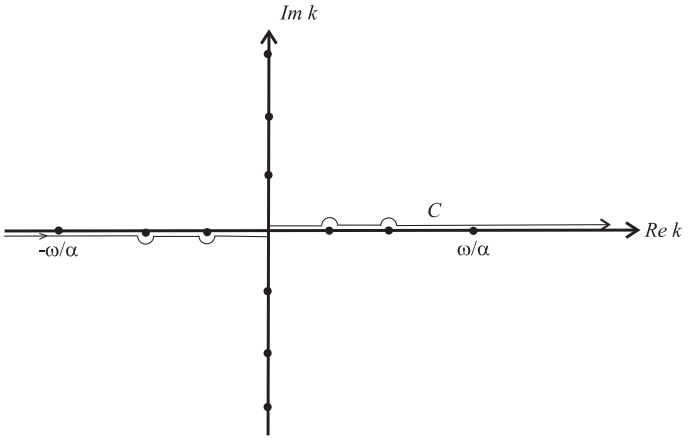

Fig. 4.19: Integration path C from $-\infty$ to $+\infty$ circumventing the poles on the real axis.

Integration path C, therefore, is, as indicated in Fig. 4.19, from $-\infty$ to $+\infty$ and circumventing the poles on the real axis.

Despite the non-uniqueness of the square root l in (4.43), $I(k)$ is a unique function of k. The reason for this is that $I(k)$ is an even function of l, thus, the sign of the square root of l does *not* matter. For more complicated wave guides, e.g., if the half-space is not rigid, $I(k)$ is not unique and the theory becomes more complicated (introduction of *branch cuts*).

Now we apply the *remainder theorem* on the closed integration path shown in Fig. 4.20 which consists of path C and a half circle with infinite radius. The *only* singularities included are the poles of $I(k)$.

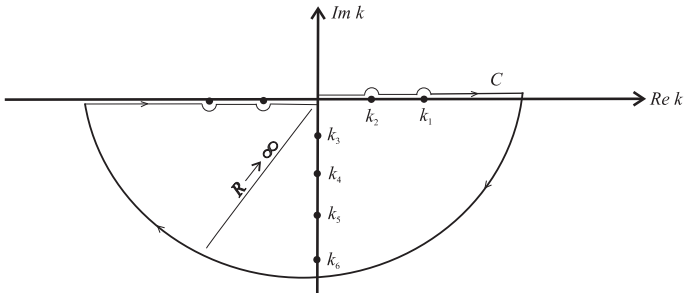

Fig. 4.20: Integration path C and half circle with infinite radius.

Then

$$\int_C + \int_L = -2\pi i \sum_{n=1}^{\infty} ResI(k)|_{k=k_n}.$$

L indicates the clockwise integration in the lower plane of Fig. 4.20, and each term in the sum is the residue of $I(k)$ at the pole $k = k_n$.

If the *asymptotic representation* of the Hankel function is used, it follows for large arguments (Appendix C, equation (C.4))

$$H_0^{(2)}(kr) \simeq \left(\frac{2}{\pi kr}\right)^{\frac{1}{2}} e^{-i\left(kr-\frac{\pi}{4}\right)}. \tag{4.44}$$

We see that their values on the semi-circle in the lower half-plane, where k has a negative imaginary part, becomes zero (for R going to ∞). The corresponding integral also goes to zero, and we have found a representation of the potential Φ as an infinite sum of residuals. The determination of the residue of the quotient $f_1(k)/f_2(k)$ at the location k_n with $f_2(k_n) = 0$ is done with the formula

$$Res\left.\frac{f_1(k)}{f_2(k)}\right|_{k=k_n} = \frac{f_1(k_n)}{f_2'(k_n)},$$

if k_n is a pole of *first* order. In our case, k_n follows from (4.41) and is either positive real or negative imaginary. The corresponding l is

$$l_n = \frac{(2n-1)\pi}{2d}.$$

Furthermore, it holds here, that $f_2(k) = \cos(ld), \quad f_2(k_n) = \cos(l_n d) = 0$ and

$$f_2'(k_n) = d\frac{k_n}{l_n}\sin(l_n d).$$

Finally,

$$\cos\left[l_n(d-h)\right] = \cos(l_n d)\cos(l_n h) + \sin(l_n d)\sin(l_n h) = \sin(l_n d)\sin(l_n h).$$

Thus,

$$Res\ I(k)|_{k=k_n} = \frac{1}{d} H_0^{(2)}(k_n r)\sin(l_n z)\sin(l_n h).$$

We, therefore, get the following *representation of the potential* Φ *as an expansion*, for which $e^{i\omega t}$ has now to be added again for completeness

$$\Phi = -\frac{2\pi i}{d}\sum_{n=1}^{\infty}\sin\left[(2n-1)\frac{\pi h}{2d}\right]\sin\left[(2n-1)\frac{\pi z}{2d}\right]H_0^{(2)}(k_n r)e^{i\omega t}. \qquad (4.45)$$

This expression not only holds for $0 \le z \le h$ but also for arbitrary depth, since according to (4.40) the same expansion can be found. From (4.45) the displacement components $\partial\Phi/\partial r$ and $\partial\Phi/\partial z$ and the pressure $p = -p_{zz} = \rho\omega^2\Phi$ can be derived.

For the ideal wave guide the field can be constructed *solely* from the contributions from the poles, each of which represents a mode, as will be shown later. For complicated wave guides, contributions in the form of curve integrals in the complex k-plane have to be added to the pole contributions. These additional contributions correspond mostly to body waves.

Modes and their properties

Each term in (4.45) represents a *mode*. This is only a definition, but it fits well into the mode concept introduced in the previous sections for *free* surface waves. If we consider, for example, the terms in (4.45) for large distances r, we can use (4.44) ($|k_n r| > 10$)

$$\Phi = \frac{-2\sqrt{2\pi}ie^{i\frac{\pi}{4}}}{d}\sum_{n=1}^{\infty}\sin\left[(2n-1)\frac{\pi h}{2d}\right]\sin\left[(2n-1)\frac{\pi z}{2d}\right]\frac{1}{(k_n r)^{\frac{1}{2}}}e^{i(\omega t - k_n r)}. \qquad (4.46)$$

The most important terms in (4.46) are those with positive k_n. Their number is finite and increases with ω. They correspond to waves with cylindrical wavefronts which propagate in $+r$-direction with the frequency dependent phase velocity

$$c_n(\omega) = \frac{\omega}{k_n} = \alpha\left[1 - \frac{(2n-1)^2\pi^2\alpha^2}{4d^2\omega^2}\right]^{-\frac{1}{2}}. \qquad (4.47)$$

If the eigenvalue problem for *free* surface waves in the same wave guide is solved (compare exercise 4.6), it follows for the *n-th free normal mode*

$$\Phi_n = A \sin\left[(2n-1)\frac{\pi z}{2d}\right] e^{i\omega\left(t-\frac{x}{c_n(\omega)}\right)}, \tag{4.48}$$

with $c_n(\omega)$ from (4.47). Furthermore, the terms in (4.46) and (4.48) agree, that describe the z-dependence agree. It, therefore, makes sense to name the single terms in (4.45) and (4.46) the *n-th forced normal mode*, if $k_n > 0$. The difference with respect to (4.48) is in the amplitude reduction proportional to $r^{-1/2}$ and in the addition of a term that depends on the source depth h. This term is named the *excitation function of the mode*. If the the source is located at a nodal plane of the free mode (4.48), the excitation function is zero, and the mode is not excited. Maximum excitation occurs, if the source is at a depth where the free mode has its maximum.

From the comparison of the free and the forced normal modes, the importance of the study of free modes becomes obvious. It describes the dispersive properties and the amplitude-depth distributions (eigen functions) of the forced normal modes and, therefore, their most important property. *This also holds for more complicated wave guides.*

The terms in (4.46) with negative imaginary k_n are not waves but represent oscillations with amplitudes that decrease exponentially in r-direction. They only contribute to the wave field near the source, where (4.45) has to be used for completeness. *The far-field is dominated by normal modes.*

The number of *nodal planes* of the n-th mode is n, and their spacing is $2d/(2n-1)$ ($n = 2, 3 \ldots$). The potential Φ, horizontal displacement $\partial\Phi/\partial r$ and pressure p have a node for $z = 0$ and a maximum for $z = d$, respectively (see Fig. 4.21). The opposite is true for the vertical displacement $\partial\Phi/\partial z$.

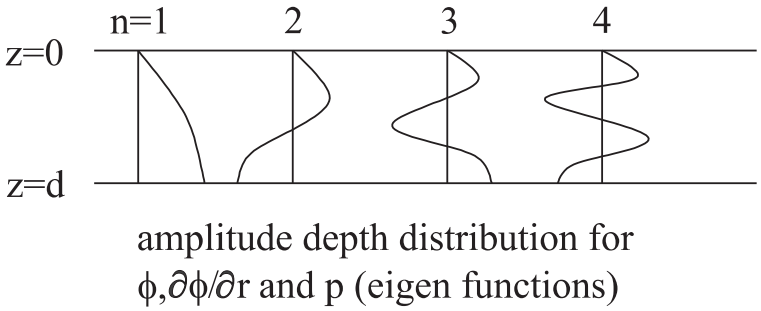

Fig. 4.21: Modes and nodal planes, n = 1, 2, 3, 4.

The phase velocity (4.47) of the n-th mode can be written as

$$c_n(\omega) = \alpha \left[1 - \left(\frac{\omega_n}{\omega}\right)^2\right]^{-\frac{1}{2}} \tag{4.49}$$

with the lower frequency limit

$$\omega_n = \frac{(2n-1)\pi\alpha}{2d}.$$

Infinitely high phase velocities can occur. According to (4.26), the group velocity is

$$U_n(\omega) = \alpha \left[1 - \left(\frac{\omega_n}{\omega}\right)^2\right]^{\frac{1}{2}}. \tag{4.50}$$

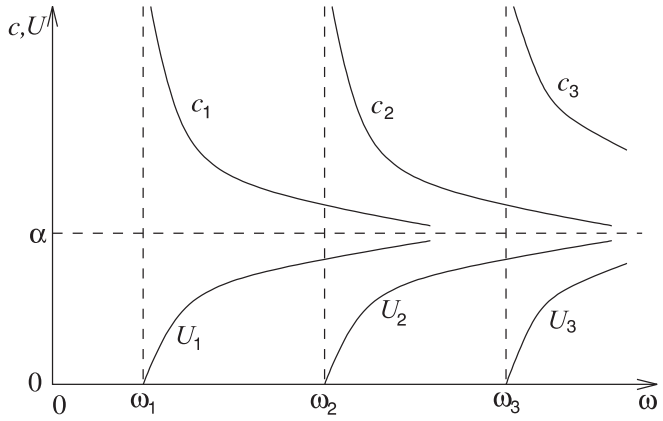

Fig. 4.22: Group and phase velocities.

An important property of the ideal wave guide with a rigid and a free interface is that the angular frequencies $\omega < \omega_1 = \pi\alpha/2d$ (or the frequencies $\nu < \alpha/4d$ and waves length $\Lambda > 4d$, respectively) *cannnot propagate undamped*. This no longer holds for the ideal wave guide with two rigid walls (compare exercise 4.6). In this case, an additional fundamental mode exists, in addition to the modes discussed before, but with different limiting frequencies. That mode can occur at all frequencies, and its phase velocity is frequency independent and equal to α.

4.2.2 The modal seismogram of the ideal wave guide

In this section, we will compute the corresponding *modal seismogram* for an arbitrary summand in (4.45), exactly. In the next section, we will use the method of stationary phase to do this.

The potential (4.45) corresponds to time harmonic excitation, i.e., for the potential of the explosion point source

$$\Phi_0 = \frac{1}{R} F\left(t - \frac{R}{\alpha}\right), \tag{4.51}$$

it holds that $F(t) = e^{i\omega t}$. From this mode of excitation, we now will move to the excitation via a delta function, $F(t) = \delta(t)$. Multiplying (4.45), without the factor $e^{i\omega t}$, with the spectrum of the delta function $\overline{F}(\omega) = 1$, gives the Fourier transform of the displacement potential. Finally, the result is transformed back into the time domain. These modal seismograms can then be convolved with realistic excitation functions $F(t)$, but the basic features can already be understood for $F(t) = \delta(t)$.

For this, we consider the n-th mode in the expansion (4.45). Its Fourier transform for excitation via a delta function is, except for geometry factors, equal to $\overline{H}_n(\omega) = iH_0^{(2)}(k_n r)$ with $k_n = (\omega^2 - \omega_n^2)^{1/2}/\alpha$. We now use the Laplace transform (compare section A.1.7)

$$h_n(s) = \overline{H}_n(-is) = iH_0^{(2)}\left[-i\frac{r}{\alpha}\left(s^2 + \omega_n^2\right)^{\frac{1}{2}}\right]$$

and the relation

$$H_0^{(2)}(-ix) = \frac{2i}{\pi} K_0(x)$$

between the Hankel function and the modified Bessel function $K_0(x)$ (see section 3.8). This gives then

$$h_n(s) = -\frac{2}{\pi} K_0\left[\frac{r}{\alpha}\left(s^2 + \omega_n^2\right)^{\frac{1}{2}}\right].$$

The original function can then be found in tables of the Laplace transform. It is zero for $t < \frac{r}{\alpha}$, and for $t > \frac{r}{\alpha}$ it holds that

$$H_n(t) = -\frac{2}{\pi} \cdot \frac{\cos\left[\omega_n\left(t^2 - \frac{r^2}{\alpha^2}\right)^{\frac{1}{2}}\right]}{\left(t^2 - \frac{r^2}{\alpha^2}\right)^{\frac{1}{2}}}.$$

Thus the n-th mode of the potential can be written as

$$\Phi_n = \begin{cases} 0 & \text{for } t < \frac{r}{\alpha} \\ \frac{4}{d}\sin\left[(2n-1)\frac{\pi h}{2d}\right]\sin\left[(2n-1)\frac{\pi z}{2d}\right]\frac{\cos\left[\omega_n\left(t^2-\frac{r^2}{\alpha^2}\right)^{\frac{1}{2}}\right]}{\left(t^2-\frac{r^2}{\alpha^2}\right)^{\frac{1}{2}}} & \text{for } t > \frac{r}{\alpha}. \end{cases} \tag{4.52}$$

That is a normal mode for *all* n since the delta function contains arbitrarily high frequencies, ensuring that the lower limiting frequency of each normal mode can be exceeded.

For simplicity, we limit the discussion in the following to the potential Φ_n. All conclusions also hold for displacement and pressure. The seismogram in Fig. 4.23 starts at time $t = r/\alpha$ with a singularity that is integrable. Then the amplitudes decrease with $1/t$, for times large compared to r/α, while oscillating. The most important feature of Φ_n is its *frequency modulation or dispersion.* The frequencies decrease from large values to the limiting frequency ω_n of the mode considered. The dispersion in the example shown is, therefore, inverse.

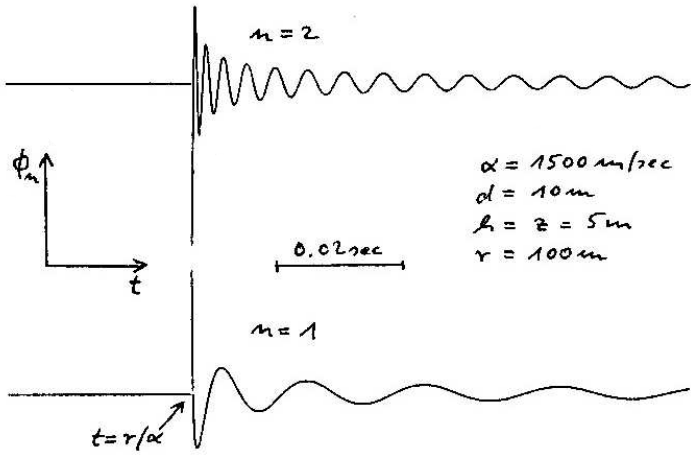

Fig. 4.23: Seismogram showing frequency modulation (dispersion).

What we have learned about the group velocity in section 4.1.5 can be confirmed with (4.52). We first ask which frequencies ω dominate at a certain time t_0 in the modal seismogram. Outside the singularity, the discussion can be limited to the cosine function in (4.52). We plan to linearise $f(t)$ near $t = t_0$ to be able to approximate the function $\cos[f(t)]$ in the neighbourhood of $t = t_0$ by the monochromatic oscillation $\cos[\varphi_0 + \omega(t_0)t]$. Here φ_0 is a phase that is independent of t, and $\omega(t_0)$ is the *instantaneous angular frequency* required. This leads to

$$\cos[f(t)] \approx \cos[f(t_0) + f'(t_0)(t - t_0)] .$$

From this, it follows that $\omega(t_0) = f'(t_0)$. If applied to (4.52), it follows

$$\omega(t_0) = \omega_n t_0 \left(t_0^2 - \frac{r^2}{\alpha^2} \right)^{-\frac{1}{2}} .$$

From this, we derive the quotient r/t_0, i.e., the velocity with which a wave group of frequency $\omega(t_0)$ propagates from the source to the receiver, and we get (with $\omega_0 = \omega(t_0)$)

$$\frac{r}{t_0} = \alpha \left[1 - \left(\frac{\omega_n}{\omega_0} \right)^2 \right]^{\frac{1}{2}} = U_n(\omega_0)$$

with $U_n(\omega_0)$ from (4.50), i.e., exactly the *group velocity* of the n-th mode. We, therefore, confirm the statement from section 4.1.5: that each frequency that is radiated from the source propagates to the receiver with the group velocity.

The *complete seismogram* in the wave guide is produced by convolving the modal seismogram (4.52) with a realistic excitation function $F(t)$, the spectrum of which has an upper limiting frequency, and sum. Only those normal modes (4.52) contribute significantly to the seismogram which have lower limiting frequencies that are smaller than the upper limiting frequency of $F(t)$. Often the response of hydro-phones and seismometers, together with the dissipative mechanisms in the wave guide, reduce the number of modes. In practise usually only a few modes contribute to the observed surface waves.

4.2.3 Computation of modal seismograms with the method of stationary phase

The computation of modal seismograms is only possible *exactly* for ideal wave guides (with rigid and/or free boundaries, respectively). In the following, an approximation is discussed and demonstrated, which gives the modal seismogram for the far-field form of a normal mode of the type of (4.46). This is the *method of stationary phase* mentioned before.

Multiplying a normal mode in (4.46) with the spectrum $\overline{F}(\omega)$ of the excitation function $F(t)$ in (4.51), then transforming back into the time domain, gives the modal seismogram as a Fourier integral. To avoid integration over negative frequencies, we use the fact that *real* functions $f(t)$ cannot only be represented as

$$f(t) = \frac{1}{2\pi} \int_{-\infty}^{+\infty} \overline{f}(\omega) e^{i\omega t} d\omega$$

but also as

$$f(t) = \frac{1}{\pi} Re \int_{0}^{\infty} \overline{f}(\omega) e^{i\omega t} d\omega.$$

This gives the modal seismogram as

$$\Phi_n = Re\left\{\frac{-2\sqrt{2}ie^{i\frac{\pi}{4}}}{\sqrt{\pi}d}\sin\left[(2n-1)\frac{\pi h}{2d}\right]\sin\left[(2n-1)\frac{\pi z}{2d}\right]\frac{1}{\sqrt{r}}\int_0^\infty \frac{\overline{F}(\omega)}{\sqrt{k_n}}e^{i(\omega t-k_n r)}d\omega\right\}. \tag{4.53}$$

The approximate computation of the integral over ω is based, as in section 4.1.5, on the fact that at times t to be considered, the phase

$$\varphi(\omega) = \omega t - k_n r \tag{4.54}$$

is usually *rapidly varying* compared to function $\overline{F}(\omega)$. Such frequencies contribute little to the integral in (4.53). This is different for frequencies with stationary phase values. Such a frequency ω_0 follows from the equation

$$\varphi'(\omega_0) = t - r\left.\frac{dk_n}{d\omega}\right|_{\omega=\omega_0} = 0$$

and depends on t. This means that the frequency ω_0, for which the group velocity is

$$U_n(\omega_0) = \left.\frac{d\omega}{dk_n}\right|_{\omega=\omega_0} = \frac{r}{t},$$

dominates the modal seismogram at time t .

From this follows the principle of *determining the group velocity* from an observed modal seismogram. For a given time t, relative to the source time, the moment frequencies and the corresponding group velocities, using t and source distance r, are determined. *The source time and epicentre* of the earthquake, therefore, have to be known. This gives a piece of the group velocity dispersion curves. One has now to verify this piece of the curve via forward modelling. The association of a certain frequency to a certain time, necessary here, is in principle not unique, but the error associated with it can be estimated. With this method, applied to surface waves of earthquakes, several important results on the structure of the Earth were found, for example, the average crustal thickness in different parts of the Earth is shown in the different branches in Fig. 4.10. A disadvantage of this method is that the result is only an average over the *whole* region between source and receiver. Therefore, today several stations are used in the interpretation of the phase velocity (compare section 4.1.4).

The *computation of the modal seismogram* requires then the following additional steps: for given time t, we expand the phase (4.54) at the frequency ω_0, which is determined by

$$U_n(\omega_0) = \frac{r}{t} \tag{4.55}$$

$$\left.\begin{array}{rcl} \varphi(\omega) & = & \varphi(\omega_0) + \frac{1}{2}\varphi''(\omega_0)(\omega-\omega_0)^2 \\ \varphi''(\omega_0) & = & \frac{r}{U_n^2(\omega_0)}\frac{dU_n}{d\omega}(\omega_0) \end{array}\right\}. \tag{4.56}$$

An *important requirement* is that $\varphi''(\omega_0) \neq 0$. Then,

$$\begin{aligned} \int_0^\infty \frac{\overline{F}(\omega)}{\sqrt{k_n}} e^{i\varphi(\omega)} d\omega &\approx \int_{\omega_0-\Delta\omega}^{\omega_0+\Delta\omega} \frac{\overline{F}(\omega)}{\sqrt{k_n}} \exp\left\{ i\left[\varphi(\omega_0) + \frac{1}{2}\varphi''(\omega_0)(\omega-\omega_0)^2\right]\right\} d\omega \\ &\approx \frac{\overline{F}(\omega_0)e^{i\varphi(\omega_0)}}{\sqrt{k_n(\omega_0)}} \int_{\omega_0-\Delta\omega}^{\omega_0+\Delta\omega} \exp\left\{\frac{i}{2}\varphi''(\omega_0)(\omega-\omega_0)^2\right\} d\omega. \end{aligned}$$

Here, we limited our discussion to the neighbourhood of the frequency ω_0, where $\varphi(\omega)$ is stationary. The other frequencies do not contribute significantly. With $x = (\omega-\omega_0)\left(\frac{1}{2}|\varphi''(\omega_0)|\right)^{1/2}$, we get

$$\begin{aligned} \int_{\omega_0-\Delta\omega}^{\omega_0+\Delta\omega} \exp\left\{\frac{i}{2}\varphi''(\omega_0)(\omega-\omega_0)^2\right\} d\omega &= \left(\frac{2}{|\varphi''(\omega_0)|}\right)^{\frac{1}{2}} \int_{-\Delta\omega\left(\frac{|\varphi''(\omega_0)|}{2}\right)^{1/2}}^{+\Delta\omega\left(\frac{|\varphi''(\omega_0|}{2}\right)^{1/2}} e^{\pm ix^2} dx \\ &\approx \left(\frac{2}{|\varphi''(\omega_0)|}\right)^{\frac{1}{2}} \int_{-\infty}^{+\infty} e^{\pm ix^2} dx \\ &= \left(\frac{2\pi}{|\varphi''(\omega_0)|}\right)^{\frac{1}{2}} e^{\pm i\frac{\pi}{4}} \end{aligned}$$

$\left(\text{with } \int_{-\infty}^{+\infty}\cos x^2 dx = \int_{-\infty}^{+\infty}\sin x^2 dx = \left(\frac{\pi}{2}\right)^{\frac{1}{2}}\right).$

The positive and the negative sign in the exponential term hold, if $\varphi''(\omega_0) > 0$ and < 0, respectively. The extension of the limits of the integration to $x = \pm\infty$ is possible, since they are proportional to $\sqrt{r}$ and r is very large. Furthermore, significant contributions to the integral come only from relatively small values of x (ca. $|x| \leq 5$). Putting all this together, the modal seismogram for the ideal wave guide in the approximation given by the method of stationary phase (with $\varphi''(\omega_0) > 0$) can be written as

$$\begin{aligned} \Phi_n &= Re\left\{ \frac{-2\sqrt{2}ie^{i\frac{\pi}{4}}}{\sqrt{\pi}d} \sin\left[(2n-1)\frac{\pi h}{2d}\right] \sin\left[(2n-1)\frac{\pi z}{2d}\right] \right. \\ &\cdot \left. \overline{F}(\omega_0)e^{i\varphi(\omega_0)} \left[\frac{2\pi}{rk_n(\omega_0)\,|\varphi''(\omega_0)|}\right]^{\frac{1}{2}} e^{i\frac{\pi}{4}} \right\}. \end{aligned} \tag{4.57}$$

Next, one uses

$$\begin{aligned} \varphi(\omega_0) &= \omega_0 t - k_n(\omega_0) r, \\ k_n(\omega_0) &= \frac{\omega_0}{\alpha}\left[1 - \left(\frac{\omega_n}{\omega_0}\right)^2\right]^{\frac{1}{2}}, \\ \frac{r}{t} &= U_n(\omega_0) = \alpha\left[1 - \left(\frac{\omega_n}{\omega_0}\right)^2\right]^{\frac{1}{2}} \end{aligned}$$

and $\varphi''(\omega_0)$ from (4.56) and deletes $\omega_0 = \omega_0(t) = \omega_n t\left(t^2 - r^2/\alpha^2\right)^{-1/2}$ from (4.57). After some calculations, and for the assumption $\overline{F}(\omega_0) = 1$, which corresponds to the excitation function $F(t) = \delta(t)$, the following *modal seismogram* can be derived (please confirm)

$$\Phi_n = \begin{cases} 0 & \text{for } t < \frac{r}{\alpha} \\ \frac{4}{d}\sin\left[(2n-1)\frac{\pi h}{2d}\right]\sin\left[(2n-1)\frac{\pi z}{2d}\right]\dfrac{\cos\left[\omega_n\left(t^2-\frac{r^2}{\alpha^2}\right)^{\frac{1}{2}}\right]}{\left(t^2-\frac{r^2}{\alpha^2}\right)^{\frac{1}{2}}} & \text{for } t > \frac{r}{\alpha}. \end{cases} \tag{4.58}$$

We, therefore, get the stringent results of (4.52). This is surprising, considering the approximations used. From this we can draw the general conclusion that the method of stationary phase is a good approximation for normal modes even for more complicated wave guides.

For frequencies ω_0 with $\varphi''(\omega_0) = 0$, i.e., with $\frac{dU_n}{d\omega}(\omega_0) = 0$ and with stationary values of the group velocity (which do not occur for ideal wave guides), the expansion in (4.56) has to be extended by one additional term. The treatment of the calculations following is, therefore, slightly different (see, for example, Appendix E). It leads to the *behaviour of Airy phases* and shows that they are usually the dominating parts of the modal seismograms (compare also Fig. 4.13).

4.2.4 Ray representation of the field in an ideal wave guide

In the last two sections we have learned that the wavefield in an ideal wave guide is composed of forced normal modes. Furthermore, we found in section 4.1.6, that free normal modes are composed of multiple reflected plane body waves in the wave guide. This raises the question, can the field of a point source in an ideal wave guide also be represented by the superposition of multiple reflections? In other words, in this case is there also a ray representation of the wave field? In addition, it is interesting to see if mode and ray representations of the wave field are then also equivalent.

We first examine the reflection of the spherical wave

$$\Phi_0 = \frac{1}{R_0} F\left(t - \frac{R_0}{\alpha}\right) \tag{4.59}$$

at the interface of the wave guide in the neighbourhood of the point source, e.g., the free surface.

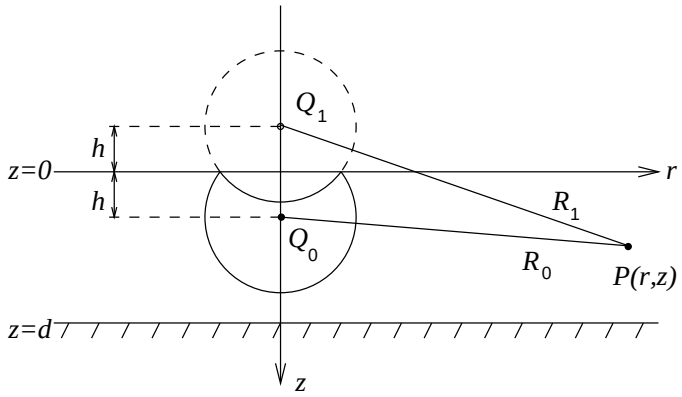

Fig. 4.24: Reflection of a spherical wave at the interface of the wave guide in the neighbourhood of the point source.

The potential of the reflection is

$$\Phi_1 = \frac{-1}{R_1} F\left(t - \frac{R_1}{\alpha}\right). \tag{4.60}$$

R_1 is the distance between $P(r,z)$ and the *image source* Q_1. As long as the reflection from the lower (rigid) interface of the wave guide has not reached the surface, the potential in the neighbourhood of the surface is $\Phi_0 + \Phi_1$ and, therefore, zero on the surface. $\Phi_0 + \Phi_1$ satisfy, therefore, for such times, the condition of no stress at the surface $z = 0$ ($p_{zz} = \rho\partial^2(\Phi_0 + \Phi_1)/\partial t^2$).

Similarly, if we consider the reflection of the spherical wave from Q_0 at the interface $z = d$, the potential of the wave reflected there can be written as

$$\Phi_2 = \frac{1}{R_2} F\left(t - \frac{R_2}{\alpha}\right), \tag{4.61}$$

where R_2 now has to be determined for a new image source with the z-coordinate $d + (d - h) = 2d - h$. That $\Phi_0 + \Phi_2$ satisfies the boundary conditions $\partial(\Phi_0 + \Phi_2)/\partial z = 0$ for $z = d$ (zero normal displacement), can be seen easily, since for points in that interface

$$
\begin{aligned}
R_0 &= R_2 \\
\frac{\partial R_0}{\partial z} &= \left.\frac{z-h}{R_0}\right|_{z=d} = \frac{d-h}{R_0} \\
\frac{\partial R_2}{\partial z} &= \left.-\frac{2d-h-z}{R_2}\right|_{z=d} = -\frac{d-h}{R_2} = -\frac{\partial R_0}{\partial z}.
\end{aligned}
$$

With the two previously considered reflections of the spherical wave originating from Q_0 at the interfaces of the wave guide, boundary conditions can only be satisfied for certain times, e.g., only as long as the reflections Φ_1 and Φ_2 have reached the opposite interface, respectively. Since they are of the same form as Φ_0, higher order reflections can be constructed in the same way. Each reflection and multiple reflection seems to come from an image source, which was created by the application of multiple mirror images of Q_0 at the interfaces (Fig. 4.25). The sign of the corresponding potential is negative if the number of reflections at the surface is odd, otherwise it is positive. Each image source corresponds to a *ray* from the source to the receiver which has undergone a certain number of reflections.

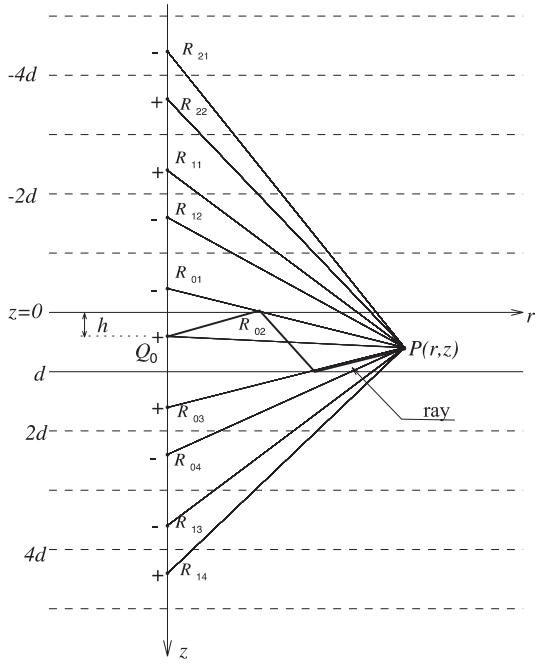

Fig. 4.25: Image sources for multiple reflections in the wave guide.

The ray concept can, without difficulties, be generalised for *solid* media (including S-waves), but this is not true for the concept of the image source. This is why, in general, and also in the case presented here, we speak of a *ray representation of the wave field*. It can be expressed as

$$\begin{aligned}\Phi &= \sum_{j=0}^{\infty}(-1)^j\left[-\frac{1}{R_{j1}}F\left(t-\frac{R_{j1}}{\alpha}\right)+\frac{1}{R_{j2}}F\left(t-\frac{R_{j2}}{\alpha}\right)\right.\\ &\left.+\frac{1}{R_{j3}}F\left(t-\frac{R_{j3}}{\alpha}\right)-\frac{1}{R_{j4}}F\left(t-\frac{R_{j4}}{\alpha}\right)\right] \qquad (4.62)\end{aligned}$$

with

$$\begin{aligned}R_{j1}^2 &= (2jd+h+z)^2+r^2\\ R_{j2}^2 &= (2jd-h+z)^2+r^2\\ R_{j3}^2 &= (2(j+1)d-h-z)^2+r^2\\ R_{j4}^2 &= (2(j+1)d+h-z)^2+r^2.\end{aligned}$$

Only those terms in (4.62) are non-zero, for which the argument is positive, and for which $F(t)$ at $t=0$ is not zero. The number of such terms is finite and increases with time.

For the ideal wave guide, the determination of the contribution of a ray is simple, since it follows the same time law as the exiting spherical wave. For other wave guides, methods like those presented in section 3.8 have to be used. The resulting numerical effort is then significantly greater and seems only justified if not too many rays have to be summed up, but that is necessary for large horizontal distances from the source where the paths of many rays become very similar. In this case, the representation of the wave field as a sum of only a few normal modes is *significantly more efficient*. The ray representation is most suited for such distances from the source where the typical normal mode properties of the wave field have *not yet* developed.

Finally, we will show that (4.62) for $F(t)=e^{i\omega t}$ and (4.39) and (4.40), respectively, are *two different representations of the same wave field*. We limit our discussion first to the case $h\le z\le d$. If $F(t)=e^{i\omega t}$ is inserted into (4.62), and the Sommerfeld integral (3.85) for a spherical wave is used for each term, it follows (the factor $e^{i\omega t}$ is again omitted)

$$\Phi = \int_0^{\infty}J_0(kr)\frac{k}{il}\sum_{j=0}^{\infty}(-1)^j\left[-\exp\left(-il\left|2jd+h+z\right|\right)\right.$$

$$
\begin{aligned}
&+\exp\left(-il\left|2jd-h+z\right|\right)\\
&+\exp\left(-il\left|2(j+1)d-h-z\right|\right)\\
&-\exp\left(-il\left|2(j+1)d+h-z\right|\right)\Big]\,dk.
\end{aligned}
$$

If $z \geq h$, the contributions are equal to the arguments *everywhere*. Then $\exp(-i2ljd)$ can be separated

$$
\begin{aligned}
\Phi \;=\; & \int_0^\infty J_0(kr)\frac{k}{il}\left[\sum_{j=0}^{\infty}\left(-e^{-2ild}\right)^j\right]\left[-\exp\left(-il\left(h+z\right)\right)\right.\\
&+\exp\left(-il\left(-h+z\right)\right)\\
&+\exp\left(-il\left(2d-h-z\right)\right)\\
&\left.-\exp\left(il\left(2d+h-z\right)\right)\right]dk.
\end{aligned}
$$

The expansion in the first square bracket has a sum of $1/(1+e^{-2ild})$. From the second square bracket, e^{-ild} can be extracted giving

$$
\begin{aligned}
\Phi \;=\; & \int_0^\infty J_0(kr)\frac{k}{2il\cos(ld)}\left[-\exp\left(il\left(d-h-z\right)\right)\right.\\
&+\exp\left(il\left(d+h-z\right)\right)\\
&+\exp\left(-il\left(d-h-z\right)\right)\\
&\left.-\exp\left(-il\left(d+h-z\right)\right)\right]dk.
\end{aligned}
$$

The remaining square bracket is equal to

$$
-2i\sin\left[l\left(d-h-z\right)\right]+2i\sin\left[l\left(d+h-z\right)\right]=4i\cos\left[l\left(d-z\right)\right]\sin\left(lh\right).
$$

Thus,

$$
\Phi = 2\int_0^\infty J_0(kr)\frac{k}{l}\frac{\cos\left[l(d-z)\right]\sin(lh)}{\cos(ld)}dk, \tag{4.63}
$$

which agrees with (4.40).

If source and receiver are exchanged in (4.62), the potential of a single ray is unchanged since it depends only on the path travelled. Therefore, exchanging z with h in (4.63) gives the potential for $0 \leq z \leq h$ which leads to (4.39). Thus, the proof of the identity of (4.62) (for $F(t) = e^{i\omega t}$) with (4.39) and (4.40), respectively, is complete.

Finally, we would like to reiterate (compare section 4.2.1) that a representation of the wave field *by normal modes alone* is only possible for ideal wave guides

which have upper and lower boundaries that are completely reflecting for all angles of incidence. In other media, additional contributions (body waves, leaky modes) occur which are not due to the poles in the complex plane like the normal modes.

Exercise 4.7

Study the polarisation of the displacement vector of the second free normal mode of the ideal wave guide (n=2 in (4.48)) as a function of depth.

Exercise 4.8

An explosive point source is located at depth h below the free surface of a liquid half-space. The displacement potential Φ is the sum of the potentials (4.59) of the direct wave and (4.60) for the reflection. Give an approximation for Φ which holds under the following conditions (dipole approximation) :

a) The dominant period of the excitation function $F(t)$ is much larger than the travel time h/α from the source to the surface.

b) The distance r to the receiver is much larger than h.

Introduce spherical coordinates R and ϑ relative to the point $r = 0$, and $z = 0$ (compare Fig. 4.24).

What is the result, if the surface is not free but rigid?

Appendix A

Laplace transform and delta function

A.1 Introduction to the Laplace transform

A.1.1 Literature

Spiegel, M.R. : Laplace Transformation, Schaum, New York, 1977

Riley, K.F., Hobson, M.P. and Bence, J.C. : Mathematical methods for physics and engineering, A comprehensive guide, Cambridge University Press, Cambridge, 2nd edition, 2002

A.1.2 Definition of the Laplace transform

The Laplace transform associates a function $f(s)$ with the function $F(t)$, or it transforms a function $F(t)$ into the function $f(s)$.

$$
\begin{aligned}
f(s) &= \int_0^\infty e^{-st} F(t) dt = \mathbf{L}\{F(t)\} \\
F(t) &= \text{original function} \\
f(s) &= \text{image function (Laplace} - \text{transform, abbreviated L} - \text{transform)}
\end{aligned}
$$

Symbolic notation: $f(s) \bullet\!\!-\!\!\circ F(t)$ ($\bullet\!\!-\!\!\circ$ = symbol of association)

$$
\begin{aligned}
t &= \text{real variable (of time)} \\
s &= \sigma + i\omega \text{ complex variable}
\end{aligned}
$$

A.1.3 Assumptions on F(t)

1. F(t) is usually a real function
2. $F(t) \equiv 0$ for $t < 0$ (satisfied for many physical parameters - causality)
3. $F(t)$ should be integrable in the interval $[0, T]$, and for $t > T$ it should hold that

$$|F(t)| < e^{\gamma t} \text{ with real } \gamma.$$

These are sufficient conditions for the existence of the L-transform $f(s)$ of $F(t)$ for complex s with Re $s > \gamma$ (*convergence half-plane*). All limited functions as, e.g., $e^{-\alpha t}$ $(\alpha > 0)$, $\sin \beta t$ *etc.* have an L-transform but also non-limited functions as $t^{-1/2}, t^n$ and $e^{\alpha t}$ $(n, \alpha > 0)$. Note assumption 2. Many functions in physics also have an L-transform. The functions t^{-1} and e^{t^2} do not have an L-transform.

A.1.4 Examples

a)

$$\begin{aligned} F(t) &= H(t) = \begin{cases} 0 & \text{for } t < 0 \\ 1 & \text{for } t \geq 0 \end{cases} \text{ Heaviside step function (unit step)} \\ f(s) &= \int_0^\infty e^{-st} dt = -\frac{1}{s}\, e^{-st}\Big|_0^\infty = \frac{1}{s} \text{ for } Re\, s > 0 \text{ (converg. half-plane)} \\ H(t) &\circ\!\!-\!\!\bullet\ \frac{1}{s} \end{aligned}$$

b)

$$\begin{aligned} F(t) &= \begin{cases} 0 & \text{for } t < 0 \\ e^{\delta t} & \text{for } t \geq 0 \end{cases} \\ f(s) &= \int_0^\infty e^{-(s-\delta)} dt = -\frac{1}{s-\delta}\, e^{-(s-\delta)t}\Big|_0^\infty = \frac{1}{s-\delta}, \quad Re\, s > \delta \\ e^{\delta t} \cdot H(t) &\circ\!\!-\!\!\bullet\ \frac{1}{s-\delta} \end{aligned}$$

For $\delta = 0$ transition to the L-transform of $H(t)$

c)

$$\frac{\sin at}{a} \cdot H(t) \circ\!\!-\!\!\bullet\ \frac{1}{s^2 + a^2}.$$

Tables of many more correspondences can be found in the literature given.

A.1.5 Properties of the Laplace transform

Similarity theorem $a > 0$

$$F(at) \circ\!\!-\!\!\bullet \int_0^\infty e^{-st} F(at)dt = \int_0^\infty e^{-\frac{s}{a}at} F(at)\frac{d(at)}{a} = \frac{1}{a}\int_0^\infty e^{-\frac{s}{a}\tau} F(\tau)d\tau$$

Therefore,

$$F(at) \circ\!\!-\!\!\bullet \frac{1}{a} f\left(\frac{s}{a}\right). \tag{A.1}$$

Thus, only the L-transform of $F(t)$ has to be known.

Example: According to section A.1.4

$$e^t \cdot H(t) \circ\!\!-\!\!\bullet \frac{1}{s-1}.$$

With the similarity theorem, it follows that

$$e^{at} \cdot H(t) \circ\!\!-\!\!\bullet \frac{1}{a}\frac{1}{\frac{s}{a}-1} = \frac{1}{s-a},$$

i.e., the result of the direct computation in section A.1.4.

Displacement theorem

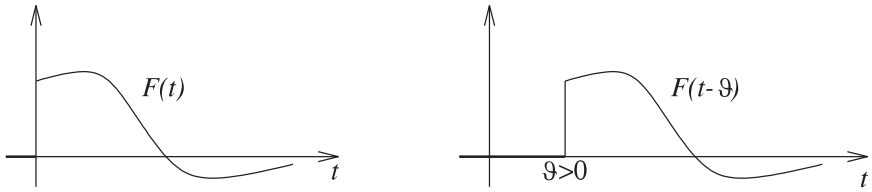

Fig. A.1: Displacement theorem.

$$\begin{aligned} F(t-\vartheta) &\circ\!\!-\!\!\bullet \int_0^\infty e^{-st} F(t-\vartheta)dt = \int_0^\infty e^{-s(\tau+\vartheta)} F(\tau)d\tau = e^{-\vartheta s} f(s) \\ F(t-\vartheta) &\circ\!\!-\!\!\bullet e^{-\vartheta s} f(s) \end{aligned} \tag{A.2}$$

Damping theorem (α arbitrary complex)

$$\begin{aligned} e^{-\alpha t} F(t) &\circ\!\!-\!\!\bullet \int_0^\infty e^{-(s+\alpha)t} F(t)dt = f(s+\alpha) \\ e^{-\alpha t} F(t) &\circ\!\!-\!\!\bullet f(s+\alpha) \end{aligned} \tag{A.3}$$

Differentiation theorem

$$F'(t) \circ\!\!-\!\!\bullet \int_0^\infty e^{-st}F'(t)dt = e^{-st}F\,(t)|_0^\infty + s\int_0^\infty e^{-st}F(t)dt$$

The first term is zero at its upper limit due to the assumption 3 from chapter A.1.3. Thus,

$$\begin{array}{rcl} F'(t) & \circ\!\!-\!\!\bullet & sf(s) - F(+0) \\ F(+0) & = & \lim\limits_{\substack{t \to 0 \\ t > 0}} \text{F(t) is the limit from the } \textit{right} \text{ side.} \end{array} \tag{A.4}$$

Generalisation:

$$\left.\begin{array}{lcl} F'(t) & \circ\!\!-\!\!\bullet & sf(s) - F(+0) \\ F''(t) & \circ\!\!-\!\!\bullet & s^2f(s) - sF(+0) - F'(+0) \\ \vdots & & \\ F^{(n)}(t) & \circ\!\!-\!\!\bullet & s^nf(s) - s^{n-1}F(+0) - s^{n-2}F'(+0) \\ & & -\ldots - sF^{(n-2)}(+0) - F^{(n-1)}(+0) \end{array}\right\} \tag{A.5}$$

Integration theorem

$$G(t) = \int_0^t F(\tau)d\tau \circ\!\!-\!\!\bullet \frac{1}{s}f(s) \tag{A.6}$$

From this, it follows that

$$G'(t) = F(t) \circ\!\!-\!\!\bullet f(s) - G(+0) = f(s).$$

Convolution theorem

$$\int_0^t F_1(\tau)F_2(t-\tau)d\tau \circ\!\!-\!\!\bullet f_1(s)f_2(s) \tag{A.7}$$

The integral is called convolution of F_1 with F_2, symbolic notation $F_1 * F_2$. Furthermore, it holds that

$$\int_0^t F_1(\tau)F_2(t-\tau)d\tau = \int_0^t F_1(t-\tau)F_2(\tau)d\tau$$

or

$$F_1 * F_2 = F_2 * F_1,$$

i.e., the convolution is commutative.

Further elementary properties of the L-transform are that it is firstly homogeneous and linear, i.e., it holds that

$$a_1F_1(t) + a_2F_2(t) \circ\!\!-\!\!\bullet\, a_1f_1(s) + a_2f_2(s),$$

and secondly, that from $F(t) \equiv 0$ it follows that $f(s) \equiv 0$ and vice versa.

An important property, which follows from the definition of the L-transform, is

$$\lim_{Re\, s \to +\infty} f(s) = 0. \tag{A.8}$$

Only *then* is a function $f(s)$ an L-transform and can be transformed back (see next chapter).

A.1.6 Back-transform

$$F(t) = \mathbf{L}^{-1}\{f(s)\} = \frac{1}{2\pi i}\int_{c-i\infty}^{c+i\infty} e^{ts}f(s)ds \tag{A.9}$$

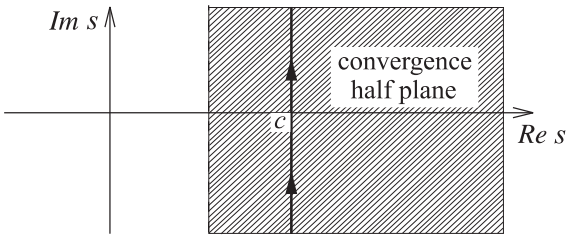

Fig. A.2: Convergence half-plane of Laplace inverse-transform.

The integration path is parallel to the imaginary axis and has to be situated in the convergence half-plane of $f(s)$, otherwise, c is arbitrary. To the right of the integration path, $f(s)$ cannot have singularities, but it can have them to the left. The integration path can be deformed in accordance with Cauchy's integral law and the remainder theorem.

A.1.7 Relation with the Fourier transform

A common representation of the Fourier transform $\overline{F}(\omega)$ of a function $F(t)$ is

$$\overline{F}(\omega) = \int_{-\infty}^{+\infty} F(t)e^{-i\omega t}dt. \tag{A.10}$$

$\overline{F}(\omega)$ is also called the *complex spectrum* of $F(t)$; ω is the angular frequency. The inverse-transform is given by

$$F(t) = \frac{1}{2\pi}\int_{-\infty}^{+\infty} \overline{F}(\omega)e^{i\omega t}d\omega. \tag{A.11}$$

This equation can be interpreted as the superposition of harmonic oscillations. This is the reason why the Fourier transform is often used in physics. If the behaviour of a system, which can be described by linear differential equations, is known for harmonic excitation, its behaviour for impulsive excitation can be determined via (A.11). To do this, the excitation has to be broken into its spectral components according to (A.10). Then, the problem is solved for each spectral component, and, finally, all spectral solutions are superimposed via (A.11). Such an approach is used in section 3.6.3 in the study of the reflection of impulsive waves at an interface.

It is often less physical, but often more elegant and simple, to use the L-transform. The connection between $\overline{F}(\omega)$ and $f(s)$ is very close for functions $F(t)$ that are zero for $t < 0$ (causality)

$$\overline{F}(\omega) = \int_{0}^{\infty} e^{-i\omega t}F(t)dt = f(i\omega),$$

i.e., the Fourier transform is also the L-transform on the imaginary axis of the complex s-plane.

In an alternative representation of the Fourier transform, the factor $\frac{1}{2\pi}$ is not in (A.11) but in (A.10). Then the Fourier transform $\overline{F}(\omega)$ is equal to $f(i\omega)/2\pi$.

A.2 Application of the Laplace transform

A.2.1 Linear ordinary differential equations with constant coefficients

Differential equation

$$\begin{aligned} L(Y) &= Y^{(n)} + a_{n-1}Y^{(n-1)} + a_{n-2}Y^{(n-2)} + \ldots + a_1Y' + a_0Y = F(t) \\ F(t) &\equiv 0 \text{ for } t < 0 \end{aligned} \tag{A.12}$$

Initial conditions

$$Y(+0) = Y_0, Y'(+0) = Y'_0, \ldots, Y^{(n-1)}(+0) = Y_0^{(n-1)}$$

L-transform of (A.12) with $Y(t) \circ\!\!-\!\!\bullet\, y(s), F(t) \circ\!\!-\!\!\bullet\, f(s)$ and (A.5)

$$\begin{aligned}\left(s^n + a_{n-1}s^{n-1} + \ldots + a_1 s + a_0\right) y(s) \quad = \quad & f(s) \\ & + \left(s^{n-1} + a_{n-1}s^{n-2} + \ldots + a_2 s + a_1\right) Y_0 \\ & + \left(s^{n-2} + a_{n-1}s^{n-3} + \ldots + a_3 s + a_2\right) Y'_0 \\ & + \ldots \\ & + \left(s + a_{n-1}\right) Y_0^{(n-2)} \\ & + Y_0^{(n-1)}.\end{aligned}$$

The polynomials can be written as

$$p_i(s) = \sum_{k=0}^{n-i} a_{k+i} s^k, \quad i = 0, 1, 2, \ldots, n, \quad a_n = 1.$$

Therefore,

$$y(s) = \frac{f(s)}{p_0(s)} + \sum_{l=1}^{n} \frac{p_l(s)}{p_0(s)} Y_0^{(l-1)}. \tag{A.13}$$

The right side contains the L-transform of the known function $F(t)$, some polynomials, the coefficients of which are known and the known initial values of the function $Y(t)$ to be solved for. If it is possible to determine the inverse transform on the right side of (A.13), the problem is solved. In the case presented here, this is not difficult. Before this is done, we discuss the comparison with the standard method to solve linear ordinary differential equations with constant coefficients.

First, in the standard method the homogeneous differential equation is solved generally (i.e., it contains n undetermined coefficients); then a special solution of the inhomogeneous differential equation is determined, e.g., by guessing or by variation of the constants. This is then the general solution of the inhomogeneous differential equation from which the n constants can be determined via the initial conditions. It is not necessary to find a general solution if the L-transform is used. Here, the solution that corresponds to the initial conditions is determined directly. That is the great advantage of this method. This advantage is even greater for the solution of partial differential equations with boundary and initial conditions and is why the L-transform is widely used. This is especially true in electronics. One consequence of this is that extensive tables with inverse transforms for many L-transforms exist.

The inverse-transform of (A.13) can be split into two steps (but that is not a necessity).

1. $f(s) \neq 0$, $Y_0 = Y_0' = \ldots = Y_0^{(n-1)} = 0$. This corresponds to the solution of the inhomogeneous differential equation with zero initial values (See section A.2.1.1).

2. $f(s) = 0$, initial value $\neq 0$. This corresponds to the solution of the homogeneous differential equation with non-zero initial conditions (See section A.2.1.2).

The sum of solution 1 and 2 is the inverse transform of (A.13) to be determined (See section A.2.1.3).

A.2.1.1 Inhomogeneous differential equations with zero initial values

This case is also of practical interest since in many cases in which a system is zero up to time $t = 0$ (i.e., $Y(t) \equiv 0$ for $t < 0$), the initial values are zero. In this case,

$$y(s) = \frac{f(s)}{p_0(s)}.$$

Since $1/p_0(s)$ for $n \geq 1$ is always an L-transform (compare (A.8)), the inverse exists

$$\frac{1}{p_0(s)} \bullet\!\!-\!\!\circ\, Q(t).$$

$Q(t)$ is the *Green's function* of the problem. The convolution theorem (A.7) then gives the solution $Y(t)$

$$Y(t) = \int_0^t F(t-\tau)Q(\tau)d\tau = \int_0^t F(\tau)Q(t-\tau)d\tau. \tag{A.14}$$

The determination of $Q(t)$ is, therefore, the remaining task. To that end, we introduce an expansion into partial fractions of $1/p_0(s)$ under the assumption that the zeros α_k of $p_0(s)$ are all *different*

$$\frac{1}{p_0(s)} = \sum_{k=1}^{n} \frac{d_k}{s-\alpha_k}$$

where d_k is the residue of $1/p_0(s)$ at the location α_k

$$d_k = \lim_{s\to\alpha_k} \frac{s-\alpha_k}{p_0(s)} = \lim_{s\to\alpha_k} \frac{1}{\frac{p_0(s)-p_0(\alpha_k)}{s-\alpha_k}} = \frac{1}{p_0'(\alpha_k)}.$$

Thus,

$$\frac{1}{p_0(s)} = \sum_{k=1}^{n} \frac{1}{p_0'(\alpha_k)} \cdot \frac{1}{s-\alpha_k}$$

.

Inverse-transform, with a result from section A.1.4, gives

$$Q(t) = H(t) \cdot \sum_{k=1}^{n} \frac{e^{\alpha_k t}}{p_0'(\alpha_k)}. \tag{A.15}$$

If α_k is real, the corresponding summand in $Q(t)$ is also real. If α_k is complex, an α_1 with $\alpha_1 = \alpha_k^*$ (the conjugate complex value to α_k) exists as part of the other zeros, since $p_0(s)$ has real coefficients. Then,

$$\begin{aligned} \frac{e^{\alpha_k t}}{p_0'(\alpha_k)} + \frac{e^{\alpha_k^* t}}{p_0'(\alpha_k^*)} &= \frac{e^{\alpha_k t}}{p_0'(\alpha_k)} + \frac{e^{(\alpha_k t)^*}}{p_0'(\alpha_k)^*} \\ &= \frac{e^{\alpha_k t}}{p_0'(\alpha_k)} + \left(\frac{e^{\alpha_k t}}{p_0'(\alpha_k)}\right)^* = 2Re\frac{e^{\alpha_k t}}{p_0'(\alpha_k)}. \end{aligned}$$

$Q(t)$ is, therefore, always real.

Relation to the usual solution method

The determination of the zeros of $p_0(s)$ is completely identical to the determination of the zeros for the characteristic equation $p_0(\lambda) = 0$ of the homogeneous differential equation. The effort involved is, therefore, the same. For the usual method, the additional effort of finding a special solution of the inhomogeneous differential equation and the determination of n constants in the solution of the homogeneous differential equation from the zero initial conditions is needed.

It is also interesting to see under which conditions on $F(t)$ the initial values of the solution

$$Y(t) = \int_0^t F(\tau)Q(t-\tau)d\tau$$

are indeed equal to zero. One can show that

$$Q^{(k)}(+0) = \lim_{s\to\infty} \frac{s^{k+1}}{p_0(s)} \qquad (k = 0, 1, \ldots, n-1),$$

and thus,

$$Q(+0) = Q'(+0) = \ldots = Q^{(n-2)}(+0) = 0, \quad Q^{(n-1)}(+0) = 1.$$

If this is used during the differentiation of $Y(t)$, it follows that

$$Y(+0) = Y'(+0) = \ldots = Y^{(n-2)}(+0) = 0,$$

and under the condition that

$$\lim_{\substack{t \to 0 \\ t > 0}} \int_0^t F(\tau) d\tau = 0 \tag{A.16}$$

it also holds that $Y^{(n-1)}(+0) = 0$. This means that due to the fact that a physical function in general satisfies (A.16) (as long as they have a defined start), the assumption of zero initial values is most often satisfied. Equation (A.14) with (A.15) is then the solution of the problem. An exception can be found in exercise A.2.

Application example

The differential equation of the mechanical resonator can be written as

$$\ddot{Y} + 2\alpha\omega_0\dot{Y} + \omega_0^2 Y = \frac{1}{m}K(t)$$

with

$$\begin{aligned} Y(t) &= \text{displacement from zero} \\ K(t) &= \text{acting force (} = 0 \text{ for t} < 0 \text{)} \\ m &= \text{mass} \\ \alpha &= \text{damping term } (\alpha = 1: \text{ aperiodic limit}) \\ \omega_0 &= \text{eigen frequency of the undamped resonator} \\ \omega &= \omega_0(1-\alpha^2)^{\frac{1}{2}} \text{ eigen frequency of the damped resonator .} \end{aligned}$$

We choose $\alpha < 1$ (*resonator case*).

The L-transform of the differential equation leads to

$$y(s) = \frac{k(s)}{mp_0(s)}$$

$$\begin{aligned}
p_0(s) &= s^2 + 2\alpha\omega_0 s + \omega_0^2 = (s-\alpha_1)(s-\alpha_2) \\
\alpha_1 &= -\omega_0\left(\alpha + i(1-\alpha^2)^{\frac{1}{2}}\right) = -\alpha\omega_0 - i\omega \\
\alpha_2 &= -\alpha\omega_0 + i\omega \\
p_0'(s) &= 2s + 2\alpha\omega_0 \\
p_0'(\alpha_1) &= -2i\omega = -p_0'(\alpha_2).
\end{aligned}$$

Thus, the Green's function can be written as

$$\begin{aligned}
Q(t) &= \frac{1}{2i\omega}\left[-e^{-\alpha\omega_0 t - i\omega t} + e^{-\alpha\omega_0 t + i\omega t}\right] \cdot H(t) \\
&= \frac{e^{-\alpha\omega_0 t}}{2i\omega}\left[e^{i\omega t} - e^{-i\omega t}\right] \cdot H(t) \\
Q(t) &= \frac{1}{\omega} e^{-\alpha\omega_0 t} \sin\omega t \cdot H(t) \\
Q(+0) &= 0,\ Q'(+0) = 1.
\end{aligned}$$

The solution of the differential equation is, therefore, $(t \geq 0)$

$$\begin{aligned}
Y(t) &= \frac{1}{\omega m}\int_0^t K(t-\tau) e^{-\alpha\omega_0\tau} \sin\omega\tau d\tau \\
&= \frac{1}{\omega m}\int_0^t K(\tau) e^{-\alpha\omega_0(t-\tau)} \sin\omega(t-\tau) d\tau. \qquad \text{(A.17)}
\end{aligned}$$

If the polynomial $p_0(s)$ has several zeros, an extension into partial fractions of $1/p_0(s)$ is also possible, but it looks different as if only simple zeros were present. Thus, the corresponding Green's function $Q(t)$ looks different (compare also the usual method of solution). Equation (A.14) is also valid in this case.

Exercise A.1

Give the solution of the inhomogeneous equation

$$L(Y) = \omega_0^2 Y_0 H(t),$$

where $H(t)$ is the Heaviside step function.

Exercise A.2

Solve the differential equation of the mechanical seismograph

$$L(Y) = -\ddot{X} \quad (X(t) = \text{ground displacement})$$

with the aid of the method of the variation of the constants and with the L-transform. Assume

$$X(t) \equiv 0 \text{ for } t < 0, \quad X(+0) = 0, \quad \dot{X}(+0) = V_0.$$

Derive the initial conditions for $Y(t)$ from physical principles and show that $Y(+0) = 0,\ \dot{Y}(+0) = -V_0$.

In both exercises, $L(Y) = \ddot{Y} + 2\alpha\omega_0\dot{Y} + \omega_0^2 Y,\ \alpha < 1$.

A.2.1.2 Homogeneous differential equations with arbitrary initial values

This case has also a practical application since it describes the *decay of oscillations* of physical systems. The important points can be learned from the following exercise.

Exercise A.3

Solve the differential equation of the eigen oscillation of a mechanical resonator with

$$L(Y) = 0,$$

with the initial conditions $Y(+0) = Y_0,\ \dot{Y}(+0) = 0$ using the L-transform, and compare the solution with the solution $L(Y)$ of exercise A.1 as done above.

A.2.1.3 Inhomogeneous differential equations with arbitrary initial values

We superimpose the solutions of section A.2.1.1 and section A.2.1.2. This means that $Y(t)$ consists of the two contributions

$$Y(t) = Y_1(t) + Y_2(t).$$

$Y_1(t)$ is the solution of the homogeneous differential equation that satisfies the initial conditions

$$Y_1(+0) = Y_0,\ Y_1'(+0) = Y_0', \ldots, Y_1^{(n-1)}(+0) = Y_0^{(n-1)}.$$

$Y_2(t)$ is the solution of the inhomogeneous differential equation with zero initial values

$$Y_2(+0) = Y_2'(+0) = \ldots = Y_2^{(n-1)}(+0) = 0.$$

$Y(t)$ satisfies the differential equation and the given initial conditions, and is, therefore, the solution of the problem.

For physical problems, the initial conditions *always* have to be derived from physical principles, for example:

1. Mechanical resonator: $\ddot{Y} + 2\alpha\omega_0\dot{Y} + \omega_0^2 Y = \frac{1}{m}K(t)$

   For $t < 0$, $Y = Y_0(t)$ is given. At time $t = 0$ the force $K(t)$ begins to act. Due to the *continuity requirement* it must, therefore, hold that

   $$Y(+0) = Y_0(-0),\ \dot{Y}(+0) = \dot{Y}_0(-0). \tag{A.18}$$

   The resonator starts at time $t = 0$ with the initial values which connect continuously to the previous values. The contribution of $Y_1(t)$ to the displacement $Y(t)$ has the initial value given in (A.18) and is, therefore, an eigen resonance, which continues the oscillation $Y_0(t)$. The forced oscillation $Y_2(t)$, given in (A.17), with zero initial values, is then superimposed on that oscillation.

2. Mechanical seismograph: $\ddot{Y} + 2\alpha\omega_0\dot{Y} + \omega_0^2 Y = -\ddot{X}$

   The ground may be at rest until the time $t = 0$. Due to the *requirement of continuity*, it follows that

   $$Y(+0) = 0,\ \dot{Y}(+0) = -\dot{X}(+0).$$

   Homogeneous equation:

   $$\ddot{Y}_1 + 2\alpha\omega_0\dot{Y}_1 + \omega_0^2 Y_1 = 0,\ Y_1(+0) = 0,\ \dot{Y}_1(+0) = -\dot{X}(+0)$$

   L-transform:

   $$\left(s^2 + 2\alpha\omega_0 s + \omega_0^2\right) y_1(s) = -\dot{X}(+0)$$

   Similar to section A.2.1.1, the eigen resonance can be written as

   $$Y_1(t) = -\frac{\dot{X}(+0)}{\omega} e^{-\alpha\omega_0 t} \sin\omega t \cdot H(t).$$

   Inhomogeneous equation:

   $$\ddot{Y}_2 + 2\alpha\omega_0\dot{Y}_2 + \omega_0^2 Y_2 = -\ddot{X},\ Y_2(+0) = \dot{Y}_2(+0) = 0$$

   L-transform:

   $$\left(s^2 + 2\alpha\omega_0 s + \omega_0^2\right) y_2(s) = -\left(s^2 x(s) - \dot{X}(+0)\right)$$

   The forced resonance, therefore, is ($t \geq 0$)

   $$Y_2(t) = -\frac{1}{\omega_0}\int_0^t \ddot{X}(\tau) e^{-\alpha\omega_0(t-\tau)} \sin\omega(t-\tau) d\tau.$$

   The complete solution $Y(t) = Y_1(t) + Y_2(t)$ is the same as in exercise A.2.

A.2.2 Partial differential equations

We now use an example to demonstrate the main points discussed so far. We will examine, unlike in section 3.4, the propagation of a compressional wave from an explosive point source. The starting point is the equation of motion of the elastic continuum without body forces.

$$\rho \frac{\partial^2 \overrightarrow{u}}{\partial t^2} = (\lambda + 2\mu) \nabla \nabla \cdot \overrightarrow{u} - \mu \nabla \times \nabla \times \overrightarrow{u} \tag{A.19}$$

(ρ=density, λ and μ=Lamé's parameters).

In our problem, for which we use spherical coordinates, the displacement $\overrightarrow{u}$ has only a radial component U, and the only spatial coordinate is the distance r from the explosive point source. In this case, $\nabla \times \overrightarrow{u}$ is zero and it holds that

$$\begin{aligned} \nabla \cdot \overrightarrow{u} &= \frac{\partial U}{\partial r} + \frac{2}{r} U \\ \nabla \nabla \cdot \overrightarrow{u} &= \left(\frac{\partial^2 U}{\partial r^2} + \frac{2}{r} \frac{\partial U}{\partial r} - \frac{2}{r^2} U, 0, 0 \right). \end{aligned}$$

With $\alpha^2 = (\lambda + 2\mu)/\rho$ (=velocity of the compressional waves), it follows from (A.19) that

$$\frac{\partial^2 U}{\partial r^2} + \frac{2}{r} \frac{\partial U}{\partial r} - \frac{2}{r^2} U - \frac{1}{\alpha^2} \frac{\partial^2 U}{\partial t^2} = 0. \tag{A.20}$$

The *boundary conditions* assumed are that for $r = r_1$ the displacement is prescribed as

$$U(r_1, t) = U_1(t). \tag{A.21}$$

The *initial conditions* are

$$U(r, 0) = \frac{\partial U}{\partial t}(r, 0) = 0. \tag{A.22}$$

$U_1(t)$, which shall be zero for $t < 0$, has to start smoothly, so that the initial conditions are also satisfied for $r = r_1$.

L-transform then gives

$$\begin{aligned} u(r, s) &= \int_0^\infty e^{-st} U(r, t) dt \\ u_1(s) &= \int_0^\infty e^{-st} U_1(t) dt \end{aligned}$$

$$\begin{aligned}\mathbf{L}\left\{\frac{\partial U}{\partial r}\right\} &= \int_0^\infty e^{-st}\frac{\partial U}{\partial r}dt = \frac{\partial}{\partial r}\int_0^\infty e^{-st}U dt = \frac{\partial}{\partial r}u(r,s)\\ \mathbf{L}\left\{\frac{\partial^2 U}{\partial r^2}\right\} &= \frac{\partial^2}{\partial r^2}u(r,s).\end{aligned}$$

With this and (A.20), equation (A.20) leads to an *ordinary* differential equation for $u(r,s)$

$$\frac{d^2u}{dr^2}+\frac{2}{r}\frac{du}{dr}-\left(\frac{2}{r^2}+\frac{s^2}{\alpha^2}\right)u=0. \tag{A.23}$$

For ordinary differential equations, the L-transform leads to an algebraic equation (polynomials). For partial differential equations in which, together with t, only *one* additional coordinate occurs (the case studied here), the L-transform leads to ordinary differential equations. For partial differential equations in which, in addition to ti, *more than one* coordinate occurs, partial differential equations are derived. In each case, the dependence on t is eliminated.

We change the variables in (A.23) to $x=\frac{rs}{\alpha}$

$$\frac{du}{dr}=\frac{du}{dx}\cdot\frac{s}{\alpha},\qquad \frac{d^2u}{dr^2}=\frac{d^2u}{dx^2}\cdot\frac{s^2}{\alpha^2}.$$

Thus, (A.23) becomes

$$x^2\frac{d^2u}{dx^2}+2x\frac{du}{dx}-\left(x^2+2\right)u=0. \tag{A.24}$$

This is a special case of the differential equations of the *modified spherical Bessel functions*

$$x^2\frac{d^2y}{dx^2}+2x\frac{dy}{dx}-\left(x^2+n(n+1)\right)y=0.$$

Compare, e.g., M. Abramovitz and I.A. Stegun: Handbook of Mathematical Functions, H. Deutsch, Frankfurt, 1985.

In our case, $n=1$, and the solution of (A.24), which has the properties (A.8) of L-transforms, is

$$u(x)=\frac{1}{x}\left(1+\frac{1}{x}\right)e^{-x}\cdot F(s),\qquad x=\frac{rs}{\alpha}. \tag{A.25}$$

As will become clear in the following, the integration constant $F(s)$ is important. We now specify (A.25) for $r=r_1$, i.e., $x=r_1s/\alpha$, thus, $u(x)$ has to become the

known L-transform $u_1(s)$ of the displacement $U_1(t)$ given at the limit $r = r_1$ (see (A.21))

$$u_1(s) = \frac{\alpha}{r_1 s}\left(1 + \frac{\alpha}{r_1 s}\right) e^{-\frac{r_1 s}{\alpha}} F(s).$$

From this, $F(s)$ can be derived. Therefore, (A.25) can be written as

$$u\,(r,s) = \frac{r_1}{r}\frac{1+\frac{\alpha}{rs}}{1+\frac{\alpha}{r_1 s}} e^{-\frac{r-r_1}{\alpha}s} u_1(s) \tag{A.26}$$

$$= \frac{r_1}{r} \cdot \left[\frac{s + \frac{\alpha}{r_1} + \frac{\alpha}{r} - \frac{\alpha}{r_1}}{s + \frac{\alpha}{r_1}} u_1(s)\right] \cdot e^{-\frac{r-r_1}{\alpha}s}.$$

The term in the square bracket can now be given as

$$u_1(s) + \alpha\left(\frac{1}{r} - \frac{1}{r_1}\right)\frac{u_1(s)}{s+\frac{\alpha}{r_1}} \bullet\!\!-\!\!\circ\, U_1(t) + \alpha\left(\frac{1}{r} - \frac{1}{r_1}\right) U_1(t) * \left[e^{-\frac{\alpha}{r_1}t} \cdot H(t)\right].$$

In the last step, the convolution theorem (A.7) was applied. If the displacement theorem (A.2) is used, the inverse transform of (A.26) follows as

$$U(r,t) = \frac{r_1}{r}\left[U_1\left(t - \frac{r-r_1}{\alpha}\right) + \alpha\left(\frac{1}{r} - \frac{1}{r_1}\right)\int_0^{t-\frac{r-r_1}{\alpha}} U_1(\vartheta) e^{-\frac{\alpha}{r_1}\left(t - \frac{r-r_1}{\alpha} - \vartheta\right)} d\vartheta\right].$$

The retardation $(r - r_1)/\alpha$ refers here not to the explosion point source, but to the sphere $r = r_1$, from which the wave starts at time $t = 0$. The retarded time is, therefore, $\tau = t - (r - r_1)/\alpha$, and the arrival of the wave at each receiver with $r > r_1$ follows from $\tau = 0$. Then

$$U(r,t) = \frac{r_1}{r}\left[U_1(\tau) + \alpha\left(\frac{1}{r} - \frac{1}{r_1}\right)\int_0^{\tau} U_1(\vartheta) e^{-\frac{\alpha}{r_1}(\tau - \vartheta)} d\vartheta\right].$$

A.3 The delta function $\delta(t)$

A.3.1 Introduction of $\delta(t)$

We examine the result (A.17) for the mechanical resonator

$$Y(t) = \frac{1}{\omega m} \int_0^t K(\tau) e^{-\alpha\omega_0(t-\tau)} \sin\omega(t-\tau) d\tau,$$

for the force $K(t) = I\delta_\epsilon(t)$, where I is a constant with the dimension of force $\times$ time (=dimension of an impulse) and

$$\delta_\epsilon(t) = \begin{cases} 0 & \text{for } t < 0 \\ \frac{1}{\epsilon} & \text{for } 0 < t < \epsilon \\ 0 & \text{for } t > \epsilon \end{cases}$$

is a square function as shown in Fig. A.3.

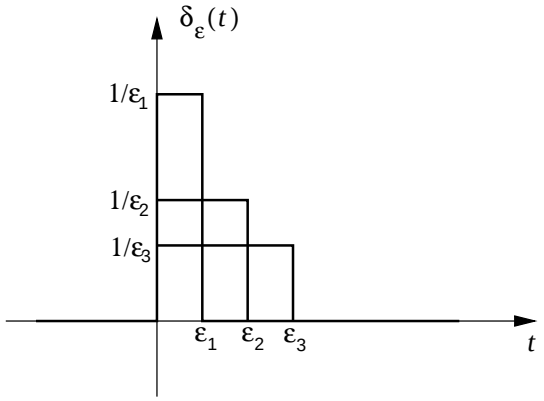

Fig. A.3: Representation of $\delta_\epsilon(t)$ as square functions.

The area under the curve $\delta_\epsilon(t)$ is always equal to 1. Therefore, independent of ϵ, always the same impulse I is transfered. Then the displacement for $t > \epsilon$ can be written as

$$\begin{aligned} Y_\epsilon(t) &= \frac{I}{\omega m\epsilon} \int_0^\epsilon e^{-\alpha\omega_0(t-\tau)} \sin\omega(t-\tau) d\tau \\ &= \frac{I}{\omega m\epsilon} \int_{t-\epsilon}^t e^{-\alpha\omega_0 u} \sin\omega\, u\, du. \end{aligned}$$

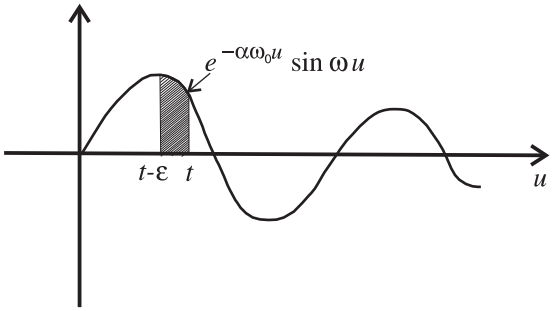

Fig. A.4: Behaviour of the term under integral in $Y_\epsilon(t)$.

The mean value theorem for integrals gives $(0 < \lambda < 1)$:

$$Y_\epsilon(t) = \frac{I}{\omega m} e^{-\alpha\omega_0(t-\lambda\epsilon)} \sin\omega(t-\lambda\epsilon). \tag{A.27}$$

The next step is the transition to $\epsilon \to 0$. For (A.27) follows the result (t is arbitrary)

$$\lim_{\epsilon\to 0} Y_\epsilon(t) = \frac{I}{\omega m} e^{-\alpha\omega_0 t} \sin\omega t H(t) = \frac{I}{m} Q(t),$$

where $Q(t)$ is the Green's function of the differential equation of the mechanical resonator (compare section A.2.1.1). For the force, the transition $\epsilon \to 0$ means that the impulse is transfered to the resonator in shorter and shorter time. It is physically plausible, that this time *then* is not important, if it is sufficiently small compared to the decay time $(\alpha\omega_0)^{-1}$ and the eigenperiod $2\pi/\omega$ of the eigen resonance of the resonator. Therefore, it makes sense to adopt the limiting case $\epsilon = 0$ also for the force, i.e.,

$$\lim_{\epsilon\to 0} K(t) = I \lim_{\epsilon\to 0} \delta_\epsilon(t) = I\delta(t),$$

where $\delta(t)$ is the *delta function*

$$\delta(t) = \lim_{\epsilon\to 0} \delta_\epsilon(t). \tag{A.28}$$

Other names are *impulse function* or *unit impulse*. It is obvious that $\delta(t)$ cannot be treated as a standard function. On the other hand, it would be wrong to study the function $\delta(t)$ separated from the ordinary functions $\delta_\epsilon(t)$. On the contrary, $\delta(t)$ has to be understood as a series of $\{\delta_\epsilon(t)\}$ with $\epsilon \to 0$. From the mathematical point of view, $\delta(t)$ is part of the *generalised* functions or *distributions*, for which extensive theories and literature exist. For our purposes,

the physical approach to the delta function given, will be sufficient. The definition of $\delta(t)$ as a series of ordinary functions is the basis of an exact theory that can also be understood by non-mathematicians; see, e.g., Riley, K.F., M.P. Hobson and S.J. Bence: Mathematical methods for physics and engineering, A comprehensive guide, Cambridge University Press, Cambridge, 2nd edition, 2002.

A.3.2 Properties of $\delta(t)$

Due to (A.28)

$$\delta(t) = 0 \text{ for } t \neq 0.$$

Furthermore, it follows from the properties of $\delta_\epsilon(t)$, that

$$\int_{-\infty}^{+\infty} \delta(t)F(t)dt = F(0).$$

The delta function, therefore, is the value of $F(t)$ at $t = 0$; such that

$$\int_{-\infty}^{+\infty} \delta(t)dt = 1.$$

Furthermore, it holds that $G(t)\delta(t) = G(0)\delta(t)$. If $G(0) = 0$, then $G(t)\delta(t) \equiv 0$. For the delta function $\delta(t - \tau)$, which is displaced by τ, it holds that

$$\delta(t - \tau) = 0 \text{ for } t \neq \tau$$

and

$$\int_{-\infty}^{+\infty} \delta(t - \tau)F(t)dt = F(\tau).$$

The definition of $\delta(t)$ is not only possible with the series $\{\delta_\epsilon(t)\}$, the functions of which are discontinuous. An alternative option is the series $\{\delta_n(t)\}$ with

$$\delta_n(t) = \left(\frac{n}{\pi}\right)^{\frac{1}{2}} e^{-nt^2}.$$

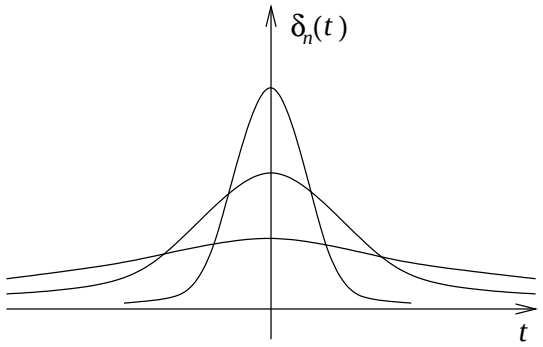

Fig. A.5: Representation of $\delta_n(t)$.

In this case,

$$\begin{aligned} \delta(t) &= \lim_{n\to\infty} \delta_n(t) \\ \int_{-\infty}^{+\infty} \delta_n(t)dt &= 1. \end{aligned}$$

With the functions $\delta_n(t)$, the derivatives of the the delta function can be defined as

$$\delta^{(k)}(t) = \lim_{n\to\infty} \delta_n^{(k)}(t).$$

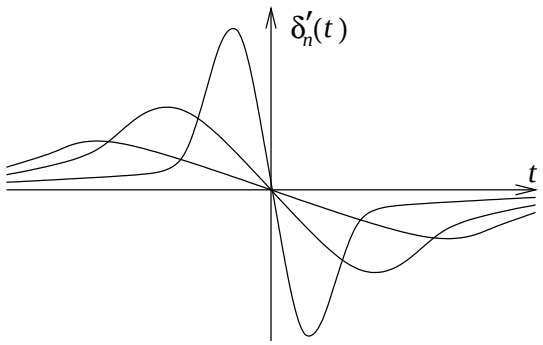

Fig. A.6: Derivative of the delta function $\delta_n(t)$.

It holds that $\delta^{(k)}(t) = 0$ for $t \neq 0$. Furthermore, it follows that

$$\begin{aligned}\int_{-\infty}^{+\infty} \delta^{(k)}(t-\tau)F(t)dt &= \lim_{n\to\infty} \int_{-\infty}^{+\infty} \delta_n^{(k)}(t-\tau)F(t)dt \\ &= \lim_{n\to\infty} (-1)^k \int_{-\infty}^{+\infty} \delta_n(t-\tau)F^{(k)}(t)dt,\end{aligned}$$

after k partial integrations. This gives

$$\int_{-\infty}^{+\infty} \delta^{(k)}(t-\tau)F(t)dt = (-1)^k F^{(k)}(\tau). \tag{A.29}$$

Finally, we discuss the *connection between the delta function and the step function H(t)* from section A.1.4. We consider the function

$$H_\epsilon(t) = \int_{-\infty}^{t} \delta_\epsilon(\tau)d\tau = \begin{cases} 0 & \text{for } t < 0 \\ \frac{t}{\epsilon} & \text{for } 0 \le t \le \epsilon \\ 1 & \text{for } t > \epsilon \end{cases}$$

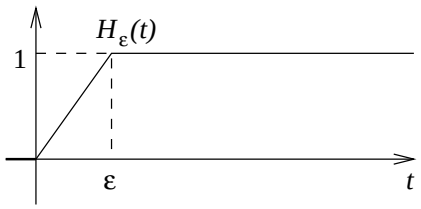

Fig. A.7: Function $H_\epsilon(t)$.

This means that

$$\delta_\epsilon(t) = H'_\epsilon(t),$$

and in the limit $\epsilon \to 0$

$$\delta(t) = H'(t).$$

The delta function is the *derivative of the step function*. The same result could have been achieved with the definition of $\delta(t)$ with the use of the functions $\delta_n(t)$.

It should also be mentioned that $H(t)$ *is dimensionless, but* $\delta(t)$ *has the inverse dimension of time.*

A.3.3 Application of $\delta(t)$

1. The option to describe *impulses of force* (and, similarly, of stress and current) will not be discussed now since that was the topic of the introduction of this appendix.

2. A *point mass* m (or similarly a point charge) can be described by the following *density*

$$\rho = m\,\delta(x)\delta(y)\delta(z).$$

This holds because $\rho = 0$ for $(x, y, z) \neq (0, 0, 0)$, and the whole mass can be described via

$$\iiint_{-\infty}^{+\infty} \rho\,dx\,dy\,dz = m \cdot \int_{-\infty}^{+\infty} \delta(x)dx \cdot \int_{-\infty}^{+\infty} \delta(y)dy \cdot \int_{-\infty}^{+\infty} \delta(z)dz = m.$$

3. The *charge distribution* of a point-like *dipole* can be described by the following *line density* $\sigma(x)$ (e.g., Coulomb per meter) on the x-axis as

$$\sigma(x) = M\delta'(x), \quad M > 0 \qquad \text{(dimension : charge * length)},$$

since we define $\sigma(x)$ by the series $\{M\delta_n'(x)\}$.

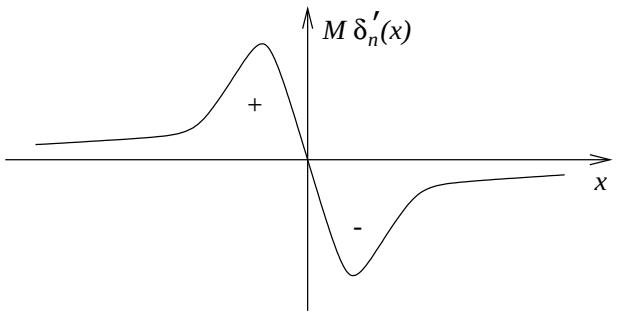

Fig. A.8: Charge distribution of a point-like dipole.

The transition $n \to \infty$ gives then two infinitely large opposite point charges, which are infinitely close to each other.

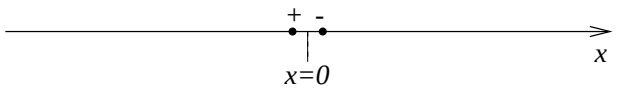

Fig. A.9: Charge distribution of a point-like dipole for two infinitely large opposite point charges, which are infinitely close to each other.

The moment of such an arrangement relative to $x = 0$ is

$$\int_{-\infty}^{+\infty} x\sigma(x)dx = M\int_{-\infty}^{+\infty} x\delta'(x)dx = -M.$$

The sign is correct, since the vector of the moment points from the negative to the positive charge. The dimension is also correct. The *spatial charge density* of the dipole would be $\sigma(x, y, z) = M \cdot \delta'(x) \cdot \delta(y) \cdot \delta(z)$ (e.g., Coulomb per cubic meter).

4. *The role of the delta function for the solution of inhomogeneous linear ordinary differential equations.*

   We start with

$$L(Y) = Y^{(n)} + a_{n-1}Y^{(n-1)} + \ldots + a_1Y' + a_0Y = \delta_\epsilon(t). \tag{A.30}$$

   The solution is, according to section A.2.1.1,

$$Y(t) = Y_\epsilon(t) = \int_0^t \delta_\epsilon(\tau)Q(t-\tau)d\tau, \tag{A.31}$$

   with $Q(t)$=Green's function, and it satisfies the initial conditions

$$Y_\epsilon(+0) = Y'_\epsilon(+0) = \ldots = Y_\epsilon^{(n-1)}(+0) = 0.$$

   The transition $\epsilon \to 0$ in (A.30) and (A.31) gives

$$L(Y) = \delta(t) \tag{A.32}$$

   with the solution

$$Y(t) = Q(t).$$

   The Green's function of a system, which can be described by a linear ordinary differential equation, is also the solution of the inhomogeneous equation, which has the delta function as the term of perturbation. Expressed differently, *the Green's function is the response function of a perturbation of the system by the delta function (impulse response).*

   The initial values of $Q(t)$ are

$$Q(+0) = Q'(+0) = \ldots = Q^{(n-2)}(+0) = 0,\ Q^{(n-1)}(+0) = 1,$$

   and are, therefore, different from those of the functions $Y_\epsilon(t)$. This is a consequence of the transition $\epsilon \to 0$. If (A.32) has, therefore, to be

solved directly, one has to use *always* zero initial values and not those, which actually hold for $Q(t)$. In that situation, it is useful to know the L-transform of $\delta(t)$

$$\mathbf{L}\{\delta(t)\} = f(s) = \int_0^\infty e^{-st}\delta(t)dt = 1.$$

Since $\delta(t)$ is a generalised function, it does *not* hold here that $\lim f(s) = 0$ for $Re\, s \to \infty$ (compare (A.8).

Now we can give the general solution of the initial value problem for a system which is at rest up to the time $t = 0$ and is then excited in an arbitrary way, a *new interpretation*. The solution (A.14), namely

$$Y(t) = \int_0^t F(t-\tau)Q(\tau)d\tau = \int_0^t F(\tau)Q(t-\tau)d\tau, \tag{A.33}$$

is derived by the convolution of the solution $Q(t)$ for the special excitation of the system by $F(t) = \delta(t)$ with an arbitrary perturbation $F(t)$.

A.3.4 Duhamel's law and linear systems

In (A.33), we choose $F(t) = H(t)$ (step function). In this case,

$$\begin{aligned} Y(t) = Y_H(t) &= \int_0^t Q(\tau)d\tau \quad \text{(step response)} \\ Y_H'(t) &= Q(t). \end{aligned}$$

Integrating by parts, it follows from (A.33)

$$Y(t) = F(t-\tau)\; Y_H(\tau)|_0^t + \int_0^t F'(t-\tau)Y_H(\tau)d\tau.$$

Thus, due to $Y_H(+0) = 0$

$$\begin{aligned} Y(t) &= F(+0)Y_H(t) + \textstyle\int_0^t F'(t-\tau)Y_H(\tau)d\tau \\ &= F(+0)Y_H(t) + \textstyle\int_0^t F'(\tau)Y_H(t-\tau)d\tau \end{aligned} \tag{A.34}$$

This is *Duhamel's law*, which describes how solutions for arbitrary $F(t)$ can be determined from those for $F(t) = H(t)$.

Generalisation

If we use $Q(t) = Y_\delta(t)$ in (A.33), it follows that

$$Y(t) = \int_0^t F(t-\tau) Y_\delta(\tau) d\tau = \int_0^t F(\tau) Y_\delta(t-\tau) d\tau. \qquad \text{(A.35)}$$

The relation between $Y_\delta(t)$ and $Y_H(t)$ is

$$Y_\delta(t) = Y'_H(t).$$

Equations (A.34) and (A.35) contain the statement that the response of a system has to be known only for very special excitations like the delta and the step functions. From this, the solution for arbitrary excitation can be given. This is not only true for systems which follow linear *ordinary* differential equations, but also for systems which can be described by *partial* differential equations or systems of *simultaneous* differential equations as long as they are linear and have *time independent* coefficients. One requirement for this to hold is that the system is at rest in the beginning. The perturbation can, depending on the problem, have a different form (e.g., force, temperature, displacement *etc.*), as indicated in Fig. A.10.

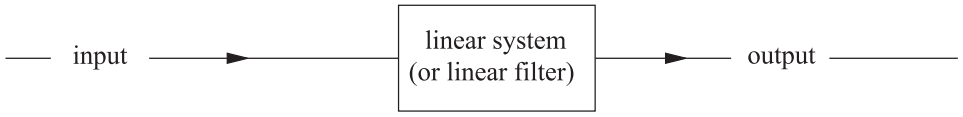

input function or perturbation function	output function or response function
$\delta(t)$	$Y_\delta(t) = Q(t)$ (impulse response)
$H(t)$	$Y_H(t) = \int_0^t Q(\tau) d\tau$ (step response)
$F(t)$	$Y(t)$ according to (A.34) or (A.35)

Fig. A.10: Linear system with input and output.

Transition into the frequency domain using the Fourier transform

The Fourier transform of $F(t)$, $Q(t)$ and $Y(t)$ is $\overline{F}(\omega), \overline{Q}(\omega)$ and $\overline{Y}(\omega)$

$$\left.\begin{matrix} \overline{F}(\omega) \\ \overline{Q}(\omega) \\ \overline{Y}(\omega) \end{matrix}\right\} = \int_{-\infty}^{+\infty} \left\{\begin{matrix} F(t) \\ Q(t) \\ Y(t) \end{matrix}\right\} e^{-i\omega t} dt.$$

The close relation with the L-transform has been discussed in section A.1.7. Therefore, it holds, as for the Fourier transform

$$\overline{Y}(\omega) = \overline{F}(\omega) \cdot \overline{Q}(\omega),$$

i.e., the Fourier transform $\overline{Y}(\omega)$ of the input function $Y(t)$ is the product of the Fourier transform $\overline{F}(\omega)$ of the input function $F(t)$ with $\overline{Q}(\omega)$ of the Green's function $Q(t)$. $\overline{Q}(\omega)$ is called the *transfer function* of the linear system or filter. Separation into absolute value and phase gives

$$\begin{aligned} \overline{Q}(\omega) &= A(\omega)e^{i}\varphi(\omega) \\ A(\omega) &= \text{amplitude characteristics of the system} \\ \varphi(\omega) &= \text{phase characteristics of the system} \end{aligned}$$

$A(\omega)$ describes the amplification or decrease of the circular frequency ω, respectively, and $\varphi(\omega)$ describes the phase shift. A monochromatic oscillation as input

$$F(t) = a \sin \omega t,$$

has the output

$$Y(t) = A(\omega) a \sin\left(\omega t + \varphi(\omega)\right).$$

The transfer function of the system has, therefore, a very physical meaning, and it is thus, used widely.

Exercise A.4

A sphere of mass m drops from the height h_1 on the mass M of a mechanical (vertical-)resonator, is reflected there and reaches the height h_2. No additional interactions between the two masses follow. Determine the displacement of mass *M:*

1. Using the homogeneous differential equation $L(Y) = 0$ and the corresponding initial conditions.
2. Using the inhomogeneous differential equation $L(Y) =?$ and zero initial values.

It holds that

$$L(Y) = \ddot{Y} + 2\alpha\omega_0\dot{Y} + \omega_0^2 Y, \quad \alpha < 1.$$

Exercise A.5

The ground displacement of the mechanical seismograph (differential equation $L(Y) = -\ddot{X}$) is given by

$$a) \quad X(t) = \frac{t^2 H(t)}{2},$$

$$b) \quad X(t) = tH(t),$$

$$c) \quad X(t) = H(t).$$

Determine, in each case, the displacement $Y(t)$ and discuss the relation between the three cases.

A.3.5 Practical approach for the consideration of non-zero initial values of the perturbation function F(t) of a linear problem

For the mechanical seismograph, the perturbation function of the differential equation is the second derivative of the ground displacement $X(t)$, and we notice that the initial values of the displacement $Y(t)$ of the mass of the seismometer depends on the initial values $X(+0)$ and $\dot{X}(+0)$, respectively (compare exercise A.2 and section A.2.1.3). This connection had to be derived from physical principles. Cases exist in which this is difficult. Therefore, we would like to have an approach, that considers the initial values of the perturbation function. In the following, we define, *contrary to the usage up to now*, the perturbation function as the function, the single (or higher) derivatives of which occur in the differential equation as inhomogeneities (we consider an arbitrary linear system). *Now* $F(t) = X(t)$ for the mechanical seismograph and not $F(t) = -\ddot{X}(t)$. We then solve the equation for $F(t) = F_n(t)$, for which the initial values are zero, up to *sufficiently* high orders. Then, one can assume that the initial values of the corresponding solution $Y_n(t)$ are also zero. Thus, $Y_n(t)$ can be written as

$$Y_n(t) = \int_0^t F_n^{(i)}(t-\tau)G(\tau)d\tau. \tag{A.36}$$

Therefore, we know the i-th order of the derivative of $F_n(t)$ $(i \geq 1)$ and the function $G(t)$.

Given a series of functions $F_n(t)$ which converge versus the perturbation function $F(t)$ to be determined (with non-zero initial values),

$$\lim_{n\to\infty} F_n(t) = F(t).$$

Compare also the comments to the definition of the delta function in chapters A.3.1 and A.3.2. Then, it follows that

$$\begin{aligned}
\lim_{n\to\infty} F_n'(t) &= F'(t) + F(+0)\delta(t) \\
\lim_{n\to\infty} F_n''(t) &= F''(t) + F(+0)\delta'(t) + F'(+0)\delta(t) \\
&\vdots \\
\lim_{n\to\infty} F_n^{(i)}(t) &= F^{(i)}(t) + \sum_{j=0}^{i-1} F^{(j)}(+0)\delta^{(i-j-1)}(t). \qquad \text{(A.37)}
\end{aligned}$$

$\delta^{(0)}(t)$ is here equal to $\delta(t)$.

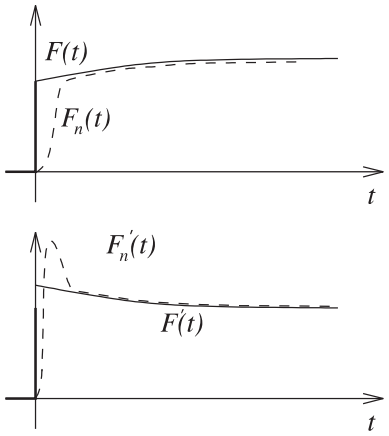

Fig. A.11: F(t) and its derivative as a function of time.

The general solution $Y(t)$ for arbitrary initial values of $F(t)$ is

$$\begin{aligned}
Y(t) &= \lim_{n\to\infty} Y_n(t) \\
&= \int_0^t F^{(i)}(t-\tau)G(\tau)d\tau + \sum_{j=0}^{i-1} F^{(j)}(+0)\int_0^t \delta^{(i-j-1)}(t-\tau)G(\tau)d\tau,
\end{aligned}$$

if (A.37) is used in(A.36). Now

$$\int_0^t \delta^{(i-j-1)}(t-\tau)G(\tau)d\tau \qquad \underset{u=t-\tau}{=} \qquad \int_0^t \delta^{(i-j-1)}(u)G(t-u)du$$

$$\begin{array}{rll} & = & (-1)^{i-j-1}\left[\dfrac{d^{i-j-1}}{du^{i-j-1}}G(t-u)\right]_{u=0} \\ \text{with (A.29)} & & \\ & = & (-1)^{i-j-1}\left[\dfrac{d^{i-j-1}}{dt^{i-j-1}}G(t-u)\right]_{u=0}(-1)^{i-j-1} \\ & = & G^{(i-j-1)}(t). \end{array}$$

The general solution of the problem for arbitrary initial values of the perturbation function $F(t)$ is then

$$Y(t) = \sum_{j=0}^{i-1} F^{(j)}(+0)G^{(i-j-1)}(t) + \int_0^t F^{(i)}(t-\tau)G(\tau)d\tau. \tag{A.38}$$

Application

Mechanical seismograph: $\ddot{Y} + 2\alpha\omega_0\dot{Y} + \omega_0^2 Y = -\ddot{X}$

The assumption that the ground displacement $X_n(t)$ starts sufficiently smooth and allows us to put the initial values of $Y_n(t)$ equal to zero

$$Y_n(+0) = \dot{Y}_n(+0) = 0.$$

The differential equation is then solved under this assumption, most easily with the L-transform (compare exercise A.2)

$$Y_n(t) = -\frac{1}{\omega}\int_0^t \ddot{X}_n(t-\tau)e^{-\alpha\omega_0\tau}\sin\omega\tau d\tau.$$

Compare with (A.36): $F_n(t) = X_n(t), i = 2,$

$$G(t) \quad = \quad -\frac{1}{\omega}e^{-\alpha\omega_0 t}\sin\omega t \cdot H(t).$$

The general solution is, according to (A.38),

$$\begin{array}{rcl} Y(t) & = & X(+0)G'(t) + \dot{X}(+0)G(t) + \displaystyle\int_0^t \ddot{X}(t-\tau)G(\tau)d\tau \\ & = & X(+0)G'(t) + \dot{X}(+0)G(t) + \displaystyle\int_0^t \ddot{X}(\tau)G(t-\tau)d\tau. \end{array}$$

This result (with $X(+0) = 0$) was derived directly, except for the sign, in the exercise mentioned above.

Appendix B

Hilbert transform

B.1 The Hilbert transform pair

The *Hilbert transform* $H(x)$ of the real function $h(x)$ is defined by the following integral (x and ξ are real)

$$H(x) = \frac{1}{\pi} P \int_{-\infty}^{+\infty} \frac{h(\xi)}{\xi - x} d\xi. \tag{B.1}$$

P is the *main value* of the integral, i.e., the singularity $\xi = x$ of the integrand has been excluded

$$P \int_{-\infty}^{+\infty} ..d\xi = \lim_{\epsilon \to 0} \left(\int_{-\infty}^{x-\epsilon} ..d\xi + \int_{x+\epsilon}^{+\infty} ..d\xi \right).$$

The *inverse Hilbert transform* can be written as (proof follows)

$$h(x) = -\frac{1}{\pi} P \int_{-\infty}^{+\infty} \frac{H(\xi)}{\xi - x} d\xi. \tag{B.2}$$

Although this is different from the Laplace and the Fourier transform, the two corresponding functions $h(x)$ and $H(x)$ have the *same argument*.

Some *analytical* Hilbert transform pairs are shown in Fig. B.1.

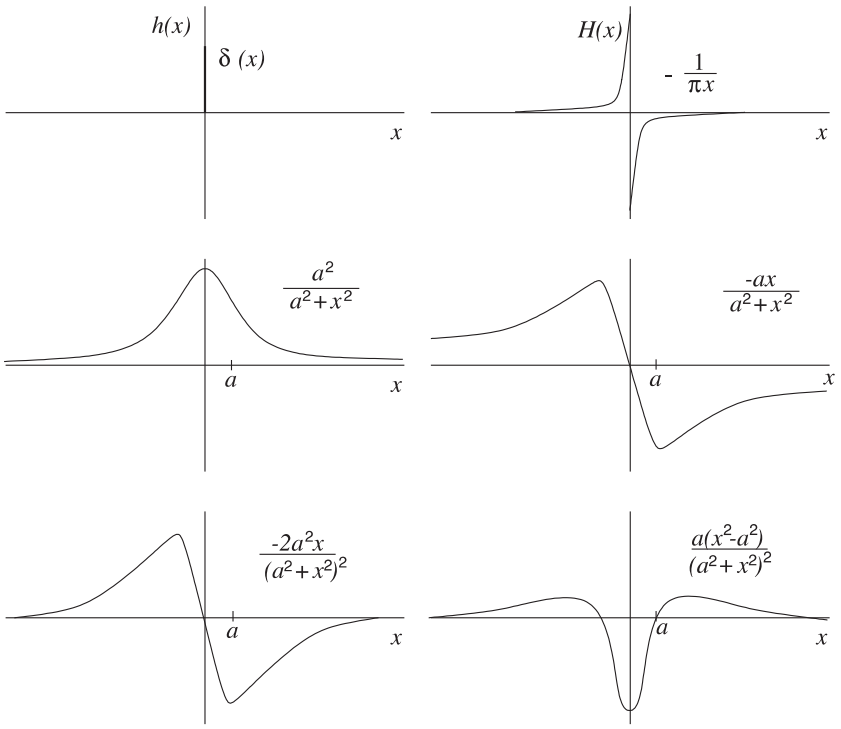

Fig. B.1: Analytical Hilbert transform pairs.

B.2 The Hilbert transform as a filter

Equation (B.1) is a convolution integral

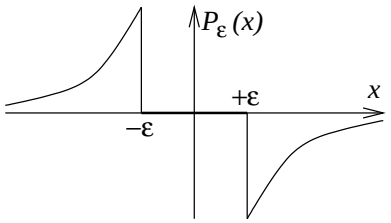

Fig. B.2: Form of $P_\epsilon(x)$.

$$H(x) = \int_{-\infty}^{+\infty} h(\xi) \cdot P\left\{\frac{-\frac{1}{\pi}}{x-\xi}\right\} d\xi = h(x) * P\left\{-\frac{1}{\pi x}\right\}$$

$$P\left\{-\frac{1}{\pi x}\right\} = \lim_{\epsilon \longrightarrow 0} P_\epsilon(x)$$
$$P_\epsilon(x) = \begin{cases} 0 & \text{for } |x| < \epsilon \\ -\frac{1}{\pi x} & \text{otherwise .} \end{cases}$$

Therefore, it holds for the Fourier transforms

$$\left.\begin{matrix} \overline{H}(\omega) \\ \overline{h}(\omega) \\ \overline{P}(\omega) \end{matrix}\right\} = \int_{-\infty}^{+\infty} \left\{\begin{matrix} H(x) \\ h(x) \\ P\left\{-\frac{1}{\pi x}\right\} \end{matrix}\right\} \cdot e^{-i\omega x} dx, \tag{B.3}$$

and according to section A.3.4,

$$\overline{H}(\omega) = \overline{h}(\omega) \cdot \overline{P}(\omega). \tag{B.4}$$

The Hilbert transform is, therefore, a *linear filter*. The Fourier transform and its inverse can be effectively calculated with the method of the Fast Fourier transform. It is, therefore, advantageous to perform the Hilbert transform in the frequency domain via (B.4). To be able to do this, one needs the *transfer function* $\overline{P}(\omega)$ *of the Hilbert transform*. From (B.3), it follows that

$$\overline{P}(\omega) = -\frac{1}{\pi} P \int_{-\infty}^{+\infty} \frac{1}{x} e^{-i\omega x} dx, \quad \overline{P}(0) = 0. \tag{B.5}$$

We compute this integral with methods from complex analysis by deforming the integration path to a semi-circle with infinite radius in the upper (lower) x-half-plane for $\omega < 0$ ($\omega > 0$), respectively,

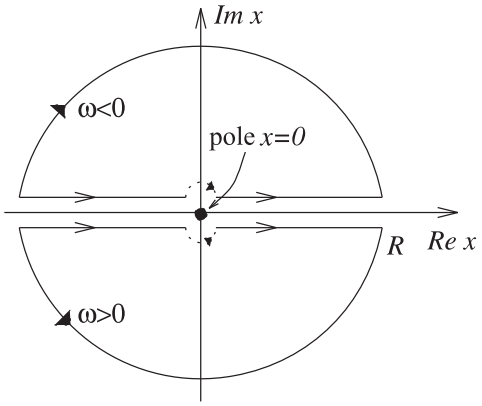

Fig. B.3: Integral path of $\overline{P}(\omega)$ in the complex plane.

$$
\begin{aligned}
P\int_{-\infty}^{+\infty}\frac{e^{-i\omega x}}{x}dx &= \int\frac{e^{-i\omega x}}{x}dx \pm \pi i Res\ \frac{e^{-i\omega x}}{x}\Big|_{x=0} \\
&= \int_{U/L}\frac{e^{-i\omega x}}{x}dx \pm \pi i, \qquad \text{(B.6)}
\end{aligned}
$$

where the upper (lower) integration path and the + (-) sign for $\omega < 0 \quad (\omega > 0)$ have to be chosen, respectively. Note that the first term on the right of the first equation has to be integrated along the real axis (excluding the pole), and the residual in the second term is identical to 1. The integration in the second equation is then along the upper (lower) half circle U (L), respectively.

With the new variable φ on the half circles, it follows that

$$x = Re^{i\varphi},\ dx = Rie^{i\varphi}d\varphi.$$

This leads to

$$
\begin{aligned}
\int_{U/L}\frac{e^{-i\omega x}}{x}dx &= i\int_{\pm\pi}^{0}\exp\left[-i\omega R\left(\cos\varphi + i\sin\varphi\right)\right]d\varphi \\
&= i\int_{\pm\pi}^{0}\exp\left[\omega R\sin\varphi - i\omega R\cos\varphi\right]d\varphi \\
&\to 0 \text{ for } R\to\infty,\ \text{since } \omega\sin\varphi < 0.
\end{aligned}
$$

Equation (B.6), therefore, reduces to

$$P\int_{-\infty}^{+\infty}\frac{e^{-i\omega x}}{x}dx = \pm\pi i,$$

and the transfer function $\overline{P}(\omega)$ in (B.5) becomes the simple expression

$$\overline{P}(\omega) = i\,sign\,\omega \text{ with } sign\,\omega = \begin{cases} -1 & \text{for } \omega < 0 \\ 0 & \text{for } \omega = 0 \\ +1 & \text{for } \omega > 0. \end{cases} \qquad \text{(B.7)}$$

If the Hilbert transform is considered as a filter of the original function, it follows from (B.4) with (B.7) that the frequency 0 is suppressed ($\overline{P}(0) = 0$), but all other frequencies remain unchanged in their amplitude ($\left|\overline{P}(\omega)\right| = 1$ for $\omega \neq 0$). At $\omega \neq 0$ only *phase shifts* are produced. With $\omega > 0$ ($\omega < 0$) a phase shift of $\pm 90^0$ results, respectively. In filter theory, the Hilbert transform is an *all-pass filter with removal of the average.*

The practical computation of the Hilbert transform $H(x)$ of $h(x)$, therefore, requires three steps:

1. Computation of the Fourier transform $\overline{h}(\omega)$ of $h(x)$
2. Multiplication with the transfer function $\overline{P}(\omega)$
3. Back transformation of $\overline{H}(\omega)$.

If the Hilbert transform is applied *twice*, it follows in the frequency domain that

$$\overline{g}(\omega) = \overline{h}(\omega) \cdot \overline{P}^2(\omega) = -\overline{h}(\omega),$$

and, therefore, $g(x) = -h(x)$. The original function $h(x)$ is, therefore, obtained, if the sign of the second Hilbert transform is reversed. This proves (B.2) for the inverse Hilbert transform.

This proof only holds for cases in which $\overline{h}(0) = 0$, i.e., in cases for which the integral over $h(x)$ is zero. The third example in Fig. B.1 is such a case. Equation (B.2) also holds if $\overline{h}(0) \neq 0$. This is shown in the second example of Fig. B.1 and can be confirmed with methods from complex analysis.

The numerical Hilbert transform, with (B.4) and (B.7) frequency $\omega = 0$, is sometimes not treated properly. For numerical reasons, it is assumed that due to $\overline{P}(0) = 0$ the integral of the Hilbert transform is *always* zero. This is not true, if $\overline{h}(0) = \int_{-\infty}^{+\infty} h(x)dx$ is not finite or not correctly defined. The first case occurs, if, e.g., $h(x)$ is a step function. The second case occurs, e.g., during the inverse-transformation of the Hilbert transform $h(x) = -ax/(a^2 + x^2)$, the decay of which with increasing $|x|$ is proportional to $-1/x$ and, therefore, not strong enough. In such cases, a constant shift of the numerical result in the ordinate direction is often sufficient. The frequency $\omega = 0$ is the only frequency for which the Hilbert transform computed numerically can then deviate from the exact result.

Appendix C

Bessel functions

In the following, only the most important equations and properties of Bessel functions with *integer order* are listed. More details can be found, e.g., in M. Abramovitz and I.A. Stegun (1985), or in Riley, K.F., M.P. Hobson and S.J. Bence (2002).

The *differential equation* of the Bessel function of integer order $n = 0, 1, 2, \ldots$ is

$$x^2 y'' + xy' + \left(x^2 - n^2\right) y = 0. \tag{C.1}$$

The two linearly independent solutions of this equation are

$$\begin{aligned} y &= J_n(x) = \text{ Bessel function of first kind and } n - \text{order} \\ y &= Y_n(x) = \begin{array}{l} \text{Bessel function of second kind and } n - \text{th order} \\ \text{or } Neumann's\, function\, of\, n - \text{th order.} \end{array} \end{aligned}$$

Representation as a series

$$\begin{aligned} J_n(x) &= \sum_{k=0}^{\infty} \frac{(-1)^k}{k!(n+k)!} \left(\frac{x}{2}\right)^{n+2k} \\ Y_n(x) &= \frac{2}{\pi}\left(0,577216 + \ln\frac{x}{2}\right) J_n(x) - \frac{1}{\pi}\sum_{k=0}^{n-1} \frac{(n-1-k)!}{k!}\left(\frac{2}{x}\right)^{n-2k} \\ &\quad -\frac{1}{\pi}\sum_{k=0}^{\infty} \frac{(-1)^k\left(\Phi_k + \Phi_{k+n}\right)}{k!(n+k)!}\left(\frac{x}{2}\right)^{n+2k} \\ \Phi_l &= \sum_{s=1}^{l} \frac{1}{s} \end{aligned}$$

The graphic representation for $x \geq 0$ is shown in Fig. C.1.

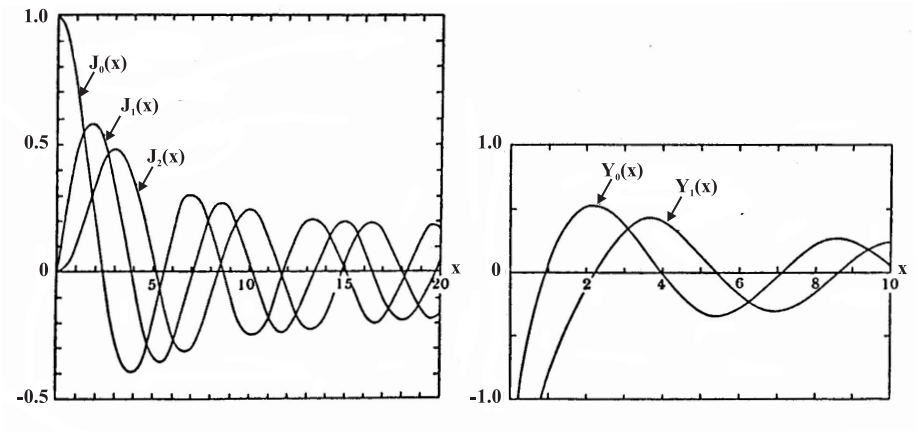

Fig. C.1: Bessel and Neumann functions.

Neumann's functions have a singularity at $x = 0$.

The *Hankel functions*, or Bessel functions of the third kind, are defined as

$$H_n^{(1)}(x) = J_n(x) + iY_n(x) \qquad \text{Hankel function of first kind} \qquad \text{(C.2)}$$

$$H_n^{(2)}(x) = J_n(x) - iY_n(x) \qquad \text{Hankel function of second kind .} \qquad \text{(C.3)}$$

$H_n^{(1)}(x)$ and $H_n^{(2)}(x)$ are linearly independent. The general solution of (C.1) is, therefore, (with the arbitrary constants A,B,C,D) either

$$y = AJ_n(x) + BY_n(x)$$

or

$$y = CH_n^{(1)}(x) + DH_n^{(2)}(x).$$

Analogies to the differential equations of the trigonometric functions (equation of oscillation)

$$y'' + n^2 y = 0$$

or their well-known solutions $\cos nx$ and $\sin nx$, and e^{inx} and e^{-inx}, respectively,

Bessel functions	Trigonometric functions
$J_n(x)$	$\cos nx$
$Y_n(x)$	$\sin nx$
$H_n^{(1)}(x)$	$e^{inx} = \cos nx + i \sin nx$
$H_n^{(2)}(x)$	$e^{-inx} = \cos nx - i \sin nx.$

Asymptotic representation for $x \gg 1$

$$\left.\begin{array}{lcl} J_n(x) & \simeq & \left(\frac{2}{\pi x}\right)^{\frac{1}{2}} \cos\left(x - \frac{n\pi}{2} - \frac{\pi}{4}\right) \\ Y_n(x) & \simeq & \left(\frac{2}{\pi x}\right)^{\frac{1}{2}} \sin\left(x - \frac{n\pi}{2} - \frac{\pi}{4}\right) \\ H_n^{(1)}(x) & \simeq & \left(\frac{2}{\pi x}\right)^{\frac{1}{2}} \exp\left[i\left(x - \frac{n\pi}{2} - \frac{\pi}{4}\right)\right] \\ H_n^{(2)}(x) & \simeq & \left(\frac{2}{\pi x}\right)^{\frac{1}{2}} \exp\left[-i\left(x - \frac{n\pi}{2} - \frac{\pi}{4}\right)\right] \end{array}\right\} \qquad \text{(C.4)}$$

Recursion formulae ($Z_n = J_n, Y_n, H_n^{(1)}$ or $H_n^{(2)}$)

$$\left.\begin{array}{lcll} \frac{2n}{x} Z_n(x) & = & Z_{n-1}(x) + Z_{n+1}(x) & (n = 1, 2, 3, \ldots) \\ Z_n'(x) & = & \frac{n}{x} Z_n(x) - Z_{n+1}(x) & (n = 0, 1, 2, \ldots) \\ Z_n'(x) & = & -\frac{n}{x} Z_n(x) + Z_{n-1}(x) & (n = 1, 2, 3, \ldots) \end{array}\right\} \qquad \text{(C.5)}$$

Special cases of the second and third recursion formulae in (C.5) are then used

$$\begin{aligned} J_0'(x) &= -J_1(x) \\ J_1'(x) &= J_0(x) - \frac{1}{x} J_1(x). \end{aligned}$$

Up until now, we have considered the variable x as real and positive. If we also assume $|x| \gg 1$, all formulae given also hold for *complex*, x and for (C.4). If complex x are used, the following relations are often useful

$$\begin{aligned} H_n^{(1)}(-x) &= -e^{-n\pi i} H_n^{(2)}(x) \\ H_n^{(2)}(-x) &= -e^{n\pi i} H_n^{(1)}(x) \end{aligned}$$

with special case $n = 0$

$$\begin{aligned} H_0^{(1)}(-x) &= -H_0^2(x) \\ H_0^{(2)}(-x) &= -H_0^{(1)}(x). \end{aligned} \qquad \text{(C.6)}$$

Appendix D

The Sommerfeld integral

We consider a time harmonic explosion point source at the origin of a cylindrical coordinate system. Its compressional potential

$$\frac{1}{R}e^{i\omega\left(t-\frac{R}{\alpha}\right)} \qquad \left(R^2=r^2+z^2\right)$$

solves the wave equation and can, therefore, be constructed from more elementary solutions of the wave equation in cylindrical coordinates (as long as cylindrical symmetry is maintained); see also discussion in section 3.7 leading to (3.83)

$$\begin{aligned} \frac{1}{R}e^{i\omega\left(t-\frac{R}{\alpha}\right)} &= e^{i\omega t}\int_0^\infty g(k)kJ_0(kr)e^{-il|z|}dk \qquad \text{(D.1)} \\ l &= \left(\frac{\omega^2}{\alpha^2}-k^2\right)^{\frac{1}{2}} \qquad \begin{array}{l}\text{(positive real or}\\ \text{negative imaginary).}\end{array} \end{aligned}$$

To determine $g(k)$, we consider (D.1) at $z=0$

$$\frac{1}{r}e^{-i\omega\frac{r}{\alpha}}=\int_0^\infty g(k)kJ_0(kr)dk \qquad \text{(D.2)}$$

and use then the *Fourier-Bessel transform*

$$\begin{aligned} g(k) &= \int_0^\infty G(r)rJ_0(kr)dr \qquad \text{(D.3)} \\ G(r) &= \int_0^\infty g(k)kJ_0(kr)dk. \qquad \text{(D.4)} \end{aligned}$$

g(k) is the Fourier-Bessel transform of *G(r)*, and *G(r)* is the inverse Fourier-Bessel transform of *g(k)*. Equation (D.2) has the form of (D.4), therefore, $G(r) = e^{-i\omega r/\alpha}/r$. Therefore, (D.3) can be used to compute *g(k)*

$$\begin{aligned} g(k) &= \int_0^\infty e^{-i\omega\frac{r}{\alpha}} J_0(kr)dr \\ &= \int_0^\infty \cos\left(\omega\frac{r}{\alpha}\right) J_0(kr)dr - i\int_0^\infty \sin\left(\omega\frac{r}{\alpha}\right) J_0(kr)dr. \end{aligned}$$

With

$$\begin{aligned} \int_0^\infty \cos\left(\omega\frac{r}{\alpha}\right) J_0(kr)dr &= \begin{cases} 0 & \text{for } 0 < k < \frac{\omega}{\alpha} \\ \left(k^2 - \frac{\omega^2}{\alpha^2}\right)^{-\frac{1}{2}} & \text{for } k > \frac{\omega}{\alpha} \end{cases} \\ \int_0^\infty \sin\left(\omega\frac{r}{\alpha}\right) J_0(kr)dr &= \begin{cases} \left(\frac{\omega^2}{\alpha^2} - k^2\right)^{-\frac{1}{2}} & \text{for } 0 < k < \frac{\omega}{\alpha} \\ 0 & \text{for } k > \frac{\omega}{\alpha}, \end{cases} \end{aligned}$$

it follows that

$$g(k) = \begin{cases} -i\left(\frac{\omega^2}{\alpha^2} - k^2\right)^{-\frac{1}{2}} & \text{for } 0 < k < \frac{\omega}{\alpha} \\ \left(k^2 - \frac{\omega^2}{\alpha^2}\right)^{-\frac{1}{2}} & \text{for } k > \frac{\omega}{\alpha}, \end{cases}$$

or simply $g(k) = \frac{1}{il}$. Inserted into (D.1), this gives the *Sommerfeld integral*

$$\frac{1}{R}e^{-i\omega\frac{R}{\alpha}} = \int_0^\infty \frac{k}{il} J_0(kr)e^{-il|z|}dk. \tag{D.5}$$

Appendix E

The computation of modal seismograms

E.1 Numerical calculations

The treatment of point sources in wave guides with *arbitrary* (horizontal) layering leads to the following general far-field form for the field values (displacement, pressure, potential *etc.*) of a normal mode

$$N(t) = r^{-\frac{1}{2}} Re \int_0^\infty \overline{M}(\omega) \exp\left[i\left(\omega t - kr\right)\right] d\omega. \tag{E.1}$$

$\overline{M}(\omega)$ consists, in principal, of factors that describe the *source spectrum*, the *excitation function* of the mode (depending on source depth, source orientation and, in general, also on ω) and their *eigen function* (amplitude-depth distribution). Wavenumber $k(\omega) = \omega/c(\omega)$ contains the *dispersion information* of the mode. Equation (4.53) is a simple special case of (E.1) with $\overline{M}(\omega) \sim k^{-1/2}(\omega)$.

Integrals of the form (E.1) can be solved efficiently with the help of the *Fast Fourier transform*. In the case of the ideal wave guide, for which the modal seismograms computed analytically are given in Fig. 4.3, the following numerical result is derived for the potential (after a low-pass filter, which has decayed to zero at the Nyquist frequency).

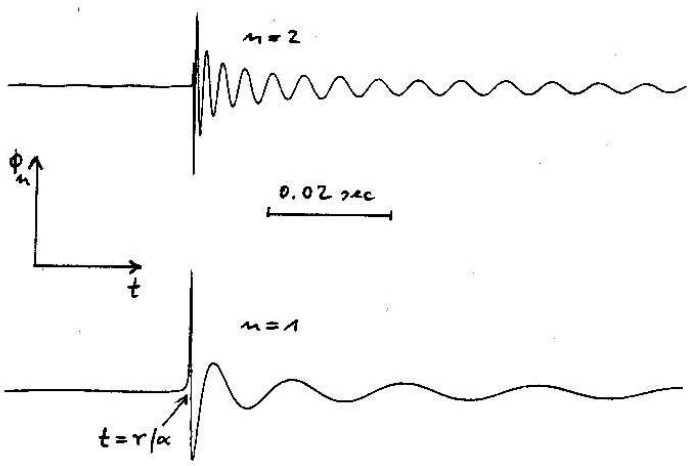

Fig. E.1: Modal seismogram for the ideal wave guide (compare to Fig. 4.23).

They agree very well with the analytical seismograms in Fig. 4.33.

If one is only interested in the study of dispersion on horizontal profiles, most times it is sufficient to consider in $\overline{M}(\omega)$ only the source spectrum. This simplifies the studies, since then only the theory of *free* surface waves is needed (for the determination of $k(\omega)$).

E.2 Method of stationary phase

The application of the method of stationary phase in integrals of the type (E.1) has been described in section 4.2.3. Here, it is shortly outlined again, since the results are needed as the basis for the treatment of the Airy phases in section E.3. It should be noted that today the results of this and the next section are not of great importance in the numerical computation of modal seismograms, since the Fast Fourier transform mentioned in section E.1 is more suited for that purpose. Here, analytical rules for the amplitude decay of surface waves with increasing distance can be derived; this is an important addition to purely numerical methods.

The phase $\varphi(\omega) = \omega t - k(\omega)r$ in (E.1) has the following derivatives with respect to ω (U = group velocity)

$$\varphi' = t - rk' = r - \frac{r}{U} \tag{E.2}$$

$$\varphi'' = -rk'' = rU^{-2}U' \tag{E.3}$$

$$\varphi''' = -rk''' = r\left(U^{-2}U'' - 2U^{-3}U'\right). \tag{E.4}$$

Stationary phase values follow from $\varphi'(\omega_0) = 0$ and are, therefore, determined by

$$U(\omega_0) = \frac{r}{t}. \tag{E.5}$$

Then

$$U'(\omega_0) \neq 0, \tag{E.6}$$

$\varphi(\omega)$ can be approximated near ω_0 by

$$\varphi(\omega) = \varphi_0 + \frac{1}{2}\varphi_0''(\omega - \omega_0)^2 \tag{E.7}$$

$(\varphi_0 = \varphi(\omega_0), \varphi_0'' = \varphi_0''(\omega_0))$. The modal seismogram can then be written in the *stationary phase approximation* as

$$\begin{aligned} N(t) &= r^{-\frac{1}{2}} Re \int_{\omega_0-\Delta\omega}^{\omega_0+\Delta\omega} \overline{M}(\omega) \exp\left[i\left(\varphi_0 + \frac{1}{2}\varphi_0''(\omega-\omega_0)^2\right)\right] d\omega \quad \text{(E.8)} \\ &\simeq r^{-\frac{1}{2}} Re\left\{\overline{M}(\omega_0) e^{i\varphi_0}\left(\frac{2}{|\varphi_0''|}\right)^{\frac{1}{2}} \int_{-\infty}^{+\infty} e^{ix^2 sign\varphi_0''} dx\right\} \end{aligned}$$

with $x = \left(\frac{|\varphi_0''|}{2}\right)^{1/2}(\omega - \omega_0)$. With (E.3), we finally derive $(U_0 = U(\omega_0), U_0' = U'(\omega_0), k_0 = k(\omega_0) = \omega_0/c(\omega_0))$

$$N(t) = \frac{U_0}{r}\left(\frac{2\pi}{|U_0'|}\right)^{\frac{1}{2}} Re\left\{\overline{M}(\omega_0)\exp\left[i\left(\omega_0 t - k_0 r + \frac{\pi}{4} sign\, U_0'\right)\right]\right\}. \tag{E.9}$$

Equation (E.9) holds under the requirement (E.6). Then ω_0, t and r are connected via (E.5) and‘ this produces the *frequency modulation* of the normal mode. Its amplitude is also time dependent; this is mostly due to $\overline{M}(\omega_0(t))$ but also partially due to U_0 and U_0' (*amplitude modulation*).

If we consider the amplitudes of the normal mode as a function of distance r, we see that they decay with r^{-1} as long as (E.9) holds. This statement concerns the amplitudes in the *time domain*; spectral amplitudes decay with $r^{-1/2}$ according to (E.1).

E.3 Airy phases

For realistic wave guides, one or several frequencies exist for which the *group velocity* is stationary. In the following, we assume that ω_0 is such a frequency. It also holds that $U'(\omega_0) = 0$, (E.6) is, therefore, violated and (E.9) no longer holds. A sufficient approximation of the phase is, in this case,

$$\varphi(\omega) = \varphi_0 + \varphi_0'(\omega - \omega_0) + \frac{1}{6}\varphi_0'''(\omega - \omega_0)^3 \tag{E.10}$$

instead of (E.7). From (E.2) and (E.4), it follows that

$$\varphi_0' = t - \frac{r}{U_0}, \qquad \varphi_0''' = rU_0^{-2}U_0''. \tag{E.11}$$

The phase is *no longer stationary at* ω_0 but has a turning point there. The third term in (E.10) has now to be considered since φ_0' changes from negative values $t < r/U_0$ to positive values for $t > r/U_0$ and, thus, the second term in (E.10) is not necessarily dominant. In analogy to (E.8), the following approximation of the modal seismogram for times near r/U_0 can be derived (*Airy phase approximation*)

$$\begin{aligned} N(t) &= r^{-\frac{1}{2}} Re \int_{\omega_0-\Delta\omega}^{\omega_0+\Delta\omega} \overline{M}(\omega) \\ &\quad \cdot \exp\left[i \left(\varphi_0 + \varphi_0'(\omega - \omega_0) + \frac{1}{6}\varphi_0'''(\omega - \omega_0)^3 \right) \right] d\omega \\ &\simeq r^{-\frac{1}{2}} Re \left\{ H \cdot b \cdot \int_{-\infty}^{+\infty} \exp\left[i \left(\varphi_0' \cdot b \cdot x + \frac{x^3}{3} sign\, \varphi_0''' \right) \right] dx \right\} \\ &= 2r^{-\frac{1}{2}} Re\{H\} \cdot b \cdot \int_0^{\infty} \cos\left[sign\, \varphi_0''' \cdot \varphi_0' \cdot b \cdot x + \frac{x^3}{3} \right] dx \end{aligned}$$

with $x = \left(\frac{|\varphi_0'''|}{2} \right)^{\frac{1}{3}} (\omega - \omega_0)$, $H = \overline{M}(\omega_0) e^{i\varphi_0}$ and $b = \left(\frac{2}{|\varphi_0'''|} \right)^{\frac{1}{3}}$.

The integral can be expressed by the *Airy function*

$$Ai(z) = \frac{1}{\pi} \int_0^{\infty} \cos\left(zx + \frac{x^3}{3} \right) dx,$$

which is shown in Fig. E.2.

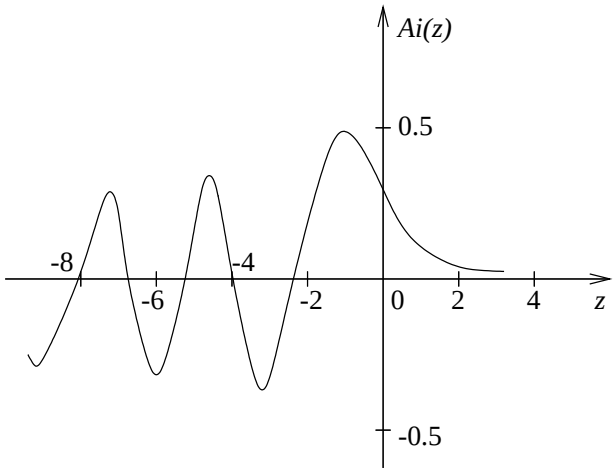

Fig. E.2: Airy function.

With (E.11), the end result for the *Airy phase* can be written as

$$\begin{aligned} N(t) &= \frac{2}{r^{\frac{5}{6}}}\left(\frac{2U_0}{|U_0''|}\right)^{\frac{1}{3}} Re\left\{\overline{M}(\omega_0)\exp\left[i(\omega_0 t - k_0 r\right]\right\} \\ &\quad \cdot Ai\left[\frac{sign\, U_0''}{r^{\frac{1}{3}}}\left(\frac{2U_0^2}{|U_0''|}\right)^{\frac{1}{3}}\left(t-\frac{r}{U_0}\right)\right]. \end{aligned} \tag{E.12}$$

This is a monochromatic oscillation with frequency ω_0 (following from $U'(\omega_0) = 0$), *the amplitude of which is modulated by the Airy function.*

If $sign\, U_0'' > 0$, i.e., if we are at a group velocity *minimum*, the modal seismogram looks qualitatively like that in Fig. E.3 (the argument z of the Airy function increases with t).

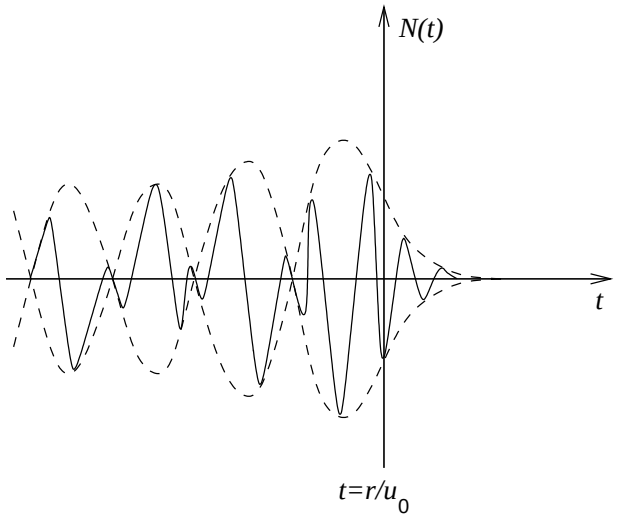

Fig. E.3: Modal seismogram.

The seismogram *ends* with strong amplitudes in the neighbourhood of the theoretical arrival times of the Airy phase. Fig. 4.13 gives quantitative results for a liquid wave guide; in the range of the Airy phases, the seismogram has been computed with the theory if this chapter.

If $sign\, U_0'' < 0$ (i.e., we are near a group velocity *maximum*), z decreases for increasing t, and the Airy function is sampled from right to left. The seismogram, therefore, *starts* with large amplitudes.

The *amplitudes of the Airy phases* decrease with $r^{-5/6}$ as a function of distance r, i.e., they decrease slower then given in (E.9). This is the reason why the Airy phase dominates for increasing distances.

Index